

Distributed smart lighting systems : sensing and control

Citation for published version (APA):

Caicedo Fernández, D. R. (2014). *Distributed smart lighting systems : sensing and control*. [Phd Thesis 1 (Research TU/e / Graduation TU/e), Electrical Engineering]. Technische Universiteit Eindhoven.
<https://doi.org/10.6100/IR774336>

DOI:

[10.6100/IR774336](https://doi.org/10.6100/IR774336)

Document status and date:

Published: 01/01/2014

Document Version:

Publisher's PDF, also known as Version of Record (includes final page, issue and volume numbers)

Please check the document version of this publication:

- A submitted manuscript is the version of the article upon submission and before peer-review. There can be important differences between the submitted version and the official published version of record. People interested in the research are advised to contact the author for the final version of the publication, or visit the DOI to the publisher's website.
- The final author version and the galley proof are versions of the publication after peer review.
- The final published version features the final layout of the paper including the volume, issue and page numbers.

[Link to publication](#)

General rights

Copyright and moral rights for the publications made accessible in the public portal are retained by the authors and/or other copyright owners and it is a condition of accessing publications that users recognise and abide by the legal requirements associated with these rights.

- Users may download and print one copy of any publication from the public portal for the purpose of private study or research.
- You may not further distribute the material or use it for any profit-making activity or commercial gain
- You may freely distribute the URL identifying the publication in the public portal.

If the publication is distributed under the terms of Article 25fa of the Dutch Copyright Act, indicated by the "Taverne" license above, please follow below link for the End User Agreement:

www.tue.nl/taverne

Take down policy

If you believe that this document breaches copyright please contact us at:

openaccess@tue.nl

providing details and we will investigate your claim.

Distributed Smart Lighting Systems: Sensing and Control

A catalogue record is available from the Eindhoven University of Technology
Library
ISBN: 978-90-386-3631-3

Cover design by Paul Verspaget, Verspaget & Bruinink design studio.

The work described in this thesis has been carried out at the Philips Research
Laboratories in Eindhoven, The Netherlands, as part of the Philips Research
programme.

© KONINKLIJKE PHILIPS N.V. 2014

All rights reserved. No part of this publication may be reproduced, stored in a
retrieval system, or transmitted, in any form or by any means, electronic, mechan-
ical, photocopying, recording or otherwise, without the prior written permission
from the copyright owner.

Distributed Smart Lighting Systems: Sensing and Control

PROEFSCHRIFT

ter verkrijging van de graad van doctor aan de Technische Universiteit
Eindhoven, op gezag van de rector magnificus prof.dr.ir. C.J. van Duijn,
voor een commissie aangewezen door het College voor Promoties, in het
openbaar te verdedigen op woensdag 25 juni 2014 om 16:00 uur

door

David Ricardo Caicedo Fernández

geboren te Guayaquil, Ecuador.

Dit proefschrift is goedgekeurd door de promotoren en de samenstelling van de promotiecommissie is als volgt:

voorzitter:	prof.dr.ir. A. C. P. M. Backx
1 ^e promotor:	prof.dr.ir. J. W. M. Bergmans
copromotoren:	dr. A. Pandharipande (Philips Research) dr.ir. F. M. J. Willems
leden:	prof.dr. U. Mitra (University of Southern California) prof.dr. G. Q. Zhang (Delft University of Technology) prof.dr. J. J. Lukkien
adviseur:	dr. S. Srinivasan (Microsoft Corporation)

Contents

1	Introduction	1
1.1	Introduction	2
1.1.1	Artificial lighting	2
1.1.2	Smart lighting systems	3
1.1.3	Occupancy information	3
1.1.4	Illumination information	5
1.1.5	Calibration	7
1.2	System architecture	9
1.2.1	System architecture for small-sized spaces	9
1.2.2	System architecture for medium-sized spaces	10
1.2.3	System architecture for large-sized spaces	11
1.2.4	Further variations on system architectures	13
1.3	Granular occupancy sensing solutions	13
1.3.1	Granular occupancy sensors	14
1.3.2	Granular occupancy sensing solutions for large-sized spaces	15
1.4	Lighting controls based on occupancy information and illuminance measurements	16
1.4.1	Illuminance measurements at the workspace plane	16
1.4.2	Illuminance measurements at the ceiling	18
1.4.3	Calibration methods	19
1.5	Outline of the thesis	20
1.6	Publications of the author	23
1.6.1	Journal Publications	23
1.6.2	Conference Publications	24
1.6.3	Other Publications	24
1.6.4	Patents Applications	25
	REFERENCES	26

2	Distributed granular occupancy sensing	31
2.1	Introduction	32
2.2	Transmission slot allocation and synchronization	34
2.2.1	Pre-processing	35
2.2.2	Pre-synchronization	37
2.2.3	Transmission slot allocation	39
2.2.4	Post-synchronization	40
2.2.5	Cross-check	41
2.3	Ultrasonic zoned presence sensing	41
2.3.1	Moving target indicator processing for movement detection	42
2.3.2	Zoning, tracking and detection rule	43
2.4	Performance evaluation	45
2.4.1	Transmission slot allocation and synchronization	46
2.4.2	Zoned presence sensing	47
2.5	Conclusions	49
2.A	Analysis of transmission slot synchronization procedure	51
	REFERENCES	56
3	Centralized lighting control with light distribution knowledge	59
3.1	Introduction	60
3.2	Lighting control solution	61
3.3	Numericals results	65
3.4	Conclusions	67
	REFERENCES	70
4	Lighting control strategies accounting for user preferences	73
4.1	Introduction	74
4.2	System model	76
4.2.1	Power consumption	77
4.2.2	Illuminance over workspace plane	78
4.2.3	User dissatisfaction	78
4.2.4	Illuminance uniformity	79
4.2.5	Localized illumination rendering	80
4.3	Illumination control	80
4.3.1	Centralized control	82
4.3.2	Distributed control	85
4.4	Simulation results	92
4.5	Conclusions	98
	REFERENCES	99

5	Distributed lighting control with light sensor measurements	101
5.1	Introduction	102
5.2	System model	103
5.2.1	Dimming of light sources	105
5.2.2	Illuminance at light sensor	106
5.3	Distributed Illumination control with local sensing and actuation: Problem formulation	107
5.4	Distributed illumination control solution	111
5.4.1	Distributed control algorithm	118
5.5	Analysis of the algorithm	120
5.5.1	Neighbor selection	123
5.6	Simulation Results	123
5.7	Conclusions and discussion	126
5.A	Sufficient conditions for (5.25)	128
	REFERENCES	133
6	Robust centralized lighting control with light sensor measurements	135
6.1	Introduction	136
6.2	Lighting system description and problem setup	137
6.2.1	Illuminance at workspace plane	138
6.2.2	Illuminance at light sensor	139
6.2.3	Calibration step	141
6.3	Problem formulation	141
6.4	Proposed method	143
6.4.1	No-daylight case	143
6.4.2	Daylight case	147
6.5	Numerical results	150
6.5.1	No-daylight scenario	152
6.5.2	Daylight scenario	155
6.6	Conclusions	157
6.A	Solution to linear programming problem (6.10)	158
6.B	Solution to linear programming problem (6.6)	160
	REFERENCES	162
7	Distributed methods for light sensor calibration	165
7.1	Introduction	166
7.2	Lighting system description	167
7.3	Problem setting	168
7.4	Proposed method	169

7.4.1	Initial calibration	170
7.4.2	Calibration tracking	173
7.4.3	Re-calibration	175
7.5	Numerical results	175
7.6	Conclusions	177
	REFERENCES	179
8	Conclusions and Further Research	181
8.1	Conclusions	182
8.1.1	Granular occupancy sensing solutions	184
8.1.2	Lighting controls when light sensors are located at the workspace plane	185
8.1.3	Lighting controls when light sensors are located at the ceiling	187
8.1.4	Calibration methods	188
8.2	Recommendations for future research	189
8.2.1	Occupancy sensing	189
8.2.2	Lighting controls	190
	Summary	191
	Curriculum vitae	195
	Acknowledgement	197

Chapter **1**

Introduction

1.1 Introduction

Light is the part of the electromagnetic radiation visible to the human eye and plays an important role in our daily lives. Without light we would not be able to see or interact with the exterior world. The two most important sources of light in indoor lighting are: *daylight* and *artificial light*. Daylight is the component that comes from the sun, and varies due to factors like time and day of year, weather conditions and geographical location. Artificial lighting is the component that results from “man-made” light sources such as fluorescent lamps, light emitting diode (LED) lamps etc.

1.1.1 Artificial lighting

Artificial lighting has become a ubiquitous part of our society and today accounts for a major fraction of electrical energy consumption in the world. In office buildings, in particular, the energy consumed due to artificial lighting can be up to 40% of the total energy consumption [1]. Reducing the energy consumption due to artificial lighting has a beneficial effect on costs associated to the operation of office buildings (*operational costs*) and the environment.

In office buildings, artificial lighting from electric light sources is used for providing indoor illumination. Electric light sources convert electrical energy into light and have the advantage that they can be easily activated or deactivated, e.g. by using light switches. Conventional *lighting systems* combine electric light sources with light switches for providing and controlling the artificial lighting. In such systems, the light switch gives the control of the lighting system to the user of the system, i.e. the occupant.

The illumination rendered by a lighting system depends on the spatial distribution of electric light sources and the *luminous intensity distribution* of each light source. The luminous intensity distribution of an electric light source denotes how much light the light source outputs in a given direction. A light source along with electrical and mechanical support constitutes a *luminaire*, and determines the effective luminous intensity distribution of the luminaire. In typical offices, luminaires with broad luminous intensity distribution patterns are spatially distributed in a grid at the ceiling for providing uniform illumination across the office.

A major factor in the energy-efficiency of lighting systems is the *luminous efficacy* of the electric light source. The luminous efficacy is the ratio between the light output and the supplied electric power of the light source. Electric light sources with large luminous efficacy are more energy-efficient because less electric power is required to produce the same light output. LED lamps have

the highest luminous efficacy when compared with current incandescent and fluorescent lamps [2]. Therefore, LED-based luminaires are desirable components in energy-efficient lighting systems.

The light output of a LED-based luminaire can be accurately controlled to a fraction of its nominal output. An advantage of reducing the light output of a LED-based luminaire is that it also reduces the energy consumption of the luminaire. Hereafter, we will refer to the act of changing the light output of a LED-based luminaire as *dimming*, and to the fraction to which the luminaire is changed as *dimming level*. The dimming capabilities of LED-based luminaires allow for a more flexible control of the lighting system.

Large energy-savings may be obtained by dimming the LED-based luminaires in lighting systems to low dimming levels. However, it is well known that an adequate level of illumination is required to perform any visual task efficiently and productively [3]. The amount of light (due to daylight and artificial lighting) incident on a given surface is known as *illuminance*. The most common criterion for assessing the quality of the illumination in offices is the average illuminance over a surface on the horizontal plane at the height of desk. In particular, in European norm EN 12464-1 [4] minimum average illuminance requirements for indoor lighting are described.

1.1.2 Smart lighting systems

With the advent of the digital age, systems have become more intelligent and automated. In lighting systems for offices, in particular, the control of the artificial lighting has been shifted partially towards the system itself. This new type of lighting system includes sensors for monitoring the environment, computing devices (*controllers*) that control the illumination based on the input from the sensors such that energy consumption is reduced while providing the required illumination, and communication units between sensors and controllers. Such a system is hereafter referred to as a *smart lighting system*.

The design of smart lighting systems for reducing energy consumption (and consequently the operational costs) should focus also on the initial investment required for deploying the system. In existing buildings, in particular, smart lighting systems that require minimal or no modifications to the existing infrastructure of the lighting system are preferred.

1.1.3 Occupancy information

Energy is wasted when the lights are kept on while no occupant is present in the office. A simple and effective control strategy to reduce energy consumption is

to turn off the lights when no occupant is present in the office. The information about whether an occupant is present or not in the office is hereafter referred to as *binary occupancy information* and is commonly provided by *occupancy sensors*. An occupancy sensor is an electronic device that monitors the presence of occupants within its sensing region. An occupancy sensor that provides binary occupancy information to the controller is hereafter referred to as *binary occupancy sensor*.

Smart lighting systems that control the artificial lighting based on binary occupancy information are desirable for energy savings, however, such systems may become a nuisance for the occupant if the lighting system is deactivated while the occupant is still in the office. The failure to detect an occupant is known as *missed detection*, while detection of an occupant who is not present is known as *false alarm*. In general, there is a trade-off between the amount of false alarms and missed detections, i.e. an increment (or decrement) in the number of false alarms results in a decrement (or increment) in the number of missed detections. Commercially available occupancy sensors are designed for limiting the number of false alarms, thus they tend to have a significant number of missed detections. In lighting systems with such sensors, a long off-timer (up to 30 minutes) is used before turning off the lights such that the occupant is not disturbed. The *reliability* of an occupancy sensor is measured by both the rate of false alarms and the rate of missed detections. Occupancy sensors with high reliability are preferred in lighting systems for reducing energy consumption while not disturbing the occupant, so that a short off-timer can be used for turning off the lights. Occupancy sensors have limited sensing regions and thus the choice of occupancy sensors depends on the size and type of the area to be monitored.

Office buildings have a large variety of workplaces such as private offices, shared offices, open offices and so on. In this work, we sort these workplaces into three categories based on their size: small-sized spaces such as private offices, medium-sized spaces such as shared offices and large-sized spaces such as open offices.

In small-sized spaces, smart lighting systems that adapt the illumination based on information from a single binary occupancy sensor over the whole space may suffice for reducing energy consumption. In medium and large-sized spaces, however, further reduction in energy consumption is achieved by also adapting the illumination based on the location of the occupant [5]. European norm EN 12464-1 [4], as an example, recommends high illumination in the region where the occupant is present and allows for a lower illumination elsewhere.

Note that in practical smart lighting systems, where LED-based luminaires have broad luminous intensity distribution patterns, changing the illumination at

a given location also influences the illumination in neighboring locations. Therefore, it makes sense to discretize the space into *control zones* such that the illumination in one control zone can be adapted by the controller with limited effect in neighboring control zones. In small-sized spaces, more than one control zone is usually not feasible while in medium-sized and large-sized spaces multiple control zones can be defined.

The presence of occupants in each control zone can be monitored by using a binary occupancy sensor in each zone. In Fig. 1.1(a), we show two control zones, each one equipped with a binary occupancy sensor (depicted as a diamond). This approach may require the deployment of several of these sensors. A different approach that provides the same information is by using a more sophisticated occupancy sensor with a sensing region that covers several control zones and that provides information about the control zones where occupants are present. The information about the location of the occupant within control zones monitored by a single occupancy sensor is hereafter referred to as *granular occupancy information* and the occupancy sensor that provides such information is referred to as a *granular occupancy sensor*. In Fig. 1.1(b), a granular occupancy sensor (depicted as a square) is monitoring two control zones.

Granular occupancy sensors that can be used in practice for smart lighting systems for offices are not presently available. Furthermore, in large-sized spaces, several of such sensors distributed across the space may be required to ensure a complete coverage of the space. Smart lighting systems with distributed sensors (e.g. granular occupancy sensors) are hereafter referred to as *distributed smart lighting systems*. A key research challenge is to develop granular occupancy sensors for medium-sized spaces and distributed systems of such sensors for large-sized spaces.

1.1.4 Illumination information

Another step towards reducing energy consumption in smart lighting systems is by dimming those luminaires over control zones with sufficient daylight [6]. This control strategy is commonly known as daylight harvesting and is usually combined with occupancy-based control of the smart lighting system.

In offices, the available light in different control zones is usually measured by using a *light sensor*. A light sensor is an electronic device with a built-in light-sensitive element that measures the amount of light that hits the element, i.e. the illuminance level at the light-sensitive element. In typical light sensors, only the light originating from specific directions is allowed to reach the light-sensitive element in the light sensor. The maximum angle with respect to an axis perpendicular to the surface of the light sensor from which light is allowed

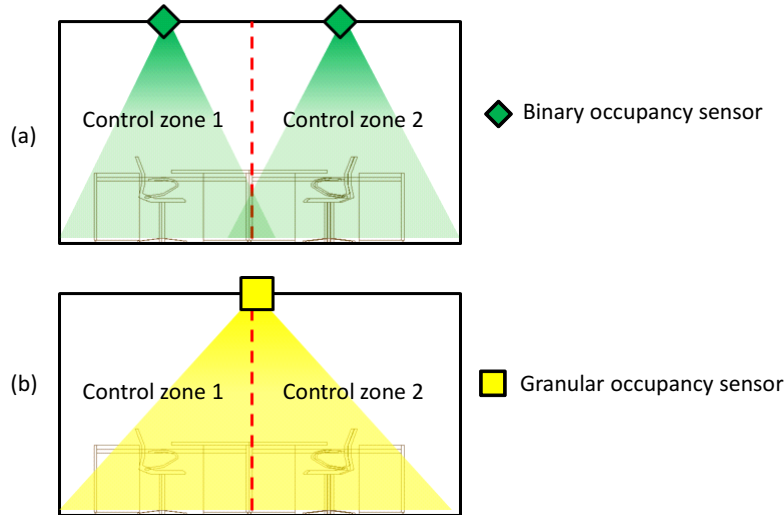


Figure 1.1: Occupancy per control zone obtained using (a) two binary occupancy sensors or (b) a single granular occupancy sensor.

to reach the light-sensitive element is known as the *half-opening angle* of the light sensor, see Fig. 1.2. Typical half-opening angles for light sensors are between 20 to 60 degrees [7].

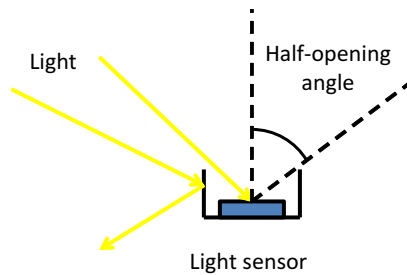


Figure 1.2: Illustration of a light sensor and its half-opening angle.

In offices, the average illuminance levels are of interest over the surface of the desks and thus locating light sensors with large half-opening angles at the desk is the most desirable choice. A light sensor with large half-opening angle measures the illuminance due to light coming from almost every direction. In small-sized spaces such as a private office, a single light sensor may suffice for measuring the illuminance levels at the desk. In comparison, medium and large-sized spaces usually have several desks distributed across the space and thus an equal amount

of light sensors needs to be deployed for measuring the illuminance level at each desk.

Illuminance measurements from light sensors located at the desk are however susceptible to occupant movements, e.g. the occupant can block the light from reaching the light sensor. Therefore, light sensors are typically located at the ceiling.

The illuminance measurements from the light sensors (at the desk or at the ceiling) provide to the controller information about the lighting conditions in the monitored space. Note that the illuminance level at a light sensor is the combination of daylight and artificial light due to multiple LED-based luminaires, and thus the same illuminance level at the light sensor could be achieved by different combinations of dimming levels at the luminaires. A key research challenge is to develop control algorithms that use information about the lighting conditions to adapt the artificial lighting such that energy consumption is reduced by finding the proper dimming levels of those luminaires over zones with sufficient light.

In this thesis, we are interested in developing controllers that adapt the illumination in distributed smart lighting systems by finding the optimum dimming levels of the LED-based luminaires based on information provided by occupancy sensors and light sensors such that energy consumption is minimized and an adequate illumination is provided. This goal is summarized as:

Goal: *To develop distributed smart lighting systems that minimize energy consumption while providing adequate illumination to the users.*

1.1.5 Calibration

At the ceiling, the light that reaches the light sensors is mainly the light reflected from objects in the field of view of the sensor such as desks, floor, walls, and so on. The ratio between the amount of light that is reflected from a surface and the light that hits that surface is known as *reflectance*. In Fig. 1.3(a) and Fig. 1.3(b), we show the path of the light measured at a light sensor at the desk and at the ceiling, respectively.

The main task of the controller is to satisfy average illuminance levels at the desks. However, a problem arises when the light sensors are located at the ceiling: *how to estimate the average illuminance levels at the desk from the illuminance levels at the light sensors at the ceiling?*

Limiting the half-opening angle of the light sensor such that only light reflected from the desk reaches the light-sensitive element would facilitate the estimation of the illuminance level at the desk. The illuminance level at the desk and the light sensor would be mainly related by the reflectance of the desk. However,

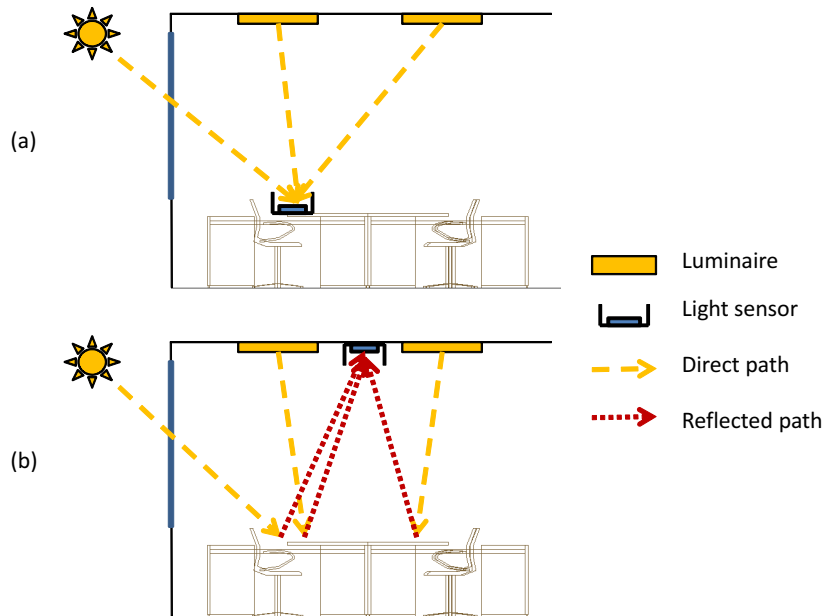


Figure 1.3: Illustration of a light sensor located (a) at the desk and (b) at the ceiling. We also show the path of the light that is measured in both cases.

in practice no prior knowledge of the size and location of desks is available during the installation of the light sensors. Furthermore, light sensors with small half-opening angles are more susceptible to changes in the reflectance of the objects within their field of view.

A straightforward solution is to map the illuminance levels at light sensors at the ceiling with the corresponding average illuminance levels at the desks. Then, the controller can infer, using this mapping, the average illuminance levels at the desks from the illuminance levels from light sensors at the ceiling and adapt the illumination accordingly.

However, finding the mapping between illuminance levels is a time-consuming procedure and in practice a simple mapping procedure is preferred, e.g. the illuminance at the light sensors at the ceiling and the average illuminance levels at the desks can be mapped when the light output of the luminaires is at maximum.

The mapping between illuminance levels is known as *calibration*. The procedures required for the correct functioning of smart lighting systems such as calibration are hereafter referred to as *commissioning*.

1.2 System architecture

Different system architectures of (distributed) smart lighting systems emerge depending on factors such as (i) the size of the spaces, (ii) the number of control zones, (iii) the number of light sensors, (iv) the number of occupancy sensors, (v) the communication between controllers and (vi) the location of light sensors. In this work, we do not consider any other type of sensors such as temperature sensors or external daylight sensors.

1.2.1 System architecture for small-sized spaces

The simplest architecture, hereafter known as Type-I, is typically used for smart lighting systems in small-sized spaces and consists of a single control zone, one or multiple LED luminaires, a single binary occupancy sensor, a single light sensor and a single controller. In Fig. 1.4, we present the components of the Type-I architecture. The controller, the binary occupancy sensor, the light sensor and the luminaire which are depicted by a triangle, diamond, circle and square, respectively. Here, we also show the connection (through a communication channel) between the controller, light sensor and binary occupancy sensor. The connections between luminaires and the controller are not shown.

In the Type-I architecture, the binary occupancy information from the occupancy sensor is used by the controller to determine whether the smart lighting system has to be activated or not. If the smart lighting system is activated, the illuminance measurement from the light sensor is used by the controller to adapt the illumination by dimming the LED luminaires such that the illuminance requirement at the light sensor is achieved.

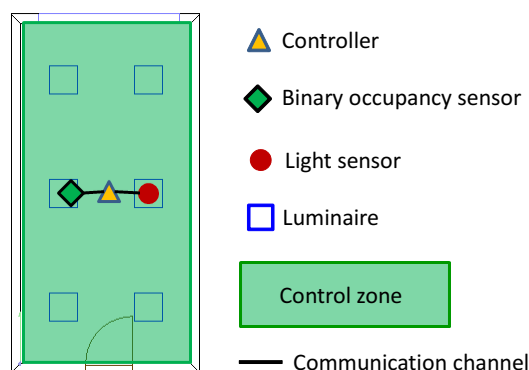


Figure 1.4: Illustration of system architecture Type-I.

1.2.2 System architecture for medium-sized spaces

In medium-sized spaces, dividing the space into control zones and adapting the illumination in each control zone, results in more energy savings when compared with Type-I (as mentioned in Section 1.1.3). Daylight is usually limited to a few control zones, in particular to those control zones near windows. Commercially available binary occupancy sensors with large sensing regions can easily provide binary occupancy information in medium-sized spaces such as shared offices [8, 9]. Therefore, having more light sensors than binary occupancy sensors in medium-sized spaces is quite common. The second architecture that we consider, hereafter referred to as Type-II, is shown in Fig. 1.5 and consists of multiple control zones, multiple luminaires, a single light sensor per control zone, a single binary occupancy sensor for the whole space and a single controller.

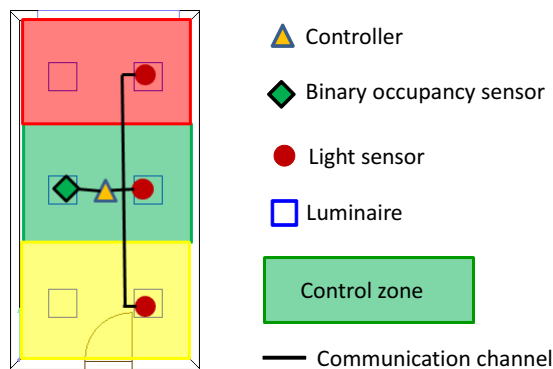


Figure 1.5: Illustration of system architecture Type-II.

In the Type-II architecture, the controller activates the distributed smart lighting system when the binary occupancy sensor reports presence of an occupant in the space. The illuminance measurements from the light sensors are used by the controller to adapt the illumination such that the illuminance requirements at each light sensor are achieved.

Further energy-savings in medium-sized spaces, when compared to Type-II architecture, are achieved by adapting the illumination requirements based on occupancy information in each control zone. As mentioned in Section 1.1.3, two approaches are possible for obtaining occupancy information at each control zone. The first approach is by placing a binary occupancy sensor at each control zone as is shown in Fig. 1.6(a). The system architecture shown in Fig. 1.6(a) is hereafter referred to as Type-III(a) and consists of multiple control zones, multiple luminaires, a single light sensor and a single binary occupancy sensor

per control zone, and a single controller. The second approach is to use a granular occupancy sensor over the space as seen in Fig. 1.6(b). System architecture Type-III(b) emerges from this approach and consists of multiple control zones, multiple luminaires, a single light sensor per control zone, a single granular occupancy sensor and a single controller.

In system architecture Type-III, both for Type-III(a) and Type-III(b), the controller uses the occupancy information in each control zone to determine the illuminance requirements per control zone, e.g. a high illuminance level if the control zone is occupied and a low illuminance level otherwise. If all the control zones are unoccupied, the controller deactivates the distributed smart lighting system. The controller uses the illuminance measurements from the light sensors to adapt the illumination such that the illuminance requirements at each light sensor are achieved.

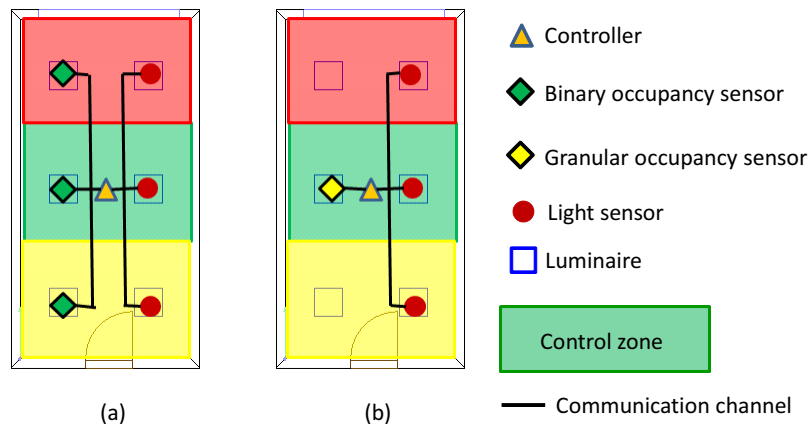


Figure 1.6: Illustration of system architectures: (a) Type-III(a) and (b) Type-III(b).

In Fig. 1.7, a diagram summarizing the different types of systems architectures (Type-I, Type-II and Type-III) for medium-sized spaces is given. Note that Type-I may be also used for medium-sized spaces but lower energy savings when compared to Type-II and Type-III are expected.

1.2.3 System architecture for large-sized spaces

In large-sized spaces such as open offices, a distributed smart lighting system with an architecture based on a combination of multiple Type-I (Type-II and/or Type-III) sub-systems is required to control and adapt the illumination in the whole space. Two variations of such system architecture emerge depending on

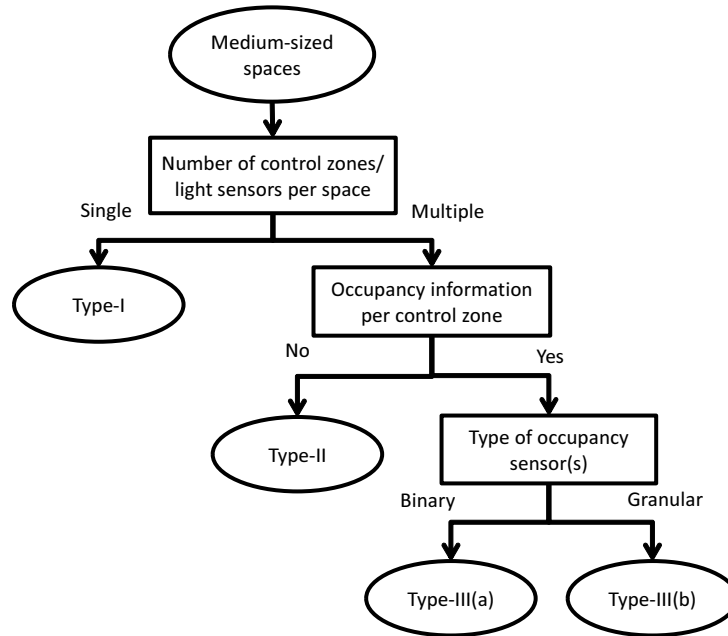


Figure 1.7: Diagram of the different system architectures for medium-sized spaces.

the communication capabilities between controllers. The two variations for a Type-I based system architecture for large-sized spaces are shown in Fig. 1.8. If the contribution from luminaires in a Type-I sub-system to the illumination in control zones of neighboring Type-I sub-systems is negligible, then no inter-zone communication channel is required as is seen in Fig. 1.8(a). Examples of such architectures are open offices divided by wall partitions into smaller cells, where the illumination from a group of luminaires may be restricted within each cell. In such an architecture, each controller adapt the illumination within its own cell (sub-system Type-I).

The second variation of Type-I based system architectures for large-sized spaces is obtained when the contribution from luminaires in a Type-I sub-system to the illumination in control zones of neighboring Type-I sub-systems is considerable. In such an architecture, an inter-zone communication channel is required as is seen in Fig. 1.8(b). The controllers in different sub-systems need to communicate to determine the dimming levels in the entire distributed smart lighting system such that the illumination requirements over the whole space are achieved.

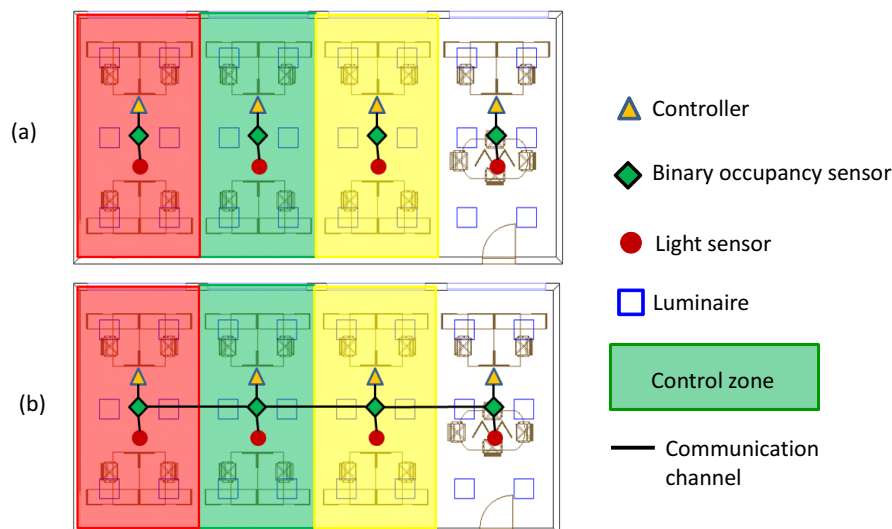


Figure 1.8: Illustration of a Type-I based system architecture for large-sized spaces (a) without a communication channel between controllers and (b) with a communication channel between controllers.

1.2.4 Further variations on system architectures

Further variations of the system architectures Type-I, Type-II and Type-III for medium and large-sized spaces may be obtained depending on the placement of light sensors: either at the ceiling or at the desks.

1.3 Granular occupancy sensing solutions

As discussed in Section 1.1.3, occupancy based lighting control strategies such as keeping the lights on when occupancy is detected and turning them off otherwise reduce energy consumption. Reliable detection of the occupant, i.e. a limited rate of missed detections and false alarms, is a desirable feature in occupancy-based lighting control strategies.

Typical technologies for obtaining occupancy information in commercial systems are: infrared, ultrasonic or a combination of both. *Passive infrared (PIR) sensors* are widely used due to their low cost and complexity. A commercial PIR sensor works by detecting the movement of an occupant between pre-defined zones, where each zone is defined by the optical pattern of the PIR's lens. It is to be noted that commercially available PIR sensors suffer from poor detection

performance of the occupant, i.e. from a large number of missed detections [10]. These sensors are designed to limit false alarms, thus slight movements of an occupant, such as typing, are not easily detected and a long off-timer is needed before deactivating lighting controls.

Commercially available *ultrasonic occupancy sensors* use Doppler shift for detecting movement. A continuous ultrasonic sinusoidal waveform is transmitted and when an occupant enters the detection range of the sensor, its movement induces a Doppler shift in the frequency of the reflected signal (*echo*) that is detected at the sensor. In general, ultrasonic occupancy sensors have fewer missed detections than PIR sensors and do not strictly require that the occupant is in line-of-sight, but ultrasonic occupancy sensors are on the other hand prone to false alarms [11]. Dual technologies that combine both PIR and ultrasonic occupancy sensors achieve a more reliable detection but have higher cost.

1.3.1 Granular occupancy sensors

Both types of commercial sensors, ultrasonic and infrared, can provide binary occupancy information within their field of view but cannot provide granular occupancy information. Granular occupancy information is desirable because it leads to substantial energy savings in medium-sized and large-sized spaces [5,12].

Radio frequency (RF) and ultra-wideband (UWB) radar technologies have been previously used to detect and localize human beings. However, RF-based radar technologies [13] are not suitable for indoor applications due to through-wall propagation properties, while UWB radar technologies [14] are currently more expensive than PIR and ultrasound technologies.

A network of PIR sensors has been studied in [15] and [16] for detection and localization of human beings. Such systems achieve good accuracy in localizing users but the cost of deploying such systems increases with the number of PIR sensors.

Vision-based systems are attractive and widely used solutions for surveillance applications [17,18], but are less attractive as granular occupancy sensors. Vision-based systems are in general more expensive than commercial occupancy sensors and are prone to privacy concerns. Furthermore, the performance of a vision-based system degrades under low-light conditions. Such conditions occur in low daylight conditions and when the lighting system is off.

Advances in micro-electro-mechanical systems (MEMS) technology have enabled the development of new commercial sensor elements that are sensitive to ultrasonic frequencies. Their adoption in smartphones in particular has driven down costs [19]. This enables the design and use of an ultrasonic sensor array at the receiver side [5]. In [5], we considered the use of a commercially available

broadbeam ultrasonic transmitter [20] with an ultrasonic receiver array for obtaining accurate location information in a wall-mounted configuration. Here, a short-pulsed ultrasonic sinusoidal signal is transmitted and the echoes processed. Distance information is derived from the time-of-flight of the echoes and angular information is obtained using beamforming techniques on the signal at the receiver side. A combination of distance and angular information provides the location of the occupant with respect to the ultrasonic array sensor. The algorithm in [5] achieved accurate location information in a wall-mounted configuration, but was not suitable for implementation in low-end microcontrollers. For practical purposes, low complexity occupancy sensing solutions are preferred. In offices, in particular, ceiling-mounted configurations are preferred due to aesthetic and functional reasons. At the ceiling, the power infrastructure of the LED-based luminaires can be reused for powering the occupancy sensors.

In this thesis, our first subgoal in this thesis is therefore:

Subgoal 1: *To design a low complexity ceiling-mounted sensing solution for providing reliable granular occupancy information.*

1.3.2 Granular occupancy sensing solutions for large-sized spaces

In large-sized spaces, such as open offices, two or more of the ultrasonic array sensors may be needed to ensure coverage over the whole area. For the proper functioning of the occupancy sensors, it is necessary to coordinate the active transmissions of each sensor. Without coordination, a sensor would not be able to distinguish between the echoes from its own active transmission and the echoes from different active transmissions. This would result in a performance degradation, e.g. an increased amount of false triggers. Common schemes for coexistence of multiple active transmissions include: time, frequency and code division. However, the narrow bandwidth of commercially-available ultrasonic transmitters [20] limits our choice to a time-multiplexing active transmission scheme. In this scheme, each ultrasonic sensor is to be assigned to a *transmission slot* such that no collisions occur with neighboring ultrasonic sensors. A transmission slot is a time window within which the ultrasonic array sensor transmits a short-pulsed ultrasonic sinusoidal signal and receives the corresponding echoes.

The coexistence problem in ultrasonic sensors has been considered in [21] and [22] where the synchronization between the transmissions of different ultrasonic sensors is achieved by using a separate communication channel. Such a solution is feasible in a system architecture for large-sized spaces with a communication channel between the controllers. However, as discussed in Section 1.2, there is a variation of system architectures for large-sized spaces for which a communication

channel does not exist. Therefore, the solutions presented in [21] and [22] that involve communication between the sensors for assigning different transmission slots, are not always feasible.

In [23], a distributed one-time transmission slot assignment protocol without a communication channel was presented. Typically, the ultrasonic sensors in distributed smart lighting systems for offices have internal clocks with low accuracy due to low cost constraints. A one-time assignment of transmission slots is thus not viable because the low accuracy in the internal clock of each sensor would lead to misalignment of the transmission slots with passage of time.

Therefore, the second subgoal in this thesis is:

Subgoal 2: *To enable the coexistence of multiple stand-alone ultrasonic occupancy sensors in an asynchronous distributed smart lighting system for large-sized spaces without communication channels between controllers.*

1.4 Lighting controls based on occupancy information and illuminance measurements

Lighting controls that adapt to occupancy information and daylight availability can achieve energy savings between 20% and 60% when compared to conventional lighting systems that do not adapt the artificial illumination [6]. In smart lighting systems with Type-I architecture, binary occupancy information is used for turning on/off the lighting system in the whole area while daylight availability is used to reduce the artificial illumination in the space. A more refined approach (as mentioned in Section 1.1.4) that can achieve larger energy savings is by individually dimming each luminaire and adapting illumination requirements depending on granular occupancy information [5]. In this approach, high illuminance levels are only provided to occupied control zones while low illuminance levels are provided to unoccupied control zones.

1.4.1 Illuminance measurements at the workspace plane

In offices, the illuminance levels are of interest over a horizontal plane at the height of the desks, hereafter referred to as *workspace plane*. The problem of creating specific illumination patterns at the workspace plane using smart lighting systems with LED-based luminaires has been considered in [24]. In [24], the goal was to determine the optimum dimming level of each LED-based luminaire such that specific illuminance patterns were rendered. Here, the illumination rendering problem was formulated as a constrained least squares problem where the sum of squared-errors between the desired and rendered illumination at specific location

1.4. LIGHTING CONTROLS BASED ON OCCUPANCY INFORMATION AND ILLUMINANCE MEASUREMENTS

at the workspace plane was minimized subject to physical constraints in the dimming level of each LED-based luminaire.

In practice, we are interested in providing constrained illuminance levels around the areas, over the workspace plane, where the occupant performs its task, i.e. the desks. The illuminance levels at the desks may be obtained, for example, by using wireless light sensor modules. Different frameworks have been considered to deal with this illumination rendering problem such as in [25–27]. In [25], a stochastic hill-climbing method for adapting the dimming levels based on illuminance measurements from light sensors on the workspace plane was proposed. A regression model was developed in [26] to estimate the influence of luminaires on light sensors on the workspace plane, based on which a control algorithm was presented. In [27], the occupants were equipped with portable wireless light sensors and a lighting control algorithm was presented.

In [5], we developed an analytical framework for the illumination rendering problem. Illuminance requirements, such as minimum illuminance levels and uniformity on the rendered illumination, were defined according to norm EN 12464-1 [4]. The rendered illumination and energy consumption of the distributed smart lighting system were modeled as functions linear in the individual dimming level of each LED-based luminaire. Thus, the energy saving problem subject to illumination constraints becomes a linear programming problem. Classical optimization techniques for solving linear programming problems are the Simplex method and interior-point methods [28]. Similar illumination models were introduced and used in [29] and [30].

The analytical framework in [5] does not consider available daylight. It is known that distributed smart lighting systems that adapt the rendered illumination based on both the available daylight and occupancy information achieve larger energy savings than those systems that only adapt to occupancy information [6, 29, 30]. The third subgoal in this thesis is therefore:

Subgoal 3: *To design lighting control algorithms that minimize energy consumption while adapting to daylight, occupancy information and satisfying minimum illuminance requirements at the workspace plane.*

The user perception of the rendered illumination is a factor that needs to be considered during the design of lighting control strategies. Dissatisfied users may disable those control strategies that do not fulfill their expectations [31], thus reducing the energy savings of such strategies. Different users have different opinions with respect to which illuminance levels are acceptable depending on the task they are going to perform. Hence, we seek to account for user preferences in the lighting control strategy. However, a problem may arise when neighboring users have conflicting preferences with respect to illuminance levels.

The fourth subgoal in this thesis is:

Subgoal 4: *To design lighting control algorithms that minimize energy consumption while taking into account user illumination preferences at the workspace.*

Experimental results from recent work in [32] support the importance of considering user preferences during the design of lighting control algorithms. In [32], the illumination problem with user preferences was formulated as a multi-objective optimization problem.

1.4.2 Illuminance measurements at the ceiling

Light sensors located at the desks have the advantage of providing measurements of the illuminance levels at the plane of interest. However, the illuminance measurements at the workspace plane are sensitive to the environment. At the workspace plane, the field of view of the light sensors may be temporarily or permanently blocked by the occupant movements, degrading the performance of the distributed smart lighting system.

An alternative, and one that is widely used in practice, is to place the light sensors at the ceiling where their view is not blocked. In this configuration, the light sensors may be co-located with the luminaires, eliminating the need for determining which group of luminaires each light sensor will control. Because the illuminance measurements are obtained in a plane different from the one where the illumination is of interest, a calibration phase is required. During the calibration phase, the target illuminance levels at the workspace plane are mapped to target illuminance levels at the light sensors. An accurate mapping ensures the equivalence between achieved illuminance levels at the ceiling and at the workspace plane.

In typical distributed smart lighting systems for large-sized spaces, a single LED-based luminaire contributes to the illumination of a limited region within its neighborhood and therefore several luminaires are required to adequately illuminate the entire space. In such systems, a distributed lighting control algorithm where communication is limited to neighbors is desirable. Distributed smart lighting systems with distributed lighting control algorithms have advantages of scalability, robustness and modularity. In [33], a heuristic distributed algorithm was proposed based on knowledge of the light distribution at the workspace plane. A multi-level lighting control strategy was presented in [34] using measurements from light sensors located at the ceiling.

The fifth subgoal in this thesis is:

1.4. LIGHTING CONTROLS BASED ON OCCUPANCY INFORMATION AND ILLUMINANCE MEASUREMENTS

Subgoal 5: *To design distributed lighting control algorithms that minimize energy consumption while satisfying illumination constraints at light sensors at the ceiling and with limited neighborhood communication requirements.*

Mapping the illuminance measurements at the ceiling with the respective illuminance measurement at the workspace plane is a time-consuming activity. For practical purposes, a coarse mapping procedure is typically performed, e.g. the illuminance levels at the light sensors are computed when all the luminaires in the lighting system are at maximum intensity and the illuminance distribution at the workspace plane is known. Thus, the actual illuminance levels at the task areas inferred from available illuminance measurements at the light sensors are only coarse approximations.

The sixth subgoal in this thesis is:

Subgoal 6: *To design distributed lighting control algorithms that minimize energy consumption while ensuring a minimum level of illumination at the workspace plane under coarse mapping between the illuminance levels at the ceiling and workspace plane.*

1.4.3 Calibration methods

The lighting control algorithms described in this thesis, and other ones in literature such as in [29] and [33], require knowledge of the illuminance contributions from each luminaire to the light sensors, hereafter referred to as *illumination gains*.

The performance of these lighting control algorithms depends highly on the accuracy of the illumination gains. Typically, the illumination gains are computed a priori during the calibration phase by turning on the luminaires one at a time and measuring illuminance values at the light sensors. Automatic methods for computing the illumination gains at each light sensor are desirable and reduce calibration (and consequently commissioning) efforts in distributed smart lighting systems.

The light sensors at the ceiling measure the amount of visible light that reaches them after being reflected from the environment, e.g. furniture. Changes in the environment may affect the amount of light reflected and thus the illumination gains. A continuous tracking of the illumination gains is needed to adapt to these changes in the environment.

Therefore, the seventh and last subgoal in this thesis is:

Subgoal 7: *To reduce the calibration efforts in asynchronous distributed smart lighting systems by developing automatic and distributed methods for computing the illumination gains.*

1.5 Outline of the thesis

In this section, we summarize the scope and key contributions of each individual chapter.

Chapter 2 addresses the first and second subgoals in this thesis. First, this chapter describes low complexity algorithms for obtaining reliable granular occupancy information using an ultrasonic array sensor located at the ceiling. The proposed solution extends the work done in [5], where a wall-mounted ultrasonic array sensor was used for localization of occupants and the algorithm was implemented in a desktop computer with no limits in the computation power. The ultrasonic array sensor consists of commercially available components: a single ultrasonic transmitter and a linear array of ultrasonic receivers. A short-pulsed ultrasonic sinusoidal signal is transmitted and the echoes are processed. Granular occupancy information is obtained by estimating distance (from time-of-flight of the echoes) and angular information (using beamforming techniques over the linear array). The complexity of the algorithm is reduced by only providing the location of the occupant within pre-defined control zones.

In distributed smart lighting systems for large-sized spaces, several of these ultrasonic array sensors may be deployed to ensure detection coverage. Due to low-cost constraints, each sensor has an internal clock with low accuracy and no communication channels between controllers are available. Two challenges emerge in such a system. One is how to allocate for each sensor a transmission slot so that interference from active transmissions of neighboring sensors is limited. The second is to guarantee that each sensor maintains its transmission slot despite the drifts due to inaccuracy in its internal clock. In Chapter 2, we propose a solution that exploits the existing cross-interference between sensors for identifying free transmissions slots and clock drifts. We consider a system architecture for large-sized spaces, in particular Type-III(b), without a communication channel between controllers.

The content of Chapter 2 is published in [35]. Additionally results on the topic of distributed occupancy sensing solutions based on ultrasonic array sensors can be found in [36–38].

Chapter 3 addresses the third subgoal in this thesis. This chapter describes centralized lighting control algorithms that adapt to daylight availability and occupancy information. The occupancy information, provided by the ultrasonic array sensor, is used to determine illuminance level targets at the workspace plane, i.e. high illuminance levels are required around the occupant and low illuminance levels elsewhere. We assume that the daylight contribution and the individual contribution of each luminaire to the workspace plane are known, e.g. by using wireless light sensors at the desks. The illumination problem is formulated as a

linear programming problem and solved using classical optimization techniques such as the Simplex method. The proposed solution is applicable to system architectures Type-II and Type-III for medium-sized spaces with light sensors at the desks. The proposed solution can also be used to control distributed smart lighting systems for large-sized spaces with a communication channel between all controllers. All the information about lighting conditions and occupancy state is communicated to a single controller, i.e. a *master controller*. The master controller adapts the artificial illumination of the entire system using the proposed algorithm. The content of Chapter 3 is based on the work published in [39].

Chapter 4 addresses the fourth subgoal in this thesis. This chapter extends the framework of Chapter 3 by considering user preferences. User preferences are modeled by piecewise linear functions. Piecewise linear functions are useful for approximating any convex (or concave) functions. We also consider methods for dealing with conflicting user preferences. A distributed lighting control algorithm with no communication constraints is developed based on a distributed implementation of the Simplex method. Here, we consider distributed smart lighting systems for large-sized spaces based on Type-I architecture with a communication channel between all controllers and light sensors at the desks. Furthermore, we compare two variations of such a system: one with individual controllers at each sub-system and a second one with a master controller. The content of Chapter 4 is published in [40].

Chapter 5 addresses the fifth subgoal in this thesis. This chapter considers a more typical office configuration in which light sensors are located at the ceiling. In this chapter, we focus on distributed smart lighting systems for large-sized spaces with communication between neighboring controllers and light sensors at the ceiling. Furthermore, we assume perfect knowledge of the mapping between illuminance levels at the light sensor at the ceiling and the corresponding illuminance levels at the workspace plane, so that the illuminance distribution at the workspace plane can be accurately inferred from the illuminance levels at the light sensors. Under these constraints, the problem is how to find the dimming levels of LED-based luminaires in distributed smart lighting systems with limited neighborhood communication capabilities so as to limit power consumption while satisfying minimum illuminance level constraints at the light sensors at the ceiling. Here, a near-optimum solution to the linear programming problem is presented. A detailed analysis of the solution is presented where bounds for optimality and stability are obtained. The content of Chapter 5 is published in [41].

Chapter 6 addresses the sixth subgoal in this thesis. This chapter assumes limited knowledge of the relationship between illuminance levels at the light

sensor at the ceiling and the corresponding illuminance levels at the workspace plane, i.e. coarse knowledge of the illuminance levels at the workspace plane is available. In this chapter, distributed smart lighting systems for large-sized spaces based on Type-I architecture with communication between neighboring controllers and light sensors at the ceiling are considered. Here, emphasis is given to guaranteeing a minimum illuminance level at the workspace plane for the considered architecture while adapting to available daylight and occupancy information. We propose a method that uses illuminance measurements at the light sensor and prior information from the calibration phase to achieve minimum illuminance levels at the workspace plane. The content of Chapter 6 is published in [42].

Chapter 7 addresses the seventh and last subgoal in this thesis. This chapter focuses on methods for estimating and tracking the illumination gains. The tracking of the illumination gains is required because they depend on the characteristics of the environment, e.g. a change in furniture may change the illumination gains. The illumination gains are important for the proper functioning of the described lighting control algorithms. We develop methods for estimating and tracking the illumination gains. The estimation problem is formulated as the solution of a system of linear equations generated by blinking the luminaires in the lighting system using semi-orthogonal dimming sequences and measuring the corresponding illuminance levels at light sensors. Furthermore, an analysis of desired properties of these sequences is presented. We consider distributed smart lighting systems for large-sized spaces with a communication channel between neighboring controllers and light sensors at the ceiling. The proposed method is also applicable when the light sensors are placed at the desks. The content of this chapter has been submitted as [43].

Finally, Chapter 8 summarizes the conclusions and results of this thesis. In this chapter, we also discuss future research challenges and directions.

1.6 Publications of the author

1.6.1 Journal Publications

1. D. Caicedo, A. Pandharipande, and M.C.J.M. Vissenberg, “Smart modular lighting control system with dual-beam luminaires”, *Lighting Research and Technology*, Accepted, 2014.
2. N. van de Meughevel, A. Pandharipande, D. Caicedo and P.P.J. van den Hof, “Distributed lighting control with daylight and occupancy adaptation”, *Energy and Buildings*, vol. 75, pp. 321 – 329, June 2014.
3. D. Caicedo, A. Pandharipande, and F. M. J. Willems, “Daylight-adaptive lighting control using light sensor calibration prior-information”, *Energy and Buildings*, vol. 73, pp. 105 – 114, April 2014.
4. D. Caicedo and A. Pandharipande, “Distributed ultrasonic zoned presence sensing system”, *IEEE Sensors Journal*, vol. 14, pp. 234 – 243, January 2014.
5. A. Pandharipande and D. Caicedo, “Adaptive illumination rendering in LED lighting systems,” *IEEE Transactions on Systems, Man, and Cybernetics–Part A: Systems and Humans*, vol. 43, pp. 1052 – 1062, May 2013.
6. D. Caicedo and A. Pandharipande, “Distributed illumination control with local sensing and actuation in networked lighting systems”, *IEEE Sensors Journal*, vol. 13, pp. 1092 – 1104, March 2013.
7. D. Caicedo and A. Pandharipande, “Ultrasonic arrays for localized presence sensing”, *IEEE Sensors Journal*, vol. 12, pp. 849–858, May 2012.
8. D. Caicedo, A. Pandharipande, and G. Leus, “Occupancy-based illumination control of LED lighting systems”, *Lighting Research and Technology*, vol. 43, pp. 217 – 234, June 2011.
9. A. Pandharipande and D. Caicedo, “Daylight integrated illumination control of LED systems based on enhanced presence sensing”, *Energy and Buildings*, vol. 43, pp. 944 – 950, April 2011.

1.6.2 Conference Publications

1. D. Caicedo, A. Pandharipande, and F. M. J. Willems, “Illumination gain estimation and tracking in a distributed lighting system,” *Submitted to IEEE Multi-Conference on Systems and Control*, 2014.
2. D. Caicedo, A. Pandharipande, and F. M. J. Willems, “Light sensor calibration and dimming sequence design in distributed lighting control systems,” *IEEE International Conference on Networking, Sensing and Control*, 2014.
3. D. Caicedo, A. Pandharipande, and F. M. J. Willems, “Detection performance analysis of an ultrasonic presence sensor,” *IEEE International Conference on Acoustics, Speech and Signal Processing*, pp. 2780 – 2784, 2013.
4. D. Caicedo and A. Pandharipande, “Daylight estimation in a faulty light sensor system for lighting control,” *IEEE International Conference on Information Fusion*, pp. 617 – 622, 2013.
5. D. Caicedo and A. Pandharipande, “Transmission slot allocation and synchronization protocol for ultrasonic sensor systems,” *IEEE International Conference on Networking, Sensing and Control*, pp. 288 – 293, 2013.
6. D. Caicedo and A. Pandharipande, “Ultrasonic array sensor for indoor presence detection,” *IEEE European Conference on Signal Processing*, pp. 175 – 179, 2012.
7. H. Wang, A. Pandharipande, D. Caicedo, and P. van den Bosch, “Distributed lighting control of locally intelligent luminaire systems,” *IEEE International Conference on Systems, Man, and Cybernetics*, pp. 3167 – 3172, 2012.
8. D. Caicedo and A. Pandharipande, “User localization using ultrasonic presence sensing systems,” *IEEE International Conference on Systems, Man, and Cybernetics*, pp. 3191 – 3196, 2012.

1.6.3 Other Publications

1. S. Srinivasan, A. Pandharipande, and D. Caicedo, “Presence detection using wideband audio-ultrasound sensor,” *IEEE Electronic Letters*, vol. 48, pp. 1577 – 1578, 2012.

1.6.4 Patents Applications

1. A. Pandharipande, D. Caicedo and M. Klompenhouwer, “Calibrating a light sensor”, WO/2014/057372.
2. A. Pandharipande and D. Caicedo, “Control of lighting devices”, WO/2013/171645.
3. T.J.J. Denteneer, O. Garcia, A. Pandharipande and D. Caicedo, “Failure detection in lighting system”, WO/2013/160791.
4. D. Caicedo, W. F. Pasveer, J. Matovina, S. M. A. T. Klein, J. M. Vangeel, R. P. A. Delnoij, W. J. Rietmann, A. Pandharipande, N. B. K. Sreedharan and G. B. Neuttiens, “Interference detection in a network of active sensors”, WO/2013/140303.
5. J. M. Vangeel, W. J. Rietman, R. P. A. Delnoij, W. F. Pasveer, J. Matovina, D. Caicedo and S. M. A. T. Klein, “Robust presence detection through audible components analysis”, WO/2013/108229.
6. A. Pandharipande and D. Caicedo, “Control unit and method for lighting control”, WO/2013/014582.
7. A. Pandharipande and D. Caicedo, “Methods for disaggregated sensing of artificial light and daylight distribution”, WO/2012/063149.
8. A. Pandharipande and D. Caicedo, “System and method for lighting control”, WO/2011/151796.
9. A. Pandharipande and D. Caicedo, “Configuration unit and method for configuring a presence detection sensor”, WO/2011/151772.
10. A. Pandharipande and D. Caicedo, “Lighting control information based analytics”, filed.
11. A. Pandharipande and D. Caicedo, “Method for slot synchronization in a distributed active presence sensing system”, filed.
12. A. Pandharipande and D. Caicedo, “Sensing protocols for multi-modal sensor systems”, filed.
13. A. Pandharipande, D. Caicedo and S. Srinivasan, “Protocols for managing cross-interference in active sensing systems”, filed.

REFERENCES

- [1] Energy Information Administration, “Commercial buildings energy consumption survey,” 2003.
- [2] Life-Cycle Assessment of Energy and Environmental Impacts of LED Lighting Products. Part 2: LED Manufacturing and Performance, http://apps1.eere.energy.gov/buildings/publications/pdfs/ssl/2012_led_lca-pt2.pdf, 2012.
- [3] J. A. Veitch, G. R. Newsham, P. R. Boyce, and C. C. Jones, “Lighting appraisal, well-being and performance in open-plan offices: A linked mechanisms approach,” *Lighting Research and Technology*, vol. 40, no. 2, pp. 133–151, 2008.
- [4] European Committee for Standardization, “EN 12464-1:2002. Light and lighting. Lighting of work places. Part 1: Indoor work places,” 2002.
- [5] D. Caicedo, “Illumination control of an LED lighting system based on localized occupancy,” Msc. thesis, TUDelft, 2010.
- [6] A. Williams, B. Atkinson, K. Garbesi, E. Page, and F. Rubinstein, “Lighting controls in commercial buildings,” *LEUKOS, The Journal of the Illuminating Engineering Society of North America*, vol. 8, no. 30, pp. 161 – 180, January 2012.
- [7] Vishay, <http://www.vishay.com/photo-detectors/ambient-light-sensor/>.
- [8] Philips, http://www.philipslightingcontrols.com/assets/cms/uploads/files/Controls_Quick_Guide_PA-7100-C_v5_web.pdf.
- [9] Lutron, <http://www.lutron.com/en-US/Products/Pages/Sensors/Occupancy-Vacancy/Occupancy.aspx>.
- [10] A. R. Kaushik and B. G. Celler, “Characterization of passive infrared sensors for monitoring occupancy pattern,” *IEEE Conference on Engineering in Medicine and Biology Society*, pp. 5257 – 5260, 2006.
- [11] X. Guo, D. K. Tiller, G. P. Henze, and C. E. Waters, “The performance of occupancy-based lighting control systems: A review,” *Lighting research and technology*, vol. 42, no. 4, pp. 415–431, 2010.
- [12] D. Caicedo and A. Pandharipande, “Ultrasonic arrays for localized presence sensing,” *IEEE Sensors Journal*, pp. 849–858, May 2012.

-
- [13] A. Lin and H. Ling, “Doppler and direction-of-arrival (DDOA) radar for multiple-mover sensing,” *IEEE Transactions on Aerospace and Electronic Systems*, pp. 1496 – 1509, 2007.
- [14] J. M. A. G. Yarovoy, L. P. Ligthart and B. Levitas, “UWB radar for human being detection,” *IEEE Aerospace and Electronic Systems Magazine*, pp. 10 – 14, 2006.
- [15] V. S. Nithya, K. Sheshadri, A. Kumar, and K. V. S. Hari, “Model based target tracking in a wireless network of passive infrared sensor nodes,” *IEEE International Conference on Signal Processing and Communications*, pp. 1–5, 2010.
- [16] Z. Zhang, X. Gao, J. Biswas, and J. K. Wu, “Moving targets detection and localization in passive infrared sensor networks,” *International Conference on Information Fusion*, pp. 1–6, 2007.
- [17] V. Takala and M. Petikainen, “Multi-object tracking using color, texture and motion,” *IEEE Conference on Computer Vision and Pattern Recognition*, 2007.
- [18] Y. Benezetha, H. Laurentb, B. Emilec, and C. Rosenbergerd, “Towards a sensor for detecting human presence and characterizing activity,” *Energy and Buildings*, vol. 43, pp. 305–314, 2011.
- [19] Knowles, http://www.knowles.com/search/prods_pdf/SPM0404UD5.PDF.
- [20] Prowave, <http://www.prowave.com.tw/pdf/T400ep14d.PDF>.
- [21] A. C. N. B. Priyantha and H. Balakrishnan, “The Cricket location-support system,” *Annual Conference on Mobile Computing and Networking*, pp. 32–43, 2000.
- [22] F. Zhang, J. Chen, H. Li, Y. Sun, and X. Shen, “Distributed active sensor scheduling for target tracking in ultrasonic sensor networks,” *ACM Mobile Networks and Applications*, 2011.
- [23] S. Srinivasan and A. Pandharipande, “Self-configuring time-slot allocation protocol for ultrasonic sensor systems,” *IEEE Sensors Journal*, 2013.
- [24] I. Moreno, “Creating a desired lighting pattern with an LED array,” *SPIE*, 2008.

- [25] M. Miki, A. Amamiya, and T. Hiroyasu, “Distributed optimal control of lighting based on stochastic hill climbing method with variable neighborhood,” *IEEE International Conference on Systems, Man and Cybernetics*, pp. 1676–1680, 2007.
- [26] S. Tanaka, M. Miki, A. Amamiya, and T. Hiroyasu, “An evolutionary optimization algorithm to provide individual illuminance in workplaces,” *IEEE International Conference on Systems, Man and Cybernetics*, pp. 941–947, 2009.
- [27] M.-S. Pan, L.-W. Yeh, Y.-A. Chen, Y.-H. Lin, and Y.-C. Tseng, “A WSN-based intelligent light control system considering user activities and profiles,” *IEEE Sensors Journal*, pp. 1710–1721, 2008.
- [28] S. Boyd and L. Vandenberghe, *Convex Optimization*. Cambridge University Press, 2004.
- [29] Y.-J. Wen and A. Agogino, “Control of wireless-networked lighting in open-plan offices,” *Lighting research and technology*, vol. 43, no. 2, pp. 235–248, 2010.
- [30] M. Fischer, W. Kui, and P. Agathoklis, “Intelligent illumination model-based lighting control,” *International Conference on Distributed Computing Systems Workshops*, pp. 245 – 249, 2012.
- [31] S. Escuyer and M. Fontoynt, “Lighting controls: a field study of office workers reactions,” *Lighting Research and Technology*, vol. 33, no. 2, p. 7796, 2001.
- [32] C. Villa and R. Labayrade, “Multi-objective optimisation of lighting installations taking into account user preferences: a pilot study,” *Lighting research and technology*, vol. 45, no. 2, pp. 176–196, 2012.
- [33] H. Wang, A. Pandharipande, D. Caicedo, and P. P. J. van den Bosch, “Distributed lighting control of locally intelligent luminaire systems,” *IEEE Conference on Systems, Man and Cybernetics*, 2012.
- [34] Y.-W. Bai and Y.-T. Ku, “Automatic room light intensity detection and control using a microprocessor and light sensors,” *IEEE Transactions on Consumer Electronics*, vol. 54, no. 3, pp. 1173 – 1176, 2008.
- [35] D. Caicedo and A. Pandharipande, “Distributed ultrasonic zoned presence sensing system,” *IEEE Sensors Journal*, vol. 14, pp. 234 – 243, January 2014.

-
- [36] D. Caicedo and A. Pandharipande, “Ultrasonic array sensor for indoor presence detection,” *European Conference on Signal Processing*, pp. 175 – 179, 2012.
- [37] D. Caicedo, A. Pandharipande, and F. M. J. Willems, “Detection performance analysis of an ultrasonic presence sensor,” *International Conference on Acoustics, Speech and Signal Processing*, pp. 2780 – 2784, 2013.
- [38] D. Caicedo and A. Pandharipande, “Transmission slot allocation and synchronization protocol for ultrasonic sensor systems,” *IEEE International Conference on Networking, Sensing and Control*, pp. 288 – 293, 2013.
- [39] A. Pandharipande and D. Caicedo, “Daylight integrated illumination control of LED systems based on enhanced presence sensing,” *Energy and Buildings*, vol. 43, pp. 944–950, April 2011.
- [40] A. Pandharipande and D. Caicedo, “Adaptive illumination rendering in LED lighting systems,” *IEEE Transactions on Systems, Man, and Cybernetics–Part A: Systems and Humans*, vol. 43, no. 5, pp. 1052 – 1062, May 2013.
- [41] D. Caicedo and A. Pandharipande, “Distributed illumination control with local sensing and actuation in networked lighting systems,” *IEEE Sensors Journal*, vol. 13, pp. 1092 – 1104, March 2013.
- [42] D. Caicedo, A. Pandharipande, and F. M. J. Willems, “Daylight-adaptive lighting control using light sensor calibration prior-information,” *Energy and Buildings*, vol. 73, pp. 105 – 114, April 2014.
- [43] D. Caicedo, A. Pandharipande, and F. M. J. Willems, “Illumination gain estimation and tracking in a distributed lighting system,” *Submitted to IEEE Multi-Conference on Systems and Control*, 2014.

Chapter 2

Distributed granular occupancy sensing*

We present a zoned presence detection system using multiple ultrasonic array sensors. In active mode, sensors transmit consecutive bursts of sinusoidal pulses over a transmission slot in a time-division multiplexed manner. We present a transmission slot synchronization method to maintain assigned transmission slots of each sensor. The proposed method is distributed and does not rely on a central coordinator or unique identifiers for the sensors. In a transmission slot, the corresponding receiver array uses moving target processing on received echoes to derive range and direction-of-arrival, defining a zone. A tracking algorithm is used to make the zoned presence detection more robust. The presented methods are evaluated using ceiling-installed ultrasonic linear array sensors in an experimental office setup.

*This chapter has been published as: D. Caicedo and A. Pandharipande, “Distributed ultrasonic zoned presence sensing system”, *IEEE Sensor Journal*, vol. 14, pp. 234 – 243, January 2014.

2.1 Introduction

Ultrasonic sensors are attractive for indoor presence detection since they offer improved sensitivity over larger detection ranges as compared to passive infrared sensors [1] at comparable costs. Continuous-wave Doppler ultrasonic sensors are already used for indoor occupancy-adaptive lighting control; user presence is derived from induced Doppler frequency shifts and used to turn on or off the lighting system. However these Doppler ultrasonic sensors like passive infrared sensors only provide binary information on occupancy state. It is known that additional energy savings may be realized by exploiting granular occupancy information [2], [3]. Fine-grained spatial occupancy can be used to achieve granular dimming in a lighting system [2] by adapting dimming levels of individual luminaires based on local occupancy conditions. Further, such information may be used to create occupancy maps [4] and analyze spatial movement patterns. Towards achieving fine-grained occupancy, we present a distributed system with multiple pulsed ultrasonic array sensors. Each ultrasonic array sensor determines occupancy in zones within its sensing region; multiple such sensors are used to achieve fine-grained spatial sensing over a large space.

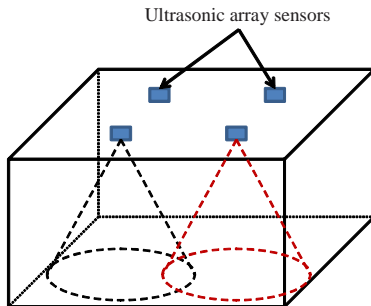


Figure 2.1: Ultrasonic array sensor system

We consider a system with N ultrasonic array sensors deployed in an indoor space as depicted in Fig. 2.1. Each ultrasonic array sensor has a broad-beam transmitter with center frequency f_c and a co-located linear array of M receiver elements, with half-wavelength inter-element separation. Each sensor monitors a region that partially overlaps with sensing regions of neighboring sensors. Overlapping sensing regions are required in practice to avoid blind spots, where the occupant is present but not detected due to insufficient sensor coverage. The transmission principle of the ultrasonic array sensor is as follows [3], [5], [6]. The transmitted waveform consists of two consecutive bursts with each containing

sinusoidal pulses of duration T followed by a quiet period that is of duration large enough so as to receive all echoes from within the sensing region. Echoes are processed at the receiver array to derive presence-related information. In [5], a prototype of a linear array sensor was presented for use in lighting control applications. For a wall-mounted configuration, receiver algorithms were developed for occupant localization in [3]. In [6], low-complexity algorithms were presented for improved presence detection in a ceiling-mounted sensor configuration. These works considered the operation of a single ultrasonic array sensor.

Given multiple active ultrasonic sensors, it is necessary to coordinate the different transmission bursts. In the absence of coordination, received echoes corresponding to transmissions from different sensors cannot be properly distinguished at a receiver array sensor, resulting in degraded detection performance. There are different approaches to coordinating multiple active transmissions. Assigning different frequencies or using coded waveforms is difficult due to limited bandwidth of commercially-available ultrasonic transmitters and limited receiver processing complexity, respectively. As such, we choose coordination in time by seeking a transmission slot assignment such that ultrasonic sensors within listening range are assigned distinct transmission slots. It is further necessary to maintain synchronization of the transmission slots given that clocks exhibit drifts in practice. We present a solution for transmission slot assignment and synchronization for a distributed ultrasonic system. We assume no central coordinator, no explicit communication and no use of sensor identifiers.

The problem of cross-interference management in ultrasonic sensor networks has been considered in [7], where an RF-ultrasonic system for location-based services is considered, and in [8], for target-tracking sensor network applications. In [7], identifiers over the RF signal are used to minimize interference amongst ultrasonic transmissions. The scheduling scheme in [8] involves explicit messaging among the sensors to determine transmission slots. Within the wireless sensor network field, the problem of distributed clock synchronization has been studied. An extensive survey on time synchronization methods for wireless sensor networks can be found in [9]. The distributed protocol in [10] extends the well-known network time protocol to sensor networks, and assumes that each sensor has a unique identifier and can explicitly message across a set of neighboring sensor nodes. The synchronization protocol in [11] involves sensors sending beacon messages using the network's physical layer broadcast and the arrival time is used as a reference for clock synchronization. A distributed synchronization protocol based on consensus was presented in [12], and relies on accurate timestamps. The distributed contention-free slot allocation protocol [13] also relies on exchanging information on transmission start times. In [14], a distributed

transmission slot assignment protocol, assuming perfect sensor synchronization, was presented.

In this paper, we consider a distributed synchronization protocol for maintaining transmission slot assignment in ultrasonic array sensors. This protocol comprises four phases: pre-synchronization, transmission slot assignment, post-synchronization and cross-check. During the first phase, a sensor not actively transmitting synchronizes with all sensors within its listening range by correlating all the echoes received within the current transmission cycle with all the echoes received in a previous transmission cycle. This phase ends when the synchronization is within the desired accuracy. Then the sensor seeks for a free transmission slot and begins to actively transmit its waveform. In the third phase, an active sensor maintains its synchronization with all sensors within listening range by correlating the echoes from a chosen transmission slot across multiple transmission cycles. The chosen transmission slot is alternated at each transmission cycle. Finally, an active sensor verifies that no neighboring sensor is transmitting at the same transmission slot by randomly skipping its transmission at a given cycle. If no overlapping transmissions are present, then no echo would be received during the respective transmission slot in this cycle. Otherwise, the active sensors seeks for a new transmission slot. This protocol thus simplifies the post-synchronization phase of the protocol presented in our earlier work [15]. We also analyze the protocol design in detail in this paper.

Finally, we describe the receiver processing for zoned presence detection. Range information, extracted from time of flight, and angular information, derived using a direction-of-arrival (DoA) beamformer, are used to define zones. We then obtain power levels in a zone using moving target detection in the received echoes corresponding to consecutive transmission bursts. A tracking vector is constructed using signal power levels in the zones and updated based on a human movement model. We use a linear receiver array to illustrate the presented principles and show performance results in an experimental setup.

2.2 Transmission slot allocation and synchronization

To allow the coexistence of multiple ultrasound array sensors, we propose allocating non-overlapping transmission slots to sensors within listening range. Each transmission slot is of duration $2T_s + \Delta T$, so it can accommodate the transmitted waveform ($2T_s$) and a safe gap (ΔT) to avoid overlapping with the previous transmission slot; this will be discussed further later in this section.

For simplicity of exposition, we assume that all sensors are within listening range of each other. Thus N transmission slots, of duration $2T_s + \Delta T$, would be

2.2. TRANSMISSION SLOT ALLOCATION AND SYNCHRONIZATION

required and so each sensor transmits its waveform over a slot after a cycle of duration $N(2T_s + \Delta T)$.

Further, we assume that each sensor has knowledge of N and the transmission slot duration $2T_s + \Delta T$. Sensor n listens in cycle k over a duration $[t_{0,n}^{(k)}, t_{0,n}^{(k)} + N(2T_s + \Delta T)]$, where $t_{0,n}^{(k)}$ is the beginning of the k -th cycle. Let sensor n have a time drift τ_n after each cycle, due to limited accuracy in its local clock. Hence, the k -th cycle of sensor n begins at time

$$t_{0,n}^{(k)} = t_{0,n}^{(k-1)} + \Upsilon_n,$$

where $\Upsilon_n = N(2T_s + \Delta T) + \tau_n$ is the cycle repetition interval of sensor n . The differences in τ_n , $n = 1, \dots, N$, cause the assigned transmission slots between sensors to be misaligned with time (see Fig. 2.2).

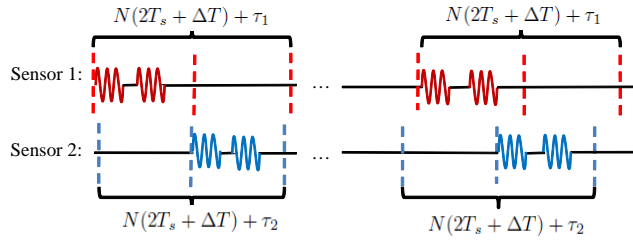


Figure 2.2: Misalignment of transmission slots due to local clock drifts for $N = 2$ sensors.

2.2.1 Pre-processing

Let the received signal during the k -th cycle at the m -th receiver of sensor n be given by $u_{m,n}^{(k)}(\tilde{t})$, where \tilde{t} is the relative time with respect to the beginning of the pulse during the k -th cycle. Hence, sensor n receives the echoes from its own transmission within the time interval $\tilde{t} \in [\Delta T, 2T_s + \Delta T)$ (the time interval $\tilde{t} \in [0, \Delta T)$ corresponds to the safe gap).

Let us recall that sensor n would received echoes from all active sensors within listening range. Hence, $u_{m,n}^{(k)}(\tilde{t})$ can be rewritten as the summation of all the echoes originating from static and moving objects due to the active transmission of each sensor, i.e.

$$u_{m,n}^{(k)}(\tilde{t}) = \sum_{i=1}^N \left[s_{m,n,i}^{(k)}(\tilde{t}) + w_{m,n,i}^{(k)}(\tilde{t}) \right], \quad (2.1)$$

where $s_{m,n,i}^{(k)}(\tilde{t})$ and $w_{m,n,i}^{(k)}(\tilde{t})$ are the received echoes originating from static and moving objects, respectively, at receiver m of sensor n due to active transmission of sensor i during the k -th cycle.

The received signal $u_{m,n}^{(k)}(\tilde{t})$ is at frequency f_c and is continuous, so we need to pre-process it. The pre-processing comprises digitizing, filtering and down-mixing the signal to zero frequency. Let the sampling rate for digitizing the signal be f_s and the number of samples over which the signal is filtered be Γ . We will refer to each filtered group of samples as a range-bin $\rho = 1, \dots, 2NR + N\bar{R}$, where

$$\begin{aligned} R &= \left\lfloor \frac{T_s f_s}{\Gamma} \right\rfloor \text{ and} \\ \bar{R} &= \left\lfloor \frac{\Delta T f_s}{\Gamma} \right\rfloor. \end{aligned}$$

Let the pre-processed signal at range-bin ρ and receiver m of sensor n be given by

$$\begin{aligned} \hat{u}_{m,n}^{(k)}(\rho) &= \frac{1}{\Gamma} \sum_{\nu=(\rho-1)\Gamma+1}^{\rho\Gamma} u_{m,n}^{(k)}\left(\frac{\nu}{f_s}\right) \times e^{-2\pi j \frac{\nu f_c}{f_s}}, \\ m &= 1, 2, \dots, M, \\ n &= 1, 2, \dots, N, \\ \rho &= 1, 2, \dots, 2NR + N\bar{R} \end{aligned}$$

and under (2.1) we can also write

$$\hat{u}_{m,n}^{(k)}(\rho) = \sum_{i=1}^N \left[\hat{s}_{m,n,i}^{(k)}(\rho) + \hat{w}_{m,n,i}^{(k)}(\rho) \right],$$

where

$$\begin{aligned} \hat{s}_{m,n,i}^{(k)}(\rho) &= \frac{1}{\Gamma} \sum_{\nu=(\rho-1)\Gamma+1}^{\rho\Gamma} s_{m,n,i}^{(k)}\left(\frac{\nu}{f_s}\right) \times e^{-2\pi j \frac{\nu f_c}{f_s}}, \\ \hat{w}_{m,n,i}^{(k)}(\rho) &= \frac{1}{\Gamma} \sum_{\nu=(\rho-1)\Gamma+1}^{\rho\Gamma} w_{m,n,i}^{(k)}\left(\frac{\nu}{f_s}\right) \times e^{-2\pi j \frac{\nu f_c}{f_s}}, \\ m &= 1, 2, \dots, M, \\ n &= 1, 2, \dots, N, \\ i &= 1, 2, \dots, N, \\ \rho &= 1, 2, \dots, 2NR + N\bar{R} \end{aligned}$$

are the downmixed and sampled signal originated from static and moving objects, respectively.

2.2.2 Pre-synchronization

During the pre-synchronization phase, a sensor which does not have an assigned transmission slot (i.e. is not actively transmitting), first synchronizes its clock to all its actively transmitting neighbors using a set of synchronization vectors. Let

$$\mathbf{p}_{m,n}^{(k)} = \left[p_{m,n}^{(k)}(1) \quad \dots \quad p_{m,n}^{(k)}(2NR + N\bar{R}) \right]^T \quad (2.2)$$

be the synchronization vector at cycle k , where

$$p_{m,n}^{(k)}(\rho) = \begin{cases} \frac{|\hat{u}_{m,n}^{(k)}(\rho)|}{\sqrt{U_{m,n}(\rho)}} & , \text{ if } U_{m,n}(\rho) \geq C_0 \sigma_{m,n}^2 \\ 0 & , \text{ otherwise,} \end{cases}$$

$$U_{m,n}(\rho) = \sum_{\gamma=r+1}^{r+2R+\bar{R}} \left| \hat{u}_{m,n}^{(k)}(\gamma) \right|^2$$

and $r = \left\lfloor \frac{\rho-1}{2R+\bar{R}} \right\rfloor (2R + \bar{R})$. The term $U_{m,n}(\rho)$ is a normalization factor, $\sigma_{m,n}^2$ is the power noise level measured at receiver element m of sensor n during those instances when no signal is received and $C_0 > 1$ is a thresholding factor.

We assume that the received signal at a given range-bin ρ^* is dominated by the received echoes of static objects due to the transmission of a given sensor [15], i^* , i.e.

$$\hat{s}_{m,n,i}^{(k)}(\rho^*) \ll \hat{s}_{m,n,i^*}^{(k)}(\rho^*), \quad \forall i, i \neq i^* \text{ and} \quad (2.3)$$

$$\hat{w}_{m,n,i}^{(k)}(\rho^*) \ll \hat{s}_{m,n,i^*}^{(k)}(\rho^*), \quad \forall i. \quad (2.4)$$

Also, the received echoes $\hat{s}_{m,n,i}^{(k)}(\rho)$ at range-bin ρ and transmission cycle k can be related to the received echoes at a shifted range-bin during the reference [15] (e.g. cycle 0) by

$$\hat{s}_{m,n,i}^{(k)}(\rho) \approx \hat{s}_{m,n,i}^{(0)}\left(g\left(\rho + \delta\rho_{n,i}^{(k)}\right)\right), \quad (2.5)$$

where

$$g(\rho) = \begin{cases} \rho - 2NR - N\bar{R} & , \text{ if } \rho > 2NR + N\bar{R} \\ \rho & , \text{ if } 1 \leq \rho \leq 2NR + N\bar{R} \\ \rho + 2NR + N\bar{R} & , \text{ if } \rho < 1, \end{cases}$$

$$\delta\rho_{n,i}^{(k)} = \left\lfloor \frac{f_s}{\Gamma} \Delta\tau_{n,i}^{(k)} \right\rfloor$$

and $\Delta\tau_{n,i}^{(k)}$ is the relative time drift between sensor n and sensor i at transmission cycle k with respect to the reference.

Hence, under assumptions (2.3), (2.4) and (2.5), we can write the ρ -th element of the synchronization vector at receiver m of sensor n during cycle k as

$$\begin{aligned} p_{m,n}^{(k)}(\rho) &\approx \sum_{i=1}^N \frac{|\hat{s}_{m,n,i}^{(k)}(\rho)|}{\sqrt{\sum_{\gamma} |\hat{s}_{m,n,i}^{(k)}(\gamma)|^2}} \\ &\approx \sum_{i=1}^N \frac{|\hat{s}_{m,n,i}^{(0)}(g(\rho + \delta\rho_{n,i}^{(k)}))|}{\sqrt{\sum_{\gamma} |\hat{s}_{m,n,i}^{(0)}(\gamma)|^2}} \end{aligned} \quad (2.6)$$

and during the reference cycle as

$$p_{m,n}^{(0)}(\rho) \approx \sum_{i=1}^N \frac{|\hat{s}_{m,n,i}^{(0)}(\rho)|}{\sqrt{\sum_{\gamma} |\hat{s}_{m,n,i}^{(0)}(\gamma)|^2}}.$$

Therefore, the relative time drift $\Delta t_n^{(k)}$ at transmission cycle k of sensor n with respect to a reference cycle can be obtained as

$$\Delta t_n^{(k)} = \Delta\rho_n^* \frac{\Gamma}{f_s}, \quad (2.7)$$

where $\Delta\rho_n^*$ is the value that maximizes the sum over all receivers of the cross-correlation between the synchronization vectors at cycle k and the reference cycle, i.e.

$$\Delta\rho_n^* = \arg \max_{\Delta\rho_n} \sum_{m=1}^M \sum_{\rho=1}^{2NR+N\bar{R}} p_{m,n}^{(k)}(\rho) p_{m,n}^{(0)}(g(\rho + \Delta\rho_n)). \quad (2.8)$$

Next, sensor n builds a history with the estimated relative time drift obtained from (2.7) during K consecutive transmission cycles. At the (κK) -th cycle, the history of relative time shifts has been completed and the estimated relative time drifts are fitted using linear regression, where the slope $\Delta c_n^{(\kappa)}$ indicates the relative time drift with respect to the reference and the height $\Delta o_n^{(\kappa)}$ indicates the current time offset with respect to the reference (e.g. cycle 0) [15].

2.2. TRANSMISSION SLOT ALLOCATION AND SYNCHRONIZATION

The beginning time of the k -th transmission cycle of sensor n is shifted by

$$t_{0,n}^{(k+1)} = \begin{cases} t_{0,n}^{(k)} + \Upsilon_n - \Delta\tilde{\tau}_n^{(k)} - \Delta o_n^{(\kappa)} & , \text{ if } k = \kappa K \\ t_{0,n}^{(k)} + \Upsilon_n - \Delta\tilde{\tau}_n^{(k)} & , \text{ otherwise,} \end{cases} \quad (2.9)$$

and the correction term is updated by

$$\Delta\tilde{\tau}_n^{(k+1)} = \begin{cases} \Delta\tilde{\tau}_n^{(k)} + \lambda_0 \Delta c_n^{(\kappa)} & , \text{ if } k = \kappa K \\ \Delta\tilde{\tau}_n^{(k)} & , \text{ otherwise,} \end{cases}$$

where $\kappa = \lfloor \frac{k}{K} \rfloor$ and $\lambda_0 \geq 0$ is an updating factor (See Appendix 2.A).

2.2.3 Transmission slot allocation

Let us assume that at cycle κ^*K , sensor n has achieved a good level of pre-synchronization with all its active neighbors (i.e. $|\Delta c_n^{(\kappa^*)}| \leq \epsilon$). Hence, sensor n proceeds to seek for a transmission slot of duration $2T_s + \Delta T$ within the cycle interval $[0, 2NT_s + N\Delta T)$. Sensor n begins its transmission slot at time

$$\tilde{t}_{0,n} = \frac{\Gamma}{f_s} (\rho_{0,n}^* - 1),$$

where $\tilde{t}_{0,n}$ is the relative time with respect to the beginning of the cycle and $\rho_{0,n}^* \in [1, 2NR + N\bar{R}]$ is chosen such that

$$\sum_{m=1}^M \left| \hat{u}_{m,n}^{(\kappa^*K)}(g(\rho)) \right|^2 < C_0 \sum_{m=1}^M \sigma_{m,n}^2, \quad \rho = \rho_{0,n}^*, \dots, \rho_{0,n}^* + 2R + \bar{R} - 1 \quad (2.10)$$

and

$$\sum_{m=1}^M \left| \hat{u}_{m,n}^{(\kappa^*K)}(g(\rho_{0,n}^* - 1)) \right|^2 > C_0 \sum_{m=1}^M \sigma_{m,n}^2. \quad (2.11)$$

Here, $\bar{R} > 0$ is a safe gap to ensure separation between active transmission of sensor n and active transmission of a neighboring sensor at the previous transmission slot. Sensor n begins its active transmission after the safe gap. Note that (2.10) ensures that a transmission free interval of at least a duration $2T_s + \Delta T$ is chosen, whereas (2.11) ensures that the assigned transmission slot is just after the end of transmission of a neighbor.

For simplicity, let us assume that sensor n shifts the beginning of its next cycle, $\kappa^*K + 1$, such that its transmission slot is at the beginning of the cycle, i.e.

$$t_{0,n}^{(\kappa^*K+1)} = t_{0,n}^{(\kappa^*K)} + \Upsilon_n - \Delta\tilde{\tau}_n^{(\kappa^*K)} + \tilde{t}_{0,n}.$$

2.2.4 Post-synchronization

Note that due to pre-processing, only relative time drifts larger than $\frac{\Gamma}{f_s}$ are detectable and can be compensated during the pre-synchronization phase. Hence, after a transmission slot has been allocated to sensor n , it requires to maintain a post-synchronization to cope with any residual time drift.

The complexity of the synchronization procedure used in Section 2.2.2 is further reduced by listening to only one neighboring transmission slot per cycle. Hence, every $(N - 1)\bar{k}$ cycles ($\bar{k} > 0$) we finish listening to all transmission slots and so we can estimate the relative time drift for sensor n with respect to all actively transmitting neighbors.

Denote

$$\bar{\mathbf{p}}_{m,n}^{(\bar{k})} = \left[\bar{p}_{m,n}^{(\bar{k})}(1) \quad \dots \quad \bar{p}_{m,n}^{(\bar{k})}(2NR + N\bar{R}) \right]^T \quad (2.12)$$

as the synchronization vector at cycle $(N - 1)\bar{k}$ of the post-synchronization phase.

At the k -th cycle ($k > \kappa^*K$), we update the entries of the synchronization vector (2.12) corresponding to the listened transmission slot, i.e.

$$\bar{p}_{m,n}^{(\bar{k})}(\rho) = \begin{cases} \frac{|\hat{u}_{m,n}^{(k)}(\rho)|}{\sqrt{U_{m,n}(\rho)}} & , \text{ if } U(\rho) \geq C_0\sigma_0^2 \\ 0 & , \text{ otherwise,} \end{cases} \quad (2.13)$$

where

$$\begin{aligned} \rho &\in [\bar{N}(2R + \bar{R}) + 1, (\bar{N} + 1)(2R + \bar{R})], \\ \bar{k} &= \left\lceil \frac{k - \kappa^*K}{N - 1} \right\rceil \text{ and} \\ \bar{N} &= k - \kappa^*K - (\bar{k} - 1)(N - 1). \end{aligned}$$

Note that the own transmission of sensor n does not provide any information of the relative time drift with respect to neighboring sensors and so it is excluded, i.e.

$$\bar{p}_{m,n}^{(\bar{k})}(\rho) = 0, \quad \rho \in [1, 2R + \bar{R}]. \quad (2.14)$$

Using the synchronization vector (2.12) with elements as defined in (2.13) and (2.14) we proceed to keep post-synchronization by estimating the relative time drift at each cycle $(N - 1)\bar{k}$ of sensor n with respect to a reference synchronization vector (e.g. $\bar{\mathbf{p}}_{m,n}^{(1)}$) following steps (2.7-2.8).

Further, the history is built during $\bar{K} = (N - 1)K$ consecutive transmission cycles. We modify the updating rule (2.9) to avoid that the chosen transmission

slot overlaps with the active transmission of a neighboring sensor in the previous transmission slot,

$$t_{0,n}^{(k+1)} = \begin{cases} t_{0,n}^{(k)} + \Upsilon_n - \Delta\tilde{\tau}_n^{(k)} + \beta_n^{(k)} - \Delta o_n^{(\bar{\kappa})} & , \text{ if } k = \bar{\kappa}\bar{K} \\ t_{0,n}^{(k)} + \Upsilon_n - \Delta\tilde{\tau}_n^{(k)} + \beta_n^{(k)} & , \text{ otherwise,} \end{cases}$$

where $\bar{\kappa} = \lfloor \frac{k}{(N-1)\bar{K}} \rfloor$ and

$$\beta_n^{(k)} = \begin{cases} 1 & , \text{ if } \sum_{m=1}^M \left| \hat{u}_{m,n}^{(k)}(\rho) \right|^2 > C_0 \sum_{m=1}^M \sigma_{m,n}^2, \\ & \rho = 1, \dots, \bar{R} \\ 0 & , \text{ otherwise.} \end{cases}$$

2.2.5 Cross-check

Sensor n verifies that no other sensor is actively transmitting with an overlapping slot by randomly skipping its transmission during a given cycle (e.g. cycle k^*) [15]. If we have that

$$\sum_{m=1}^M \left| \hat{u}_{m,n}^{(k^*)}(\rho) \right|^2 < C_0 \sum_{m=1}^M \sigma_{m,n}^2, \quad \rho = \bar{R} + 1, \dots, 2\bar{R} + \bar{R},$$

then sensor n is the only one transmitting. Otherwise, there is another sensor actively transmitting at the same transmission slot and so sensor n stops transmitting and repeats the procedures for pre-synchronization, discussed in Section 2.2.2, and transmission slot allocation, as detailed in Section 2.2.3.

2.3 Ultrasonic zoned presence sensing

At sensor n , we process the received signal corresponding to its active transmission. At each receiver element of sensor n , we obtain a difference signal by subtracting the received echoes (at zero frequency) corresponding to consecutive transmitted bursts. Zones are defined as pairs of group-range and DoA, and the power values in each zone using the difference signal is computed. A zone with observed movement is identified as one that has the largest signal-to-noise ratio (SNR) exceeding a pre-defined threshold. Finally, a tracking algorithm provides a score, related to the confidence of user movement in a zone, based on which zoned presence is determined.

2.3.1 Moving target indicator processing for movement detection

We limit the monitored region of sensor n to a maximum range D_0 (i.e. any occupant located at a distance larger than D_0 is considered to be out of the monitored region of sensor n). Hence, we only process those ranges within the interval $[1, R_0]$, where $R_0 = \left\lceil \frac{2D_0}{v_s} \right\rceil \leq R$. Note that any echo coming from a static object is the same for any two consecutive signals $\hat{u}_{m,n}^{(k)}(\rho + \bar{R})$ and $\hat{u}_{m,n}^{(k)}(\rho + R + \bar{R})$, $\rho = 1, 2, \dots, R_0$. Thus, if we calculate the difference signal for range-bin $\rho = 1, 2, \dots, R_0$,

$$\begin{aligned} \Delta u_{m,n}^{(k)}(\rho) &= \hat{u}_{m,n}^{(k)}(\rho + \bar{R}) - \hat{u}_{m,n}^{(k)}(\rho + R + \bar{R}) \\ &= \left[\hat{s}_{m,n,n}^{(k)}(\rho + \bar{R}) + \hat{w}_{m,n,n}^{(k)}(\rho + \bar{R}) \right] \\ &\quad - \left[\hat{s}_{m,n,n}^{(k)}(\rho + R + \bar{R}) + \hat{w}_{m,n,n}^{(k)}(\rho + R + \bar{R}) \right] \\ &= \hat{w}_{m,n,n}^{(k)}(\rho + \bar{R}) - \hat{w}_{m,n,n}^{(k)}(\rho + R + \bar{R}), \end{aligned}$$

then only those echoes coming from moving objects remain [3], [16].

We implement a low complexity algorithm for range and DoA estimation. We combine P consecutive range-bins into a single group-range. Let the group-range ζ comprise the range-bins $[(\zeta - 1)P + 1, \zeta P]$. Hence, we have

$$Z = \left\lceil \frac{R_0}{P} \right\rceil$$

group-ranges. We further monitor over a set of Q discrete steering angles,

$$\mathcal{A} = \{\Theta_1, \Theta_2, \dots, \Theta_Q\}.$$

We calculate the SNR of the received signal per group-range ζ and angle Θ_q as

$$F^{(k)}(\zeta, \Theta_q) = \frac{\sum_{\rho=(\zeta-1)P+1}^{\min\{R_0, \zeta P\}} \left| \mathbf{a}(\Theta_q)^H \Delta \mathbf{u}_n^{(k)}(\rho) \right|^2}{\sigma^2(\zeta, \Theta_q)}, \quad (2.15)$$

where

$$\Delta \mathbf{u}_n^{(k)}(\rho) = \left[\Delta u_{1,n}^{(k)}(\rho), \dots, \Delta u_{M,n}^{(k)}(\rho) \right]^T$$

and

$$\mathbf{a}(\Theta_q) = \left[1, e^{j\pi \sin(\Theta_q)}, \dots, e^{j\pi(M-1) \sin(\Theta_q)} \right]^T$$

is the response of the linear array to a signal coming from angle Θ_q [17]. Here, $\sigma^2(\zeta, \Theta_q)$ is the noise power level at location $\{\zeta, \Theta_q\}$. The noise power level is measured at periods when the room is unoccupied. The largest peak of (2.15) over all steering angles $\{\Theta_q\}$ at a given range ζ corresponds to the location of a possible occupant. Let the pair $\{\zeta, \Theta_{q^*}\}$ be the location with the largest SNR at range ζ .

We further decrease complexity by analyzing only those locations where a possible occupant is observed with high reliability. A possible occupant is observed at location $\{\zeta, \Theta_{q^*}\}$ with high reliability when

$$F^{(k)}(\zeta, \Theta_{q^*}) \geq C_d. \quad (2.16)$$

2.3.2 Zoning, tracking and detection rule

We implement a simple tracking algorithm to improve the performance of presence detection and zoning. We consider that an occupant's movement must satisfy some constraints on temporal motion continuity [18], i.e. the current zone of the occupant depends on the occupant's previous zone.

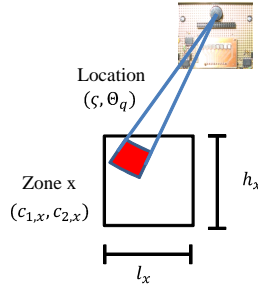


Figure 2.3: Division of the sensing region into zones; each location is mapped into a pre-defined zone.

We divide the sensed region into X zones along the scanning direction of the ultrasonic array sensor as shown in Fig. 2.3. Let \mathcal{L}_x be the set of locations $\{\zeta, \Theta_q\}$ with possible occupants during the k -th transmission belonging to zone x . The location $\{\zeta, \Theta_{q^*}\}$ that satisfies (2.16) belongs to zone x if

$$\begin{aligned} c_{2,x} - \frac{h_x}{2} &\leq \frac{(\zeta-1)P\Gamma}{f_s} \cos \Theta_{q^*} \leq c_{2,x} + \frac{h_x}{2} \text{ and} \\ c_{1,x} - \frac{l_x}{2} &\leq \frac{(\zeta-1)P\Gamma}{f_s} \sin \Theta_{q^*} \leq c_{1,x} + \frac{l_x}{2}, \end{aligned} \quad (2.17)$$

where $\{c_{1,x}, c_{2,x}\}$, h_x , l_x are the center coordinates, height and width of zone x , respectively. Further, let \mathcal{X} be the set of zones with possible occupants during the k -th transmission. Zone x belongs to \mathcal{X} if during the k -th transmission exists a location (ζ, Θ_{q^*}) such that (2.16) and (2.17) are satisfied.

We assign to each zone x , a score $\Psi_x^{(k)}$ to indicate the confidence that an occupant is present in zone x at transmission cycle k given its previous observed zones. This scores accumulates with each new observation from the occupant's zone.

Let $\Psi^{(k)}$ be the vector of size X with scores $\{\Psi_x^{(k)}\}$ during the k -th transmission. Each element in the score vector $\Psi^{(k)}$ depends on the previous score vector $\Psi^{(k-1)}$. Let us assume that an occupant during current transmission cycle k is observed at zone $x^* \in \mathcal{X}$, then the confidence that the occupant was at a given zone during previous transmission $k-1$ decreases monotonically with distance. This idea is captured by the function

$$f_1(x^* - x) = \begin{cases} 1 & , \quad \text{if } x^* - x = 0 \\ 0.5 & , \quad \text{if } |x^* - x| \leq \alpha_1 \\ 0 & , \quad \text{otherwise} \end{cases}$$

which indicates the confidence that the occupant was at zone x given that currently it is observed at zone $x^* \in \mathcal{X}$. Hence, we update the element $\Psi_{x^*}^{(k)}$, $x^* \in \mathcal{X}$, as follows

$$\Psi_{x^*}^{(k)} = G \left\{ \sum_{(\zeta, \Theta_{q^*}) \in \mathcal{L}_{x^*}} \frac{F^{(k)}(\zeta, \Theta_{q^*})}{C_d} + \max_x \left\{ \Psi_x^{(k-1)} f_1(x^* - x) \right\} \right\},$$

where $G\{\}$ is an operator that ensures that the tracking score is within a valid range $[0, \Omega]$.

Other elements of the score matrix (i.e. $x \notin \mathcal{X}$) are updated as follows

$$\Psi_x^{(k)} = G \left\{ \sum_{x^* \in \mathcal{X}} \sum_{(\zeta, \Theta_{q^*}) \in \mathcal{L}_{x^*}} \frac{F^{(k)}(\zeta, \Theta_{q^*})}{C_d} f_2(x^* - x) + \Psi_x^{(k-1)} - \beta \right\},$$

where

$$f_2(x^* - x) = \begin{cases} 1 & , \quad \text{if } x^* - x = 0 \\ 0.5 & , \quad \text{if } |x^* - x| \leq \alpha_2 \\ 0 & , \quad \text{otherwise,} \end{cases}$$

indicates the confidence that the occupant is at zone x given that it is observed at zone x^* .

In the case when no occupant is observed at current transmission cycle k (i.e. (2.16) is not satisfied), then all the elements of the score matrix are updated with

$$\Psi_x^{(k)} = \mathbf{G} \left\{ \Psi_x^{(k-1)} - \beta \right\}, \forall x.$$

The factors $\alpha_1 \geq 0$ and $\alpha_2 \geq 0$ are propagation factors and $0 < \beta \leq 1$ is a decreasing factor. The factor β ensures that those zones wherein no occupant is observed any longer decrease their tracking score with time.

When a score element in the vector $\Psi^{(k)}$ is larger than tracking threshold C_{Th} , then presence is declared in the whole region. Note that a larger value for C_{Th} corresponds to a larger delay for declaring presence in the whole region. Let us consider the scenario where the echoes of an occupant moving in the room have a SNR of C_d . Hence, we would require at least C_{Th} transmission cycles before detecting the occupant. On the other hand, a smaller C_{Th} corresponds to faster detection of an occupant. However, any sudden peak in the received power (e.g. due to air fluctuations) would trigger false alarms. Further, after presence is declared, the occupant is localized to a given zone when the tracking score in that zone is larger than a zoning threshold C_z . In a similar way, the zone is declared as unoccupied when the tracking score is below the zoning threshold C_z .

The whole region is declared as unoccupied when none of the scores exceed C_{Th} , i.e.

$$\Psi_x^{(k)} < C_{Th}, \quad x = 1, 2, \dots, X,$$

for a period larger than K_{Th} transmissions.

Note that presence is declared for at least K_{Th} transmissions and at most

$$\left\lceil \frac{\Omega}{\beta} \right\rceil + K_{th} \tag{2.18}$$

transmissions after the last occupant has left the room. Hence, the parameter K_{Th} has to be chosen larger than the expected maximum number of transmissions without detection of the occupant (i.e. no movement of the occupant). Furthermore, $\Omega > C_{Th}$ and $0 < \beta \leq 1$ are chosen such that (2.18) is within system requirements.

2.4 Performance evaluation

Experiments were performed in a typical office space of length 8 m and width 5 m, with the sensors ceiling-mounted at a height of about 3 m. In the first

experiment, we tested the performance of the transmission slot allocation and synchronization algorithm using $N = 4$ ultrasonic array sensors distributed in a 2 by 2 grid with a separation in length and width of 2.5 m. The location of the sensors labeled S1, S2, S3 and S4 were $(1.25, -1.25, 0)$, $(1.25, 1.25, 0)$, $(-1.25, -1.25, 0)$ and $(-1.25, 1.25, 0)$, respectively, where the origin was defined at the center of the ceiling.

For the second experiment, we evaluated the performance of the zoned presence sensing algorithm. In this experiment, we installed a single prototype ultrasonic array sensor, labeled S0, in a ceiling-mounted configuration situated at the origin.

Each ultrasonic sensor consists of a single transmitter and a co-located linear array of $M = 4$ receivers with inter-element separation of 4.3 mm. The transmitter was of model 400ST120 [19] at central frequency $f_c = 40$ kHz and bandwidth of 2 kHz. The receivers were of model SPM0404UD5 [20]. The parameters of the transmitted waveform were $T = 2$ ms, $T_s = 60$ ms and $\Delta T = 5$ ms. This choice of parameters is large enough so that echoes due to signal propagation from an active transmission die out, before an active transmission from a neighboring sensor ensues. Further, we limit the monitored area of each sensor to a maximum range $D_0 = 4$ m which is large enough for covering a typical work space within an open office. This choice of parameters corresponds to $R = 60$, $R_0 = 26$ and $\bar{R} = 5$ range-bins.

2.4.1 Transmission slot allocation and synchronization

During the experiment, all the ultrasonic sensors were connected to a single computer that provided a timing reference for comparison. Asynchronous behavior of the system was emulated by artificially adding a time drifts to each ultrasonic sensor. The artificial time drifts from sensors S1-S4 were respectively $\tau_1 = 0.813$ ms, $\tau_2 = -0.01$ ms, $\tau_3 = 0.15$ ms, and $\tau_4 = -0.23$ ms.

The noise power level is measured during the first cycles when there are no active transmissions. We consider that if the received power at a given instant of time is less than $C_0 = 2$ times the power noise level, then that instant of time is transmission free. The history of time drift is collected during $K = 20$ consecutive cycles before estimating a compensation factor. Further, we choose $\epsilon = 0.01$ ms/cycle as a good level of pre-synchronization.

We present the results over the performance of the transmission slot allocation and synchronization algorithm in Figs. 2.4 and 2.5. In Fig. 2.4, we show the difference between the beginning of the assigned transmissions of each ultrasonic sensor (S1-S4) with respect to S1 (i.e. $t_{0,n}^{(k)} - t_{0,1}^{(k)}$, $n = 1, \dots, 4$). It can be seen from Fig. 2.4 that the separation between the beginning of assigned transmissions

of each ultrasonic sensor is around 125 ms and it is kept over the duration of the whole experiment.

In Fig. 2.5 we can observe more details of the variations in the separation between the beginning of the assigned transmissions of S1 and S2 (i.e. synchronization). These variations are due to multipath effects and the presence of occupants in the room. Nevertheless, these variations do not result in overlapping of the assigned transmission slots. Finally, in Fig. 2.6, we show the standard deviation in the difference between the beginning of the transmissions of each ultrasonic sensor (S1-S4) averaged across other sensors. We show that the proposed method achieves performance comparable to the reference method of [15], at a lower complexity.

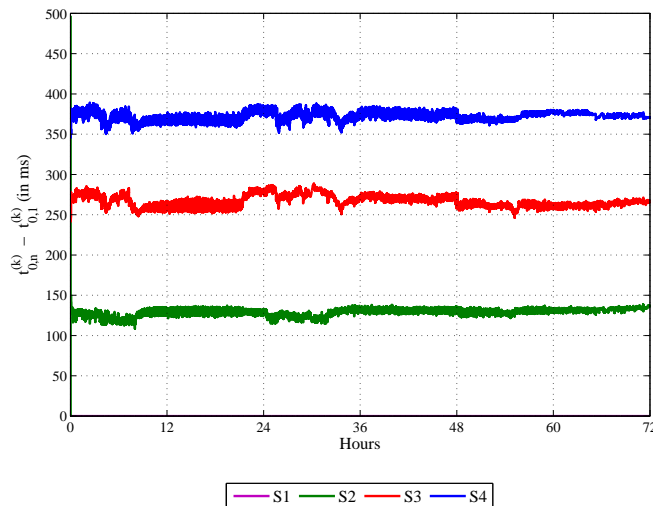


Figure 2.4: Synchronization results with respect to S1.

2.4.2 Zoned presence sensing

The design parameters in the receiver array processing are summarized in Table 2.1. We average the signal over $\Gamma = 200$ samples (i.e. 1 ms at sampling rate $f_s = 200$ kHz). This corresponds to filtering out all echoes with a Doppler frequency larger than 1 kHz (i.e. filter out all moving sources with a radial speed larger than 4 m/s). We further combine $P = 2$ consecutive ranges into a single group-range in order to decrease the complexity of the algorithm. A further simplification is achieved by monitoring 18 DoA angles.

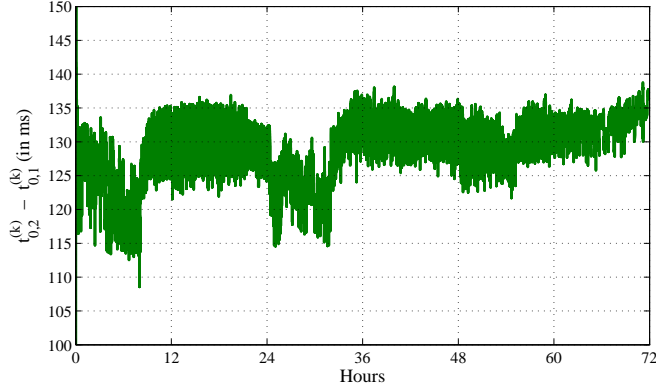


Figure 2.5: Synchronization results of S2 with respect to S1.

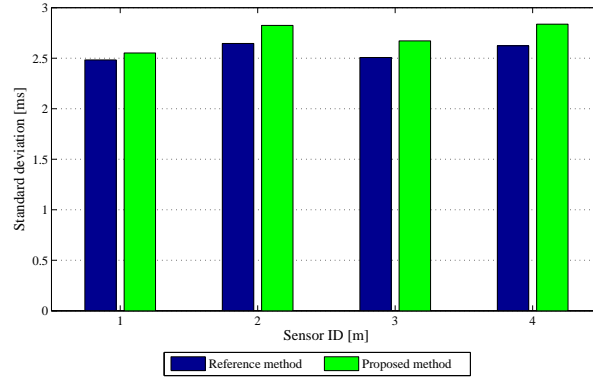


Figure 2.6: Comparison of standard deviation of proposed method and reference method.

We divide the sensed region into $X = 17$ zones. The x -th zone is centered at location $\{0.5x - 4.5, 2\}$. Using these parameter values, the tracking vector is reduced to size 17×1 . An occupant between consecutive transmissions can only change the position between adjacent zones ($\alpha_1 = 1$ zone).

We consider that an occupant is observed when the received power is at least $C_d = 5$ times the power noise level. Further, we require at least 3 consecutive observations of the occupant to declare a room as occupied ($C_{Th} = 3$) and a tracking score of $C_z = 200$ for localizing an occupant within a zone. Before

declaring a room as unoccupied, we require at least $K_{Th} = 600$ transmissions (around 20 s) without any observation of movement.

Table 2.1: Parameters of zoned presence sensing algorithm

Parameter	Value
\mathcal{A}	$\{-90^\circ, -80^\circ, \dots, 70^\circ, 80^\circ\}$
Z	13 group-ranges
α_2	1 zone
β	1
Ω	255
h_x	2 m
l_x	0.5 m

We tested the accuracy of the proposed zoned presence sensing algorithm by standing at predefined distances from the ultrasonic array sensor $-3, -2, -1, 0, 1, 2, 3$ m. The results of the experiment are shown in Fig. 2.7. We can see that the system achieves an accuracy of 1 m around the location of the occupant.

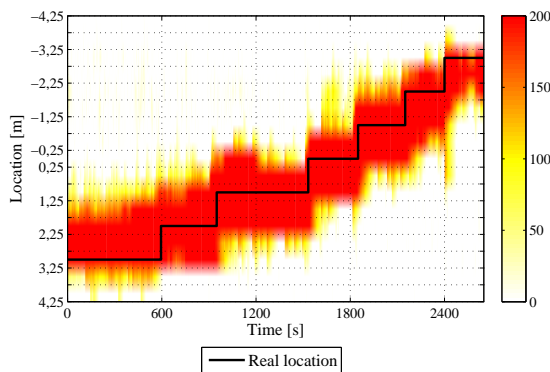


Figure 2.7: Performance evaluation of zoning algorithm.

2.5 Conclusions

We considered an ultrasonic array sensor system and presented a distributed transmission slot synchronization method and developed algorithms for zones presence detection. Our solution for synchronization was based on listening to

the echoes due to active transmission of neighboring sensors and aligning transmission slots based on the deviation from the expected arrival time of the echoes and the actual arriving time. Further, these echoes were used to decide which transmission slots were occupied by neighboring sensors and then choose a free transmission slot for transmission. Our solution for zoned presence sensing consisted of determining zones with largest SNR due to user movements. Tracking of user movement over zones was used to improve detection and zoning performance.

Appendix

2.A Analysis of transmission slot synchronization procedure

For simplicity of analysis, let us assume that the power of all received echoes are normalized to 1 (i.e. $U_{m,n}(\rho) = 1, \forall m, n, \rho$). The objective function in (2.8) can be rewritten as

$$\begin{aligned}
 &= \mathcal{F}^{-1} \left\{ \mathcal{F} \left\{ \sum_{m=1}^M \sum_{\rho=1}^{2NR+N\bar{R}} p_{m,n}^{(k)}(\rho) p_{m,n}^{(0)}(g(\rho+\Delta\rho_n)) \right\} \right\} \\
 &= \mathcal{F}^{-1} \left\{ \sum_{m=1}^M \mathcal{F} \left\{ \sum_{\rho=1}^{2NR+N\bar{R}} p_{m,n}^{(k)}(\rho) p_{m,n}^{(0)}(g(\rho+\Delta\rho_n)) \right\} \right\} \\
 &= \mathcal{F}^{-1} \left\{ \sum_{m=1}^M \sum_{\substack{i=1 \\ i \neq n}}^N S_{m,n,i}^{(k)}(\omega) (S_{m,n,i}^{(0)}(\omega))^* \right\} \\
 &= \sum_{\omega=1}^{2NR+N\bar{R}} \sum_{m=1}^M \sum_{\substack{i=1 \\ i \neq n}}^N S_{m,n,i}^{(k)}(\omega) (S_{m,n,i}^{(0)}(\omega))^* e^{j\pi(\omega-1)\frac{\Delta\rho_n}{NR+\frac{N}{2}\bar{R}}}, \quad (2.19)
 \end{aligned}$$

where $\mathcal{F} \{ \}$ is the discrete Fourier transform (DFT), $()^*$ is the conjugate operator and

$$\begin{aligned}
 S_{m,n,i}^{(k)}(\omega) &= \mathcal{F} \left\{ \left| s_{m,n,i}^{(k)}(\rho) \right| \right\} \\
 &= \sum_{\rho=1}^{2NR+N\bar{R}} \left| s_{m,n,i}^{(k)}(\rho) \right| e^{-j\pi(\omega-1)\frac{\rho-1}{NR+\frac{N}{2}\bar{R}}} \quad (2.20)
 \end{aligned}$$

is the DFT of the absolute value of received echoes from static objects.

Using (2.5) and properties of DFT we have that (2.20) becomes

$$S_{m,n,i}^{(k)}(\omega) \approx S_{m,n,i}^{(0)}(\omega) e^{-j\pi(\omega-1)\frac{\delta\rho_{n,i}^{(k)}}{NR+\frac{N}{2}\bar{R}}}$$

and so we can rewrite (2.19) as

$$\begin{aligned}
 &= \sum_{m=1}^M \sum_{\substack{i=1 \\ i \neq n}}^N \sum_{\omega=1}^{2NR+N\bar{R}} \left| S_{m,n,i}^{(0)}(\omega) \right|^2 e^{j\pi(\omega-1) \frac{\Delta\rho_n - \delta\rho_{n,i}^{(k)}}{NR + \frac{N}{2}\bar{R}}} \\
 &= \sum_{m=1}^M \sum_{\substack{i=1 \\ i \neq n}}^N \left| S_{m,n,i}^{(0)}(1) \right|^2 + \\
 &\quad 2 \sum_{m=1}^M \sum_{\substack{i=1 \\ i \neq n}}^N \sum_{\omega=2}^{NR + \frac{N}{2}\bar{R}} \left| S_{m,n,i}^{(0)}(\omega) \right|^2 \cos\left(\pi(\omega-1) \frac{\Delta\rho_n - \delta\rho_{n,i}^{(k)}}{NR + \frac{N}{2}\bar{R}} \right). \quad (2.21)
 \end{aligned}$$

A solution, $\Delta\rho_n^*$, that maximizes (2.21) is obtained from

$$\sum_{m=1}^M \sum_{\substack{i=1 \\ i \neq n}}^N \sum_{\omega=2}^{NR + \frac{N}{2}\bar{R}} \left| S_{m,n,i}^{(0)}(\omega) \right|^2 \frac{\pi(\omega-1)}{NR + \frac{N}{2}\bar{R}} \sin\left(\pi(\omega-1) \frac{\Delta\rho_n^* - \delta\rho_{n,i}^{(k)}}{NR + \frac{N}{2}\bar{R}} \right) = 0. \quad (2.22)$$

If $\left| \Delta\rho_n^* - \delta\rho_{n,i}^{(k)} \right| \ll 1$, $\forall i$, (i.e. $\left| \delta\rho_{n,i}^{(k)} - \delta\rho_{n,l}^{(k)} \right| \ll 1$, $\forall i, \forall l$), then we can approximate (2.22) by

$$\begin{aligned}
 \sum_{m=1}^M \sum_{\substack{i=1 \\ i \neq n}}^N \sum_{\omega=2}^{NR + \frac{N}{2}\bar{R}} \left| S_{m,n,i}^{(0)}(\omega) \right|^2 \frac{\pi(\omega-1)}{NR + \frac{N}{2}\bar{R}} \left(\pi(\omega-1) \frac{\Delta\rho_n^* - \delta\rho_{n,i}^{(k)}}{NR + \frac{N}{2}\bar{R}} \right) &= 0, \\
 \sum_{m=1}^M \sum_{\substack{i=1 \\ i \neq n}}^N \sum_{\omega=2}^{NR + \frac{N}{2}\bar{R}} \left| S_{m,n,i}^{(0)}(\omega) \right|^2 (\omega-1)^2 \left(\Delta\rho_n^* - \delta\rho_{n,i}^{(k)} \right) &= 0
 \end{aligned}$$

and so the solution to (2.21) is approximately

$$\Delta\rho_n^* = \frac{\sum_{m=1}^M \sum_{\substack{i=1 \\ i \neq n}}^N \sum_{\omega=2}^{NR + \frac{N}{2}\bar{R}} \left| S_{m,n,i}^{(0)}(\omega) \right|^2 (\omega-1)^2 \delta\rho_{n,i}^{(k)}}{\sum_{m=1}^M \sum_{\substack{i=1 \\ i \neq n}}^N \sum_{\omega=2}^{NR + \frac{N}{2}\bar{R}} \left| S_{m,n,i}^{(0)}(\omega) \right|^2 (\omega-1)^2}.$$

2.A. ANALYSIS OF TRANSMISSION SLOT SYNCHRONIZATION PROCEDURE

Hence, the solution to (2.8) would approximately be given by a weighted average of the relative time drift between all sensors,

$$\Delta t_n^{(\kappa K+k)} \approx \frac{\Gamma}{f_s} \sum_m \sum_{\substack{i=1 \\ i \neq n}}^N \eta_{m,n,i} \delta \rho_{n,i}^{(\kappa K+k)},$$

where

$$\eta_{m,n,i} = \frac{\sum_{w=2}^{NR+\frac{N}{2}\bar{R}} \left| S_{m,n,i}^{(0)}(w) \right|^2 (\omega - 1)^2}{\sum_{m=1}^M \sum_{\substack{i=1 \\ i \neq n}}^N \sum_{\omega=2}^{NR+\frac{N}{2}\bar{R}} \left| S_{m,n,i}^{(0)}(\omega) \right|^2 (\omega - 1)^2} \quad (2.23)$$

is a weighting factor. Note that the weighting factor (2.23) assigns a larger weight to high spectral components of the signal. Hence, if the received signal at receiver m of sensor n due to active transmission of sensor i has large fluctuations (i.e. several peaks due to multiple echoes), then sensor n would keep a tighter synchronization with respect to sensor i .

Let us assume that the time drifts of sensor i from transmission cycle $\kappa K + 1$ to $(\kappa + 1)K$ are equal to

$$\delta \rho_{n,i}^{(\kappa K+k)} = \left[k \frac{f_s}{\Gamma} \left(\tau_n - \Delta \tilde{\tau}_n^{(\kappa K)} - \tau_i + \Delta \tilde{\tau}_i^{(\kappa K)} \right) \right], \quad k = 1, \dots, K,$$

that is, the time drift between two consecutive transmission is constant and equal to $(\tau_n - \Delta \tilde{\tau}_n^{(\kappa K)} - \tau_i + \Delta \tilde{\tau}_i^{(\kappa K)})$.

Hence, we have that

$$\begin{aligned} \Delta c_n^{(\kappa)} &= \frac{\Gamma}{f_s K} \Delta t_n^{((\kappa+1)K)} + e_n^{(\kappa)} \\ &= \sum_m \sum_{\substack{i=1 \\ i \neq n}}^N \eta_{m,n,i} \left(\tau_n - \Delta \tilde{\tau}_n^{(\kappa K)} - \tau_i + \Delta \tilde{\tau}_i^{(\kappa K)} \right) + e_n^{(\kappa)}, \end{aligned}$$

where $e_n^{(\kappa)}$ is the error associated to the estimation at sensor n . Thus, the cor-

rection term at transmission cycle $(\kappa + 1)K$ is given by

$$\begin{aligned}
 \Delta \tilde{\tau}_n^{((\kappa+1)K)} &= \Delta \tilde{\tau}_n^{(\kappa K)} + \lambda_0 e_n^{(\kappa)} + \\
 &\quad \lambda_0 \sum_m \sum_{\substack{i=1 \\ i \neq n}}^N \eta_{m,n,i} \left(\tau_n - \Delta \tilde{\tau}_n^{(\kappa K)} - \tau_i + \Delta \tilde{\tau}_i^{(\kappa K)} \right) \\
 &= \Delta \tilde{\tau}_n^{(\kappa K)} + \lambda_0 e_n^{(\kappa)} - \lambda_0 \sum_{\substack{i=1 \\ i \neq n}}^N \tilde{\eta}_{n,i} \left(\Delta \tilde{\tau}_n^{(\kappa K)} - \Delta \tilde{\tau}_i^{(\kappa K)} \right) \\
 &\quad + \lambda_0 \sum_{\substack{i=1 \\ i \neq n}}^N \tilde{\eta}_{n,i} (\tau_n - \tau_i) \\
 &= (1 - \lambda_0) \Delta \tilde{\tau}_n^{(\kappa K)} + \lambda_0 \sum_{\substack{i=1 \\ i \neq n}}^N \tilde{\eta}_{n,i} \Delta \tilde{\tau}_i^{(\kappa K)} \\
 &\quad + \lambda_0 \sum_{\substack{i=1 \\ i \neq n}}^N \tilde{\eta}_{n,i} (\tau_n - \tau_i) + \lambda_0 e_n^{(\kappa)}, \tag{2.24}
 \end{aligned}$$

where $\tilde{\eta}_{n,i} = \sum_m \eta_{m,n,i}$.

A further simplification can be done for the scenario when the update of the correction term is performed at the same cycle for all ultrasonic array sensors. Then, we can rewrite (2.24) in matrix form as

$$\begin{aligned}
 \Delta \tilde{\boldsymbol{\tau}}^{((\kappa+1)K)} &= (\mathbf{I} - \lambda_0 \mathbf{C}) \Delta \tilde{\boldsymbol{\tau}}^{(\kappa K)} + \lambda_0 \mathbf{b} + \lambda_0 \mathbf{e}^{(\kappa)} \\
 &= \sum_{\xi=0}^{\kappa} (\mathbf{I} - \lambda_0 \mathbf{C})^\xi \left(\lambda_0 \mathbf{b} + (\mathbf{I} - \lambda_0 \mathbf{C}) \Delta \tilde{\boldsymbol{\tau}}^{(0)} + \lambda_0 \mathbf{e}^{(\kappa)} \right), \tag{2.25}
 \end{aligned}$$

where

$$\mathbf{b} = \begin{bmatrix} \sum_{\substack{i=1 \\ i \neq 1}}^N \tilde{\eta}_{1,i} (\tau_1 - \tau_i) \\ \sum_{\substack{i=1 \\ i \neq 2}}^N \tilde{\eta}_{2,i} (\tau_2 - \tau_i) \\ \vdots \\ \sum_{\substack{i=1 \\ i \neq N}}^N \tilde{\eta}_{N,i} (\tau_N - \tau_i) \end{bmatrix}, \quad \Delta \tilde{\boldsymbol{\tau}}^{(\kappa K)} = \begin{bmatrix} \Delta \tilde{\tau}_1^{(\kappa K)} \\ \Delta \tilde{\tau}_2^{(\kappa K)} \\ \vdots \\ \Delta \tilde{\tau}_N^{(\kappa K)} \end{bmatrix},$$

2.A. ANALYSIS OF TRANSMISSION SLOT SYNCHRONIZATION
PROCEDURE

$$\mathbf{e}^{(\kappa)} = \begin{bmatrix} e_1^{(\kappa)} \\ e_2^{(\kappa)} \\ \vdots \\ e_N^{(\kappa)} \end{bmatrix}, \quad \mathbf{C} = \begin{bmatrix} 1 & -\tilde{\eta}_{1,2} & \dots & -\tilde{\eta}_{1,N} \\ -\tilde{\eta}_{2,1} & 1 & \dots & -\tilde{\eta}_{2,N} \\ \vdots & \vdots & \ddots & \vdots \\ -\tilde{\eta}_{N,1} & -\tilde{\eta}_{N,2} & \dots & 1 \end{bmatrix}$$

and \mathbf{I} is the identity matrix of size $N \times N$.

It can be noted that (2.25) converges [21] when

$$\max |\text{eig}(\lambda_0 \mathbf{C})| < 1.$$

The maximum eigenvalue of \mathbf{C} is upper bounded by

$$\begin{aligned} \max |\text{eig}(\mathbf{C})| &\leq \max_n \sum_i |[C]_{n,i}| \\ &= 1 + \max_n \sum_{i \neq n} \tilde{\eta}_{n,i} \\ &= 2. \end{aligned}$$

Hence, an upper bound for λ_0 to ensure stability is given by

$$\lambda_0 < \frac{1}{2}.$$

REFERENCES

- [1] H. J. Keller, “Advanced passive infrared presence detectors as key elements in integrated security and building automation systems,” *IEEE Conference on Security Technology*, pp. 75–77, 1993.
- [2] D. Caicedo and A. Pandharipande, “Distributed illumination control with local sensing and actuation in networked lighting systems,” *IEEE Sensors Journal*, vol. 13, pp. 1092 – 1104, March 2013.
- [3] D. Caicedo and A. Pandharipande, “Ultrasonic arrays for localized presence sensing,” *IEEE Sensors Journal*, pp. 849–858, May 2012.
- [4] B. N. R. Melfi, B. Rosenblum and K. Christensen, “Ultrasonic arrays for localized presence sensing,” *International Green Computing Conference and Workshops*, 2011.
- [5] A. Pandharipande and D. Caicedo, “Daylight integrated illumination control of LED systems based on enhanced presence sensing,” *Energy and Buildings*, vol. 43, pp. 944–950, April 2011.
- [6] D. Caicedo and A. Pandharipande, “Ultrasonic array sensor for indoor presence detection,” *European Conference on Signal Processing*, pp. 175 – 179, 2012.
- [7] A. C. N. B. Priyantha and H. Balakrishnan, “The Cricket location-support system,” *Annual Conference on Mobile Computing and Networking*, pp. 32–43, 2000.
- [8] F. Zhang, J. Chen, H. Li, Y. Sun, and X. Shen, “Distributed active sensor scheduling for target tracking in ultrasonic sensor networks,” *ACM Mobile Networks and Applications*, 2011.
- [9] K. Romer, P. Blum, and L. Meier, “Time synchronization and calibration in wireless sensor networks,” *Handbook of Sensor Networks: Algorithms and Architectures*, pp. 199–237, 2005.
- [10] S. Ganeriwal, R. Kumar, and M. B. Srivastava, “Timing-sync protocol for sensor networks,” *International Conference on Embedded Networked Sensor Systems*, pp. 138–149, 2003.
- [11] J. Elson, L. Girod, and D. Estrin, “Fine-grained network time synchronization using reference broadcasts,” *Symposium on Operating Systems Design and Implementation*, 2002.

-
- [12] L. Schenato and G. Gamba, “A distributed consensus protocol for clock synchronization in wireless sensor network,” *IEEE Conference on Decision and Control*, pp. 2289–2294, 2007.
- [13] J. Degeysys, I. Rose, A. Patel, and R. Nagpal, “DESYNC: Self-Organizing Desynchronization and TDMA on Wireless Sensor Networks,” *International Symposium on Information Processing in Sensor Networks*, pp. 11–20, 2007.
- [14] S. Srinivasan and A. Pandharipande, “Self-configuring time-slot allocation protocol for ultrasonic sensor systems,” *IEEE Sensors Journal*, 2013.
- [15] D. Caicedo and A. Pandharipande, “Transmission slot allocation and synchronization protocol for ultrasonic sensor systems,” *IEEE International Conference on Networking, Sensing and Control*, pp. 288 – 293, 2013.
- [16] M. Skolnik, *Introduction to Radar Systems*, 3rd ed. McGraw-Hill, 2002.
- [17] D. H. Johnson and D. E. Dudgeon, *Array Signal Processing: Concepts and Techniques*. Prentice Hall, 1993.
- [18] L. Dong and S. C. Schwartz, “Object tracking by finite-state Markov process,” *IEEE International Conference on Acoustics, Speech and Signal Processing*, vol. 1, pp. I–897 – I–900, 2007.
- [19] Prowave, <http://www.prowave.com.tw/pdf/T400ep14d.PDF>.
- [20] Knowles, http://www.knowles.com/search/prods_pdf/SPM0404UD5.PDF.
- [21] K. Ogata, *Discrete-time control systems*, 2nd ed. Prentice-hall, 1995.

Chapter 3

Centralized lighting control with light distribution knowledge*

Light emitting diodes (LEDs) are considered to become the dominant source of illumination in the future, offering long life times, energy efficiency and flexible tunability. The flexibility of adapting LED parameters offers multiple degrees of freedom in designing LED based lighting systems. In this paper, we consider energy-efficient illumination control design of LED based lighting systems in office spaces. Our goal is to determine the optimum dimming levels of the LED sources so as to minimize the power consumption while rendering (i) uniform illumination at a given illumination level in workspace regions that are occupied, and (ii) a minimum illumination level of lower value in unoccupied regions, while taking daylight distribution over the workspace plane into account. We further propose a method to estimate and disaggregate illumination contributions of daylight and the different LED sources at the workspace plane. The performance of our proposed control solution is evaluated under different occupancy scenarios.

*This chapter has been published as: A. Pandharipande and D. Caicedo, "Daylight integrated illumination control of LED systems based on enhanced presence sensing", *Energy and Buildings*, pp. 944 – 950, April 2011.

3.1 Introduction

Energy efficiency is one of the design drivers of smart lighting systems and more generally of green buildings. In office buildings, lighting alone constitutes about 25-35% of the total energy consumed [1]. Energy consumption of a lighting system may be addressed by incorporating energy-efficient light sources, properly designing lighting controls and controlling lighting systems based on sensing information regarding occupancy and daylight.

Light emitting diodes (LEDs) are an attractive choice as an energy-efficient illumination source that can provide long life times, dynamic lighting effects and greater design flexibility. The flexibility in controlling individual LEDs can be used to render dynamic lighting in LED based systems while realizing savings in energy.

In this paper, we consider illumination rendering from an LED based lighting system in an office setting. The lighting system under consideration comprises of multiple LED based light sources, photosensors and an occupancy sensor. We are interested in the multiple facets that contribute to energy-efficient system design: enhanced occupancy sensing, and illumination control optimization that takes into account occupancy information and daylight contributions. Illumination control relates to the determination of LED dimming levels according to some design criteria. In this paper, our design goal is to minimize the power consumption by determining the optimum dimming levels of LEDs so as to render an illumination level of L_o in occupied regions and a minimum illumination level of L_u elsewhere, while taking into account daylight illumination over the workspace plane. The illumination levels L_o and L_u are chosen according to office workspace lighting recommendations [2]. Occupied regions are determined using the ultrasonic occupancy sensor presented in the chapter 2.

Several studies [3], [4], [5] (and references within), [6] have shown that considerable energy savings can be realized by designing lighting systems that are adapted to presence of occupants. In its simplest form, occupancy information is used to control an entire lighting system in a room to provide illumination only when the room is determined to be occupied. The presence of occupants is determined by simple motion detectors, e.g., passive infrared sensor, ultrasound sensor or a combination thereof. The information that is output from these sensors is a binary value indicative of whether the monitored space is occupied or not. Such information can only be used to realize energy gains when the monitored space is empty in its entirety, and thus has limited energy saving potential. For instance, in a multi-occupant office, if there is only a single person present, the entire lighting system would be on. Further, it is not possible to exploit the degrees of design freedom that an LED system has to offer.

The problem of illumination rendering in LED based systems has been considered in [7], [8]. The goal in [7] was to determine the dimming levels required to create specific illumination patterns using a mean-squared error approach. In [8], the design of the LED radiation pattern was studied with the goal of uniform illumination rendering. Such illumination control approaches require that individual LEDs be controllable. Methods for doing so using code division multiplexing and frequency division multiplexing have been proposed in [9] and [10,11] respectively. Strategies for integrated daylight-artificial light control based on computational models were presented in [12]. Field tests showing the savings obtained by daylighting offices have been reported in [13]. Lighting control design that accounts for daylight and occupancy was considered in [14].

The paper is organized as follows. The illumination control problem is formulated in Section 3.2, and takes location of occupants into account. We describe methods to disaggregate illumination contributions of daylight and the LED based light sources at the workspace plane. Numerical results showing the performance of the proposed illumination control solution are presented in Section 3.3. Conclusions are drawn in Section 3.4.

3.2 Lighting control solution

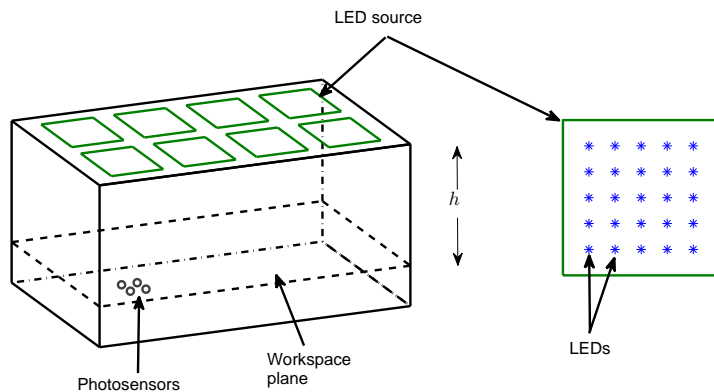


Figure 3.1: LED based lighting system

We consider an LED based lighting system with a total number of N LED based light sources and K photosensors arranged on the workspace plane. An example configuration is shown in Figure 3.1, where a number of LEDs together

CHAPTER 3. CENTRALIZED LIGHTING CONTROL WITH LIGHT DISTRIBUTION KNOWLEDGE

comprise an LED based light source². In certain configurations, the photosensor could be coupled to the light source, in which case $K = N$. The location of the i -th LED source is given by coordinates (x_i, y_i) and is assumed to be known from the commissioning plan. We consider a simple illumination model for the LED source. The total illuminance achieved from an LED source is the aggregated superposition of the illuminance from individual LEDs in that source. For the i -th LED source, let (x_{i_v}, y_{i_v}) be the coordinates of the v -th LED, $v = 1, \dots, V$. Employing the widely used generalized Lambertian function [15], [16], [17] to model the far-field illumination pattern of an LED, the illuminance achieved at a location (x, y) in the workspace plane (at a distance h from the ceiling) from a LED source located at (x_i, y_i) is thus given by

$$E_i(x, y; h) = A \sum_{v=1}^V \left[1 + \frac{\|(x, y) - (x_{i_v}, y_{i_v})\|_2^2}{h^2} \right]^{-\frac{m+3}{2}} \quad (3.1)$$

with

$$A = \frac{(m+1)A_0}{2\pi h^2}$$

where A_0 is the luminous flux of the light and $m > 0$ is the Lambertian mode. This mode is related to the semi-angle of the light beam at half power, $\Phi_{\frac{1}{2}}$, by

$$m = -\frac{\ln(2)}{\ln\left(\cos\left(\Phi_{\frac{1}{2}}\right)\right)}.$$

We assume a frequency division multiplexing based system [11] wherein each LED source is assigned a distinct frequency. The illumination intensity of the LED source is controlled using pulse width modulation (PWM) [18]. The duty cycle of the PWM waveform is the dimming level of the LED source. Hence, the average power consumed by the i -th LED source at dimming level d_i over one waveform cycle is

$$P_i(d_i) \approx d_i P_{on} \quad (3.2)$$

where P_{on} is the power consumption while the source is on (the approximation in (3.2) is under the assumption that the power consumption in the off state is negligibly small). Denote by \mathbf{d} , the $N \times 1$ dimming vector, given by

$$\mathbf{d} = [d_1, d_2, \dots, d_N],$$

²We shall use the terms ‘‘LED based light source’’ and ‘‘LED source’’ interchangeably to refer to a source that is based on a collection of embed LEDs

where $0 \leq d_i \leq 1$ is the dimming level of the i -th LED source. The value $d_i = 0$ means that the LED is dimmed off while $d_i = 1$ represents that the LED is at its maximum illumination. In practice, d_i takes values from a finite discrete set of values $\{l_1, l_2, \dots, l_Q\}$, where the l_q 's represent dimming levels and $l_1 = 0, l_Q = 1$.

The workspace plane is parallel to the ceiling at a distance h from it, and is the plane over which a particular illumination rendering is desired. For clarity of exposition, we will not introduce a z -coordinate to distinguish the two planes since the difference will be clear from the context.

The office is additionally equipped with an occupancy detection sensor as the one described in chapter 2. Assume there are J occupants in the office. The locations $(x_j, y_j), j = 1, \dots, J$ of occupants in the office are determined by the occupancy detection sensor. Define the occupied region R_o as the collection of all points that are within a distance r_0 from an occupied location:

$$R_o = \{(x, y) : \|(x, y) - (x_j, y_j)\|_2 \leq r_0, \quad j = 1, \dots, J\} \quad (3.3)$$

and its area by Ω . The constant r_0 may be chosen as per workspace norms and occupant visual comfort.

We desire uniform illumination at level L_o in the occupied region R_o . In the unoccupied area, it is desired to have a minimal illumination level of L_u . Levels L_o and L_u are chosen as per office illumination norms. In practice, uniform illumination is in the sense that variations in the illumination level about the value L_o must be below a certain threshold, C_o . This notion is analytically captured by illumination contrast. Denote the total illuminance at a point (x, y) in the workspace plane (at distance h from the ceiling) by $E_T(x, y; h; \mathbf{d})$, when the dimming levels of the LED sources are given by dimming vector \mathbf{d} . The illuminance contrast between $E_T(x, y; h; \mathbf{d})$ and L_o is defined as [19],

$$C(E_T(x, y; h; \mathbf{d}), L_o) = \frac{E_T(x, y; h; \mathbf{d}) - L_o}{L_o}. \quad (3.4)$$

The total illuminance is the combined illumination contribution of every LED source and the daylight. Denoting by $D(x, y; h)$ and $E_i(x, y; h)$ the illuminance in the workspace plane at location (x, y) and a distance h due to daylight and the i -th LED source respectively, we have

$$E_T(x, y; h; \mathbf{d}) = D(x, y; h) + \sum_{i=1}^N d_i E_i(x, y; h). \quad (3.5)$$

Given that the illumination levels vary about L_o , we furthermore require that the mean illumination level over R_o be L_o .

CHAPTER 3. CENTRALIZED LIGHTING CONTROL WITH LIGHT DISTRIBUTION KNOWLEDGE

The goal is to determine the dimming levels of the LED sources so as to achieve the desired illumination rendering with minimum power consumption. This illumination control problem can be mathematically formalized as follows. We want to determine the optimum dimming vector \mathbf{d}^* that solves

$$\mathbf{d}^* = \arg \min_{\mathbf{d}} \sum_{i=1}^N P_i(d_i)$$

$$\text{s.t.} \quad \begin{cases} |C(E_T(x, y; h; \mathbf{d}), L_o)| \leq C_o, & \forall (x, y) \in R_o \\ \frac{1}{\Omega} \int_{(x, y) \in R_o} E_T(x, y; h; \mathbf{d}) \partial x \partial y = L_o \\ E_T(x, y; h; \mathbf{d}) \geq L_u, & \forall (x, y) \notin R_o \\ d_i \in \{l_1, l_2, \dots, l_Q\}, & i = 1, \dots, N. \end{cases} \quad (3.6)$$

Some comments are due regarding feasibility of (3.6). If the contribution of the daylight illumination level is higher than $L_o(1 + C_o)$ at certain points in the workspace plane, then the first constraint cannot be met if these points lie in R_o . This is so because, even with all the LED sources in off state, the total illumination level (which is the contribution of the daylight level) would be higher than $L_o(1 + C_o)$ at certain points, and thus the contrast would be greater than C_o . To deal with this, we discard all points that have a daylight illumination level higher than L_o from our optimization problem. In certain cases, high daylight leads to an undesirable glare which affects visual comfort levels of occupants. This may be accounted by taking glare control, which can be achieved through electronic blinds, into our problem formulation.

Before solving (3.6), the following aspect need to be addressed: How do we determine how much illumination comes from daylight and individual LED sources, given illumination values at locations in the workspace plane?

Our solution involves a configuration step and signal processing techniques. During configuration, light intensity measurements are taken at a number of points in the workspace plane. These measurements may be taken by having the light sources turned on at dimming levels specified by vector \mathbf{d}_s . Correspondingly, let the measurements of the sensor at location (x, y) in the workspace plane be $E_T(x, y; h; \mathbf{d}_s)$. Now based on these signal measurements, we obtain estimates of $\{E_i(x, y; h)\}$. This is done by estimating the frequencies of the sources using, for instance, the techniques described in [10] or [11]. Since the duty cycles are known a priori, the summed signal contribution of the LED sources is subsequently determined. Estimates of $D(x, y; h)$ can then be obtained after subtracting the total signal contribution of the LED sources from the received signals.

We now turn our attention to solving (3.6). Observe that the objective function as well as the constraints are linear in the optimization variables $\{d_i\}$. The optimization problem is thus a linear programming problem [20] and can be

solved using a Simplex algorithm [21]. The computational complexity of the Simplex algorithm is $3(N + W)$ [20], where W is the number of constraints in the optimization problem resulting when (3.6) is discretized and slack variables are incorporated [22]. On the other hand, a full-search has exponential complexity of N^Q , where Q is the number of dimming levels.

3.3 Numericals results

We now present simulation results showing the performance of the proposed control algorithm, labeled ODA. The baseline control algorithm for comparison is one that optimizes the LED system so as to provide uniform illumination across the entire room taking room-level occupancy into account. The underlying optimization problem is one where R_o in (3.6) covers the entire workspace plane of the office room. A simplex algorithm is used to obtain the dimming levels and is labeled UIA. We shall assume parameter values of $L_o = 600$ lx, $L_u = 300$ lx and $C_o = 0.3$, consistent with workspace office lighting norms [2]. The parameter $r_0 = 1$ m, and an 8-bit uniform dimming corresponding to $Q = 256$ is assumed. We consider two occupancy scenarios, with the location of users being determined by the occupancy detection sensor described in chapter 2.

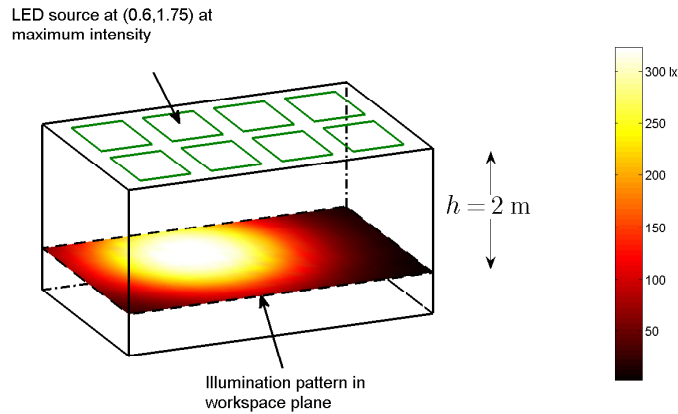


Figure 3.1: Illumination pattern of an LED

We consider an office test room of length 4.5m and width 3m, with the workspace plane located about 2m from the ceiling. There are $N = 8$ LED sources on the ceiling in the configuration shown in Figure 3.1, comprising of 25 LEDs arranged in a 5×5 uniform square grid with 0.1 m of separation between

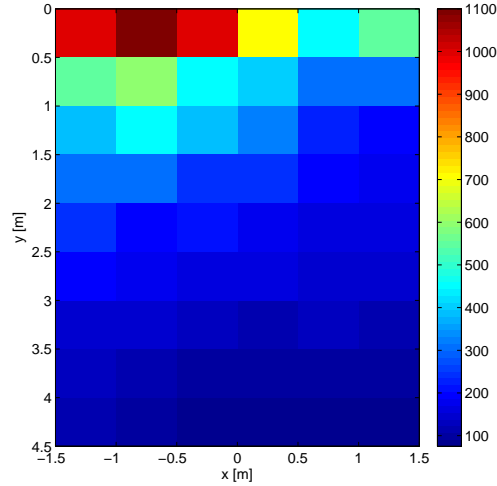


Figure 3.2: Daylight distribution (in lx)

LEDs. The spacing of the LED sources is 0.9 m along the length and 1.2 m along the width, as measured between the center of the grid. The individual LED is of type LUXEON model [15] that has a Lambertian radiation pattern with a half-power beam angle of 60 degrees and a maximum intensity of 14.3 lx. As an example illustration, the illumination pattern in the workspace plane when the LED source located at (0.6, 1.75) is at full dimming level is shown in Figure 3.1. We assume that the dimming level of the source is tunable at a group level, i.e. LEDs within a source are at the same dimming level. Extension to the case where all individual LEDs are tunable is straightforward. In Figure 3.2, we show the spatial distribution of daylight across the workspace plane. A window was located at one end of the room, which is reflected in the high illumination values seen in the top part of Figure 3.2.

In the first occupancy scenario, we consider a single user. The user is located at the coordinate (0, 2.25). For this setting, we show the resulting illumination pattern under ODA in Figure 3.3 and the corresponding dimming levels of the LED sources in Figure 3.4. Note from Figure 3.3 that points close to the window have illumination levels greater than 600 lx and comprise the region that is unfeasible. Correspondingly, LED sources close to the window are thus dimmed off as seen in Figure 3.4. In Figure 3.5, we show the power savings for different occupancy locations of the user in the room. Note that the savings are greater at occupant locations close to the window, more specifically, at locations where the

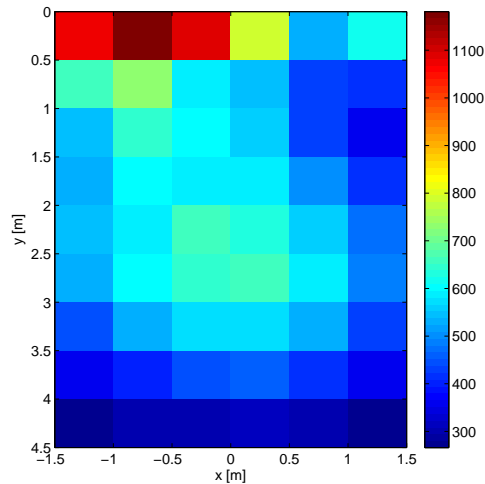


Figure 3.3: Illumination pattern obtained using ODA for an occupant located at the center of the room

daylight levels are higher. This means that the contribution required from the LED sources to meet the illumination requirements at such points is minimal, translating to power savings.

In the second occupancy scenario, we consider two occupants located at $(0, 1.5)$ and $(0, 3)$. Here we analyze the power savings for different amounts of occupancy overlap, i.e. the fraction of time that both occupants are at their workspace. These results are depicted in Figure 3.6. The largest gain in power savings is when only a single occupant is present at any given time, with the savings decreasing as the overlap increases. However, note that the power saving does not change substantially with occupancy overlap. This is since a large portion of the region around the occupant located at $(0, 1.5)$ is already adequately illuminated by daylight and the contribution required from the LED sources is minimal. In general, for lower daylight levels and larger room sizes, we would expect greater power savings at low levels of occupancy overlap.

3.4 Conclusions

We developed a framework for energy-efficient illumination control of LED systems that takes into account location of occupants and daylight distribution. The location information is input to the illumination control algorithm to optimize

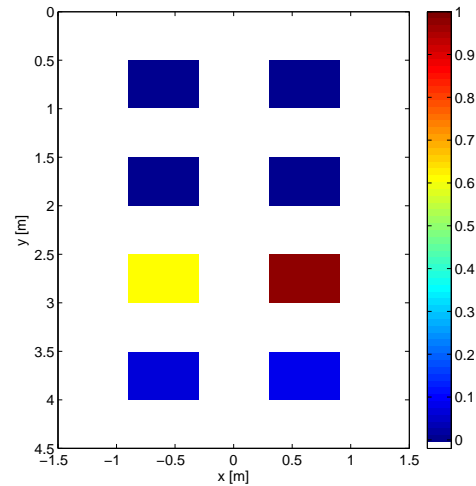


Figure 3.4: Optimized dimming levels under ODA of LED sources for an occupant located at the center of the room

dimming levels of the multiple LED sources in order to achieve the desired illumination rendering. We then considered different occupancy scenarios and showed that substantial energy savings can be obtained using our proposed strategy. Further work will involve extensive field tests to understand the impact of specific occupancy patterns on the energy savings that may be realized.

Acknowledgement

We thank Dr. Hongming Yang, Eindhoven University of Technology, for valuable discussions and feedback on the paper.

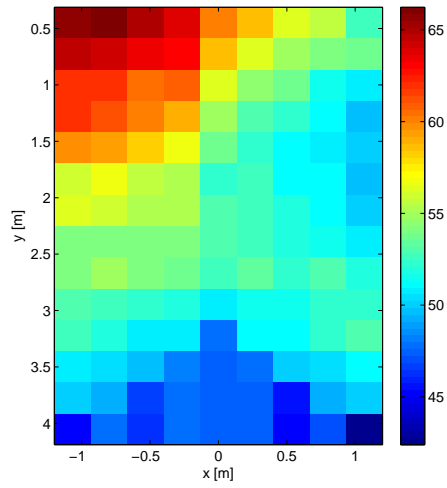


Figure 3.5: Power savings for different locations of the occupant in the room

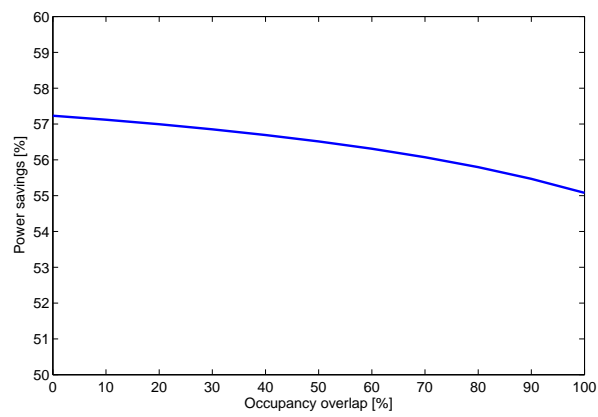


Figure 3.6: Power savings for different levels of occupancy overlap for two occupants

REFERENCES

- [1] Energy Information Administration, “Commercial buildings energy consumption survey,” 2003.
- [2] European Committee for Standardization, “EN 12464-1:2002. Light and lighting. Lighting of work places. Part 1: Indoor work places,” 2002.
- [3] P. R. Boyce, J. A. Veitch, G. R. Newsham, C. C. Jones, J. Heerwagen, M. Myer, and C. M. Hunter, “Occupant use of switching and dimming controls in offices,” *Lighting Research and Technology*, vol. 38, no. 4, pp. 358 – 376, 2006.
- [4] V. Garg and N. K. Bansal, “Smart occupancy sensors to reduce energy consumption,” *Energy and Buildings*, vol. 32, no. 1, pp. 81 – 87, 2000.
- [5] B. Roisin, M. Bodart, A. Deneyer, and P. D. Herdt, “Lighting energy savings in offices using different control systems and their real consumption,” *Energy and Buildings*, vol. 40, no. 4, pp. 514 – 523, 2008.
- [6] D. Wang, C. C. Federspiel, and F. Rubinstein, “Modeling occupancy in single person offices,” *Energy and Buildings*, vol. 37, no. 2, pp. 121 – 126, 2005.
- [7] I. Moreno, “Creating a desired lighting pattern with an LED array,” *SPIE*, 2008.
- [8] H. Yang, J. W. M. Bergmans, T. C. W. Schenk, J. M. G. Linnartz, and R. Rietman, “Uniform illumination rendering using an array of LEDs: A signal processing perspective,” *IEEE Transactions on Signal Processing*, vol. 57, pp. 1044 – 1057, March 2009.
- [9] J. M. G. Linnartz, L. Feri, H. Yang, S. B. Colak, and T. C. W. Schenk, “Code division-based sensing on illumination contributions in solid-state lighting systems,” *IEEE Transactions on Signal Processing*, vol. 57, no. 10, October 2009.
- [10] H. Yang, J. W. M. Bergmans, and T. C. W. Schenk, “Illumination sensing in LED lighting systems based on frequency-division multiplexing,” *IEEE Transactions on Signal Processing*, vol. 57, pp. 4269 – 4281, November 2009.
- [11] H. Yang, T. C. W. Schenk, J. W. M. Bergmans, and A. Pandharipande, “Enhanced illumination sensing using multiple harmonics for LED lighting

- systems,” *IEEE Transactions on Signal Processing*, vol. 58, pp. 5508 – 5522, November 2010.
- [12] C. P. Kurian, R. S. Aithal, J. Bhat, and V. I. George, “Robust control and optimisation of energy consumption in daylight-artificial light integrated schemes,” *Lighting Research and Technology*, vol. 40, no. 1, pp. 7 – 24, March 2008.
- [13] D. H. W. Li and J. C. Lam, “Evaluation of lighting performance in office buildings with daylighting controls,” *Energy and Buildings*, vol. 33, no. 8, pp. 793 – 803, 2001.
- [14] V. Singhvi, A. Krause, C. Guestrin, J. H. G. Jr., and H. S. Matthews, “Intelligent light control using sensor networks,” *International Conference on Embedded Networked Sensor Systems*, pp. 218 – 229, 2005.
- [15] Lumileds, “LUXEON LED Radiation Patterns: Light Distribution Patterns,” <http://www.lumileds.com/technology/radiationpatterns.cfm>.
- [16] I. Moreno and C. Sun, “Modeling the radiation pattern of LEDs,” *Optics Express*, vol. 16, no. 3, pp. 1810 – 1819, February 2008.
- [17] C. Sun, W. T. Chien, I. Moreno, C. C. Hsieh, and Y.-C. Lo, “Analysis of the far-field region of LEDs,” *Optics Express*, vol. 17, no. 16, pp. 13 918 – 13 927, 2009.
- [18] Y. Gu, N. Narendran, T. Dong, and H. Wu, “Spectral and luminous efficacy change of high-power LEDs under different dimming methods,” *International Conference on Solid State Lighting, SPIE*, vol. 6337, p. 63370J, 2006.
- [19] P. R. Boyce, *Human Factors in Lighting*, 2nd ed. New York: Taylor and Francis, 2003.
- [20] D. G. Luenberger and Y. Ye, *Linear and Nonlinear Programming*, 3rd ed. Springer, 2008.
- [21] G. B. Dantzig, *Linear Programming and Extensions*, 1st ed. Princeton University Press, 1963.
- [22] D. Caicedo, A. Pandharipande, and G. Leus, “Occupancy based illumination control of LED lighting systems,” *Lighting Research and Technology*, vol. 43, no. 2, pp. 217–234, August 2011.

CHAPTER 3. CENTRALIZED LIGHTING CONTROL WITH LIGHT
DISTRIBUTION KNOWLEDGE

Chapter 4

Lighting control strategies accounting for user preferences*

We consider energy-efficiency and user-comfort driven design of indoor light emitting diode (LED) lighting control systems, by achieving spatial illumination rendering adapted to presence and daylight conditions and user preference for the amount of rendered illuminance. A localized illumination rendering strategy for lighting control is presented where a given level of uniform illuminance is provided with a certain user satisfaction level over a user-occupied zone, and a lower illuminance level is maintained in unoccupied zones. Under these illuminance constraints, our objective is to minimize a weighted sum of power consumed in localized illumination rendering and the net user dissatisfaction with the rendered illumination. This is achieved by determining the dimming levels for controlling the multiple LED luminaires. Algorithms for centralized and distributed lighting control are proposed. Simulation results are presented to evaluate the performance of the algorithms in achieving power savings and meeting user preferences of illumination levels.

*This chapter has been published as: A. Pandharipande and D. Caicedo, "Adaptive illumination rendering in LED lighting systems", *IEEE Transactions on Systems, Man, and Cybernetics – Part A: Systems and Humans*, vol. 43, no. 5, pp. 1052 – 1062, May 2013.

4.1 Introduction

It has been widely recognized that the visual lighting environment in offices has an influence on the comfort and productivity of occupants [1–3]. Office lighting is a major constituent of electrical usage in buildings [4]. There has thus been great interest in the design of intelligent lighting systems in office spaces driven by user comfort and energy savings [3, 5–10]. We consider an intelligent lighting system as one that has sensing, communication and control as integral elements, in addition to luminaires to provide the basic function of illumination rendering, and that can adapt to sensing information inputs and user preferences. We are interested in methods for controlling such lighting systems to achieve adaptive illumination rendering.

We consider a lighting system with multiple light emitting diode (LED) luminaires on the ceiling. LEDs are set to become the primary illumination source bringing in benefits such as longer life times and greater design flexibility. In particular, LED luminaires offer easy and accurate dimming capability. Thus it is possible to achieve illumination rendering flexibly in a LED luminaire based lighting system by individually dimming each luminaire. In office workplace lighting, illumination rendering over the workspace plane is of interest. The workspace plane, divided in to a number of logical spatial zones, is the horizontal plane typically at occupant desk height. We are interested in localized illumination rendering where we desire an illuminance distribution in an occupied zone to be rendered with a certain illumination uniformity and at an average illuminance value that is at a certain level of user satisfaction, and a lower illuminance to be provided in unoccupied zones. Note that the illuminance at any point is due to daylight and the illuminance contributions of the LED luminaires. Our goal is to minimize a weighted sum of the power consumed in localized illumination rendering and the user dissatisfaction with the rendered illumination. This is done by determining the optimum dimming levels of the LED luminaires. The optimization thus results in a lighting system that is optimally adapted to integrate daylight, provides illumination where needed and in the amount that accounts for individual user preferences. We shall consider centralized and distributed lighting control scenarios under which this optimization is performed.

The presence sensing, light sensing, and communication elements are integral to the lighting control system. We consider a presence sensing system that can determine local occupancy in every zone. This can be achieved using a stand-alone sensor or using multiple sensors, with a sensor embedded in every LED luminaire. Subsequently, occupancy information in zones is conveyed to the lighting controller. Similarly, light sensing to determine daylight distribution over a zone may be done using a stand-alone sensor, e.g., a vision sensor, or using

an array of light sensors, e.g., photodiodes. This information is then conveyed to the lighting controller. The sensing systems are assumed to be connected to the lighting control system via reliable communication links.

While substantial literature exists on lighting control strategies from a qualitative view and based on field tests, there is limited work reported on lighting control design from an analytical standpoint. Different frameworks for lighting control have been considered recently in [5, 6, 8–12]. A decision-theoretic approach to centralized control was considered in [8] to achieve optimum tradeoff between meeting occupant comfort and reducing operational costs by lowering energy usage. Distributed lighting control systems were considered in [9] and [12]. A stochastic hill-climbing method was proposed in [12], with the model assuming illuminance sensors on the workspace plane. Under a similar assumption on the sensors, a regression model was developed in [9] to estimate the influence of lamps on illuminance sensors on the workspace plane, based on which a control algorithm was presented. In [5, 10], the lighting control problem was studied in a scenario in which users are equipped with portable wireless light sensors. Binary and gaussian satisfaction models were considered to model user-requirements of illumination levels, and the resulting optimization was solved using linear programming and sequential quadratic programming methods respectively. In [6], a centralized lighting control was presented to achieve illumination rendering that accounted for presence and daylight sensing information. The illumination sensing aspect of the lighting control problem was treated in [13] by considering a frequency-division multiplexed lighting system wherein the output of each light source is modulated by a distinct frequency.

In this paper, we develop an analytical framework for lighting control to achieve localized illumination rendering while balancing power consumption with user preferences, thus extending the lighting system control model presented in [6]. User preference is accounted for by modeling the user dissatisfaction with illumination rendered over the respective occupied zone. We further present algorithms for solving the resulting optimization problem in a centralized as well as a distributed lighting control scenario.

The paper is organized as follows. The lighting system and the various elements constituting illumination control are described in Section 4.2. Illumination control is formulated as an optimization problem in Section 4.3, and shown to be a linear programming problem. Centralized and distributed control algorithms are described to obtain the optimum dimming levels. Simulation results are presented in Section 4.4 to validate the performance of our algorithms. Conclusions are drawn in Section 4.5.

Notation: For a matrix \mathbf{A} , $[\mathbf{A}]_{i,j}$ denotes the element in row i and column j

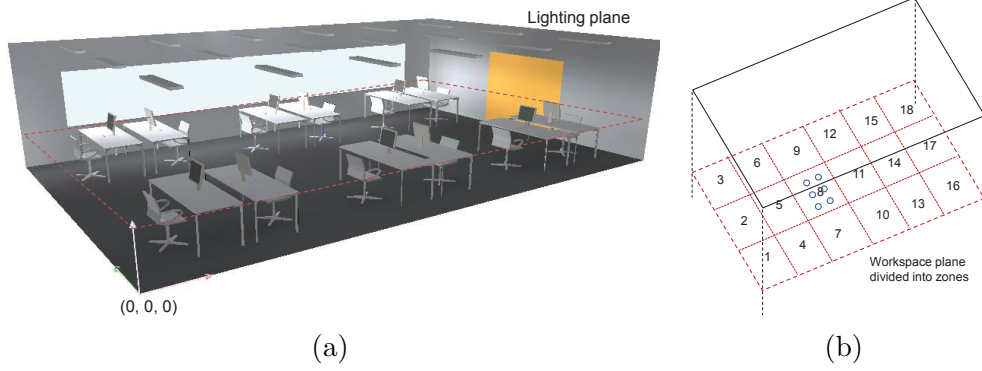


Figure 4.1: (a) Lighting system in an office room, (b) Depiction of zones in the workspace plane.

of \mathbf{A} ; $[\mathbf{A}]_{i,:}$ is a row vector corresponding to row i of \mathbf{A} ; \mathbf{A}^T denotes the transpose of \mathbf{A} . For a row vector \mathbf{b} , $[\mathbf{b}]_i$ denotes the element in column i . Given an $n \times m$ matrix \mathbf{A} and $n \times 1$ vector \mathbf{x} , the matrix $[\mathbf{A} \ \mathbf{x}]$ denotes an $n \times (m + 1)$ matrix with the column \mathbf{x} concatenated after the columns of \mathbf{A} .

4.2 System model

We consider a lighting system in an indoor office as depicted in Fig. 4.1(a). The lighting system comprises of M LED luminaires in the ceiling arranged in a grid configuration on a plane we shall refer to as the lighting plane. Parallel to this plane is the workspace plane, a plane over which illumination rendering is of interest. This plane is typically at a height corresponding to desks of occupants. We divide the workspace plane into M logical zones, over which illuminance is evaluated at different discrete locations, as depicted in Fig. 4.1(b) (with evaluation points illustrated for zone 8). The set of discrete points located within the m -th zone is given by $R_m = \{r_{m,1}, r_{m,2}, \dots, r_{m,N_m}\}$, where $r_{m,i}$ is the coordinate of point i and N_m is the number of evaluation locations in zone m . Each zone either contains exactly one desk space that a user may occupy or none at all (e.g., corresponding to the central row in Fig. 4.1).

We are interested in rendering illumination such that in an occupied zone, the illumination level is achieved with a certain level of user satisfaction and pre-defined illumination uniformity, and in an unoccupied zone, a minimum level of illuminance is provided. We seek to achieve a balance between the power consumption and user satisfaction with the rendered illumination in the occupied

zone. Towards this, our objective is to minimize a weighted sum of the power consumed in illumination rendering and the user dissatisfaction with the rendered illumination, by determining the optimum dimming levels of the LED sources.

We consider centralized and distributed control scenarios in controlling the luminaires. These scenarios respectively provide different options in embedding the control intelligence at either a central control unit, or at multiple controllers with the control function at the luminaire level. In centralized lighting control, a central controller coordinates information inputs from the presence and light sensing systems and computes the dimming levels of the LED luminaires to realize localized illumination rendering over the office space while minimizing the objective function. These optimum dimming levels are then signaled to the respective LEDs. The presence sensing system indicates zone occupancies to the central controller. The light sensing system provides the daylight distribution to the central controller. The light distributions of the LED luminaires may additionally be input during an initial configuration phase to the controller. In the other distributed lighting control scenario, the dimming level of each LED luminaire is determined by an associated controller. Further, the m -th zone is said to be associated to the m -th controller, where the association reflects that the localized illumination rendering constraints over the m -th zone are tied to the m -th controller. Each controller has knowledge of local occupancy and daylight distribution in its associated zone. It also has knowledge of the objective function and the number of controllers and constraints. Based on this information and coordination with other controllers, it determines the dimming level of its LED luminaire such that the objective function is minimized such that localized illumination rendering constraints over the office space are satisfied. We assume the controllers can communicate with each other reliably.

In the following sections, we present an analytical formulation of the optimization problem. We first formalize the objective function and constraints of the optimization problem.

4.2.1 Power consumption

Let d_m , where $0 \leq d_m \leq 1$, be the dimming level of the m -th LED luminaire. The value $d_m = 0$ means that the LED is dimmed off completely, while $d_m = 1$ represents that the LED is at its maximum luminance. Dimming of LEDs is typically done using pulse width modulation (PWM) [14], where the dimming level corresponds to the duty cycle of the PWM waveform. Let \mathbf{d} be the $M \times 1$ dimming vector of the lighting system given by

$$\mathbf{d} = [d_1, d_2, \dots, d_M]^T,$$

indicating that the m -th LED is at dimming level d_m .

The power consumption of an LED is directly proportional to the dimming level. Denote the average power consumption of the m -th LED at dimming level d_m by $P_m(d_m)$. We then have,

$$P_m(d_m) = P_{on}d_m, \quad (4.1)$$

where P_{on} is the power consumption of the LED in ON-state.

4.2.2 Illuminance over workspace plane

The illuminance at a point in the workspace plane is the combined illumination contribution due to the LED luminaires and daylight. Denote the illuminance in the workspace plane at location (x, y, z) due to the m -th LED source at dimming level d_m as $E_m(x, y, z; d_m)$. We shall assume that

$$E_m(x, y, z; d_m) = d_m E_m(x, y, z; 1),$$

that is, the illuminance scales linearly with the dimming level. This assumption holds well for LED lighting. In Fig. 4.2, we plot $E_m(x, y, z; d_m)/E_m(x, y, z; 1)$ versus d_m for different points $(x, y, 1.88)$, over the workspace plane at a distance of 1.88 m from the lighting plane. Here, results are shown for LED luminaire indexed 8 in Fig. 4.1 and type Philips BCS640 W21L120 1xLED48/840 [15]. We can see that $E_m(x, y, z; d_m)/E_m(x, y, z; 1)$ shows very small variations across locations and is linear in d_m with slope of unity.

Let $D(x, y, z)$ denote the illuminance due to daylight. The total illuminance at (x, y, z) in the workspace plane, given that the lighting system is at dimming vector \mathbf{d} , can then be written as

$$E_T(x, y, z; \mathbf{d}) = \sum_{m=1}^M d_m E_m(x, y, z; 1) + D(x, y, z). \quad (4.2)$$

In practice, the mappings $E_m(\cdot)$ may be computed a priori in a configuration phase. Similarly the daylight spatial distribution $\{D(x, y, z)\}$ may be estimated using a light sensing system.

4.2.3 User dissatisfaction

We introduce the following model to capture the dissatisfaction of a user with the rendered illumination over the occupied zone. The dissatisfaction of user m is given by the function $U_m(\bar{E}_{T,m}(\mathbf{d}), E_{D,m})$, where $\bar{E}_{T,m}(\mathbf{d})$ is the average of

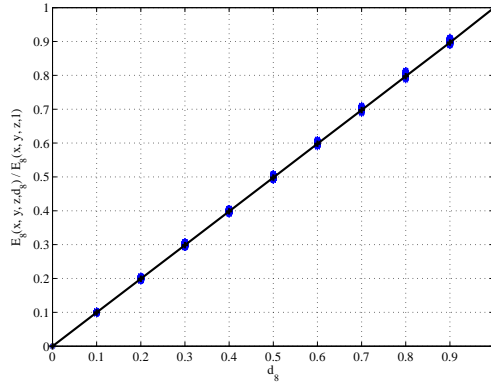


Figure 4.2: Linearity of $E_m(x, y, z; d_m)/E_m(x, y, z; 1)$ in d_m

the total illumination over zone m , and $E_{D,m}$ is the desired average illumination level,

$$U_m(\bar{E}_{T,m}(\mathbf{d}), E_{D,m}) = \begin{cases} \beta_{m,1}(\bar{E}_{T,m}(\mathbf{d}) - E_{D,m}) & \text{if } \bar{E}_{T,m}(\mathbf{d}) \leq E_{D,m} \\ \beta_{m,2}(\bar{E}_{T,m}(\mathbf{d}) - E_{D,m}) & \text{otherwise,} \end{cases} \quad (4.3)$$

where $\beta_{m,1} < 0$ and $\beta_{m,2} > 0$ are constants. Thus $U_m = 0$ if the average illuminance $\bar{E}_{T,m}(\mathbf{d})$ in a user-occupied zone is equal to the desired level $E_{D,m}$. Else, U_m is proportional to the difference $|E_{D,m} - \bar{E}_{T,m}(\mathbf{d})|$, with respective proportionality factors $\beta_{m,1}$, if $\bar{E}_{T,m}(\mathbf{d}) \leq E_{D,m}$, and $\beta_{m,2}$ otherwise. That is, user dissatisfaction increases if the value $\bar{E}_{T,m}(\mathbf{d})$ is further from $E_{D,m}$.

We note that a more general model using a convex piecewise linear function may be used to describe user dissatisfaction, wherein piecewise linear functions are used to describe the amount of dissatisfaction at different values of $\bar{E}_{T,m}(\mathbf{d})$ with respect to the desired level $E_{D,m}$. Our proposed methods apply to this general model as well; however, for the sake of simplicity we shall work with the simple two-piece linear dissatisfaction function described in (4.3).

4.2.4 Illuminance uniformity

In practice, uniform illumination means that variations in the illumination level must be below a certain threshold. The uniformity distortion in illumination pattern $\{E(x, y, z; d)\}$ may be characterized using illuminance contrast, which is given by the variations of the illuminance $E(x, y, z; d)$ values at different locations (x, y, z) with respect to an illuminance level L , and is given by Weber's law [16,

Chapter 2],

$$C(E(x, y, z; d), L) = \frac{E(x, y, z; d) - L}{L}. \quad (4.4)$$

The distribution $\{E(x, y, z; d)\}$ is considered uniform, with a uniformity contrast of C_{th} , over a set of points R with respect to illuminance level L if

$$|C(E(x, y, z; d), L)| \leq C_{th} \quad \forall (x, y, z) \in R. \quad (4.5)$$

The recommended contrast for sufficiently uniform illumination in [17] is 30% for office lighting, which we shall adopt.

4.2.5 Localized illumination rendering

Under localized illumination rendering, in an occupied zone we want to render an illuminance level that is attained as per user satisfaction levels in that zone with a certain illumination uniformity. For a zone m that is occupied, this constraint may be formulated as

$$|C(E_T(x, y, z; \mathbf{d}), \bar{E}_{T,m}(\mathbf{d}))| \leq C_{th}, \quad \forall (x, y, z) \in R_m \text{ and } m \in \mathcal{S}_o,$$

where \mathcal{S}_o is the index set corresponding to occupied zones, and $\bar{E}_{T,m}(\mathbf{d})$ is the average of the illuminance level attained at dimming level \mathbf{d} over R_m . In an unoccupied zone, we desire a minimum level of illuminance L_{min} . Thus in an unoccupied zone m ,

$$E_T(x, y, z; \mathbf{d}) \geq L_{min}, \quad \forall (x, y, z) \in R_m \text{ and } m \in \mathcal{S}_u$$

where \mathcal{S}_u is the index set corresponding to unoccupied zones.

4.3 Illumination control

Our objective function is a weighted sum of the total power consumed in localized illumination rendering and the net user dissatisfaction with the rendered illumination. In each zone m , let α_m denote the weighting factor that is used to balance power consumption with the dissatisfaction of the user with the average illumination rendered in that zone. We have $0 < \alpha_m < 1$, for $m = 1, \dots, M$. The net user dissatisfaction is the sum of the dissatisfaction functions over all zones. The illumination control problem is to determine the optimum dimming vector for the LED lighting system such that the objective function is minimized subject to localized illumination rendering constraints and constraints on the dimming

levels. Using the analytical models developed in Section 4.2, this optimization problem can be written as

$$\begin{aligned} \min_{\mathbf{d}} \quad & \sum_{m=1}^M \left\{ \alpha_m \eta P_{on} d_m + (1 - \alpha_m) U_m(\bar{E}_{T,m}(\mathbf{d}), E_{D,m}) \right\} \\ \text{s.t.} \quad & \begin{cases} |C(E_T(x, y, z; \mathbf{d}), \bar{E}_{T,m}(\mathbf{d}))| \leq C_{th}, \forall (x, y, z) \in R_m \text{ and } m \in \mathcal{S}_o \\ E_T(x, y, z; \mathbf{d}) \geq L_{min}, \forall (x, y, z) \in R_m \text{ and } m \in \mathcal{S}_u \\ 0 \leq d_m \leq 1, \quad m = 1, \dots, M, \end{cases} \end{aligned} \quad (4.6)$$

where $\eta > 0$ is a normalizing constant to make the objective function in 4.6 dimensionless. Note that the constraints in (4.6) are linear in the optimization variables $\{d_m\}$. While the objective function is a non-linear function, we shall show that (4.6) can be cast as a linear programming problem.

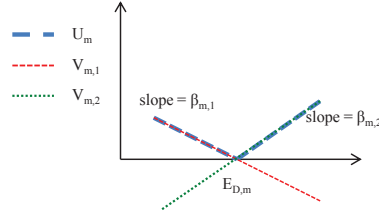


Figure 4.1: User dissatisfaction functions

Define the extended dissatisfaction functions, as illustrated in Fig. 4.1,

$$V_{m,l}(\bar{E}_{T,m}(\mathbf{d}), E_{D,m}) = \beta_{m,l}(\bar{E}_{T,m}(\mathbf{d}) - E_{D,m}), \quad l = 1, 2,$$

for $m = 1, \dots, M$. We may then write

$$U_m(\bar{E}_{T,m}(\mathbf{d}), E_{D,m}) = \max_{l=1,2} V_{m,l}(\bar{E}_{T,m}(\mathbf{d}), E_{D,m}).$$

Thus, the objective function can be written as

$$\sum_{m=1}^M \left\{ \alpha_m \eta P_{on} d_m + (1 - \alpha_m) \max_{l=1,2} V_{m,l}(\bar{E}_{T,m}(\mathbf{d}), E_{D,m}) \right\}. \quad (4.7)$$

Note that for a given \mathbf{d} and fixed m ,

$$\max_{l=1,2} \left\{ \alpha_m \eta P_{on} d_m + (1 - \alpha_m) V_{m,l}(\bar{E}_{T,m}(\mathbf{d}), E_{D,m}) \right\}$$

CHAPTER 4. LIGHTING CONTROL STRATEGIES ACCOUNTING FOR USER PREFERENCES

is equivalent to determining the smallest number t_m , such that the following inequalities hold,

$$\alpha_m \eta P_{on} d_m + (1 - \alpha_m) V_{m,l} (\bar{E}_{T,m}(\mathbf{d}), E_{D,m}) \leq t_m, \quad l = 1, 2. \quad (4.8)$$

We can thus rewrite the optimization problem (4.6) as

$$\begin{aligned} & \min_{\mathbf{d}, \mathbf{t}} \sum_{m=1}^M t_m \\ \text{s.t.} & \begin{cases} \alpha_m \eta P_{on} d_m + (1 - \alpha_m) V_{m,l} (\bar{E}_{T,m}(\mathbf{d}), E_{D,m}) \leq t_m \\ \quad \text{for } m = 1, \dots, M, \text{ and } l = 1, 2, \\ |C(E_T(x, y, z; \mathbf{d}), \bar{E}_{T,m}(\mathbf{d}))| \leq C_{th}, \forall (x, y, z) \in R_m \text{ and } m \in \mathcal{S}_o \\ E_T(x, y, z; \mathbf{d}) \geq L_{min}, \forall (x, y, z) \in R_m \text{ and } m \in \mathcal{S}_u \\ 0 \leq d_m \leq 1, \quad m = 1, \dots, M, \end{cases} \end{aligned} \quad (4.9)$$

where $\mathbf{t} = [t_1, t_2, \dots, t_M]$. Problem (4.9) now is in the form of a linear programming problem [18].

We shall present algorithms for obtaining the optimum dimming vector by solving (4.9) for centralized and distributed lighting control systems.

4.3.1 Centralized control

In centralized lighting control, there is a central controller that receives all sensing inputs and has knowledge of the global variables. The controller computes the optimum dimming vector that optimizes (4.9) and the dimming values are applied at the LED luminaires.

In order to write (4.9) in the standard matrix form of a linear programming problem [19], we evaluate the constraints in (4.9) for the m -th zone over the respective set of locations,

$$R_m = \{r_{m,1}, r_{m,2}, \dots, r_{m,N_m}\}.$$

The constraints in (4.9) can then be put in the following matrix form,

$$\mathbf{K}_m \mathbf{d} - \mathbf{T}_m \mathbf{t} \leq \mathbf{b}_m, \quad m = 1, \dots, M.$$

The entries of matrices \mathbf{K}_m , \mathbf{T}_m and vector \mathbf{b}_m are given by, if the m -th zone is

occupied,

$$\mathbf{K}_m = \begin{bmatrix} \alpha_m \eta P_{on} \mathbf{e}_m^T + (1 - \alpha_m) \beta_{m,1} \mathbf{a}_m^T \\ \alpha_m \eta P_{on} \mathbf{e}_m^T + (1 - \alpha_m) \beta_{m,2} \mathbf{a}_m^T \\ \mathbf{c}_{m,1}^T - (1 + C_{th}) \mathbf{a}_m^T \\ -\mathbf{c}_{m,1}^T + (1 - C_{th}) \mathbf{a}_m^T \\ \vdots \\ \mathbf{c}_{m,N_m}^T - (1 + C_{th}) \mathbf{a}_m^T \\ -\mathbf{c}_{m,N_m}^T + (1 - C_{th}) \mathbf{a}_m^T \end{bmatrix},$$

$$\mathbf{T}_m = \begin{bmatrix} \mathbf{e}_m^T \\ \mathbf{e}_m^T \\ \mathbf{0}_{1 \times M} \\ \mathbf{0}_{1 \times M} \\ \vdots \\ \mathbf{0}_{1 \times M} \\ \mathbf{0}_{1 \times M} \end{bmatrix}, \quad \mathbf{b}_m = \begin{bmatrix} (1 - \alpha_m) \beta_{m,1} (E_{D,m} - \bar{D}_m) \\ (1 - \alpha_m) \beta_{m,2} (E_{D,m} - \bar{D}_m) \\ -D(r_{m,1}) + (1 + C_{th}) \bar{D}_m \\ D(r_{m,1}) - (1 - C_{th}) \bar{D}_m \\ \vdots \\ -D(r_{m,N_m}) + (1 + C_{th}) \bar{D}_m \\ D(r_{m,N_m}) - (1 - C_{th}) \bar{D}_m \end{bmatrix}$$

or, if unoccupied, given by

$$\mathbf{K}_m = \begin{bmatrix} \alpha_m \eta P_{on} \mathbf{e}_m^T + (1 - \alpha_m) \beta_{m,1} \mathbf{a}_m^T \\ \alpha_m \eta P_{on} \mathbf{e}_m^T + (1 - \alpha_m) \beta_{m,2} \mathbf{a}_m^T \\ -\mathbf{c}_{m,1}^T \\ \vdots \\ -\mathbf{c}_{m,N_m}^T \end{bmatrix},$$

$$\mathbf{T}_m = \begin{bmatrix} \mathbf{e}_m^T \\ \mathbf{e}_m^T \\ \mathbf{0}_{1 \times M} \\ \vdots \\ \mathbf{0}_{1 \times M} \end{bmatrix}, \quad \mathbf{b}_m = \begin{bmatrix} (1 - \alpha_m) \beta_{m,1} (E_{D,m} - \bar{D}_m) \\ (1 - \alpha_m) \beta_{m,2} (E_{D,m} - \bar{D}_m) \\ -L_{min} + D(r_{m,1}) \\ \vdots \\ -L_{min} + D(r_{m,N_m}) \end{bmatrix}$$

where

$$\mathbf{a}_m = \frac{1}{N_m} \sum_{(x,y,z) \in R_m} \begin{bmatrix} E_1(x, y, z) \\ E_2(x, y, z) \\ \vdots \\ E_M(x, y, z) \end{bmatrix},$$

$$\bar{D}_m = \frac{1}{N_m} \sum_{(x,y,z) \in R_m} D(x, y, z),$$

$$\mathbf{c}_{m,n} = [E_1(r_{m,n}) \quad \dots \quad E_M(r_{m,n})]^T,$$

CHAPTER 4. LIGHTING CONTROL STRATEGIES ACCOUNTING FOR USER PREFERENCES

$\mathbf{0}_{N \times M}$ is a matrix of 0s of size $N \times M$ and \mathbf{e}_m is a vector of length M with all element 0 except the m -th element which is equal to 1. $D(r)$ denotes the daylight value evaluated at location r .

To deal with some of the elements of \mathbf{t} being negative, we introduce new variable vectors \mathbf{t}^+ and \mathbf{t}^- , whose elements are non-negative. Subsequently, (4.9) can be rewritten in matrix form as

$$\begin{aligned} & \min_{\mathbf{t}} \mathbf{1}^T \mathbf{t}^+ - \mathbf{1}^T \mathbf{t}^- \\ \text{s.t. } & \begin{cases} \mathbf{Kd} - \mathbf{Tt}^+ + \mathbf{Tt}^- + \mathbf{Ss} = \mathbf{b} \\ 0 \leq d_m \leq 1, \quad m = 1, \dots, M \\ s_{m,r} \geq 0, \quad m = 1, \dots, M \text{ and } r = 1, \dots, \bar{N}_m \\ t_m^+ \geq 0, \quad m = 1, \dots, M \\ t_m^- \geq 0, \quad m = 1, \dots, M \end{cases} \end{aligned} \quad (4.10)$$

where $\mathbf{1}$ is a vector of 1s,

$$\begin{aligned} \mathbf{K} &= \begin{bmatrix} \mathbf{K}_1 \\ \vdots \\ \mathbf{K}_M \end{bmatrix}, \quad \mathbf{T} = \begin{bmatrix} \mathbf{T}_1 \\ \vdots \\ \mathbf{T}_M \end{bmatrix}, \\ \mathbf{S} &= \begin{bmatrix} \mathbf{S}_1 \\ \vdots \\ \mathbf{S}_M \end{bmatrix}, \quad \mathbf{b} = \begin{bmatrix} \mathbf{b}_1 \\ \vdots \\ \mathbf{b}_M \end{bmatrix}, \\ \mathbf{S}_m &= [\mathbf{0}_{\bar{N}_m \times \bar{N}_1} \quad \dots \quad \mathbf{I}_{\bar{N}_m} \quad \dots \quad \mathbf{0}_{\bar{N}_m \times \bar{N}_M}], \\ \mathbf{t}^+ &= [t_1^+, t_2^+, \dots, t_M^+]^T, \\ \mathbf{t}^- &= [t_1^-, t_2^-, \dots, t_M^-]^T, \\ \mathbf{s} &= [\mathbf{s}_1^T \quad \mathbf{s}_2^T \quad \dots \quad \mathbf{s}_M^T]^T, \\ \mathbf{s}_m &= [s_{m,1}, s_{m,2}, \dots, s_{m,\bar{N}_m}]^T, \\ \bar{N}_m &= \begin{cases} 2N_m + 2, & \text{if } m \in \mathcal{S}_o \\ N_m + 2, & \text{if } m \in \mathcal{S}_u, \end{cases} \end{aligned}$$

and \mathbf{I}_N is the identity matrix of size $N \times N$.

The linear programming optimization problem in (4.10) can be now solved using the two-phase simplex method [19] for bounded variables. Phase-I of the method provides a basic feasible solution of the problem, if one exists. In Phase-II, the simplex method improves towards an optimal solution starting from the basic feasible solution.

4.3.2 Distributed control

The distributed lighting control scenario is relevant in lighting systems where the desire is to embed the intelligence at the luminaire level, rather than at a centralized unit. In distributed lighting control, each controller determines the dimming level of its associated luminaire based on knowledge of local constraints over the associated zone and information exchange with other controllers. Note that the constraints in (4.10) are distributed across all the controllers. We propose the use of a distributed implementation of the two-phase simplex method. The presented algorithm extends the basic simplex method in [20] to the case of bounded variables and such that each controller can determine the dimming level of its associated luminaire.

Let the m -th controller own a local tableau given by

$$\mathbf{A}_m = [\mathbf{K}_m \quad -\mathbf{T}_m \quad \mathbf{T}_m \quad \mathbf{S}_m \quad \mathbf{b}_m].$$

Note that the total number of columns in \mathbf{A}_m is equal to $\bar{M} = 3M + \sum_m \bar{N}_m + 1$ (total number of variables plus one).

Additionally, the m -th controller owns the variables $Bound_m$ and Row_m . The variable $Bound_m$ indicates if d_m is at its lower bound ($Bound_m = 0$) or upper bound ($Bound_m = 1$).

The variable Row_m is used to obtain the value of d_m as

$$d_m = \begin{cases} 1 - [\mathbf{A}_m]_{Row_m, \bar{M}} & , \text{ if } Row_m > 0 \text{ and } Bound_m = 1 \\ [\mathbf{A}_m]_{Row_m, \bar{M}} & , \text{ if } Row_m > 0 \text{ and } Bound_m = 0 \\ 1 & , \text{ if } Row_m = 0 \text{ and } Bound_m = 1 \\ 0 & , \text{ if } Row_m = 0 \text{ and } Bound_m = 0. \end{cases} \quad (4.11)$$

In order to avoid degeneracy in the simplex method (i.e. a basic variable is equal to zero), we initialize the variables $\{d_m\}$ with the upper bound, i.e. $d_m = 1$, $m = 1, \dots, M$. Accordingly, we modify the tableau \mathbf{A}_m as

$$\begin{aligned} [\mathbf{A}_m]_{r, \bar{M}} &= [\mathbf{A}_m]_{r, \bar{M}} - \sum_{q=1}^M [\mathbf{A}_m]_{r, q}, \quad r = 1, \dots, \bar{N}_m, \\ [\mathbf{A}_m]_{r, q} &= -[\mathbf{A}_m]_{r, q}, \quad r = 1, \dots, \bar{N}_m \text{ and } q = 1, \dots, M. \end{aligned}$$

CHAPTER 4. LIGHTING CONTROL STRATEGIES ACCOUNTING FOR USER PREFERENCES

Using these values, the initial solution for the problem is

$$\begin{aligned}
 \mathbf{d}^{(0)} &= \mathbf{1}, \\
 \mathbf{t}^{+(0)} &= \mathbf{0}_{M \times 1}, \\
 \mathbf{t}^{-(0)} &= \mathbf{0}_{M \times 1}, \\
 s_{m,r}^{(0)} &= [\mathbf{A}_m]_{r,\bar{M}}, \quad r = 1, \dots, \bar{N}_m, \quad m = 1, \dots, M, \\
 \text{Bound}_m &= 1, \quad m = 1, \dots, M \text{ and} \\
 \text{Row}_m &= 0, \quad m = 1, \dots, M.
 \end{aligned}$$

In most cases, this solution is not feasible, i.e. $\{\exists s_{m,r}^{(0)} : s_{m,r}^{(0)} < 0, r = 1, \dots, \bar{N}_m, m = 1, \dots, M\}$. Hence, during Phase-I of the simplex method we find a feasible starting solution, i.e. a solution which does not violate any constraint ($\{\nexists s_{m,r}^{(0)} : s_{m,r}^{(0)} < 0, r = 1, \dots, \bar{N}_m, m = 1, \dots, M\}$). This is achieved by minimizing the sum of violation of constraints

$$\min \sum_{\{\forall r \forall m : s_{m,r} < 0\}} -s_{m,r}.$$

Accordingly, the objective function for Phase-I is

$$f^{\mathbf{I}} = \mathbf{c}^{\mathbf{I}} [\mathbf{d}^T \quad \mathbf{t}^{+T} \quad \mathbf{t}^{-T} \quad \mathbf{s}^T]^T,$$

where

$$\mathbf{c}^{\mathbf{I}} = \sum_{\{\forall r \forall m : s_{m,r} < 0\}} \left[[\mathbf{K}_m]_{r,:} \quad -[\mathbf{T}_m]_{r,:} \quad [\mathbf{T}_m]_{r,:} \quad [\mathbf{S}_m]_{r,:} \right]^T.$$

Also denote

$$\mathbf{p}^{\mathbf{I}} = [\mathbf{c}^{\mathbf{I}} \quad f^{\mathbf{I}}].$$

Note that Phase-I ends when the objective function reaches zero (there is no constraint which is violated) or the problem is determined to be unfeasible.

After a feasible solution has been found in Phase-I, we proceed to improve it by minimizing the objective function for Phase-II given by

$$f^{\mathbf{II}} = \mathbf{1}^T \mathbf{t}^+ - \mathbf{1}^T \mathbf{t}^-,$$

which is the original objective function in (4.10). Denote

$$\mathbf{p}^{\mathbf{II}} = [\mathbf{0}_{1 \times M} \quad \mathbf{1}^T \quad -\mathbf{1}^T \quad \mathbf{0}_{1 \times \bar{N}_1} \quad \dots \quad \mathbf{0}_{1 \times \bar{N}_M} \quad -f^{\mathbf{II}}].$$

The two-phase distributed simplex algorithm is described as follows in the form of pseudo-code:

1. For each controller, execute routine 1. Transmit the local minimum $\{\mu_m\}$ to the other controllers
2. Obtain the global minimum between all the controllers. Execute routine 2.
3. If $Case_{m^*}$ is (a), then go to step 4. Otherwise, execute routine 3 in the controller to which the global minimum belongs (m^* -th controller).
4. If $Case_{m^*}$ is (b) or (c), then wait till *Pivot* is received from the m^* -th controller. Execute routine 4.
5. Repeat procedure from step 1.

CHAPTER 4. LIGHTING CONTROL STRATEGIES ACCOUNTING FOR USER PREFERENCES

Routine 1 Local minimum for the m -th controller

Let the local minimum be denoted by

$$\mu_m = \{ \textit{Value}_m; \textit{Case}_m; \textit{IndexVariable}_m; \textit{IndexRow}_m \}$$

where

\textit{Value}_m : Minimum value for the m -th controller,

\textit{Case}_m : ID of the case that has the minimum value

$\textit{IndexVariable}_m$: Index of the variable to be modified.

$\textit{IndexRow}_m$: Index of the row for pivoting.

Require: \mathbf{p}^{I} (or \mathbf{p}^{II}), \mathbf{A}_m

if Phase-I **then**

$$\hat{q} \leftarrow \arg \min_q \left\{ [\mathbf{p}^{\text{I}}]_q, q = 1, \dots, \bar{M} - 1 \right\}$$

else

$$\hat{q} \leftarrow \arg \min_q \left\{ [\mathbf{p}^{\text{II}}]_q, q = 1, \dots, \bar{M} - 1 \right\}$$

end if

$\textit{IndexVariable}_m \leftarrow \hat{q}$

if $\hat{q} \leq M$ **then**

$$\textit{Ratio}_a \leftarrow 1$$

end if

if $\exists r : [\mathbf{A}_m]_{r, \hat{q}} > 0$ **then**

$$\hat{r} \leftarrow \arg \min_r \left\{ \frac{[\mathbf{A}_m]_{r, \bar{M}}}{[\mathbf{A}_m]_{r, \hat{q}}} : [\mathbf{A}_m]_{r, \hat{q}} > 0 \text{ and } r = 1, \dots, \bar{N}_m \right\}$$

$$\textit{Ratio}_b \leftarrow \frac{[\mathbf{A}_m]_{\hat{r}, \bar{M}}}{[\mathbf{A}_m]_{\hat{r}, \hat{q}}}$$

end if

if $\textit{Row}_m > 0$ **and** $[\mathbf{A}_m]_{\textit{Row}_m, \hat{q}} < 0$ **then**

$$\textit{Ratio}_c \leftarrow \frac{[\mathbf{A}_m]_{\textit{Row}_m, \bar{M}-1}}{[\mathbf{A}_m]_{\textit{Row}_m, \hat{q}}}$$

end if

Continue...

Routine 1 Local minimum for the m -th controller

...Continue
 Choose minimum amongst $\{Ratio_a, Ratio_b, Ratio_c\}$
if $Ratio_a$ is the minimum **then**
 $Value_m \leftarrow Ratio_a$
 $Case_m \leftarrow (a)$
 $IndexRow_m \leftarrow 0$
else if $Ratio_b$ is the minimum **then**
 $Value_m \leftarrow Ratio_b$
 $Case_m \leftarrow (b)$
 $IndexRow_m \leftarrow \hat{r}$
else if $Ratio_c$ is the minimum **then**
 $Value_m \leftarrow Ratio_c$
 $Case_m \leftarrow (c)$
 $IndexRow_m \leftarrow Row_m$
end if

Routine 2 Global minimum

Let the global minimum be denoted by

$$\{IDController, IDOwnerVariable, \mu_{m^*}\}$$

where

IDController: ID of the controller that owns the global minimum ,

IDOwnerVariable: ID of the controller that must know the value of the variable.

Require: $\{\mu_m\}$, a set of local minimums from all the controllers.

$m^* \leftarrow \arg \min_m \{Value_m\}$
 $IDController \leftarrow m^*$
if $IndexVariable_{m^*} \leq M$ **then**
 $IDOwnerVariable \leftarrow IndexVariable_{m^*}$
else
 $IDOwnerVariable \leftarrow m^*$
end if

CHAPTER 4. LIGHTING CONTROL STRATEGIES ACCOUNTING FOR USER PREFERENCES

Routine 3 Transmit row from m^* -th controller

Let $q^* = IndexVariable_{m^*}$ and $r^* = IndexRow_{m^*}$ where $\{IDController; IDOwnerVariable; \mu_{m^*}\}$ is the global minimum.

if $Case_{m^*} = (b)$ **then**

$$[A_{m^*}]_{r^*,q} \leftarrow \frac{[A_{m^*}]_{r^*,q}}{[A_{m^*}]_{r^*,q^*}}, q = 1, \dots, \bar{M}$$

else if $Case_{m^*} = (c)$ **then**

Change $Bound_m$ to its opposite bound

$$[A_{m^*}]_{r^*,\bar{M}} \leftarrow [A_{m^*}]_{r^*,\bar{M}} - 1$$

$$[A_{m^*}]_{r^*,m^*} \leftarrow -[A_{m^*}]_{r^*,m^*}$$

$$[A_{m^*}]_{r^*,q} \leftarrow \frac{[A_{m^*}]_{r^*,q}}{[A_{m^*}]_{r^*,q^*}}, q = 1, \dots, \bar{M}$$

$$Row_{m^*} \leftarrow 0$$

end if

Transmit $Pivot = [A_{m^*}]_{r^*,:}$

Routine 4a Interchange rows for the m -th controller

Let $\{IDController; IDOwnerVariable; \mu_{m^*}\}$ be the global minimum.

if $IndexVariable_{m^*} \leq M$ **then**

if $m = IDController$ **and** $m \neq IDOwnerVariable$ **then**

Delete $IndexRow_{m^*}$ -th row from the tableau A_m

$IDController \leftarrow IDOwnerVariable$

else if $m \neq IDController$ **and** $m = IDOwnerVariable$ **then**

Add $Pivot$ to the beginning of the tableau A_m

$IndexRow_{m^*} \leftarrow 1$

$IDController \leftarrow m$

end if

end if

Routine 4 Update local tableau for the m -th controller

Let $q^* = \text{IndexVariable}_{m^*}$ and $r^* = \text{IndexRow}_{m^*}$ where $\{IDController; IDOwnerVariable; \mu_{m^*}\}$ is the global minimum.

Require: *Pivot*

if $Case_{m^*} = (a)$ **then**

$$[\mathbf{A}_m]_{r, \bar{M}} \leftarrow [\mathbf{A}_m]_{r, \bar{M}} - [\mathbf{A}_m]_{r, q^*}, \quad r = 1, \dots, \bar{N}_m$$

$$[\mathbf{A}_m]_{r, q^*} \leftarrow -[\mathbf{A}_m]_{r, q^*}, \quad r = 1, \dots, \bar{N}_m$$

if Phase-I **then**

$$[\mathbf{p}^I]_{\bar{M}} \leftarrow [\mathbf{p}^I]_{\bar{M}} - [\mathbf{p}^I]_{q^*}$$

$$[\mathbf{p}^I]_{q^*} \leftarrow -[\mathbf{p}^I]_{q^*}$$

end if

$$[\mathbf{p}^{II}]_{\bar{M}} \leftarrow [\mathbf{p}^{II}]_{\bar{M}} - [\mathbf{p}^{II}]_{q^*}$$

$$[\mathbf{p}^{II}]_{q^*} \leftarrow -[\mathbf{p}^{II}]_{q^*}$$

if $m = IDController$ **then**

Change $Bound_m$ to its opposite bound

end if

else if $Case_{m^*} = (b)$ **or** $Case_{m^*} = (c)$ **then**

Call Routine 4a

Perform Gaussian-Jordan elimination in \mathbf{A}_m with *Pivot*
(exclude the r^* -th row if $m = IDController$)

if Phase-I **then**

$$\mathbf{p}^I \leftarrow \mathbf{p}^I - [\mathbf{p}^I]_{q^*} \times \text{Pivot}$$

end if

$$\mathbf{p}^{II} \leftarrow \mathbf{p}^{II} - [\mathbf{p}^{II}]_{q^*} \times \text{Pivot}$$

if $q^* \leq M$ **and** $m = IDController$ **then**

$$Row_m = r^*$$

end if

end if

Some comments about the procedure. The procedure terminates Phase-I (or Phase-II) when no more messages are exchanged between the controllers or all the elements of \mathbf{p}^I (or \mathbf{p}^{II}) are larger than zero in Routine 1.

The final tableau of the procedure after executing Phase-I is used as the initial tableau for Phase-II. Let \mathbf{A}_m^* be the resulting matrix after finishing Phase-II. The optimum dimming level d_m^* for the LED in the m -th controller is obtained from the respective matrix \mathbf{A}_m^* using (4.11).

4.4 Simulation results

In this Section, we present simulation results to show the performance of the proposed control schemes in an office setting. The office has length 12 m and width 7.5 m with the workspace plane at a height of 1.88 m from the lighting plane as shown in fig. 4.1, with the model generated in DIALux [21]. A top view of the office layout is depicted in Fig. 4.1. There are eighteen LED luminaires of type Philips BCS640 W21L120 1xLED48/840, spaced 2 m along the length and 2.5 m along the width. The luminaire indexing in Fig. 4.1 also corresponds to that of the controllers for the distributed lighting control scenario. The office has a window on one side (top part in Fig. 4.1) for daylight ingress.

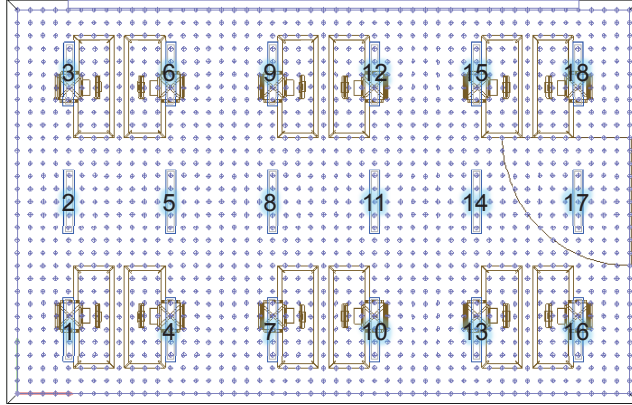


Figure 4.1: Top view of example office

As reference, we consider a strategy in which the dimming levels of the luminaires are set such that 500 lux illuminance is achieved across the workspace plane with a uniformity contrast of 30%. To render this illumination, the luminaires are set at a dimming level of 0.85. Note that this value of dimming level depends on factors such as luminaire-type, configuration of luminaire grid, office room layout, and as such has to be computed for a given office lighting setting.

We now consider the centralized control scheme with the following parameters. The value of $\eta = 1/P_{on}$, $\beta_{m,1} = -1/25$, $\beta_{m,2} = 1/50$, $m = 1, \dots, 18$, $\alpha_1 = \alpha_{13} = 0.2$, $\alpha_9 = \alpha_{18} = 0.6$, and $\alpha_m = 0.8$ in the remaining zones. In occupied zones, the contrast $C_{th} = 0.3$ with a desired average illuminance level of 500 lux. In unoccupied zones, a desired average illuminance level of 300 lux is chosen, with $L_{min} = 270$ lux.

To evaluate performance, we first consider the solution of optimization prob-

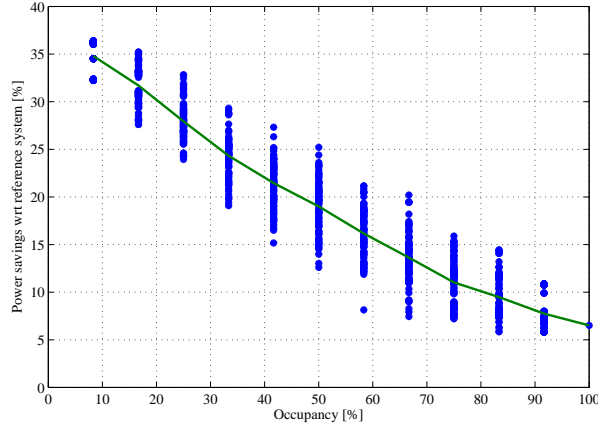


Figure 4.2: Power saving under proposed control strategy in comparison with reference systems (no daylight case)

lem (4.10) without daylight contribution (i.e. with $D(x, y, z) = 0$). We simulated 100 occupancy realizations at different percentages of occupancy. Fig. 4.2 shows the power savings achieved under the proposed localized illumination rendering strategy relative to the reference control strategy. For instance, at an occupancy level of 50%, there is about 19% power savings on an average under the proposed strategy with the savings varying between 13% and 25% depending on the particular occupancy realization. Note in Fig. 4.2 that at a given percentage of occupancy, the power savings show variations. This is since the power savings depend on occupant locations as well as daylight contribution in a zone, or the illuminance required further from artificial light to meet the illuminance constraints. In Figs. 4.3 and 4.4, we show the illuminance distribution and the dimming levels upon optimization for a specific occupancy realization where zones 1, 9, 13 and 18 are occupied. We note that under the optimum dimming solution shown in Fig. 4.4, some of the luminaires in zones adjacent to the occupied ones also dim up to meet the illumination rendering constraints. This is particularly evident in zones at the corners of the room. In Fig. 4.5, the average illuminance over each zone is shown along with the desired average illuminance values. Note that the deviation from the desired average illuminance value for users in zones 1 and 13 is smaller in comparison to that for users in zones 9 and 18, due to the larger weights that these users assigned to their satisfaction levels. Also a deviation in average illuminance values in unoccupied zones 4, 10, 15 and 16 is observed since these are adjacent to occupied zones and the dimming levels

CHAPTER 4. LIGHTING CONTROL STRATEGIES ACCOUNTING FOR USER PREFERENCES

of the associated luminaires are high in order to meet the illumination rendering constraints.

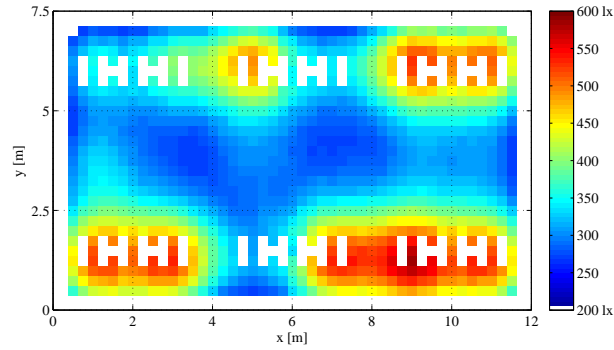


Figure 4.3: Illumination rendering over workspace plane under proposed control strategy (no daylight case)

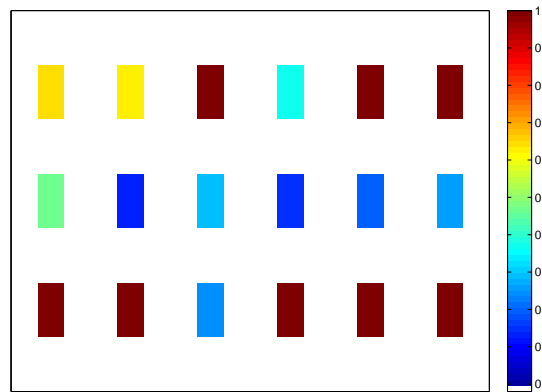


Figure 4.4: Optimum dimming levels of LED luminaires under proposed control strategy (no daylight case)

We now consider the daylight contribution with the same occupancy realization as before. The daylight distribution is depicted in Fig. 4.6. Upon optimizing (4.10), the resulting illuminance distribution is shown in Fig. 4.7 and the op-

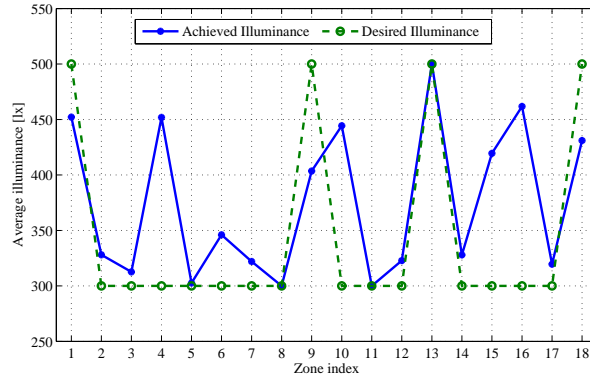


Figure 4.5: Comparison of achieved and desired average illuminance values in different zones (no daylight case)

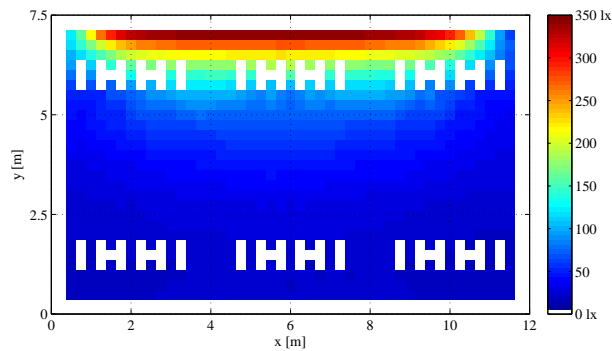


Figure 4.6: Daylight distribution over workspace plane

imum dimming values in Fig. 4.8. In Fig. 4.9, the average illuminance over each zone is shown along with the desired average illuminance values. The average illuminance values in occupied zones are close to the desired levels, while in unoccupied zones 2, 4, 10, 14 and 15, deviations from the minimum required illuminance are observed, these being adjacent to occupied zones.

The optimum solution under the distributed lighting control scenario is the same as in the centralized control scenario and is hence not shown. However the

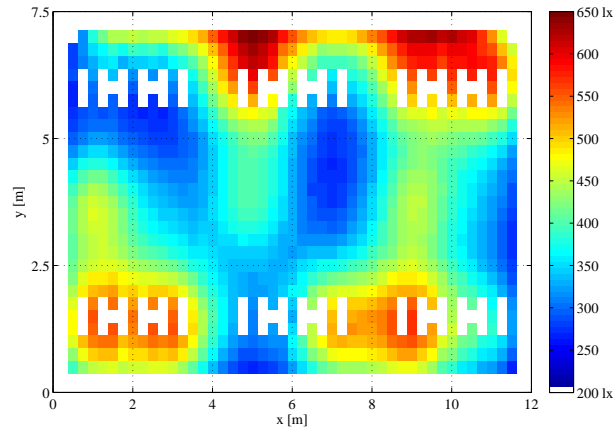


Figure 4.7: Illumination rendering over workspace plane under proposed control strategy (considering daylight case)

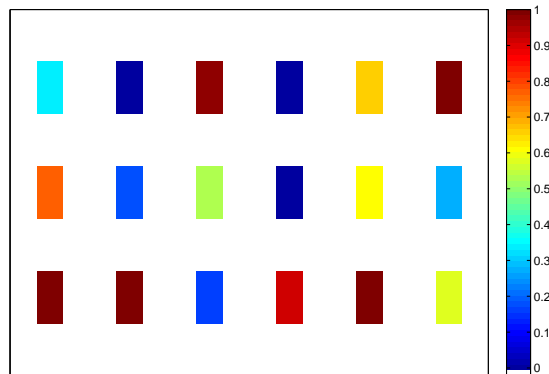


Figure 4.8: Optimum dimming levels of LED luminaires under proposed control strategy (considering daylight case)

computational complexity of the controllers under the two scenarios is different. Given a problem instance, i.e. for a fixed number of variables but possibly variable number of constraints, the computational complexity is linear in the number of constraints [22]. The number of constraints is the number of rows in the local tableau of the controller. We hence compare the number of rows in the local tableau per controller under both scenarios. In Fig. 4.10, we show the ratio of the

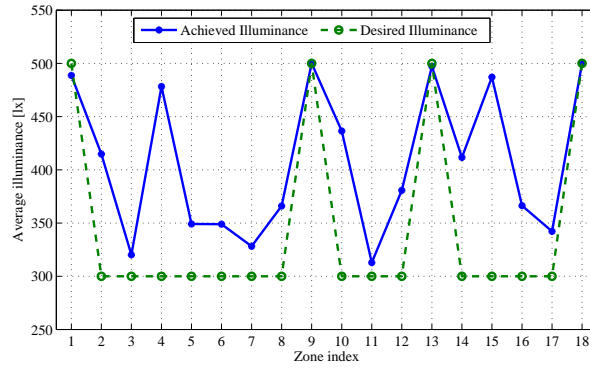


Figure 4.9: Comparison of achieved and desired average illuminance values in different zones (considering daylight case)

number of rows in the centralized controller to the number of rows per controller in the distributed lighting control system as a gain factor. Here, 100 occupancy realizations were considered. Clearly, a distributed implementation allows for less computationally complex controllers. This comes at additional communication across the controllers; however, in a networked distributed lighting system, this communication is at a negligible overhead.

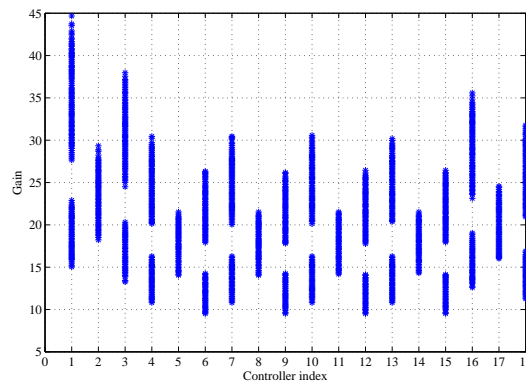


Figure 4.10: Gain in computational complexity per controller in the distribution lighting control system in comparison to the central controller

4.5 Conclusions

We have presented algorithms for centralized and distributed LED lighting control to achieve a balance between power minimization and user satisfaction with the rendered illuminance under a localized illumination rendering strategy. The proposed algorithms adapt to presence over zones, daylight distribution and user preference of illuminance levels. The performance of the proposed control strategy in achieving power saving and user satisfaction was shown using simulations in a multi-occupant office environment.

REFERENCES

- [1] F. Linhart and J.-L. Scartezzini, “Minimizing lighting power density in office rooms equipped with anidolic daylighting systems,” *Solar Energy*, vol. 84, no. 4, pp. 587–595, 2010.
- [2] D. H. W. Li and J. C. Lam, “Evaluation of lighting performance in office buildings with daylighting controls,” *Energy and Buildings*, vol. 33, no. 8, pp. 793 – 803, 2001.
- [3] J. A. Veitch, G. R. Newsham, P. R. Boyce, and C. C. Jones, “Lighting appraisal, well-being and performance in open-plan offices: A linked mechanisms approach,” *Lighting Research and Technology*, vol. 40, no. 2, pp. 133–151, 2008.
- [4] Energy Information Administration, “Commercial buildings energy consumption survey,” 2003.
- [5] M.-S. Pan, L.-W. Yeh, Y.-A. Chen, Y.-H. Lin, and Y.-C. Tseng, “A WSN-based intelligent light control system considering user activities and profiles,” *IEEE Sensors Journal*, pp. 1710–1721, 2008.
- [6] A. Pandharipande and D. Caicedo, “Daylight integrated illumination control of LED systems based on enhanced presence sensing,” *Energy and Buildings*, vol. 43, pp. 944–950, April 2011.
- [7] B. Roisin, M. Bodart, A. Deneyer, and P. D. Herdt, “Lighting energy savings in offices using different control systems and their real consumption,” *Energy and Buildings*, vol. 40, no. 4, pp. 514 – 523, 2008.
- [8] V. Singhvi, A. Krause, C. Guestrin, J. H. G. Jr., and H. S. Matthews, “Intelligent light control using sensor networks,” *International Conference on Embedded Networked Sensor Systems*, pp. 218 – 229, 2005.
- [9] S. Tanaka, M. Miki, A. Amamiya, and T. Hiroyasu, “An evolutionary optimization algorithm to provide individual illuminance in workplaces,” *IEEE International Conference on Systems, Man and Cybernetics*, pp. 941–947, 2009.
- [10] L.-W. Yeh, C.-Y. Lu, C.-W. Kou, Y.-C. Tseng, and C.-W. Yi, “Autonomous light control by wireless sensor and actuator networks,” *IEEE Sensors Journal*, pp. 1029–1041, June 2010.

CHAPTER 4. LIGHTING CONTROL STRATEGIES ACCOUNTING FOR USER PREFERENCES

- [11] D. Caicedo, A. Pandharipande, and G. Leus, “Occupancy based illumination control of LED lighting systems,” *Lighting Research and Technology*, vol. 43, no. 2, pp. 217–234, August 2011.
- [12] M. Miki, A. Amamiya, and T. Hiroyasu, “Distributed optimal control of lighting based on stochastic hill climbing method with variable neighborhood,” *IEEE International Conference on Systems, Man and Cybernetics*, pp. 1676–1680, 2007.
- [13] H. Yang, T. C. W. Schenk, J. W. M. Bergmans, and A. Pandharipande, “Enhanced illumination sensing using multiple harmonics for LED lighting systems,” *IEEE Transactions on Signal Processing*, vol. 58, pp. 5508 – 5522, November 2010.
- [14] Y. Gu, N. Narendran, T. Dong, and H. Wu, “Spectral and luminous efficacy change of high-power LEDs under different dimming methods,” *International Conference on Solid State Lighting, SPIE*, vol. 6337, p. 63370J, 2006.
- [15] http://www.lighting.philips.com/main/connect/tools_literature/dialux_and_other_downloads.wpd.
- [16] P. R. Boyce, *Human Factors in Lighting*, 2nd ed. New York: Taylor and Francis, 2003.
- [17] European Committee for Standardization, “EN 12464-1:2002. Light and lighting. Lighting of work places. Part 1: Indoor work places,” 2002.
- [18] D. Bertsimas and J. Tsitsiklis, *Introduction to Linear Optimization*. Athena Scientific, 1997.
- [19] D. G. Luenberger and Y. Ye, *Linear and Nonlinear Programming*, 3rd ed. Springer, 2008.
- [20] H. Dutta and H. Kargupta, “Distributed linear programming and resource management for data mining in distributed environments,” *IEEE International Conference on Data Mining Workshops*, pp. 543–552, 2008.
- [21] DIALux, <http://www.dial.de/DIAL/en/dialux.html>.
- [22] G. Yarmish and R. V. Slyke, “A distributed, scaleable simplex method,” *Journal of Supercomputing*, vol. 49, no. 3, pp. 373–381, 2009.

Distributed lighting control with light sensor measurements*

We consider the problem of illumination control in a networked lighting system wherein luminaires have local sensing and actuation capabilities. Each luminaire (i) consists of a light emitting diode (LED) based light source dimmable by a local controller, (ii) is actuated based on sensing information from a presence sensor, that determines occupant presence, and a light sensor, that measures illuminance, within their respective fields of view, and (iii) a communication module to exchange control information within a local neighborhood. We consider distributed illumination control in such an intelligent lighting system to achieve presence-adaptive and daylight-integrated spatial illumination rendering. The rendering is specified as target values at the light sensors, and under these constraints, a local controller has to determine the optimum dimming levels of its associated LED luminaire so that the power consumed in rendering is minimized. The formulated optimization problem is a distributed linear programming problem with constraints on exchanging control information within a neighborhood. A distributed optimization algorithm is presented to solve this problem and its stability and convergence are studied. Sufficient conditions, in terms of parameter selection, under which the algorithm can achieve a feasible solution are provided. The performance of the algorithm is evaluated in an indoor office setting in terms of achieved illuminance rendering and power savings.

*This chapter has been published as: D. Caicedo and A. Pandharipande, "Distributed illumination control with local sensing and actuation in networked lighting systems", *IEEE Sensors Journal*, vol. 13, pp. 1092 – 1104, March 2013.

5.1 Introduction

Advances in semiconductors have brought in a new generation of light sources in the form of light emitting diodes (LEDs). Miniaturization and rapid cost-downs from semiconductorization has also made it possible for greater integration of sensing, communication, computation and control functions into luminaires. This has made intelligent LED luminaires feasible, that (i) are dimmable by an associated local controller, (ii) can be actuated based on local sensing inputs such as presence detection and light intensity measurement within the sensor field of view, and (iii) can exchange control information within a local neighborhood using a communication module. We address the problem of illumination control in a system of such intelligent luminaires to achieve energy-efficient illumination rendering over the workspace.

We consider illumination control for indoor office general lighting applications. Office lighting is one of the major constituents of electrical energy consumption in buildings [1]. As such, energy-efficient strategies for illumination rendering in lighting systems are of interest. We consider presence-adaptive, daylight-integrated illumination rendering in this paper. In particular, we want to achieve uniform illumination at an average illuminance of L_{WP}^o in an occupied zone and a lower average illuminance of L_{WP}^u otherwise over the workspace plane. Local occupancy in a zone is determined by a presence sensor. In office lighting, the illumination distribution achieved at the workspace plane, typically corresponding to desk level, is of most interest. This is a horizontal plane at a certain vertical height from the ceiling plane, in which the luminaires are located. Illuminance is however measured in practice using light sensors placed in the ceiling. As such, light measurement is in a plane different from the one where the spatial illumination rendering is desired. Also, a light sensor measures a spatial average of the light distribution in its field of view. A light sensor calibration step is thus employed to obtain target sensor values. These target light sensor illuminance values then specify the rendering constraints to be satisfied under distributed control. The specifics of the lighting system are described in Section 5.2.

For a given realization of occupancy and daylight distribution in the office space, the local controller needs to determine the dimming level of its associated luminaire using local presence and light sensor measurements and communication with controllers in its neighborhood. This problem is mathematically a distributed linear programming problem with constraints on information exchange, and is formulated in Section 5.3. We present a distributed optimization algorithm to obtain a suboptimum solution to this problem, and is described in Section 5.4. A bound is further obtained on the deviation of the resulting power consumption from that obtained under optimum dimming. In Section 5.5, we analyze stability

and convergence of the proposed algorithm. Sufficient conditions are provided for specifying the neighborhood for exchanging control information such that the algorithm can achieve the target sensor values, i.e. a feasible solution is obtained.

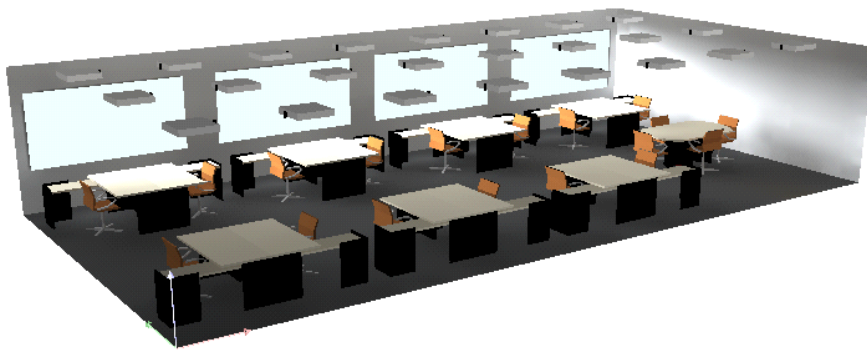
We evaluate the performance of the distributed illumination control algorithm with an example open office lighting simulation. The performance is evaluated based on the achieved illumination rendering and power savings. A comparison is made with an optimum centralized control algorithm. These numerical results are presented in Section 5.6.

Different lighting control approaches exist in literature [2–8], depending on the system architecture, connectivity and optimization algorithms employed. A numerical optimization approach to energy-efficient central control of polychromatic solid state lighting systems was presented in [2]. Under a centralized control system, a simplex algorithm was used in [3] to solve the resulting optimization problem for achieving illumination rendering adapted to occupancy, with [4] extending the control system to take daylight variations into account. In [5], user preferences for lighting conditions were additionally accounted for, assuming availability of rich light sensing information at the workspace plane, and centralized and distributed simplex algorithms were presented. The distributed simplex algorithm in [5] however requires information exchange between all controllers in the system. In [6], a heuristic distributed algorithm was proposed, again assuming availability of rich light sensing information at the workspace plane. Under different system considerations, linear programming and sequential quadratic programming approaches were used for centralized lighting control [7], [8]. A sensing solution to disaggregate daylight and artificial light was proposed in [9], which may be used to simplify daylight-adaptive lighting control.

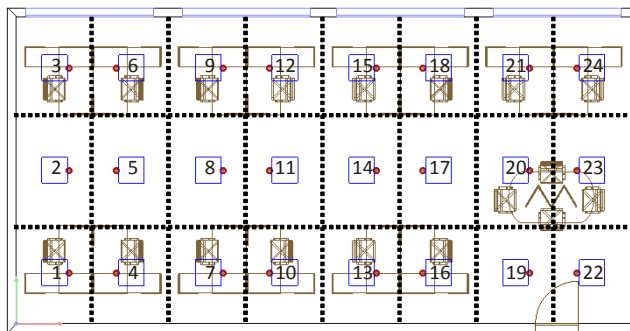
5.2 System model

Consider a lighting system in an indoor office with M LED luminaires arranged in the ceiling, an example illustration shown in Fig. 5.1(a) with $M = 24$. Parallel to the ceiling is the workspace plane, a plane over which spatial illumination rendering is of interest. The workspace plane is assumed to be divided into M logical zones, as shown in the example of Fig. 5.1(b). Each luminaire contains a local controller, an LED light source, a light sensor, a presence sensor and a communication module. Typically, a photodiode or a light dependent resistor may be used as a light sensor. Common modalities for presence sensing are passive infrared and ultrasound. We shall assume a simplified presence and light sensor model. We assume a light sensor with a well-defined sensing region defined by its opening angle. We assume that the presence sensing region is

CHAPTER 5. DISTRIBUTED LIGHTING CONTROL WITH LIGHT
SENSOR MEASUREMENTS



(a)



(b)

Figure 5.1: (a) Lighting system in an example office room, (b) Depiction of logical zones in the workspace plane (blue rectangles depict luminaires and red circles depict light sensors).

constrained to a zone, and that there are no missed detections or false alarms. In practice, the sensing region may extend further and an occupant outside the zone might be detected by the presence sensor. Furthermore, a missed detection over a zone would lead to specification of a lower average illuminance value to be achieved, while a false alarm would lead to higher average illuminance requirement. As a result, in the former case, the rendered illumination upon lighting control might lead to occupant dissatisfaction and in the latter case additional power consumption.

The local controller determines the dimming level of the associated LED luminaire, such that the resulting illumination rendered from the lighting system achieves target illuminance values at the light sensors. The target illuminance at the light sensor is the mapped value of the required average illuminance in the corresponding zone in the workspace plane, and is done in a dark room calibration step. Denote the target illuminance level at the m -th light sensor when the m -th zone is occupied (respectively, unoccupied) as L_m^o (respectively, L_m^u). We assume that after calibration, the measured illuminance at the m -th light sensor when the n -th luminaire is at maximum intensity is proportional to the average illuminance over the corresponding zone at the workspace plane.

We consider a distributed control scenario for illumination rendering with only neighborhood communication. Communication can be achieved using IEEE 802.15.4 radios [10] or visible light communications IEEE 802.15.7 [11]. Each controller only knows dimming level information of its own luminaire and that from its closest neighbors. Light sensing and presence information in a zone is only known locally to the corresponding controller. The local controllers also know the global occupancy/vacancy state in the office space so that the corresponding target average illuminance values in their associated zones may be set. Based on sensing information and coordination with neighboring controllers, each controller determines the dimming level of its luminaire such that the total power consumption is minimized while achieving the illumination rendering constraints as specified at the light sensors. We assume that each controller can communicate reliably with neighboring controllers.

5.2.1 Dimming of light sources

We assume that the LED light source is dimmed using pulse width modulation [12]. Let d_n , where $0 \leq d_n \leq 1$, be the dimming level of the n -th luminaire. The value $d_n = 0$ means that the LED luminaire is dimmed off completely, while $d_n = 1$ represents that the luminaire is at its maximum luminance level. Let \mathbf{d}

CHAPTER 5. DISTRIBUTED LIGHTING CONTROL WITH LIGHT
SENSOR MEASUREMENTS

be the $M \times 1$ dimming vector for the luminaires of the lighting system given by

$$\mathbf{d} = [d_1, d_2, \dots, d_M]^T,$$

indicating that the n -th LED luminaire is at dimming level d_n .

5.2.2 Illuminance at light sensor

The measured illuminance at the light sensor at the ceiling is the combined illuminance contribution due to the luminaires and daylight reflected from the objects (e.g. furniture) in the office. Denote $\hat{E}_{m,n}(d_n)$ to be the measured illuminance at the m -th light sensor when the n -th luminaire is at dimming level d_n , in the absence of daylight and when the other luminaires are turned off. We assume that the illuminance scales linearly with the dimming level, i.e.

$$\hat{E}_{m,n}(d_n) = d_n \hat{E}_{m,n}(1). \quad (5.1)$$

This assumption holds well for LED luminaires. In particular in Fig. 5.2, we plot $\hat{E}_{m,n}(d_n)/\hat{E}_{m,n}(1)$ versus d_n for luminaire 9 w.r.t. light sensors 5, 6, 8, 9, 11, 12 for the office lighting system in Fig. 5.1 to illustrate that linearity holds. These illuminance values are obtained from photometric data from an implementation model of the lighting system in DIALux [13].

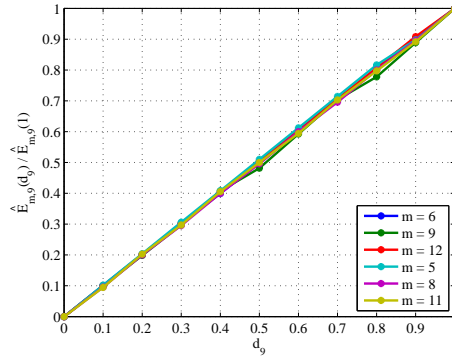


Figure 5.2: Linearity of light sensor illuminance values with respect to dimming level of luminaire 9.

The total illuminance at the m -th sensor at the ceiling, given that the lighting system is at dimming vector \mathbf{d} and under daylight, can then be written as

$$\bar{L}_m(\mathbf{d}) = \sum_{n=1}^M d_n \hat{E}_{m,n}(1) + \hat{O}_m,$$

5.3. DISTRIBUTED ILLUMINATION CONTROL WITH LOCAL SENSING AND ACTUATION: PROBLEM FORMULATION

where \hat{O}_m is the illuminance due to daylight measured at the m -th sensor. In practice, the mappings $\hat{E}_{m,n}(\cdot)$ may be computed a priori in a configuration phase by turning on the luminaires one at a time and measuring illuminance values at the light sensors.

5.3 Distributed Illumination control with local sensing and actuation: Problem formulation

Our objective is to minimize the power consumption of the lighting system subject to illuminance constraints at the light sensors and limited neighbor communication across local controllers. Formally, the global optimization problem may be posed as follows.

$$\begin{aligned} \mathbf{d}^* = \arg \min_{\mathbf{d}} \quad & \sum_{m=1}^M d_m \\ \text{s.t.} \quad & \begin{cases} \sum_{n=1}^M d_n \hat{E}_{m,n}(1) + \hat{O}_m \geq \hat{L}_m, & m = 1, \dots, M, \\ 0 \leq d_m \leq 1, & m = 1, \dots, M, \\ \{m\} \rightarrow \mathcal{N}_m, & m = 1, \dots, M. \end{cases} \end{aligned} \quad (5.2)$$

In the above,

$$\hat{L}_m = \begin{cases} L_m^o, & \text{if the } m\text{-th zone is occupied} \\ L_m^u, & \text{otherwise,} \end{cases}$$

is the target illuminance level at the m -th light sensor. In (5.2), the constraint $\{m\} \rightarrow \mathcal{N}_m$ means that the m -th controller can only communicate with controllers in a corresponding neighbor set, \mathcal{N}_m , where \mathcal{N}_m is the set of indices of N_m neighbors from the m -th controller,

$$\mathcal{N}_m = [\nu_{m,1}, \nu_{m,2}, \dots, \nu_{m,N_m}].$$

For simplicity, we assume reciprocity, i.e. if controller m is in the neighbor set of n , then controller n is also in the neighbor set of m . A local controller m has information on local occupancy in its associated zone and thus knows the appropriate target illuminance level \hat{L}_m , it has illuminance mappings $\{\hat{E}_{m,n}(1)\}$, $n \in \mathcal{N}_m \cup \{m\}$, and has the current measured illuminance value \bar{L}_m . Based on this information and exchange of control information, the local controllers seek a solution to (5.2).

CHAPTER 5. DISTRIBUTED LIGHTING CONTROL WITH LIGHT
SENSOR MEASUREMENTS

Note that the objective function and the first two sets of constraints in (5.2) are linear in the variables d_m . Upon introduction of slack variables $\{s_m\}$ and $\{t_m\}$ to write (5.2) in standard form [14], the problem may be rewritten in matrix form as

$$\begin{aligned} \mathbf{d}^* &= \arg \min_{\mathbf{d}, \mathbf{s}, \mathbf{t}} \mathbf{1}^T \mathbf{d} \\ \text{s.t.} & \begin{cases} \hat{\mathbf{E}}\mathbf{d} - \mathbf{s} = \hat{\mathbf{L}} - \hat{\mathbf{O}} \\ \mathbf{d} + \mathbf{t} = \mathbf{1} \\ d_m \geq 0, & m = 1, \dots, M, \\ s_m \geq 0, & m = 1, \dots, M, \\ t_m \geq 0, & m = 1, \dots, M, \\ \{m\} \rightarrow \mathcal{N}_m & m = 1, \dots, M, \end{cases} \end{aligned} \quad (5.3)$$

where

$$\begin{aligned} \hat{\mathbf{E}} &= \begin{bmatrix} \hat{E}_{1,1}(1) & \hat{E}_{1,2}(1) & \dots & \hat{E}_{1,M}(1) \\ \hat{E}_{2,1}(1) & \hat{E}_{2,2}(1) & \dots & \hat{E}_{2,M}(1) \\ \vdots & \vdots & \ddots & \vdots \\ \hat{E}_{M,1}(1) & \hat{E}_{M,2}(1) & \dots & \hat{E}_{M,M}(1) \end{bmatrix}, \\ \hat{\mathbf{L}} &= [\hat{L}_1, \hat{L}_2, \dots, \hat{L}_M]^T, \\ \hat{\mathbf{O}} &= [\hat{O}_1, \hat{O}_2, \dots, \hat{O}_M]^T, \\ \mathbf{s} &= [s_1, s_2, \dots, s_M]^T, \\ \mathbf{t} &= [t_1, t_2, \dots, t_M]^T, \end{aligned}$$

and $\mathbf{1}$ is the vector of 1s of size $M \times 1$. Also, $\hat{\mathbf{E}}$ is the illuminance transfer matrix relating the effect of the luminaires at the light sensors.

If we do not consider the neighbor communication constraints, problem (5.3) is a linear programming problem. A solution to this problem can be found by solving the primal problem

$$\begin{aligned} P_{min} &= \min_{\mathbf{d}, \mathbf{s}, \mathbf{t}} \mathbf{1}^T \mathbf{d} \\ \text{s.t.} & \begin{cases} \hat{\mathbf{E}}\mathbf{d} - \mathbf{s} = \hat{\mathbf{L}} - \hat{\mathbf{O}} \\ \mathbf{d} + \mathbf{t} = \mathbf{1} \\ d_m \geq 0, & m = 1, \dots, M, \\ s_m \geq 0, & m = 1, \dots, M, \\ t_m \geq 0, & m = 1, \dots, M, \end{cases} \end{aligned} \quad (5.4)$$

5.3. DISTRIBUTED ILLUMINATION CONTROL WITH LOCAL SENSING
AND ACTUATION: PROBLEM FORMULATION

and the associated dual problem

$$\begin{aligned}
 D_{min} &= \max_{\mathbf{u}, \mathbf{v}, \mathbf{w}} \left(\hat{\mathbf{L}} - \hat{\mathbf{O}} \right)^T \mathbf{u} - \mathbf{1}^T \mathbf{v} \\
 \text{s.t.} &\begin{cases} \hat{\mathbf{E}}^T \mathbf{u} - \mathbf{v} + \mathbf{w} = \mathbf{1} \\ u_m \geq 0, & m = 1, \dots, M, \\ v_m \geq 0, & m = 1, \dots, M, \\ w_m \geq 0, & m = 1, \dots, M, \end{cases} \quad (5.5)
 \end{aligned}$$

such that

$$\begin{aligned}
 d_m w_m &= 0, & m = 1, \dots, M \\
 s_m u_m &= 0, & m = 1, \dots, M \\
 t_m v_m &= 0, & m = 1, \dots, M
 \end{aligned} \quad (5.6)$$

where

$$\begin{aligned}
 \mathbf{u} &= [u_1, u_2, \dots, u_M]^T, \\
 \mathbf{v} &= [v_1, v_2, \dots, v_M]^T, \\
 \mathbf{w} &= [w_1, w_2, \dots, w_M]^T.
 \end{aligned}$$

For any feasible solution to the primal and dual problem that satisfies conditions in (5.6), the following condition holds [15, Chapter 5]

$$\left(\hat{\mathbf{L}} - \hat{\mathbf{O}} \right)^T \mathbf{u} - \mathbf{1}^T \mathbf{v} = \mathbf{1}^T \mathbf{d}. \quad (5.7)$$

Now, if we consider the neighbor communication constraint, then we need to limit all terms to the available information. It can be noted that we have all the required information for solving the primal problem in (5.4), given that

$$\begin{aligned}
 \hat{\mathbf{E}}\mathbf{d} + \mathbf{s} &= \hat{\mathbf{L}} - \hat{\mathbf{O}} \\
 \hat{\mathbf{E}}\mathbf{d} + \hat{\mathbf{O}} + \mathbf{s} &= \hat{\mathbf{L}} \\
 \bar{\mathbf{L}}(\mathbf{d}) + \mathbf{s} &= \hat{\mathbf{L}}
 \end{aligned}$$

where

$$\bar{\mathbf{L}}(\mathbf{d}) = \hat{\mathbf{E}}\mathbf{d} + \hat{\mathbf{O}}$$

and

$$\bar{\mathbf{L}}(\mathbf{d}) = [\bar{L}_1(\mathbf{d}) \quad \bar{L}_2(\mathbf{d}) \quad \dots \quad \bar{L}_M(\mathbf{d})]^T.$$

CHAPTER 5. DISTRIBUTED LIGHTING CONTROL WITH LIGHT
SENSOR MEASUREMENTS

However, we do not have all the information to solve the dual problem in (5.5). Thus, the additional constraints implies a change into

$$D_{max} = \max_{\tilde{\mathbf{u}}, \tilde{\mathbf{v}}, \tilde{\mathbf{w}}} \left(\hat{\mathbf{L}} - \hat{\mathbf{O}} \right)^T \tilde{\mathbf{u}} - \mathbf{1}^T \tilde{\mathbf{v}}$$

$$\text{s.t.} \begin{cases} \tilde{\mathbf{E}}^T \tilde{\mathbf{u}} - \tilde{\mathbf{v}} + \tilde{\mathbf{w}} = \mathbf{1} \\ \tilde{u}_m \geq 0, & m = 1, \dots, M, \\ \tilde{v}_m \geq 0, & m = 1, \dots, M, \\ \tilde{w}_m \geq 0, & m = 1, \dots, M \end{cases} \quad (5.8)$$

where $\tilde{\mathbf{E}}$ is the matrix containing only neighbor information where each element is given by

$$[\tilde{\mathbf{E}}]_{m,n} = \begin{cases} \hat{E}_{m,n} & , \text{ if } n \in \mathcal{N}_m \text{ or } m = n \\ 0 & , \text{ otherwise.} \end{cases}$$

The primal problem associated to the dual problem in (5.8) is given by

$$P_{max} = \min_{\tilde{\mathbf{d}}, \tilde{\mathbf{s}}, \tilde{\mathbf{t}}} \mathbf{1}^T \tilde{\mathbf{d}}$$

$$\text{s.t.} \begin{cases} \tilde{\mathbf{E}} \tilde{\mathbf{d}} - \tilde{\mathbf{s}} = \hat{\mathbf{L}} - \hat{\mathbf{O}} \\ \tilde{\mathbf{d}} + \tilde{\mathbf{t}} = \mathbf{1} \\ \tilde{d}_m \geq 0, & m = 1, \dots, M, \\ \tilde{s}_m \geq 0, & m = 1, \dots, M, \\ \tilde{t}_m \geq 0, & m = 1, \dots, M. \end{cases} \quad (5.9)$$

We propose to find a suboptimal solution to (5.3) by seeking a vector

$$[\mathbf{d}^{*T} \quad \mathbf{s}^{*T} \quad \mathbf{t}^{*T} \quad \tilde{\mathbf{u}}^{*T} \quad \mathbf{v}^{*T} \quad \tilde{\mathbf{w}}^{*T}]^T \quad (5.10)$$

that is a feasible solution for the primal problem (5.4) and dual problem (5.8), i.e.

$$\begin{cases} \tilde{\mathbf{E}}^T \tilde{\mathbf{u}}^* - \mathbf{v}^* + \tilde{\mathbf{w}}^* = \mathbf{1} \\ \tilde{\mathbf{E}} \mathbf{d}^* - \mathbf{s}^* = \hat{\mathbf{L}} - \hat{\mathbf{O}} \\ \mathbf{d}^* + \mathbf{t}^* = \mathbf{1} \end{cases} \quad (5.11)$$

and all the variables $\{d_m^*\}$, $\{s_m^*\}$, $\{t_m^*\}$, $\{\tilde{u}_m^*\}$, $\{v_m^*\}$ and $\{\tilde{w}_m^*\}$ are non-negative.

Furthermore, this vector also satisfies the complementary conditions

$$d_m^* \tilde{w}_m^* = 0, \quad m = 1, \dots, M \quad (5.12a)$$

$$s_m^* \tilde{u}_m^* = 0, \quad m = 1, \dots, M \quad (5.12b)$$

$$t_m^* \tilde{v}_m^* = 0, \quad m = 1, \dots, M. \quad (5.12c)$$

If the complementary conditions in (5.12b) are satisfied, then

$$\begin{aligned}
 \tilde{\mathbf{u}}^{*T} \mathbf{s}^* &= 0 \\
 \tilde{\mathbf{u}}^{*T} \left(\hat{\mathbf{E}} \mathbf{d}^* - \hat{\mathbf{L}} + \hat{\mathbf{O}} \right) &= 0 \\
 \tilde{\mathbf{u}}^{*T} \hat{\mathbf{E}} \mathbf{d}^* - \tilde{\mathbf{u}}^{*T} \hat{\mathbf{L}} + \tilde{\mathbf{u}}^{*T} \hat{\mathbf{O}} &= 0 \\
 \tilde{\mathbf{u}}^{*T} \hat{\mathbf{E}} \mathbf{d}^* &= \tilde{\mathbf{u}}^{*T} \hat{\mathbf{L}} - \tilde{\mathbf{u}}^{*T} \hat{\mathbf{O}}
 \end{aligned}$$

and if (5.12a) and (5.12c) are satisfied, then

$$\begin{aligned}
 \tilde{\mathbf{w}}^{*T} \mathbf{d}^* &= 0 \\
 \left(\mathbf{1} - \check{\mathbf{E}}^T \tilde{\mathbf{u}}^* + \tilde{\mathbf{v}}^* \right)^T \mathbf{d}^* &= 0 \\
 \mathbf{1}^T \mathbf{d}^* - \tilde{\mathbf{u}}^{*T} \check{\mathbf{E}} \mathbf{d}^* + \tilde{\mathbf{v}}^{*T} \mathbf{d}^* &= 0 \\
 \tilde{\mathbf{u}}^{*T} \check{\mathbf{E}} \mathbf{d}^* - \tilde{\mathbf{v}}^{*T} \mathbf{d}^* &= \mathbf{1}^T \mathbf{d}^* \\
 \tilde{\mathbf{u}}^{*T} \check{\mathbf{E}} \mathbf{d}^* - \tilde{\mathbf{v}}^{*T} (\mathbf{1} - \mathbf{t}^*) &= \mathbf{1}^T \mathbf{d}^*. \tag{5.13}
 \end{aligned}$$

Note that because $\{d_m^*\}$ and $\{\tilde{u}_m^*\}$ are non-negative, we have

$$\tilde{\mathbf{u}}^{*T} \hat{\mathbf{E}} \mathbf{d}^* \geq \tilde{\mathbf{u}}^{*T} \check{\mathbf{E}} \mathbf{d}^*$$

and so (5.13) becomes

$$\begin{aligned}
 \tilde{\mathbf{u}}^{*T} \hat{\mathbf{E}} \mathbf{d}^* - \tilde{\mathbf{v}}^{*T} (\mathbf{1} - \mathbf{t}^*) &\geq \mathbf{1}^T \mathbf{d}^* \\
 \tilde{\mathbf{u}}^{*T} \hat{\mathbf{L}} - \tilde{\mathbf{u}}^{*T} \hat{\mathbf{O}} - \tilde{\mathbf{v}}^{*T} \mathbf{1} &\geq \mathbf{1}^T \mathbf{d}^* \\
 \tilde{\mathbf{u}}^{*T} \hat{\mathbf{L}} - \tilde{\mathbf{u}}^{*T} \hat{\mathbf{O}} - \tilde{\mathbf{v}}^{*T} \mathbf{1} &\geq \mathbf{1}^T \mathbf{d}^*. \tag{5.14}
 \end{aligned}$$

Using (5.4), (5.7), (5.8) and (5.9),

$$\begin{aligned}
 P_{max} = D_{max} &\geq \tilde{\mathbf{u}}^{*T} \hat{\mathbf{L}} - \tilde{\mathbf{u}}^{*T} \hat{\mathbf{O}} - \tilde{\mathbf{v}}^{*T} \mathbf{1} \\
 P_{min} &\leq \mathbf{1}^T \mathbf{d}^*
 \end{aligned}$$

and combining with (5.13), the suboptimal solution (5.10) to problem (5.3) is bounded as follows

$$P_{min} \leq \mathbf{1}^T \mathbf{d}^* \leq P_{max}.$$

5.4 Distributed illumination control solution

We first provide a brief outline of our proposed control solution. First the complementary conditions (5.12a) - (5.12c) are linearized around an initial point

$$\mathbf{x}^{(0)} = \left[\mathbf{d}^{(0)T} \quad \mathbf{s}^{(0)T} \quad \mathbf{t}^{(0)T} \quad \tilde{\mathbf{w}}^{(0)T} \quad \tilde{\mathbf{u}}^{(0)T} \quad \tilde{\mathbf{v}}^{(0)T} \right]^T.$$

CHAPTER 5. DISTRIBUTED LIGHTING CONTROL WITH LIGHT
SENSOR MEASUREMENTS

Then, we seek for a intermediate solution

$$\mathbf{x}^* = [\mathbf{d}^{*T} \quad \mathbf{s}^{*T} \quad \mathbf{t}^{*T} \quad \tilde{\mathbf{w}}^{*T} \quad \tilde{\mathbf{u}}^{*T} \quad \tilde{\mathbf{v}}^{*T}]^T$$

that minimizes the violation of complementary conditions and that is in the neighborhood of $\mathbf{x}^{(0)}$ such that the system of equations in (5.11) are satisfied and all the variables are non-negative. The intermediate solution \mathbf{x}^* is obtained by an iterative approach as detailed later in this section. Then, we repeat this procedure by linearizing the complementary conditions (5.12a) - (5.12c) around point \mathbf{x}^* . We repeat these steps till the difference between two consecutive solutions is within a predefined limit.

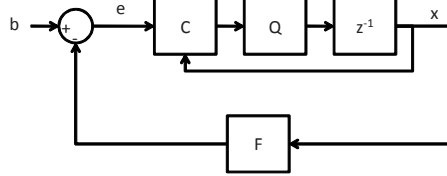


Figure 5.1: Controller feedback loop

Let us model problem (5.3) as a control system as depicted in Fig. 5.1 with two loops. The inner loop ensures that the system of equations in (5.11) are satisfied and all variables are non-negative after convergence. Let us assume that the inner loop converges after K iterations (see Section 5.5 for convergence analysis). The outer loop moves further the solution after the inner loop has converged (i.e. iteration κK , $\kappa = 0, 1, \dots$) towards satisfying complementary conditions in (5.12a) - (5.12c). In Fig. 5.1,

$$\begin{aligned} \mathbf{e}^{(k)} &= \mathbf{b}^{(k)} - \mathbf{F}\mathbf{x}^{(k-1)} \\ \mathbf{F} &= \begin{bmatrix} \mathbf{0} & \mathbf{0} & \mathbf{0} & \mathbf{I} & \tilde{\mathbf{E}}^T & -\mathbf{I} \\ \mathbf{E} & -\mathbf{I} & \mathbf{0} & \mathbf{0} & \mathbf{0} & \mathbf{0} \\ \mathbf{I} & \mathbf{0} & \mathbf{I} & \mathbf{0} & \mathbf{0} & \mathbf{0} \end{bmatrix}, \\ \mathbf{x}^{(k)} &= \begin{bmatrix} \mathbf{d}^{(k)} \\ \mathbf{s}^{(k)} \\ \mathbf{t}^{(k)} \\ \tilde{\mathbf{w}}^{(k)} \\ \tilde{\mathbf{u}}^{(k)} \\ \tilde{\mathbf{v}}^{(k)} \end{bmatrix}, \quad \mathbf{e}^{(k)} = \begin{bmatrix} e_1^{(k)} \\ e_2^{(k)} \\ e_3^{(k)} \end{bmatrix}, \quad \mathbf{b}^{(k)} = \begin{bmatrix} \mathbf{1} \\ \mathbf{L}^{(k)} - \mathbf{O}^{(k)} \\ \mathbf{1} \end{bmatrix}, \end{aligned}$$

$$\begin{aligned}
 \mathbf{E} &= \Phi \hat{\mathbf{E}}, & \tilde{\mathbf{E}} &= \Phi \tilde{\mathbf{E}}, \\
 \mathbf{L}^{(k)} &= \Phi \hat{\mathbf{L}}^{(k)}, & \mathbf{O}^{(k)} &= \Phi \hat{\mathbf{O}}^{(k)}, \\
 \Phi &= \text{diag} \{ [\phi_1 \ \phi_2 \ \dots \ \phi_M] \}, \\
 \mathbf{x}^{(k)} &= [x_1^{(k)} \ x_2^{(k)} \ \dots \ x_{4M}^{(k)}]^T, \\
 \mathbf{e}_1^{(k)} &= [e_{1,1}^{(k)} \ e_{1,2}^{(k)} \ \dots \ e_{1,M}^{(k)}]^T, \\
 \mathbf{e}_2^{(k)} &= [e_{2,1}^{(k)} \ e_{2,2}^{(k)} \ \dots \ e_{2,M}^{(k)}]^T, \\
 \mathbf{e}_3^{(k)} &= [e_{3,1}^{(k)} \ e_{3,2}^{(k)} \ \dots \ e_{3,M}^{(k)}]^T,
 \end{aligned}$$

block \mathbf{C} is the controller to be designed, z^{-1} is a unit delay and $\text{diag}\{\cdot\}$ is a diagonal matrix with entries in the main diagonal equal to the corresponding entries of the vector in the argument. The vectors $\mathbf{L}^{(k)}$ and $\mathbf{O}^{(k)}$ are the normalized target illuminance and normalized daylight illuminance contribution at sensors during iteration k , respectively. Similarly, \mathbf{E} and $\tilde{\mathbf{E}}$ are normalized versions of matrices $\hat{\mathbf{E}}$ and $\tilde{\mathbf{E}}$, respectively. Here, Φ is a normalization matrix where

$$\phi_m = \frac{\xi_m}{\sum_{n \in \mathcal{N}_m} \hat{E}_{m,n}(1)}$$

and $\xi_m > 0$ is a design parameter. Also, we refer to the (m, n) -th element in matrix \mathbf{E} and $\tilde{\mathbf{E}}$ as $E_{m,n}$ and $\tilde{E}_{m,n}$, respectively.

The operator \mathbf{Q} ensures that all variables $\{s_m^{(k)}\}$, $\{t_m^{(k)}\}$, $\{\tilde{u}_m^{(k)}\}$, $\{\tilde{v}_m^{(k)}\}$ and $\{\tilde{w}_m^{(k)}\}$ are non-negative and

$$0 \leq d_m^{(k)} \leq 1, \quad m = 1, \dots, M.$$

We design the inner loop such that we solve the subproblem,

$$\begin{aligned}
 \mathbf{x}^* &= \arg \min_{\mathbf{x}} \|(\mathbf{Y}^{(\kappa)})^T \mathbf{x}\|^2 + \|\mathbf{x} - \mathbf{x}^{(\kappa K)}\|^2 \\
 \text{s.t.} &\begin{cases} \mathbf{F}\mathbf{x} = \mathbf{b} \\ x_p \geq 0, \quad p = 1, 2, \dots, 6M, \end{cases} \quad (5.15)
 \end{aligned}$$

where

$$\mathbf{Y}^{(\kappa)} = \tilde{\mathbf{Y}}^{(\kappa)} \left(\tilde{\mathbf{Y}}^{(\kappa)} (\tilde{\mathbf{Y}}^{(\kappa)})^T \right)^{-\frac{1}{2}}$$

$$\tilde{\mathbf{Y}}^{(\kappa)} = \begin{bmatrix} \text{diag} \left\{ \tilde{\mathbf{w}}^{(\kappa K)} \right\} & \mathbf{0} & \mathbf{0} \\ \mathbf{0} & \text{diag} \left\{ \tilde{\mathbf{u}}^{(\kappa K)} \right\} & \mathbf{0} \\ \mathbf{0} & \mathbf{0} & \text{diag} \left\{ \tilde{\mathbf{v}}^{(\kappa K)} \right\} \\ \text{diag} \left\{ \mathbf{d}^{(\kappa K)} \right\} & \mathbf{0} & \mathbf{0} \\ \mathbf{0} & \text{diag} \left\{ \mathbf{s}^{(\kappa K)} \right\} & \mathbf{0} \\ \mathbf{0} & \mathbf{0} & \text{diag} \left\{ \mathbf{t}^{(\kappa K)} \right\} \end{bmatrix},$$

and $(\mathbf{Y}^{(\kappa)})^T \mathbf{x}$ is a linearization of complementary conditions (5.12a) - (5.12c) around vector $\mathbf{x}^{(\kappa K)}$,

$$\begin{aligned} 2d_m \tilde{w}_m &= d_m^{(\kappa K)} \tilde{w}_m + d_m \tilde{w}_m^{(\kappa K)}, \quad m = 1, \dots, M \\ 2s_m \tilde{u}_m &= s_m^{(\kappa K)} \tilde{u}_m + s_m \tilde{u}_m^{(\kappa K)}, \quad m = 1, \dots, M \\ 2t_m \tilde{v}_m &= t_m^{(\kappa K)} \tilde{v}_m + t_m \tilde{v}_m^{(\kappa K)}, \quad m = 1, \dots, M. \end{aligned}$$

In the outer loop, we update the matrix $\mathbf{Y}^{(\kappa)}$ at each iteration κK .

The problem in (5.15) is solved iteratively in the inner loop by

$$\mathbf{x}^{(\kappa K+1)} = \mathbf{Q} \left\{ \boldsymbol{\beta}^{(\kappa)} \mathbf{x}^{(\kappa K)} + \alpha \boldsymbol{\beta}^{(\kappa)} \Delta \mathbf{x}^{(\kappa K)} \right\}$$

and

$$\begin{aligned} \mathbf{x}^{(\kappa K+\tilde{k})} &= \mathbf{Q} \left\{ \mathbf{x}^{(\kappa K+\tilde{k}-1)} + \alpha \boldsymbol{\beta}^{(\kappa)} \Delta \mathbf{x}^{(\kappa K+\tilde{k})} \right\} \\ \tilde{k} &= 2, \dots, K, \end{aligned}$$

where

$$\boldsymbol{\beta}^{(\kappa)} = \left(\mathbf{Y}^{(\kappa)} (\mathbf{Y}^{(\kappa)})^T + \mathbf{I} \right)^{-1},$$

$$\Delta \mathbf{x}^{(k)} = \begin{bmatrix} \Delta \mathbf{d}^{(k)} \\ \Delta \mathbf{s}^{(k)} \\ \Delta \mathbf{t}^{(k)} \\ \Delta \tilde{\mathbf{w}}^{(k)} \\ \Delta \tilde{\mathbf{u}}^{(k)} \\ \Delta \tilde{\mathbf{v}}^{(k)} \end{bmatrix} = \mathbf{G} \mathbf{e}^{(k)}, \quad \mathbf{G} = \begin{bmatrix} \mathbf{0} & \tilde{\mathbf{E}}^T & \mathbf{I} \\ \mathbf{0} & -\mathbf{I} & \mathbf{0} \\ \mathbf{0} & \mathbf{0} & \mathbf{I} \\ \mathbf{I} & \mathbf{0} & \mathbf{0} \\ \tilde{\mathbf{E}} & \mathbf{0} & \mathbf{0} \\ -\mathbf{I} & \mathbf{0} & \mathbf{0} \end{bmatrix},$$

$$\mathbf{e}^{(k)} = \mathbf{b}^{(k)} - \mathbf{F} \mathbf{x}^{(k-1)}$$

and $\alpha \geq 0$ is a scaling factor.

Furthermore, $\beta^{(\kappa)}$ can be rewritten as

$$\begin{bmatrix} \mathbf{H}_d^{(\kappa)} & \mathbf{0} & \mathbf{0} & -\mathbf{H}_{dw}^{(\kappa)} & \mathbf{0} & \mathbf{0} \\ \mathbf{0} & \mathbf{H}_s^{(\kappa)} & \mathbf{0} & \mathbf{0} & -\mathbf{H}_{su}^{(\kappa)} & \mathbf{0} \\ \mathbf{0} & \mathbf{0} & \mathbf{H}_t^{(\kappa)} & \mathbf{0} & \mathbf{0} & -\mathbf{H}_{tv}^{(\kappa)} \\ -\mathbf{H}_{dw}^{(\kappa)} & \mathbf{0} & \mathbf{0} & \mathbf{H}_w^{(\kappa)} & \mathbf{0} & \mathbf{0} \\ \mathbf{0} & -\mathbf{H}_{su}^{(\kappa)} & \mathbf{0} & \mathbf{0} & \mathbf{H}_u^{(\kappa)} & \mathbf{0} \\ \mathbf{0} & \mathbf{0} & -\mathbf{H}_{tv}^{(\kappa)} & \mathbf{0} & \mathbf{0} & \mathbf{H}_v^{(\kappa)} \end{bmatrix}$$

where $\mathbf{H}_d^{(0)}$, $\mathbf{H}_s^{(0)}$, $\mathbf{H}_t^{(0)}$, $\mathbf{H}_w^{(0)}$, $\mathbf{H}_u^{(0)}$, $\mathbf{H}_v^{(0)}$, $\mathbf{H}_{dw}^{(0)}$, $\mathbf{H}_{su}^{(0)}$ and $\mathbf{H}_{tv}^{(0)}$ are diagonal matrices with entries in the main diagonal given by

$$\begin{aligned} [\mathbf{H}_d^{(\kappa)}]_{m,m} &= \frac{2(d_m^{(\kappa K)})^2 + (\tilde{w}_m^{(\kappa K)})^2}{2(d_m^{(\kappa K)})^2 + 2(\tilde{w}_m^{(\kappa K)})^2}, \\ [\mathbf{H}_s^{(\kappa)}]_{m,m} &= \frac{2(s_m^{(\kappa K)})^2 + (\tilde{u}_m^{(\kappa K)})^2}{2(s_m^{(\kappa K)})^2 + 2(\tilde{u}_m^{(\kappa K)})^2}, \\ [\mathbf{H}_t^{(\kappa)}]_{m,m} &= \frac{2(t_m^{(\kappa K)})^2 + (\tilde{v}_m^{(\kappa K)})^2}{2(t_m^{(\kappa K)})^2 + 2(\tilde{v}_m^{(\kappa K)})^2}, \\ [\mathbf{H}_w^{(\kappa)}]_{m,m} &= \frac{2(\tilde{w}_m^{(\kappa K)})^2 + (d_m^{(\kappa K)})^2}{2(d_m^{(\kappa K)})^2 + 2(\tilde{w}_m^{(\kappa K)})^2}, \\ [\mathbf{H}_u^{(\kappa)}]_{m,m} &= \frac{2(\tilde{u}_m^{(\kappa K)})^2 + (s_m^{(\kappa K)})^2}{2(s_m^{(\kappa K)})^2 + 2(\tilde{u}_m^{(\kappa K)})^2}, \\ [\mathbf{H}_v^{(\kappa)}]_{m,m} &= \frac{2(\tilde{v}_m^{(\kappa K)})^2 + (t_m^{(\kappa K)})^2}{2(t_m^{(\kappa K)})^2 + 2(\tilde{v}_m^{(\kappa K)})^2}, \\ [\mathbf{H}_{dw}^{(\kappa)}]_{m,m} &= \frac{d_m^{(\kappa K)} \tilde{w}_m^{(\kappa K)}}{2(d_m^{(\kappa K)})^2 + 2(\tilde{w}_m^{(\kappa K)})^2}, \\ [\mathbf{H}_{su}^{(\kappa)}]_{m,m} &= \frac{s_m^{(\kappa K)} \tilde{u}_m^{(\kappa K)}}{2(s_m^{(\kappa K)})^2 + 2(\tilde{u}_m^{(\kappa K)})^2}, \\ [\mathbf{H}_{tv}^{(\kappa)}]_{m,m} &= \frac{t_m^{(\kappa K)} \tilde{v}_m^{(\kappa K)}}{2(t_m^{(\kappa K)})^2 + 2(\tilde{v}_m^{(\kappa K)})^2}. \end{aligned}$$

CHAPTER 5. DISTRIBUTED LIGHTING CONTROL WITH LIGHT
SENSOR MEASUREMENTS

Hence we have, for the m -th controller

$$\Delta d_m^{(k)} = E_{m,m} e_{2,m}^{(k)} + \sum_{n \in \mathcal{N}_m} E_{n,m} e_{2,n}^{(k)} + e_{3,m}^{(k)}, \quad (5.17a)$$

$$\Delta s_m^{(k)} = -e_{2,m}^{(k)}, \quad (5.17b)$$

$$\Delta t_m^{(k)} = e_{3,m}^{(k)}, \quad (5.17c)$$

$$\Delta \tilde{u}_m^{(k)} = E_{m,m} e_{1,m}^{(k)} + \sum_{n \in \mathcal{N}_m} E_{m,n} e_{1,n}^{(k)}, \quad (5.17d)$$

$$\Delta \tilde{v}_m^{(k)} = -e_{1,m}^{(k)}, \quad (5.17e)$$

$$\Delta \tilde{w}_m^{(k)} = e_{1,m}^{(k)}, \quad (5.17f)$$

where

$$e_{1,m}^{(k)} = 1 - E_{m,m} \tilde{u}_m^{(k-1)} - \sum_{n \in \mathcal{N}_m} E_{n,m} \tilde{u}_n^{(k-1)} + \tilde{v}_m^{(k-1)} - \tilde{w}_m^{(k-1)}, \quad (5.18a)$$

$$e_{2,m}^{(k)} = L_m^{(k)} - \tilde{L}_m^{(k)}(\mathbf{d}^{(k)}) + s_m^{(k-1)}, \quad (5.18b)$$

$$e_{3,m}^{(k)} = 1 - d_m^{(k-1)} - t_m^{(k-1)} \quad (5.18c)$$

and

$$\begin{aligned} \tilde{L}_m^{(k)}(\mathbf{d}^{(k)}) &= \sum_{n=1}^M d_n^{(k)} E_{m,n} + O_m^{(k)} \\ &= \phi_m \left(\sum_{n=1}^M d_n^{(k)} \hat{E}_{m,n}(1) + \hat{O}_m^{(k)} \right) \\ &= \phi_m \bar{L}_m^{(k)}(\mathbf{d}^{(k)}). \end{aligned} \quad (5.19)$$

Here, $\bar{L}_m^{(k)}(\mathbf{d}^{(k)})$ is the measured illuminance at the m -th light sensor during iteration k due to dimming vector $\mathbf{d}^{(k)}$ and daylight contribution $\hat{O}_m^{(k)}$, and $\tilde{L}_m^{(k)}(\mathbf{d}^{(k)})$ is its normalized value. Note that the computation of (5.18b) does not require an estimation of daylight contribution, $\hat{O}_m^{(k)}$, but only the normalized measured illuminance at the m -th light sensor, $\tilde{L}_m^{(k)}(\mathbf{d}^{(k)})$.

The updating term $\Delta d_m^{(k)}$ can be approximated as

$$\Delta d_m^{(k)} \approx \widehat{\Delta d}_{m,0}^{(k-1)} + \sum_{n=1}^{N_m} \widehat{\Delta d}_{m,n}^{(k-1)},$$

where

$$\widehat{\Delta d}_{m,0}^{(k)} = E_{m,m} e_{2,m}^{(k)} + e_{3,m}^{(k)} \quad (5.20)$$

is the proposed variation of dimming level of the m -th controller for its associated luminaire and

$$\widehat{\Delta d}_{m,n}^{(k)} = E_{\nu_{m,n},m} e_{2,\nu_{m,n}}^{(k)}, \quad n = 1, \dots, N_m \quad (5.21)$$

is the variation of dimming level of the m -th controller proposed by the n -th neighbor.

Similarly, the error term $e_{1,m}^{(k-1)}$ can be rewritten as

$$e_{1,m}^{(k)} = \Delta e_{m,0}^{(k-1)} + \sum_{n=1}^{N_m} \Delta e_{m,n}^{(k-1)}$$

where

$$\Delta e_{m,0}^{(k)} = 1 - E_{m,m} \tilde{u}_m^{(k)} + \tilde{v}_m^{(k)} - \tilde{w}_m^{(k)} \quad (5.22)$$

is the own estimated error of the m -th controller and

$$\Delta e_{m,n}^{(k)} = -E_{\nu_{m,n},m} \tilde{u}_{\nu_{m,n}}^{(k)}, \quad n = 1, \dots, N_m \quad (5.23)$$

is the error of the m -th controller estimated by the n -th neighbor.

Finally, by combining both loops we have the following updating formula for the m -th controller

$$\begin{bmatrix} d_m^{(k+1)} \\ s_m^{(k+1)} \\ t_m^{(k+1)} \\ \tilde{w}_m^{(k+1)} \\ \tilde{u}_m^{(k+1)} \\ \tilde{v}_m^{(k+1)} \end{bmatrix} = \mathbf{Q} \left\{ \gamma_m^{(k)} \begin{bmatrix} d_m^{(k)} \\ s_m^{(k)} \\ t_m^{(k)} \\ \tilde{w}_m^{(k)} \\ \tilde{u}_m^{(k)} \\ \tilde{v}_m^{(k)} \end{bmatrix} + \alpha \beta_m^{(\kappa)} \begin{bmatrix} \Delta d_m^{(k)} \\ \Delta s_m^{(k)} \\ \Delta t_m^{(k)} \\ \Delta \tilde{w}_m^{(k)} \\ \Delta \tilde{u}_m^{(k)} \\ \Delta \tilde{v}_m^{(k)} \end{bmatrix} \right\} \quad (5.24)$$

where

$$\gamma_m^{(k)} = \begin{cases} \beta_m^{(\kappa)} & , \text{ if } k = \kappa K \\ \mathbf{I}_6 & , \text{ otherwise} \end{cases}$$

and

$$\begin{aligned}\beta_m^{(\kappa)} &= \left(\mathbf{Y}_m^{(\kappa)} \left(\mathbf{Y}_m^{(\kappa)} \right)^T + \mathbf{I}_6 \right)^{-1}, \\ \mathbf{Y}_m^{(\kappa)} &= \tilde{\mathbf{Y}}_m^{(\kappa)} \left(\tilde{\mathbf{Y}}_m^{(\kappa)} \left(\tilde{\mathbf{Y}}_m^{(\kappa)} \right)^T \right)^{-\frac{1}{2}} \\ \tilde{\mathbf{Y}}_m^{(\kappa)} &= \begin{bmatrix} \tilde{w}_m^{(\kappa K)} & \mathbf{0} & \mathbf{0} \\ \mathbf{0} & \tilde{u}_m^{(\kappa K)} & \mathbf{0} \\ \mathbf{0} & \mathbf{0} & \tilde{v}_m^{(\kappa K)} \\ d_m^{(\kappa K)} & \mathbf{0} & \mathbf{0} \\ \mathbf{0} & s_m^{(\kappa K)} & \mathbf{0} \\ \mathbf{0} & \mathbf{0} & t_m^{(\kappa K)} \end{bmatrix}\end{aligned}$$

where \mathbf{I}_6 is the identity matrix of size 6×6 .

5.4.1 Distributed control algorithm

We assume that the system initializes with all the luminaires off. That is

$$d_m^{(0)} = 0, \quad m = 1, \dots, M.$$

Additionally, all the variables $\{s_m^{(0)}\}$, $\{t_m^{(0)}\}$, $\{\tilde{u}_m^{(0)}\}$, $\{\tilde{v}_m^{(0)}\}$ and $\{\tilde{w}_m^{(0)}\}$ are initialized with zero.

Let the transmitted message at iteration k from the m -th controller be denoted by

$$\mu_m^{(k)} = \begin{bmatrix} \left\{ d_m^{(k)}, e_{1,m}^{(k)} \right\} \\ \left\{ \nu_{m,1}, \widehat{\Delta d}_{m,1}^{(k)}, \Delta e_{m,1}^{(k)} \right\} \\ \vdots \\ \left\{ \nu_{m,N_m}, \widehat{\Delta d}_{m,N_m}^{(k)}, \Delta e_{m,N_m}^{(k)} \right\} \end{bmatrix},$$

where

- $d_m^{(k)}$: Current dimming level of the m -th luminaire,
- $e_{1,m}^{(k)}$: Current error of the m -th controller,
- $\nu_{m,n}$: Index of the n -th neighbor, $n = 1, \dots, N_m$,
- $\widehat{\Delta d}_{m,n}^{(k)}$: Proposed variation for the dimming level of the luminaire of the n -th neighbor, $n = 1, \dots, N_m$,

5.4. DISTRIBUTED ILLUMINATION CONTROL SOLUTION

$\Delta e_{m,n}^{(k)}$: Estimated error of the n -th neighbor, $n = 1, \dots, N_m$.

The pseudo-code for the distributed lighting control algorithm is presented in *Algorithm 1*.

Algorithm 1 Local lighting control in m -th controller

Require: Set of received messages $\{\mu_n^{(k-1)} : n \in \mathcal{N}_m\}$
 Scaling factor α
 Normalization factor ϕ_m
 Current light measurement, $\bar{L}_m^{(k)}(\mathbf{d}^{(k)})$
 Current target illuminance, $\hat{L}_m^{(k)}$
 Maximum number of iteration of inner loop, K
 Threshold for changing dimming level, ϵ_d

loop

Normalization

$$\tilde{L}_m^{(k)}(\mathbf{d}^{(k)}) \leftarrow \phi_m \bar{L}_m^{(k)}(\mathbf{d}^{(k)})$$

$$L_m^{(k)} \leftarrow \phi_m \hat{L}_m^{(k)}$$

$$E_{m,n} \leftarrow \phi_m \hat{E}_{m,n}(1), \quad n \in \mathcal{N}_m$$

Estimate errors terms

$$e_{1,m}^{(k)} \leftarrow \Delta e_{m,0}^{(k-1)} +$$

$$\sum \left\{ \Delta e_{i,j}^{(k-1)} : \nu_{i,j} = m, i \in \mathcal{N}_m \wedge j = 1, \dots, N_m \right\}$$

Use equations (5.18b) - (5.18c)

Estimate updating terms

$$\Delta d_m^{(k)} \leftarrow \widehat{\Delta d}_{m,0}^{(k-1)} +$$

$$\sum \left\{ \widehat{\Delta d}_{i,j}^{(k-1)} : \nu_{i,j} = m, i \in \mathcal{N}_m \wedge j = 1, \dots, N_m \right\}$$

Use equations (5.17b)-(5.17f)

$$\kappa \leftarrow \lfloor \frac{k}{K} \rfloor$$

Continue...

Algorithm 1 Local lighting control in m -th controller

...Continue

if $\kappa K = k$ **then**

 Update matrix $\beta_m^{(\kappa)}$

$\gamma_m^{(k)} \leftarrow \beta_m^{(\kappa)}$

else

$\gamma_m^{(k)} \leftarrow \mathbf{I}_6$

end if

 Update terms

 Use equation (5.24)

if $\|d_m^{(k)} - d_m^{(k-1)}\| > \epsilon_d$ **then**

 Calculate propose terms

 Use equations (5.20), (5.21), (5.22) and (5.23)

 Transmit message $\mu_m^{(k)}$ to neighbors in \mathcal{N}_m

end if

end loop

5.5 Analysis of the algorithm

In this section, we establish conditions under which the controller is stable and converges to a feasible solution \mathbf{x}^* for both the primal problem (5.4) and the dual problem (5.8) such that the complementary conditions (5.12a)-(5.12c) are satisfied. We assume that \mathbf{b} is constant during the inner and outer loop.

Let us establish conditions on matrix \mathbf{G} for stability and convergence of the inner loop to a feasible intermediate solution \mathbf{x}^* to exist.

First, we consider the inner loop without the operator \mathbf{Q} . Let $\mathbf{x}^{(0)}$ be the initial vector. It can be shown using classic control theory that the system is stable and converges to solution $\bar{\mathbf{x}}^*$ [16, Chapter 5],

$$\begin{aligned} \bar{\mathbf{x}}^* &= \arg \min_{\mathbf{x}} \|(\mathbf{Y}^{(0)})^T \mathbf{x}\|^2 + \|\mathbf{x} - \mathbf{x}^{(0)}\|^2 \\ &\text{s.t. } \mathbf{F}\mathbf{x} = \mathbf{b} \end{aligned}$$

when

$$\max \left\{ \left| \text{eig} \left(\mathbf{I} - \alpha \mathbf{F} \beta^{(0)} \mathbf{G} \right) \right| \right\} < 1. \quad (5.25)$$

Choose parameters χ_i, χ and N such that the following holds

$$\sum_{n \in \mathcal{N}_i} E_{i,n} = \chi_i \sum_n E_{i,n}, \quad \forall i, \quad (5.26a)$$

$$\sum_{n \notin \mathcal{N}_i} E_{i,n} = (1 - \chi_i) \sum_n E_{i,n}, \quad \forall i, \quad (5.26b)$$

$$\chi_i \leq \chi, \quad \forall i, \quad (5.26c)$$

$$N_i \geq N, \quad \forall i. \quad (5.26d)$$

Then sufficient conditions for (5.25) to hold are

$$0 < \xi \leq \frac{\sqrt{1.25^2 + \left(\frac{M-1}{\sqrt{2}}\right) \left(\frac{\chi}{1-\chi}\right)} - 1.25}{2(M-1)}, \quad (5.27)$$

with $\xi_i \leq \xi, \forall i$, and

$$0 < \alpha \leq \min \left\{ \frac{1}{2.25 + (\xi + 0.25)\xi N}, \frac{\chi}{\chi + M\xi^2 + 1.25\xi}, \frac{1}{2.25 + N\xi} \right\}. \quad (5.28)$$

The proof is provided in Appendix 5.A.

Additionally if condition in (5.25) is satisfied, then we have the following property at each iteration k in the inner loop [16, Chapter 4]

$$\|\mathbf{x}^{(k)} - \bar{\mathbf{x}}^*\| < \|\mathbf{x}^{(k-1)} - \bar{\mathbf{x}}^*\|. \quad (5.29)$$

Now, let us consider the effect of the nonlinear operator \mathbf{Q} . Given that operator \mathbf{Q} is projecting over a convex set which contains \mathbf{x}^* , where \mathbf{x}^* is a solution to (5.15), then we have the following property [17]

$$\|\mathbf{Q}\{\mathbf{x}^{(k)}\} - \mathbf{x}^*\| \leq \|\mathbf{x}^{(k)} - \mathbf{x}^*\|. \quad (5.30)$$

Note that the equality only holds when $\mathbf{Q}\{\mathbf{x}^{(k)}\} = \mathbf{x}^{(k)}$.

Let us consider that during the first K' iterations the intermediate solution vectors $\{\mathbf{x}^{(k)}\}, k = 0, 1, \dots, K'$ satisfy

$$\mathbf{Q}\{\mathbf{x}^{(k)}\} = \mathbf{x}^{(k)}, \quad k = 0, 1, \dots, K'.$$

Hence, we have for each iteration $k = 0, 1, \dots, K'$,

$$\|\mathbf{x}^{(k)} - \mathbf{x}^*\|^2 = \|\mathbf{x}^{(k)} - \bar{\mathbf{x}}^*\|^2 + \|\bar{\mathbf{x}}^* - \mathbf{x}^*\|^2 + 2(\mathbf{x}^{(k)} - \bar{\mathbf{x}}^*)^T(\bar{\mathbf{x}}^* - \mathbf{x}^*)$$

CHAPTER 5. DISTRIBUTED LIGHTING CONTROL WITH LIGHT
SENSOR MEASUREMENTS

and using (5.29), we have

$$\left\| \mathbf{x}^{(k)} - \mathbf{x}^* \right\| < \left\| \mathbf{x}^{(k-1)} - \mathbf{x}^* \right\|. \quad (5.31)$$

Then, after combining with (5.30), we have at iteration $K' + 1$,

$$\left\| \mathbf{Q} \left\{ \mathbf{x}^{(K'+1)} \right\} - \mathbf{x}^* \right\| < \left\| \mathbf{x}^{(K'+1)} - \mathbf{x}^* \right\| < \left\| \mathbf{x}^{(K')} - \mathbf{x}^* \right\|$$

and also

$$\mathbf{e}^{(K'+1)} = \left\| \mathbf{FQ} \left\{ \mathbf{x}^{(K'+1)} \right\} - \mathbf{b} \right\| < \left\| \mathbf{F} \mathbf{x}^{(K')} - \mathbf{b} \right\|.$$

At iteration $K' + 1$, the j -th variable in vector $\mathbf{x}^{(K)}$ reaches its lower bound (or upper bound) and cannot be further reduced (or increased). If the system is controllable (i.e. it is possible to transfer the system from any initial illuminance state to any desired illuminance state [16, pp. 379]), then there exists a control path from $\mathbf{x}^{(K')}$ to \mathbf{x}^* which does not modify the j -th variable further. Moreover, this path reduces the error in each iteration and so

$$\lim_{k \rightarrow \infty} \left\| \mathbf{e}^{(k)} \right\| = 0.$$

Thus, the inner loop is stable and converges to a feasible solution \mathbf{x}^* .

In the outer loop the solution $\mathbf{x}^{((\kappa-1)K)}$ is moved towards a new intermediate solution $\mathbf{x}^{(\kappa K)}$ where

$$\left\| (\mathbf{Y}^{(\kappa)})^T \mathbf{x}^{(\kappa K)} \right\|^2 + \left\| \mathbf{x}^{(\kappa K)} - \mathbf{x}^{((\kappa-1)K)} \right\|^2 \leq \left\| (\mathbf{Y}^{(\kappa-1)})^T \mathbf{x}^{((\kappa-1)K)} \right\|^2$$

It can be noted that when the solution has converged (i.e. $\mathbf{x}^{(\kappa K)} = \mathbf{x}^{((\kappa-1)K)} = \mathbf{x}^{(\tilde{\kappa}K)}$), then

$$\left\| (\mathbf{Y}^{(\kappa)})^T \mathbf{x}^{(\kappa K)} \right\|^2 = \left\| (\mathbf{Y}^{(\kappa-1)})^T \mathbf{x}^{((\kappa-1)K)} \right\|^2,$$

where $\mathbf{x}^{(\tilde{\kappa}K)}$ is the solution that minimizes

$$\begin{aligned} \left\| (\mathbf{Y}^{(\tilde{\kappa})})^T \mathbf{x}^{(\tilde{\kappa}K)} \right\|^2 &= \sum_m \frac{(d_m^{(\tilde{\kappa}K)} \tilde{w}^{(\tilde{\kappa}K)})^2}{(d_m^{(\tilde{\kappa}K)})^2 + (\tilde{w}^{(\tilde{\kappa}K)})^2} + \frac{(s_m^{(\tilde{\kappa}K)} \tilde{u}^{(\tilde{\kappa}K)})^2}{(s_m^{(\tilde{\kappa}K)})^2 + (\tilde{u}^{(\tilde{\kappa}K)})^2} \\ &\quad + \frac{(t_m^{(\tilde{\kappa}K)} \tilde{v}^{(\tilde{\kappa}K)})^2}{(t_m^{(\tilde{\kappa}K)})^2 + (\tilde{v}^{(\tilde{\kappa}K)})^2}. \end{aligned} \quad (5.32)$$

Furthermore, the minimum of (5.32) is achieved only when all the complementary conditions in (5.12a) - (5.12c) are satisfied. Hence, we have that $\mathbf{x}^{(\tilde{\kappa}K)} = \mathbf{x}^*$.

5.5.1 Neighbor selection

The selection of neighbors in the proposed control algorithm depends on the controllability of the system. A sufficient condition for the system to be controllable is that the m -th controller achieves the target illuminance at the m -th light sensor independently from other controllers outside its neighborhood, i.e.

$$\sum_{n \in \mathcal{N}_m} \hat{E}_{m,n}(1) > L_m^o. \quad (5.33)$$

5.6 Simulation Results

In this section, we present simulation results to show the performance of the proposed control scheme. The office has length 14.4 m and width 7.4 m with height of the ceiling of 2.86 m. The distance of the ceiling to the workspace plane is 1.93 m. There are $M = 24$ luminaires arranged in a grid of 3 by 8, with light sensors co-located with the luminaires, as shown in Fig. 5.1. The beam profile of the luminaire was the same as used in [6]. The luminaire indexing in Fig. 5.2 also corresponds to that of the controllers and zones. The office has windows on one side of the room for daylight.

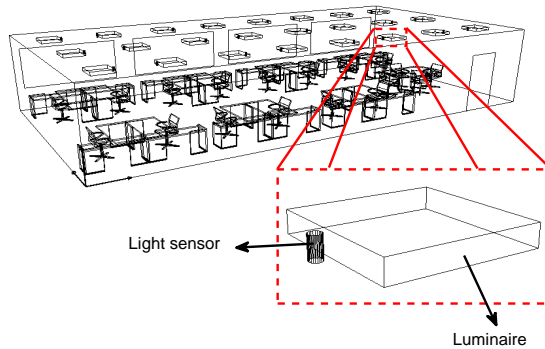


Figure 5.1: Room configuration

We consider a light sensor with a half opening angle of 20 degrees. Since there is no readily available model for a light sensor in DIALux, we created a model to emulate a light sensor. This was done by creating an opaque cylinder with an opening on the bottom end facing the workspace plane. The illuminance was measured at a point along the main axis so as to emulate a half opening angle of 20 degrees.

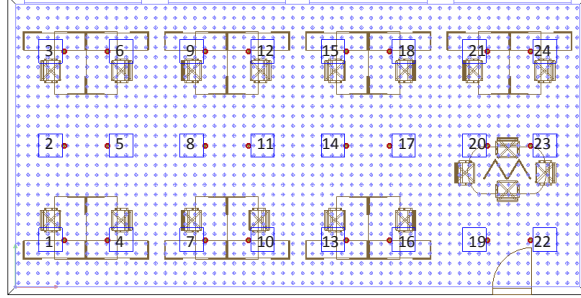


Figure 5.2: Top view of office room

The minimum desired average illuminance value L_{WP}^u in an unoccupied zone is chosen to be 300 lux, and in an occupied zone to be $L_{\text{WP}}^o = 500$ lux, following recommended norms for office lighting [18]. The target intensity when the m -th zone is empty, L_m^u , is calculated by setting all the luminaires such that 300 lx is achieved across the room, i.e. $d_m = 0.51$, $m = 1, \dots, M$. That is equivalent to

$$L_m^u = 0.51 \sum_{n=1}^N \hat{E}_{m,n}(1), \quad m = 1, \dots, M.$$

Similarly, we calculate the target intensity when the m -th zone is occupied, L_m^o , with a dimming level such that 500 lx is achieved across the room. In this case, all the luminaires are at dimming level 0.85, and

$$L_m^o = 0.85 \sum_{n=1}^N \hat{E}_{m,n}(1), \quad m = 1, \dots, M.$$

The resulting target illuminance values at the light sensors are shown in Fig. 5.3. Note that the target illuminance at the light sensor are not uniform, due to differences in reflectance across zones in the workspace plane.

The daylight data is obtained from DIALux using clear sky settings for 11 November, 2011 in Amsterdam. The daylight distribution is simulated from 7:00 to 20:00 hours. An average occupancy level of 50% was used in each zone along the simulated day.

The updating time of the dimming levels per controller is set to 4 seconds. Also, each controller broadcasts its message to its neighbors every 4 seconds. We assume the neighborhood of the m -th controller to be the closest controllers to it

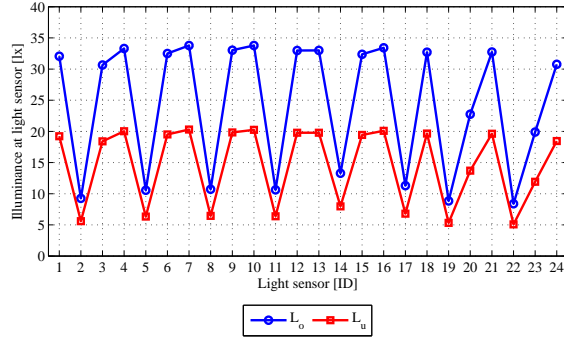


Figure 5.3: Target illuminance values at light sensors

(i.e. $N = 10$). Furthermore, this neighborhood corresponds to $\chi = 0.85$. Hence, we choose parameter $\xi = 0.1$ (satisfying (5.27)), normalization factor

$$\phi_m = \frac{0.1}{\sum_{n \in \mathcal{N}_m} \hat{E}_{m,n}(1)}, \forall m$$

and scaling factor $\alpha = 0.3$ (satisfying (5.28)). The threshold for transmitting a message is set to $\epsilon_d = 0.001$ and $K = 30$.

We calculate the power savings with respect to a reference static rendering, in which the dimming levels of the luminaires are set to a fixed level 0.85 such that an illuminance level of 500 lux is achieved over the workspace plane.

The power savings of our proposed scheme, which we will refer as NCLC (Neighbor Communication Lighting Control), are compared with a centralized implementation of the optimal control for (5.9) and (5.4), which we will refer as COC_{\max} and COC_{\min} , respectively. The power savings achieved by NCLC along the simulated day are shown in Fig. 5.4. We note that the savings achieved by NCLC are within the limits COC_{\max} and COC_{\min} .

The rendering solution at a given time instance (10:53 hours) is depicted in Figs. 5.5 and 5.6. We can note that the luminaires close to the windows are dimmed down due to larger daylight contribution. The differences between target illuminance and achieved illuminance at the sensors are shown in Fig. 5.7. As expected, the achieved illuminance is no smaller than the target illuminance. Note that the illuminance values at the light sensors that are closer to the windows are much higher than the target illuminance values due to the large contribution of daylight over the corresponding zones.

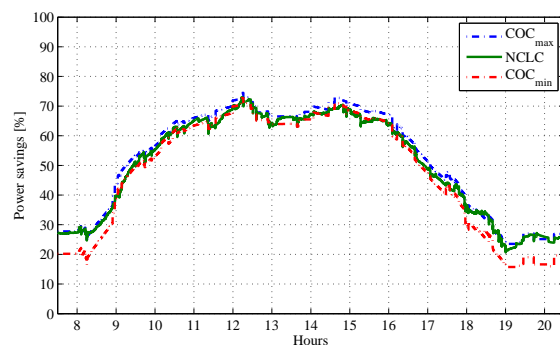


Figure 5.4: Power savings NCLC wrt COC_{\max} and COC_{\min}

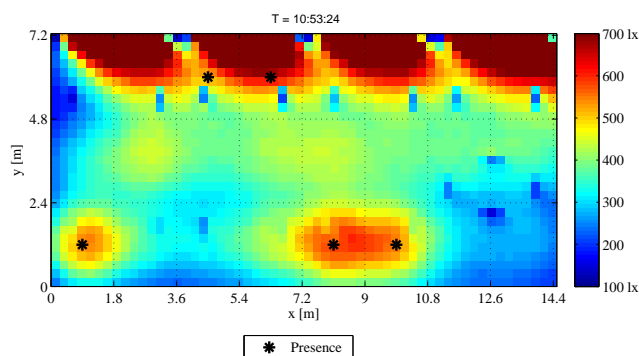


Figure 5.5: Illuminance distribution at workspace plane at 10:53 hours

5.7 Conclusions and discussion

We presented a distributed algorithm for illumination control under local presence and light sensing, with networking constraints on exchanging control information. Sufficient conditions were provided under which the algorithm can achieve the target light sensor values, calibrated to achieve a corresponding desired spatial illumination rendering in the workspace plane. The performance of the distributed control algorithm was evaluated in an open office room and shown to result in substantial power savings when compared to the luminaires being at a fixed dimming level, with no presence or daylight adaptation.

In this paper, we assumed a simplified presence and light sensor model. Im-

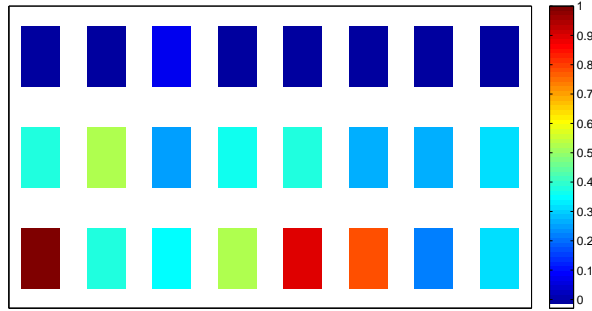


Figure 5.6: Dimming levels at 10:53 hours

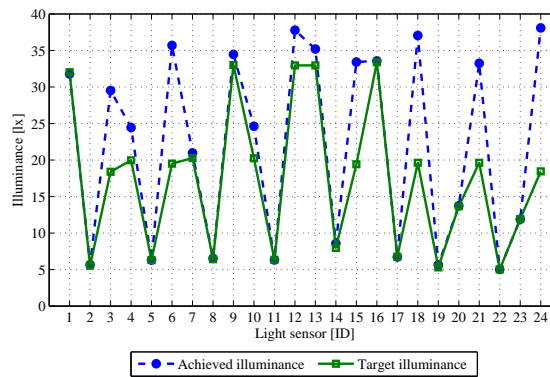


Figure 5.7: Target vs Achieved illuminance values at light sensors at 10:53 hours

provements in presence sensor technology [19] minimize detection errors and as such the rendered illumination is close to the desired one. In our analysis, we had assumed perfect light sensor calibration. In practice, this may not be the case. Further, light sensor readings may show fluctuations. Considering such sensor imperfections and evaluating their impact on lighting control is a topic for further investigation.

The developed distributed sensing and control framework may be extended to other illumination applications, e.g. [20]. Developing appropriate analytical models and control solutions for such an application would be interesting future work.

Appendix

5.A Sufficient conditions for (5.25)

Sufficient conditions for (5.25) to hold are

$$\operatorname{Re} \left\{ \operatorname{eig} \left(\mathbf{F} \boldsymbol{\beta}^{(0)} \mathbf{G} \right) \right\} > 0 \quad (5.34a)$$

$$\operatorname{Re} \left\{ \operatorname{eig} \left(\mathbf{F} \boldsymbol{\beta}^{(0)} \mathbf{G} \right) \right\} > \operatorname{Im} \left\{ \operatorname{eig} \left(\mathbf{F} \boldsymbol{\beta}^{(0)} \mathbf{G} \right) \right\} \quad (5.34b)$$

$$\alpha \left| \operatorname{eig} \left(\mathbf{F} \boldsymbol{\beta}^{(0)} \mathbf{G} \right) \right| < 1 \quad (5.34c)$$

for any eigenvalue of $\mathbf{F} \boldsymbol{\beta}^{(0)} \mathbf{G}$.

Note that $\mathbf{F} \boldsymbol{\beta}^{(0)} \mathbf{G}$ can be rewritten as the summation of a symmetric matrix $\mathbf{P} = \mathbf{G}^T (\boldsymbol{\beta}^{(0)} - \tilde{\boldsymbol{\beta}}^{(0)}) \mathbf{G}$,

$$\mathbf{P} = \begin{bmatrix} P_{1,1} & P_{1,2} & P_{1,3} \\ P_{2,1} & P_{2,2} & P_{2,3} \\ P_{3,1} & P_{3,2} & P_{3,3} \end{bmatrix}.$$

where

$$\begin{aligned} P_{1,1} &= \mathbf{H}_w^{(0)} + \tilde{\mathbf{E}}^T \mathbf{H}_u^{(0)} \tilde{\mathbf{E}} + \mathbf{H}_v^{(0)}, \\ P_{1,2} &= -\mathbf{H}_{dw}^{(0)} \tilde{\mathbf{E}}^T + \tilde{\mathbf{E}}^T \mathbf{H}_{su}^{(0)}, \\ P_{1,3} &= -\mathbf{H}_{dw}^{(0)} + \mathbf{H}_{tv}^{(0)}, \\ P_{2,1} &= -\tilde{\mathbf{E}} \mathbf{H}_{dw}^{(0)} + \mathbf{H}_{su}^{(0)} \tilde{\mathbf{E}}, \\ P_{2,2} &= \tilde{\mathbf{E}} \mathbf{H}_d^{(0)} \tilde{\mathbf{E}}^T + 0.5 \mathbf{H}_s^{(\kappa)}, \\ P_{2,3} &= \tilde{\mathbf{E}} \mathbf{H}_d^{(0)}, \\ P_{3,1} &= -\mathbf{H}_{dw}^{(0)} + \mathbf{H}_{tv}^{(0)}, \\ P_{3,2} &= \mathbf{H}_d^{(0)} \tilde{\mathbf{E}}^T, \\ P_{3,3} &= \mathbf{H}_d^{(0)} + \mathbf{H}_t^{(0)}, \end{aligned}$$

and

$$\tilde{\boldsymbol{\beta}}^{(0)} = \begin{bmatrix} 0 & 0 & 0 & 0 & 0 & 0 \\ 0 & 0.5 \mathbf{H}_s^{(0)} & 0 & 0 & 0 & 0 \\ 0 & 0 & 0 & 0 & 0 & 0 \\ 0 & 0 & 0 & 0 & 0 & 0 \\ 0 & 0 & 0 & 0 & 0 & 0 \\ 0 & 0 & 0 & 0 & 0 & 0 \end{bmatrix},$$

and an asymmetric matrix $\bar{\mathbf{P}} = \mathbf{F}\boldsymbol{\beta}^{(0)}\mathbf{G} - \mathbf{P}$,

$$\bar{\mathbf{P}} = \begin{bmatrix} \mathbf{0} & \mathbf{0} & \mathbf{0} \\ -\bar{\mathbf{E}}\mathbf{H}_{dw}^{(0)} & \bar{\mathbf{E}}\mathbf{H}_d^{(0)}\tilde{\mathbf{E}}^T + 0.5\mathbf{H}_s^{(0)} & \bar{\mathbf{E}}\mathbf{H}_d^{(0)} \\ \mathbf{0} & \mathbf{0} & \mathbf{0} \end{bmatrix}.$$

where $\bar{\mathbf{E}} = \mathbf{E} - \tilde{\mathbf{E}}$.

Hence, conditions (5.34a) and (5.34b) are satisfied when

$$\operatorname{Re} \{ \operatorname{eig}(\mathbf{P}) \} > 0 \quad (5.35a)$$

$$\operatorname{Re} \{ \operatorname{eig}(\mathbf{P}) \} > \operatorname{Im} \{ \operatorname{eig}(\mathbf{P}) \} \quad (5.35b)$$

$$\operatorname{Re} \{ \operatorname{eig}(\bar{\mathbf{P}}) \} > 0 \quad (5.35c)$$

$$\operatorname{Re} \{ \operatorname{eig}(\bar{\mathbf{P}}) \} > \operatorname{Im} \{ \operatorname{eig}(\bar{\mathbf{P}}) \} \quad (5.35d)$$

for any eigenvalue of \mathbf{P} and $\bar{\mathbf{P}}$, respectively.

Note that all the entries in the main diagonal of $\mathbf{H}_d^{(0)}$, $\mathbf{H}_s^{(0)}$, $\mathbf{H}_t^{(0)}$, $\mathbf{H}_w^{(0)}$, $\mathbf{H}_u^{(0)}$ and $\mathbf{H}_v^{(0)}$ are within the range $[0.5, 1]$. Similarly, all the entries in the main diagonal of $\mathbf{H}_{dw}^{(0)}$, $\mathbf{H}_{su}^{(0)}$ and $\mathbf{H}_{tv}^{(0)}$ are within the range $[0, 0.25]$. Hence, $(\boldsymbol{\beta}^{(0)} - \tilde{\boldsymbol{\beta}}^{(0)})$ is diagonal dominant with non-negative elements in the main diagonal (i.e. positive semidefinite) and so condition (5.35a) is satisfied. Additionally, given that \mathbf{P} is symmetric we have that its eigenvalues are real and so condition (5.35b) is satisfied.

Using Gershgorin circle theorem [21, Chapter 6], we have that any eigenvalue of $\bar{\mathbf{P}}$ satisfies for at least one i^*

$$\begin{aligned} \left(\operatorname{eig}(\bar{\mathbf{P}}) - [\bar{\mathbf{P}}]_{i^*,i^*} \right)^2 &\leq \left(\sum_{j \neq i^*} |[\bar{\mathbf{P}}]_{i^*,j}| \right)^2 \\ \left(\operatorname{Re} \{ \operatorname{eig}(\bar{\mathbf{P}}) \} - [\bar{\mathbf{P}}]_{i^*,i^*} \right)^2 + \left(\operatorname{Im} \{ \operatorname{eig}(\bar{\mathbf{P}}) \} \right)^2 &\leq \left(\sum_{j \neq i^*} |[\bar{\mathbf{P}}]_{i^*,j}| \right)^2 \end{aligned}$$

and by using (5.35d) then

$$\begin{aligned} \left(\operatorname{Re} \{ \operatorname{eig}(\bar{\mathbf{P}}) \} \right)^2 &\geq \left(\sum_{j \neq i^*} |[\bar{\mathbf{P}}]_{i^*,j}| \right)^2 - \left(\operatorname{Re} \{ \operatorname{eig}(\bar{\mathbf{P}}) \} - [\bar{\mathbf{P}}]_{i^*,i^*} \right)^2, \\ 2 \left(\operatorname{Re} \{ \operatorname{eig}(\bar{\mathbf{P}}) \} \right)^2 &- 2 [\bar{\mathbf{P}}]_{i^*,i^*} \operatorname{Re} \{ \operatorname{eig}(\bar{\mathbf{P}}) \} \\ &+ \left([\bar{\mathbf{P}}]_{i^*,i^*} \right)^2 - \left(\sum_{j \neq i^*} |[\bar{\mathbf{P}}]_{i^*,j}| \right)^2 \geq 0 \end{aligned} \quad (5.36)$$

We have that (5.36) is true if

$$\begin{aligned}
& \left([\bar{\mathbf{P}}]_{i,i}\right)^2 - 2\left(\left([\bar{\mathbf{P}}]_{i,i}\right)^2 - \left(\sum_{j \neq i} |[\bar{\mathbf{P}}]_{i,j}|\right)^2\right) \leq 0, \forall i \\
& - \left([\bar{\mathbf{P}}]_{i,i}\right)^2 + \left(\sum_{j \neq i} |[\bar{\mathbf{P}}]_{i,j}|\right)^2 \leq 0, \forall i \\
& [\bar{\mathbf{P}}]_{i,i} \geq \sqrt{2} \sum_{j \neq i} |[\bar{\mathbf{P}}]_{i,j}|, \forall i.
\end{aligned} \tag{5.37}$$

Hence, sufficient conditions to (5.35c) and (5.35d) are given by (5.37) and so

$$\begin{aligned}
0.5 \left[\mathbf{H}_s^{(0)}\right]_{i,i} & \geq \sqrt{2} \left(\sum_{j \neq i} \sum_{\substack{n \notin \mathcal{N}_j \\ n \in \mathcal{N}_j}} E_{i,n} \left[\mathbf{H}_d^{(0)}\right]_{n,n} E_{j,n} \right. \\
& \left. + \sum_{n \notin \mathcal{N}_i} E_{i,n} \left[\mathbf{H}_d^{(0)}\right]_{n,n} + \sum_{n \notin \mathcal{N}_i} E_{i,n} \left[\mathbf{H}_{dw}^{(0)}\right]_{n,n} \right), \forall i
\end{aligned} \tag{5.38}$$

Note that the following inequalities hold

$$\begin{aligned}
\sum_{n \in \mathcal{N}_j} E_{i,n} E_{j,n} & \leq \sum_m E_{i,m} \sum_{n \in \mathcal{N}_j} E_{j,n}, \forall i, j, \\
\sum_{n \in \mathcal{N}_i} E_{i,n}^2 & \leq \left(\sum_{n \in \mathcal{N}_i} E_{i,n} \right)^2, \forall i.
\end{aligned}$$

and due to reciprocity between neighbors we have the following equality

$$\sum_{n:i \in \mathcal{N}_n} E_{n,i} = \sum_{n \in \mathcal{N}_i} E_{n,i}, \forall i.$$

Let $\xi_i \leq \xi$, $\forall i$ and so the following inequalities hold

$$\begin{aligned}
\sum_{n \in \mathcal{N}_i} E_{i,n} & \leq \xi, \forall i, \\
\sum_{n \in \mathcal{N}_i} E_{n,i} & \leq N\xi, \forall i.
\end{aligned}$$

Now suppose conditions (5.26a-5.26d) hold. Hence, (5.38) becomes

$$\begin{aligned}
 0.25 &\geq \sqrt{2} \left(\sum_{j \neq i} \sum_{\substack{n \notin \mathcal{N}_j \\ n \in \mathcal{N}_j}} E_{i,n} E_{j,n} + 1.25 \sum_{n \notin \mathcal{N}_i} E_{i,n} \right), \\
 0.25 &\geq \sqrt{2} \left(\sum_{j \neq i} \sum_{m \notin \mathcal{N}_i} E_{i,m} \sum_{n \in \mathcal{N}_j} E_{j,n} + 1.25 \left(\frac{1-\chi}{\chi} \right) \sum_{n \in \mathcal{N}_i} E_{i,n} \right), \\
 0.25 &\geq \sqrt{2} \left(\sum_{j \neq i} \left(\frac{1-\chi}{\chi} \right) \sum_{m \in \mathcal{N}_i} E_{i,m} \xi + 1.25 \left(\frac{1-\chi}{\chi} \right) \xi \right), \\
 0.25 &\geq \sqrt{2} \left(\sum_{j \neq i} \left(\frac{1-\chi}{\chi} \right) \xi^2 + 1.25 \left(\frac{1-\chi}{\chi} \right) \xi \right), \\
 0.25 &\geq \sqrt{2} \left((M-1) \left(\frac{1-\chi}{\chi} \right) \xi^2 + 1.25 \left(\frac{1-\chi}{\chi} \right) \xi \right), \\
 (M-1) \xi^2 + 1.25 \xi - \frac{\chi}{4\sqrt{2}(1-\chi)} &\leq 0,
 \end{aligned}$$

thus

$$\xi \leq \frac{\sqrt{1.25^2 + \left(\frac{M-1}{\sqrt{2}} \right) \left(\frac{\chi}{1-\chi} \right)} - 1.25}{2(M-1)}.$$

A sufficient condition to (5.34c) is

$$\alpha \sum_j \left(\left| [\mathbf{P}]_{i,j} \right| + \left| [\bar{\mathbf{P}}]_{i,j} \right| \right) \leq 1, \forall i$$

and so

$$\alpha \left(2.25 + \sum_j \sum_{\substack{i \in \mathcal{N}_n \\ j \in \mathcal{N}_n}} E_{n,i} E_{n,j} + 0.25 \sum_{n: i \in \mathcal{N}_n} E_{n,i} \right) \leq 1, \quad (5.39a)$$

$$\alpha \left(1 + \sum_j \sum_{n \in \mathcal{N}_j} E_{i,n} E_{j,n} + 1.25 \sum_n E_{i,n} \right) \leq 1, \quad (5.39b)$$

$$\alpha \left(2.25 + \sum_{n: i \in \mathcal{N}_n} E_{n,i} \right) \leq 1. \quad (5.39c)$$

CHAPTER 5. DISTRIBUTED LIGHTING CONTROL WITH LIGHT
SENSOR MEASUREMENTS

Using (5.39a) we have

$$\begin{aligned}
& \alpha \left(2.25 + \sum_{n:i \in \mathcal{N}_n} E_{n,i} \sum_{j \in \mathcal{N}_n} E_{n,j} + 0.25 \sum_{n:i \in \mathcal{N}_n} E_{n,i} \right) \leq 1 \\
& \alpha \left(2.25 + \xi \sum_{n \in \mathcal{N}_i} E_{n,i} + 0.25 \sum_{n \in \mathcal{N}_i} E_{n,i} \right) \leq 1 \\
& \alpha \left(2.25 + (\xi + 0.25) \sum_{n \in \mathcal{N}_i} E_{n,i} \right) \leq 1 \\
& \alpha \left(2.25 + (\xi + 0.25) N \xi \right) \leq 1 \\
& \alpha \leq \frac{1}{2.25 + (\xi + 0.25) \xi N}.
\end{aligned}$$

Similarly, from (5.39b) and (5.39c) we obtain respectively

$$\begin{aligned}
& \alpha \left(1 + \sum_j \sum_m E_{i,m} \sum_{n \in \mathcal{N}_j} E_{j,n} + 1.25 \sum_n E_{i,n} \right) \leq 1 \\
& \alpha \left(1 + \sum_j \frac{\xi}{\chi} \xi + 1.25 \frac{\xi}{\chi} \right) \leq 1 \\
& \alpha \left(1 + \frac{M \xi^2}{\chi} + 1.25 \frac{\xi}{\chi} \right) \leq 1 \\
& \alpha \leq \frac{\chi}{\chi + M \xi^2 + 1.25 \xi}
\end{aligned}$$

and

$$\begin{aligned}
& \alpha \left(2.25 + \sum_{n \in \mathcal{N}_i} E_{n,i} \right) \leq 1 \\
& \alpha (2.25 + N \xi) \leq 1 \\
& \alpha \leq \frac{1}{2.25 + N \xi}.
\end{aligned}$$

Summing up, sufficient conditions to (5.25) are given by (5.27) and (5.28).

REFERENCES

- [1] Buildings Energy Data Book, <http://buildingsdatabook.eren.doe.gov/>, 2011.
- [2] M. Aldrich, N. Zhao, and J. Paradiso, “Energy efficient control of polychromatic solid-state lighting using a sensor network,” *International Conference on Solid State Lighting, SPIE*, vol. 7784, August 2010.
- [3] D. Caicedo, A. Pandharipande, and G. Leus, “Occupancy based illumination control of LED lighting systems,” *Lighting Research and Technology*, vol. 43, no. 2, pp. 217–234, August 2011.
- [4] A. Pandharipande and D. Caicedo, “Daylight integrated illumination control of LED systems based on enhanced presence sensing,” *Energy and Buildings*, vol. 43, pp. 944–950, April 2011.
- [5] A. Pandharipande and D. Caicedo, “Adaptive illumination rendering in LED lighting systems,” *IEEE Transactions on Systems, Man, and Cybernetics—Part A: Systems and Humans*, vol. 43, no. 5, pp. 1052 – 1062, May 2013.
- [6] H. Wang, A. Pandharipande, D. Caicedo, and P. P. J. van den Bosch, “Distributed lighting control of locally intelligent luminaire systems,” *IEEE Conference on Systems, Man and Cybernetics*, 2012.
- [7] M.-S. Pan, L.-W. Yeh, Y.-A. Chen, Y.-H. Lin, and Y.-C. Tseng, “A WSN-based intelligent light control system considering user activities and profiles,” *IEEE Sensors Journal*, pp. 1710–1721, 2008.
- [8] L.-W. Yeh, C.-Y. Lu, C.-W. Kou, Y.-C. Tseng, and C.-W. Yi, “Autonomous light control by wireless sensor and actuator networks,” *IEEE Sensors Journal*, pp. 1029–1041, June 2010.
- [9] H. Yang and A. Pandharipande, “Disaggregated daylight-artificial light sensing,” *IEEE Sensors Journal*, vol. 12, no. 12, pp. 3438–3445, 2012.
- [10] F. J. Bellido-Outeirino, J. M. Flores-Arias, F. Domingo-Perez, A. G. de Castro, and A. Moreno-Munoz, “Building lighting automation through the integration of DALI with wireless sensor networks,” *IEEE Transactions on Consumer Electronics*, pp. 47–52, 2012.
- [11] S. Rajagopal, R. D. Roberts, and S.-K. Lim, “IEEE 802.15.7 visible light communication: modulation schemes and dimming support,” *IEEE Communications Magazine*, pp. 72–82, March 2012.

CHAPTER 5. DISTRIBUTED LIGHTING CONTROL WITH LIGHT
SENSOR MEASUREMENTS

- [12] Y. Gu, N. Narendran, T. Dong, and H. Wu, “Spectral and luminous efficacy change of high-power LEDs under different dimming methods,” *International Conference on Solid State Lighting, SPIE*, vol. 6337, p. 63370J, 2006.
- [13] DIALux, <http://www.dial.de/DIAL/en/dialux.html>.
- [14] D. G. Luenberger and Y. Ye, *Linear and Nonlinear Programming*, 3rd ed. Springer, 2008.
- [15] S. Boyd and L. Vandenberghe, *Convex Optimization*. Cambridge University Press, 2004.
- [16] K. Ogata, *Discrete-time control systems*, 2nd ed. Prentice-hall, 1995.
- [17] A. Nedic, A. Ozdaglar, and P. A. Parrilo, “Constrained consensus and optimization in multi-agent networks,” *IEEE Transactions on Automatic Control*, vol. 55, no. 4, pp. 922–938, April 2010.
- [18] European Committee for Standardization, “EN 12464-1:2002. Light and lighting. Lighting of work places. Part 1: Indoor work places,” 2002.
- [19] D. Caicedo and A. Pandharipande, “Ultrasonic array sensor for indoor presence detection,” *European Conference on Signal Processing*, pp. 175 – 179, 2012.
- [20] I. Moreno, “Image-like illumination with LED arrays: design,” *Optics Letters*, vol. 37, no. 5, pp. 839–841, 2012.
- [21] R. A. Horn and C. R. Johnson, *Matrix Analysis*. Cambridge University Press, 1990.

Chapter 6

Robust centralized lighting control with light sensor measurements*

We consider a daylight-adaptive lighting control system to adapt dimming levels of artificial light sources with changing daylight, under illumination constraints specified at the horizontal workspace plane of an occupant. We propose a control method for achieving a minimum illuminance at the workspace plane using illuminance measurements at light sensors situated at the ceiling, and additional prior-information from sensor calibration. The proposed method results in a linear programming optimization problem with inequality constraints. Using simulations with photometric data, we compare our sub-optimum solution with the solution where knowledge of the illuminance mapping from the light sensors to workspace illuminance values is available, and with a reference method that is based on satisfying illuminance constraints specified at the light sensors.

*This chapter has been published as: D. Caicedo, A. Pandharipande and F. M. J. Willems. "Daylight-adaptive lighting control using light sensor calibration prior-information", *Energy and Buildings*, vol. 73, pp. 105–114, April 2014.

6.1 Introduction

A major part of the total energy consumption in commercial buildings corresponds to artificial lighting [1]. For this reason, several works have focussed on minimizing energy consumption in lighting systems [2–4]. Limited energy consumption may be achieved by providing low illumination levels, but as shown in [5], low illumination levels will also decrease satisfaction, performance and productivity in the office. Further, this approach goes against the European guidelines for illumination levels in offices provided by norms EN12464-1 [6].

Daylight-adaptive lighting control provides an effective method for energy saving while providing the required illumination levels [2]. This is achieved by adapting the dimming levels of the light sources to produce an artificial illuminance distribution such that when combined with the varying daylight distribution results in a net illuminance distribution that meets the desired illuminance constraints.

The performance of daylight-adaptive lighting control strategies is determined by light sensor measurements. Light sensors should preferably be located in the plane of interest, i.e. the workspace plane [7–11]. In [7], [8], [9], centralized lighting control schemes were considered assuming knowledge of light distributions at the workspace plane. In [10], light sensors were placed at the workspace plane, and in [11], a system was considered wherein light sensors were carried by occupants. While it is advantageous to place light sensors directly at the plane where the light distribution is of interest, the light sensor measurements become more sensitive to changes in the environment, e.g. movement of occupants and is thus undesirable.

A different approach, and one widely used in practice, is to place the light sensors at the ceiling plane as in [4] and [12]. The light sensor measures illuminance within its sensor field of view. In such a system configuration, the light sensor measurements are in a plane different than the plane of interest, i.e. the illuminance measurements are at the ceiling and not at the workspace. Hence, we have limited knowledge about the light distribution at the workspace plane.

In this paper, we consider a lighting system with light sensors co-located at light sources. The light sensor measurements are input to a central controller that determines dimming levels of each light source. The objective of the central controller is to minimize power consumption while maintaining a minimum average illuminance level in various zones in the workspace plane, where zones are a logical partitioning of the workspace plane. Because the light sensors are located in the ceiling plane and not in the workspace plane, a calibration step is required where a relationship between the measured illuminance value at the light sensors in the ceiling plane and the average illuminance value at the workspace

plane is obtained. Using the measurements from the calibration step, the central controller translates the illuminance constraints in the workspace plane into illuminance constraints in the ceiling plane. An accurate relationship can be obtained by measuring all the possible illuminance distributions at the workspace plane and the corresponding illuminance values at the light sensors. This procedure is however time consuming and so a simplified calibration step is used in practice. Typically, the simplified calibration step is performed during night (dark-room calibration) using an additional light meter [13]. In this step, the light sources are dimmed to a reference value, and the corresponding reference average illuminance values at zones in the workspace plane and reference illuminance values at the light sensors are measured. In some scenarios, using the measurements from the simplified calibration step leads to a lighting system that satisfies the illuminance constraints at the light sensors in the ceiling plane but not the illuminance constraints at the workspace plane.

In our proposed method, we design a central controller that trades-off between power savings and the minimum achievable average illuminance levels at the zones in the workspace plane. The minimum achievable average illuminance level at each zone in the workspace plane for a given dimming vector is formulated as the solution to a constrained optimization problem with a mix of linear and non-convex constraints. We use the calibration prior-information (i.e. reference dimming levels and illuminance measurements) and measured illuminance values at the light sensors to obtain a lower bound, which is linear in the dimming vector, for this constrained optimization problem. We then incorporate the lower bound as an additional constraint in the power minimization problem and solve it, thus resulting in a sub-optimum power saving given the illumination rendering constraints at the workspace plane. The resulting optimization problem is a linear programming problem with inequality constraints. Using photometric data from an indoor open-office scenario, we compare our proposed solution with two other methods: the first one, where knowledge of the illuminance mapping from the light sensors to workspace illuminance values is known; and the second one, where illuminance constraints are specified at the light sensors as in [4].

6.2 Lighting system description and problem setup

We consider a lighting system in an indoor office as depicted in Fig. 6.1, with P light sources. Each light source is embedded with a light sensor that has a limited field of view defined by its opening angle. Parallel to the ceiling is the workspace plane where the spatial illuminance distribution is of interest. The workspace plane is assumed to be divided into P logical zones, as shown in Fig. 6.1. Denote



Figure 6.1: Top view of office room showing zones

$\mathbf{d} = [d_1, d_2, \dots, d_P]$ to be the dimming vector containing dimming levels, d_n ($0 \leq d_n \leq 1$), of the n -th light source.

The dimming level of each LED light source is determined by the central controller, under the constraint that the resulting illumination rendered from the lighting system satisfies a minimum target average illuminance level in each zone in the workspace plane. Denote the target average illuminance level at the m -th workspace zone, when the m -th zone is occupied (respectively, unoccupied), as W_m^o (respectively, W_m^u).

6.2.1 Illuminance at workspace plane

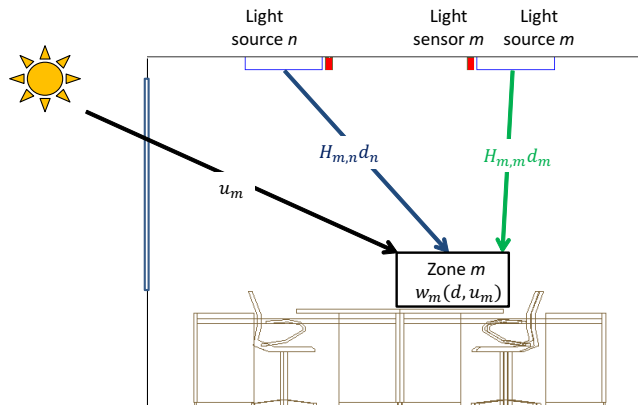


Figure 6.2: Average illuminance at zone m at the workspace due to contribution from artificial light and daylight.

The average net illuminance at the m -th zone in the workspace plane, given

dimming vector \mathbf{d} and under daylight, may be written as

$$w_m(\mathbf{d}, u_m) = \sum_{n=1}^P H_{m,n} d_n + u_m,$$

where $\sum_{n=1}^P H_{m,n} d_n$ and u_m are the illuminance contributions due to lighting system and daylight at the m -th zone, respectively, as seen in Fig. 6.2. Here, $H_{m,n} \geq 0$ is the unknown illuminance contribution to the average in the m -th zone when the n -th light source is at maximum intensity, with all other light sources turned off.

In practice, illuminance values at the workspace place cannot be measured; instead, only illuminance measurements at light sensors are available.

6.2.2 Illuminance at light sensor

The measured illuminance at a light sensor in the ceiling is the net illuminance due to contributing light sources and daylight reflected from the objects (e.g. furniture) in the office. Denote $E_{m,n}$ as the measured illuminance at the m -th light sensor when the n -th light source is at maximum intensity, in the absence of daylight. We assume that the illuminance scales linearly with the dimming level. This assumption holds well for practical light sources, e.g. LED light sources.

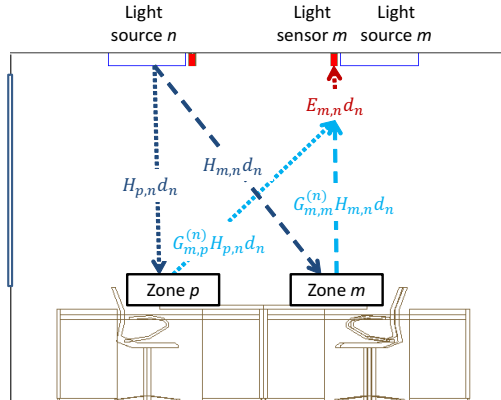


Figure 6.3: Illuminance contribution at light sensor m due to artificial light from light source n reflected from zone m and p .

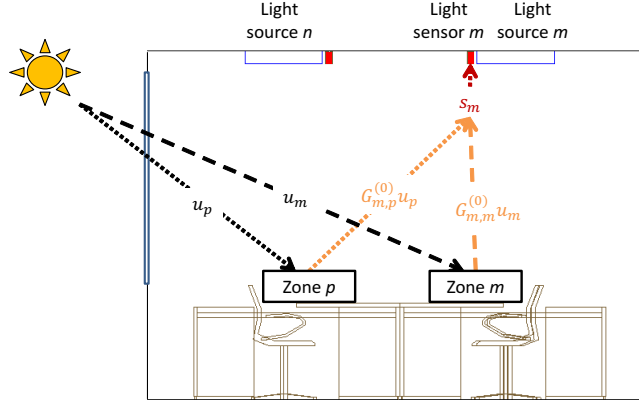


Figure 6.4: Illuminance contribution at light sensor m due to daylight reflected from zone m and p .

The net illuminance at the m -th sensor at the ceiling, given that the lighting system is at dimming vector \mathbf{d} and under daylight, can then be written as

$$l_m(\mathbf{d}, s_m) = \sum_{n=1}^P E_{m,n} d_n + s_m, \quad (6.1)$$

where $\sum_{n=1}^P E_{m,n} d_n$ is the illuminance due to the lighting system and s_m is the illuminance due to daylight measured at the m -th sensor, as seen in Figs. 6.3 and 6.4, respectively. In practice, the mappings $E_{m,n}$ may be computed a priori in a calibration phase by turning on the light sources to the maximum intensity one at a time and measuring illuminance values at the light sensors.

Further, we can relate the average illuminance values at the workspace plane and illuminance values at light sensors by

$$\sum_n E_{m,n} d_n = \sum_n \sum_p G_{m,p}^{(n)} H_{p,n} d_n, \quad (6.2)$$

$$s_m = \sum_p G_{m,p}^{(0)} u_p, \quad (6.3)$$

where $G_{m,p}^{(n)} \geq 0$ is the illuminance contribution at the m -th light sensor when the average illuminance at the p -th zone due to the n -th light source is at the maximum (see Figs. 6.3 and 6.4). Here, $G_{m,p}^{(0)} \geq 0$ is the illuminance contribution at the m -th light sensor when the average illuminance at the p -th zone due to daylight is u_p . Note that we do not have knowledge of $\{G_{m,p}^{(n)}\}$ or $\{G_{m,p}^{(0)}\}$.

6.2.3 Calibration step

A dark-room calibration step is performed with the lighting system set to a reference dimming vector $\mathbf{d}^* = [d_1^*, \dots, d_P^*]^T$. During this step, we obtain the reference average illuminance values at the workspace plane $\mathbf{W}^* = [W_1^*, \dots, W_P^*]^T$ using an additional light meter and measure the reference illuminance values at light sensors $\mathbf{L}^* = [L_1^*, \dots, L_P^*]^T$, where $W_P^* = w_p(\mathbf{d}^*, 0)$ and $L_P^* = l_p(\mathbf{d}^*, 0)$

The transfer matrix

$$\mathbf{E} = \begin{bmatrix} E_{1,1} & \dots & E_{1,P} \\ \vdots & \ddots & \vdots \\ E_{P,1} & \dots & E_{P,P} \end{bmatrix},$$

with (m, n) -th element $E_{m,n} = \sum_p G_{m,p}^{(n)} H_{p,n}$, is also determined during this step, as discussed in Section 6.2.2, by turning on individual light sources one at a time at maximum dimming and making illuminance measurements at the light sensors. Note that the individual terms $\{G_{m,p}^{(n)}\}$ and $\{H_{p,n}\}$ are not measured.

6.3 Problem formulation

Our problem is to obtain the dimming vector \mathbf{d}^* that minimizes the power consumption of the lighting system such that the net illuminance at the workspace plane, $\{w_m(\mathbf{d}, u_m)\}$, is larger than a target illuminance level. Note that minimizing the power consumption is equivalent to minimizing the sum of dimming levels of the P light sources [4], [7]. Define

$$\mathbf{H} = \begin{bmatrix} H_{1,1} & \dots & H_{1,P} \\ \vdots & \ddots & \vdots \\ H_{P,1} & \dots & H_{P,P} \end{bmatrix}, \quad \mathbf{G}^{(n)} = \begin{bmatrix} G_{1,1}^{(n)} & \dots & G_{1,P}^{(n)} \\ \vdots & \ddots & \vdots \\ G_{P,1}^{(n)} & \dots & G_{P,P}^{(n)} \end{bmatrix},$$

and $\mathbf{u} = [u_1, \dots, u_P]^T$. Note that the only knowledge we have of \mathbf{H} , $\mathbf{G}^{(n)}$ and \mathbf{u} is that

- [P1] all entries of \mathbf{H} , $\mathbf{G}^{(n)}$ and \mathbf{u} are non-negative;
- [P2] under reference dimming vector \mathbf{d}^* , we obtain average illuminance distribution at the workspace \mathbf{W}^* and illuminance values at light sensors \mathbf{L}^* ; and
- [P3] transfer matrix \mathbf{H} and $\mathbf{G}^{(n)}$ are related by $\sum_q G_{p,q}^{(n)} H_{q,n} = E_{p,n}$, $\forall p, n$.

CHAPTER 6. ROBUST CENTRALIZED LIGHTING CONTROL WITH
LIGHT SENSOR MEASUREMENTS

Further, we assume that

- [A1] zone m is only illuminated by a limited set of light sources within its neighborhood. Let \mathcal{N}_m denotes the index set of neighborhood light sources of zone m . Thus, we have $H_{m,n} = 0, n \notin \mathcal{N}_m$;
- [A2] the illuminance contributions of the m -th and n -th light sources to the net illuminance of the m -th zone at the workspace satisfy the following relation:
 $H_{m,n} \leq \xi_{m,n} H_{m,m}, \forall m, n \in \mathcal{N}_m$;
- [A3] the illuminance contribution from light source m to zone m is larger than the illuminance contribution from other light sources, i.e. $\xi_{m,n} \leq 1, \forall m, n \in \mathcal{N}_m$; and
- [A4] any light source that contributes to the net illuminance of the m -th zone, also contributes to the illuminance value of the m -th light sensor. Hence, the ratio between terms $G_{m,m}^{(m)}$ and $G_{m,m}^{(n)}$ is bounded, i.e. $\frac{G_{m,m}^{(m)}}{G_{m,m}^{(n)}} \leq \psi_{m,n}, \forall m, n, \psi_{m,n} > 0$.

Assumption [A1] is reasonable because in a typical lighting system for offices, the illuminance contribution of a light source to the net illuminance of a given zone decreases with the separation between the zone and the light source. Hence, the contribution from non-neighboring further-off light sources to a particular zone is negligible. Further, the major contributor to the net illuminance of the zone is its own light source, followed by the illuminance contribution from neighboring light sources (assumptions [A2] and [A3]). Lastly, assumption [A4] is reasonable because the workspace disperses the incident light in all directions.

Using the prior-information [P1]-[P3] and assumptions [A1]-[A4], we can formulate the problem as

$$\mathbf{d}^* = \arg \min_{\mathbf{d}} \sum_{n=1}^P d_n \quad \text{s.t.}$$

$$\begin{cases} e_m(\mathbf{d}, W_m - u_m) \leq \eta W_m, & m = 1, \dots, M \end{cases} \quad (6.4a)$$

$$\begin{cases} 0 \leq d_n \leq 1, & n = 1, \dots, P, \end{cases} \quad (6.4b)$$

where

$$e_m(\mathbf{d}, W_m - u_m) = \max_{\mathbf{H}, \mathbf{G}^{(n)}, t_m} t_m \quad \text{s.t.}$$

$$\left\{ \begin{array}{l} \sum_{n \in \mathcal{N}_m} H_{m,n} d_n + t_m = W_m - u_m \end{array} \right. \quad (6.5a)$$

$$\left\{ \begin{array}{l} \sum_{n \in \mathcal{N}_p} H_{p,n} d_n^* = W_p^*, \forall p \end{array} \right. \quad (6.5b)$$

$$\left\{ \begin{array}{l} H_{p,n} \geq 0, \forall p, n \in \mathcal{N}_p \end{array} \right. \quad (6.5c)$$

$$\left\{ \begin{array}{l} H_{p,n} \leq \xi_{p,n} H_{p,p}, \forall p, n \in \mathcal{N}_p \end{array} \right. \quad (6.5d)$$

$$\left\{ \begin{array}{l} \sum_q G_{p,q}^{(n)} H_{q,n} = E_{p,n}, \forall p, n \end{array} \right. \quad (6.5e)$$

$$\left\{ \begin{array}{l} G_{q,p}^{(n)} \geq 0, \forall q, n, p. \end{array} \right. \quad (6.5f)$$

The problem in (6.5) provides us with the maximum difference between target and achieved illuminance level over all feasible matrices \mathbf{H} . Hence, constraint (6.4a) indicates that the difference between target and achieved illuminance level at zone m in the worst-case scenario should be smaller than ηW_m . Here, $\{\xi_{m,n} \geq 0\}$ and $0 \leq \eta \leq 1$ are parameters of the system.

6.4 Proposed method

In this section, we propose a method to obtain a sub-optimum solution to problem (6.4).

6.4.1 No-daylight case

Let us consider the no-daylight case (i.e. $u_m = 0, \forall m$). First of all, we find a solution to the simplest version of problem (6.5). We only consider constraints (6.5a)-(6.5c), i.e.

$$\begin{aligned} \bar{e}_m(\mathbf{d}, W_m) &= \max_{\mathbf{H}, t_m} t_m \\ \text{s.t.} \quad &\left\{ \begin{array}{l} \sum_{n \in \mathcal{N}_m} H_{m,n} d_n + t_m = W_m \\ \sum_{n \in \mathcal{N}_p} H_{p,n} d_n^* = W_p^*, \forall p \\ H_{p,n} \geq 0, \forall p, n \in \mathcal{N}_p. \end{array} \right. \end{aligned} \quad (6.6)$$

Note that $e_m(\mathbf{d}, W_m) \leq \bar{e}_m(\mathbf{d}, W_m), \forall m$, i.e. it provides an upper-bound to the optimal solution of problem (6.5).

CHAPTER 6. ROBUST CENTRALIZED LIGHTING CONTROL WITH
LIGHT SENSOR MEASUREMENTS

The problem in (6.6) is a linear programming problem with solution (see 6.B) given by

$$\bar{e}_m(\mathbf{d}, W_m) = W_m - W_m^* \min_{n \in \mathcal{N}_m} \left\{ \frac{d_n}{d_n^*} \right\}. \quad (6.7)$$

Then, using (6.7), we can rewrite constraint (6.4a) as

$$\begin{aligned} W_m - W_m^* \min_{n \in \mathcal{N}_m} \left\{ \frac{d_n}{d_n^*} \right\} &\leq \eta W_m \\ \min_{n \in \mathcal{N}_m} \left\{ \frac{d_n}{d_n^*} \right\} &\geq (1 - \eta) \frac{W_m}{W_m^*} \end{aligned}$$

and so

$$d_n \geq (1 - \eta) \frac{W_m}{W_m^*} d_n^*, \quad n \in \mathcal{N}_m, \quad \forall m. \quad (6.8)$$

Solution (6.8) means that all light sources that contribute to the net average illuminance at zone m should be at a dimming level larger than the reference dimming level times a scaling factor, $(1 - \eta) \frac{W_m}{W_m^*}$.

Using (6.8), we can obtain a simple sub-optimum solution to our optimization problem in (6.4) as

$$d_n^* = \max_{m: n \in \mathcal{N}_m} \left\{ (1 - \eta) \frac{W_m}{W_m^*} d_n^* \right\}, \quad \forall n. \quad (6.9)$$

Second, we add constraint (6.5d) to problem (6.6), i.e.

$$\begin{aligned} \bar{e}_m(\mathbf{d}, W_m) &= \max_{\mathbf{H}, t_m} t_m \\ \text{s.t.} \quad &\begin{cases} \sum_{n \in \mathcal{N}_m} H_{m,n} d_n + t_m = W_m \\ \sum_{n \in \mathcal{N}_p} H_{p,n} d_n^* = W_p^*, \forall p \\ H_{p,n} \geq 0, \quad \forall p, n \in \mathcal{N}_p, \\ H_{p,n} \leq \xi_{p,n} H_{p,p}, \quad \forall p, n \in \mathcal{N}_p. \end{cases} \end{aligned} \quad (6.10)$$

The problem in (6.10) is also a linear programming problem with solution equal to the minimum value of t_m (see 6.A) that satisfies

$$\begin{cases} t_m = W_m - \frac{W_m^*}{d_m^*} \left[d_m - \sum_{\substack{q \neq m \\ \wedge q \in \mathcal{N}_m}} \mu_{m,q} \xi_{m,q} \right], \\ t_m \geq W_m - \frac{W_m^*}{d_n^*} \left[d_n + \mu_{m,n} \right], \quad n \neq m \wedge n \in \mathcal{N}_m, \\ \mu_{m,n} \geq 0, \quad n \neq m \wedge n \in \mathcal{N}_m. \end{cases} \quad (6.11)$$

Next, we replace constraint (6.4a) by (6.11) and obtain

$$\begin{cases} W_m - \frac{W_m^*}{d_m^*} \left[d_m - \sum_{\substack{q \neq m \\ \wedge q \in \mathcal{N}_m}} \mu_{m,q} \xi_{m,q} \right] \leq \eta W_m, \\ W_m - \frac{W_m^*}{d_n^*} \left[d_n + \mu_{m,n} \right] \leq \eta W_m, n \neq m \wedge n \in \mathcal{N}_m, \\ \mu_{m,n} \geq 0, n \neq m \wedge n \in \mathcal{N}_m. \end{cases} \quad (6.12)$$

Let us rewrite the set of equations in (6.12) as

$$\begin{cases} d_m \geq (1 - \eta) \frac{W_m}{W_m^*} d_m^* + \sum_{\substack{q \neq m \\ \wedge q \in \mathcal{N}_m}} \mu_{m,q} \xi_{m,q}, \\ \mu_{m,n} \geq \max \left\{ 0, (1 - \eta) \frac{W_m}{W_n^*} d_n^* - d_n \right\}, n \neq m \wedge n \in \mathcal{N}_m. \end{cases} \quad (6.13)$$

We can see from solution (6.13) that the additional intensity of light source m (over its scaled reference dimming level, $(1 - \eta) \frac{W_m}{W_m^*} d_m^*$) should compensate for the missing intensity of all its neighbors (with respect to the scaled reference dimming levels, $\{(1 - \eta) \frac{W_m}{W_n^*} d_n^*, n \neq m \wedge n \in \mathcal{N}_m\}$).

Lastly, we consider the non-linear constraint (6.5e) and constraint (6.5f). Note that the solution in (6.11) depends on the terms $\{\xi_{m,n}\}$. Hence, we use constraints (6.5e) and (6.5f) to upper-bound these terms as

$$\xi_{m,n} = \frac{H_{m,n}}{H_{m,m}} \leq \min \left\{ 1, \frac{E_{m,n} G_{m,m}^{(m)} \gamma_m}{E_{m,m} G_{m,m}^{(n)}} \right\} \leq \min \left\{ 1, \frac{E_{m,n} \gamma_m \psi_{m,n}}{E_{m,m}} \right\}. \quad (6.14)$$

Here, we use

$$E_{m,n} = \sum_p G_{m,p}^{(n)} H_{p,n} = G_{m,m}^{(n)} H_{m,n} + \sum_{p \neq m} G_{m,p}^{(n)} H_{p,m} \geq G_{m,m}^{(n)} H_{m,n}$$

and

$$E_{m,m} = \sum_p G_{m,p}^{(m)} H_{p,m} \leq H_{m,m} \sum_p G_{m,p}^{(m)} = H_{m,m} G_{m,m}^{(m)} \gamma_m,$$

where

$$\gamma_m = 1 + \sum_{p \neq m} \frac{G_{m,p}^{(m)}}{G_{m,m}^{(m)}}.$$

CHAPTER 6. ROBUST CENTRALIZED LIGHTING CONTROL WITH LIGHT SENSOR MEASUREMENTS

Finally, we obtain a sub-optimal solution to our optimization problem in (6.4) by solving the linear programming problem

$$\mathbf{d}^* = \arg \min_{\mathbf{d}, \{\mu_{m,n}\}} \sum_{n=1}^P d_n$$

$$\text{s.t.} \begin{cases} d_m - \sum_{\substack{q \neq m \\ \wedge q \in \mathcal{N}_m}} \mu_{m,q} \xi_{m,q} \geq (1 - \eta) \frac{W_m}{W_m^*} d_m^*, \quad \forall m \\ d_n + \mu_{m,n} \geq (1 - \eta) \frac{W_m}{W_m^*} d_n^*, \quad \forall m, n \neq m \wedge n \in \mathcal{N}_m \\ \mu_{m,n} \geq 0, \quad \forall m, n \neq m \wedge n \in \mathcal{N}_m \\ 0 \leq d_n \leq 1, \quad n = 1, \dots, P, \end{cases} \quad (6.15)$$

where we replace constraints (6.4a) by (6.11) and use the upper-bounds of terms $\{\xi_{m,n}\}$ given by equation (6.14). The linear programming problem in (6.15) can be solved using known techniques like interior-point or Simplex algorithms [14].

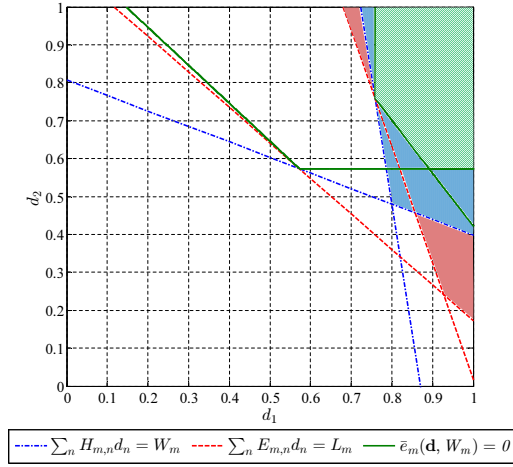


Figure 6.1: Geometric view of constraints

In Fig. 6.1, we provide a geometric view of constraints in (6.11). For this example, we consider $P = 2$ light sources and zones;

$$\mathbf{E} = \begin{bmatrix} 12.24 & 3.88 \\ 12.78 & 13.88 \end{bmatrix}, \quad \mathbf{H} = \begin{bmatrix} 540 & 80 \\ 180 & 440 \end{bmatrix},$$

$$\mathbf{d}^* = \begin{bmatrix} 0.9 \\ 0.9 \end{bmatrix}, \quad \mathbf{W} = \begin{bmatrix} 470.4 \\ 355.2 \end{bmatrix}, \quad \mathbf{L} = \begin{bmatrix} 11.7 \\ 15.9 \end{bmatrix},$$

with parameters $\eta = 0$ and $\xi_{m,n} = 1$, $m = 1, 2$ and $n = 1, 2$. Here, $\mathbf{L} = [L_1, \dots, L_P]^T$ are the corresponding target illuminance levels at the light sensors, where

$$L_p = \frac{W_p}{W_p^*} L_p^*. \quad (6.16)$$

The pair of inequality constraints $\sum_n H_{m,n} \mathbf{d} \geq W_m$, $m = 1, 2$, define the actual set of feasible solutions. This feasible set is depicted in Fig. 6.1 as the blue vertical and green diagonal patterned region. The optimum solution is given by point $[0.8, 0.48]^T$.

We can see that the pair of inequality constraints at the light sensor

$$\sum_n E_{m,n} \mathbf{d} \geq I_m, \quad m = 1, 2$$

extends outside the feasible solution space (red horizontal patterned region). The achieved solution using this pair of inequality constraints is the point $[0.92, 0.25]^T$. This solution is outside the actual set of feasible solution, i.e. it is in the red horizontal patterned region.

Finally, our new pair of constraints $\bar{e}_m(\mathbf{d}, W_m) \leq 0$, $m = 1, 2$, defines a set of feasible solutions that are within the actual set (green diagonal patterned region). The corresponding solution is given by point $[0.88, 0.57]^T$.

Further, we can see that all the constraints for the m -th zone intersect at the same point $\left[\frac{W_m}{W_m^*} d_1^*, \frac{W_m}{W_m^*} d_2^* \right]^T$. Note that this point depends on the reference dimming vector, target and reference average illuminance values at the workspace plane.

6.4.2 Daylight case

In this section, we consider the daylight case. First of all, for a given $H_{m,n}$, we can rewrite the daylight contribution at the m -th workspace zone as

$$\begin{aligned} u_m &= \sum_{n \in \mathcal{N}_m} H_{m,n} z_n^* + r_m, \\ 0 &\leq r_m \leq u_m, \\ z_n^* &\geq 0. \end{aligned} \quad (6.17)$$

Here, $\{z_m^*\}$ are compensation terms for the daylight at the m -th light sensor, $\sum_{n \in \mathcal{N}_m} H_{m,n} z_n^*$ is the estimated daylight at the workspace using terms $\{H_{m,n}\}$

CHAPTER 6. ROBUST CENTRALIZED LIGHTING CONTROL WITH
LIGHT SENSOR MEASUREMENTS

and $\{z_m^*\}$; and r_m is the associated residual. The bounds in r_m are necessary conditions to avoid under- or over-estimating the daylight.

Next, we proceed to bound the vector \mathbf{z}^* that satisfies constraints in (6.17). We define the bounds based on the Euclidean norm of the vector, $\|\mathbf{z}^*\|$. A lower-bound is 0, i.e. no daylight compensation, $z_m = 0, \forall m$. Note that the constraints in (6.17) define a convex set and so exists a vector \mathbf{z}^* in this set that satisfies,

$$\|\mathbf{z}^*\| \leq \|\bar{\mathbf{z}}\|, \quad (6.18)$$

where $\bar{\mathbf{z}}$ is the vector in \mathbb{R}^P such that $\mathbf{H}\bar{\mathbf{z}} = \mathbf{u}$, i.e. $r_m = 0, m = 1, \dots, P$.

However, we do not know \mathbf{u} and so we cannot obtain $\bar{\mathbf{z}}$. We only know daylight contribution at light sensors $\mathbf{s} = \mathbf{l}(\mathbf{d}, \mathbf{s}) - \mathbf{E}\mathbf{d}$, where

$$\begin{aligned} \mathbf{l}(\mathbf{d}, \mathbf{s}) &= [l_1(\mathbf{d}, s_1), \dots, l_P(\mathbf{d}, s_P)]^T \text{ and} \\ \mathbf{s} &= [s_1, \dots, s_P]^T. \end{aligned} \quad (6.19)$$

Thus, we can only obtain a vector $\mathbf{z}^* \in \mathbb{R}^P$ that satisfies $\mathbf{E}\mathbf{z}^* = \mathbf{s}$. Next, we can write

$$\begin{aligned} \|\mathbf{z}^*\| &= \|\mathbf{E}^{-1}\mathbf{s}\| = \left\| \mathbf{E}^{-1} \left(\bar{\mathbf{G}}\mathbf{u} + (\mathbf{G}^{(0)} - \bar{\mathbf{G}})\mathbf{u} \right) \right\| \\ &= \left\| \mathbf{E}^{-1} \left(\mathbf{E}\bar{\mathbf{z}} + (\mathbf{G}^{(0)} - \bar{\mathbf{G}})\mathbf{u} \right) \right\| \\ &\leq \|\bar{\mathbf{z}}\| + \left\| \mathbf{E}^{-1}(\mathbf{G}^{(0)} - \bar{\mathbf{G}})\mathbf{u} \right\|, \end{aligned} \quad (6.20)$$

where $\bar{\mathbf{G}} = \mathbf{E}\mathbf{H}^{-1}$ is a transfer matrix from zones to sensors, $(\mathbf{G}^{(0)} - \bar{\mathbf{G}})\mathbf{u}$ is the term associated with the mismatch between matrices $\bar{\mathbf{G}}$ and $\mathbf{G}^{(0)}$; and $\mathbf{s} = \bar{\mathbf{G}}\mathbf{u} + (\mathbf{G}^{(0)} - \bar{\mathbf{G}})\mathbf{u}$.

If we combine (6.18) and (6.20), then we can constraint our search space to those vectors \mathbf{z} such that

$$\|\mathbf{z}\| \leq \beta \|\mathbf{z}^*\|, \quad (6.21)$$

where $0 \leq \beta \leq 1$ determines how close the solution is from the upper-bound.

Hence, we seek for a vector \mathbf{z}^* that minimizes residuals $\{r_m\}$ such that (6.21) is satisfied for a given β , i.e.

$$\begin{aligned} \mathbf{z}^* &= \arg \min_{\mathbf{z}} \|\mathbf{E}\mathbf{z} - \mathbf{s}\|^2 \\ \text{s.t.} &\begin{cases} \mathbf{E}\mathbf{z} \leq \mathbf{s}, \\ \|\mathbf{z}\| \leq \beta \|\mathbf{z}^*\|, \\ z_n \geq 0, n = 1, \dots, P. \end{cases} \end{aligned} \quad (6.22)$$

Note that (6.22) is a quadratic constrained quadratic programming problem.

Using (6.17) and (6.22), we can rewrite the problem in (6.6) as

$$\begin{aligned} \bar{e}_m(\mathbf{d}, W_m - u_m) &= \max_{\mathbf{H}, \bar{t}_m} \bar{t}_m \\ \text{s.t. } &\begin{cases} \sum_{n \in \mathcal{N}_m} H_{m,n} \bar{d}_n + \bar{t}_m = W_m \\ \sum_{n \in \mathcal{N}_p} H_{p,n} d_n^* = W_p^*, \forall p \\ H_{p,n} \geq 0, \forall p, n \in \mathcal{N}_p, \end{cases} \end{aligned} \quad (6.23)$$

and the problem in (6.10) as

$$\begin{aligned} \bar{e}_m(\mathbf{d}, W_m - u_m) &= \max_{\mathbf{H}, \bar{t}_m} \bar{t}_m \\ \text{s.t. } &\begin{cases} \sum_{n \in \mathcal{N}_m} H_{m,n} \bar{d}_n + \bar{t}_m = W_m \\ \sum_{n \in \mathcal{N}_p} H_{p,n} d_n^* = W_p^*, \forall p \\ H_{p,n} \leq \xi_{p,n} H_{p,p}, \forall p, n \in \mathcal{N}_p \\ H_{p,n} \geq 0, \forall p, n \in \mathcal{N}_p, \end{cases} \end{aligned} \quad (6.24)$$

where we introduce variables

$$\begin{aligned} \bar{t}_m &= t_m + r_m, \\ \bar{d}_n &= d_n + z_n^*, \forall n. \end{aligned}$$

Note that the term r_m determines how tight the bounds in (6.23) and (6.24) are under daylight.

Using a similar procedure as given in Section 6.4.1, we rewrite constraint (6.4a) with the optimum solution of (6.23) as

$$d_n \geq (1 - \eta) \frac{W_m}{W_m^*} d_n^* - z_n^*, \quad n \in \mathcal{N}_m, \forall m \quad (6.25)$$

and with the optimum solution of (6.24) as

$$\begin{cases} d_m \geq (1 - \eta) \frac{W_m}{W_m^*} d_m^* + \sum_{\substack{q \neq m \\ \wedge q \in \mathcal{N}_m}} \mu_{m,q} \xi_{m,q} - z_m^*, \\ \mu_{m,n} \geq \max \left\{ 0, (1 - \eta) \frac{W_m}{W_n^*} d_n^* - d_n - z_n^* \right\}, \quad n \neq m \wedge n \in \mathcal{N}_m. \end{cases} \quad (6.26)$$

Finally, using (6.25), we can obtain a simple sub-optimum solution to our optimization problem as

$$d_n^* = \max \left\{ 0, \max_{m: n \in \mathcal{N}_m} \left\{ (1 - \eta) \frac{W_m}{W_m^*} d_n^* - z_n^* \right\} \right\}, \quad \forall n, \quad (6.27)$$

CHAPTER 6. ROBUST CENTRALIZED LIGHTING CONTROL WITH
LIGHT SENSOR MEASUREMENTS

analogous to (6.9). An improved sub-optimum solution is obtained by solving the linear programming problem

$$\mathbf{d}^* = \arg \min_{\mathbf{d}, \{\mu_{m,n}\}} \sum_{n=1}^P d_n$$

$$\text{s.t.} \begin{cases} d_m - \sum_{\substack{q \neq m \\ \wedge q \in \mathcal{N}_m}} \mu_{m,q} \xi_{m,q} \geq (1 - \eta) \frac{W_m}{W_m^*} d_m^* - z_m^*, \quad \forall m \\ d_n + \mu_{m,n} \geq (1 - \eta) \frac{W_m}{W_m^*} d_n^* - z_n^*, \quad \forall m, n \neq m \wedge n \in \mathcal{N}_m \\ \mu_{m,n} \geq 0, \quad \forall m, n \neq m \wedge n \in \mathcal{N}_m \\ 0 \leq d_n \leq 1, \quad n = 1, \dots, P, \end{cases} \quad (6.28)$$

where we use (6.26) and (6.22). This is analogous to the solution (6.15) in Section 6.4.1.

6.5 Numerical results

In this Section, we present numerical results to evaluate the performance of the proposed method. The dimensions of the office are: 14.4 m (length) \times 7.2 m (width) \times 2.7 m (ceiling height). The distance of the ceiling to the workspace plane is 1.94 m. There are $P = 24$ light sources, with co-located light sensors, arranged in a grid of 3-by-8 as shown in Fig. 6.1. The light source indexing in Fig. 6.1 also corresponds to that of the zones. The office has windows on one side of the room for daylight. We consider a light sensor with a half-opening angle of 45 degrees.

The reference average illuminance at the workspace, \mathbf{W}^* , is 600 lux, with variations within 20%. This illuminance distribution may be realized by setting the lighting system to the reference dimming vector $\mathbf{d}^* = 0.9 \times \mathbf{1}$, where $\mathbf{1}$ is a vector of ones of size 24×1 . In Table 6.1, we show the reference illuminance for each zone at the workspace plane and light sensor (under dimming vector \mathbf{d}^*).

We assume the neighborhood of the m -th light source to include the closest light sources. The target average illuminance values at the workspace when the m -th zone is occupied and unoccupied are respectively

$$W_m^o = \min(500, w_m(\mathbf{d}^*, 0)) \quad \text{and} \quad W_m^u = \min(300, w_m(\mathbf{d}^*, 0)).$$

We compare our proposed method given by (6.28) with a reference method that minimizes the power consumption subject to illuminance constraints at the

Index [m]	W_m^*	L_m^*	Index [m]	W_m^*	L_m^*
1	413	104	13	498	109
2	468	54	14	567	62
3	428	100	15	515	103
4	489	107	16	498	109
5	554	56	17	565	59
6	506	101	18	512	102
7	497	110	19	494	55
8	565	59	20	555	94
9	514	104	21	501	100
10	497	110	22	423	53
11	567	60	23	477	90
12	515	104	24	429	100

Table 6.1: Reference average illuminance per zone and reference illuminance at light sensor

light sensors, i.e.

$$\mathbf{d}^{(ceiling)} = \arg \min_{\mathbf{d}} \sum_{n=1}^P d_n \quad \begin{cases} \mathbf{E}\mathbf{d} \geq \mathbf{L} - \mathbf{s} \\ 0 \leq d_n \leq 1, n = 1, \dots, P, \end{cases} \quad (6.29)$$

where the elements of \mathbf{L} are given by (6.16). The reference method corresponds to a central controller that adapts the dimming levels of the light sources based only on the measured illuminance values at the light sensors at the ceiling. The target illuminances, \mathbf{L} , are the translated target illuminance values from the zones in the workspace plane to the corresponding light sensors at the ceiling plane.

Also, we compare our solution with the solution obtained when the transfer matrix from light sources to workspace zones, \mathbf{H} , is known, i.e.

$$\mathbf{d}^{(workplane)} = \arg \min_{\mathbf{d}} \sum_{n=1}^P d_n \quad \begin{cases} \mathbf{H}\mathbf{d} \geq \mathbf{W} - \mathbf{u} \\ 0 \leq d_n \leq 1, n = 1, \dots, P. \end{cases} \quad (6.30)$$

CHAPTER 6. ROBUST CENTRALIZED LIGHTING CONTROL WITH LIGHT SENSOR MEASUREMENTS

Full knowledge of \mathbf{H} corresponds to a lighting system where the light sensors are located at the workspace plane.

The power savings of the proposed method and when the light sensors are located at the workspace plane are calculated with respect to a lighting system without daylight-adaptive lighting control (the lighting system is set to dimming vector $\mathbf{d}^{(no-control)} = 0.9 \times \mathbf{1}$ when there is occupancy in the room), i.e.

$$100\% \frac{\mathbf{1}^T \mathbf{d}^{(no-control)} - \mathbf{1}^T \mathbf{d}^*}{\mathbf{1}^T \mathbf{d}^{(no-control)}} \text{ and}$$

$$100\% \frac{\mathbf{1}^T \mathbf{d}^{(no-control)} - \mathbf{1}^T \mathbf{d}^{(workspace)}}{\mathbf{1}^T \mathbf{d}^{(no-control)}},$$

respectively.

We choose parameters $\eta = 0$ and $\beta = 0.75$ for our simulations.

6.5.1 No-daylight scenario

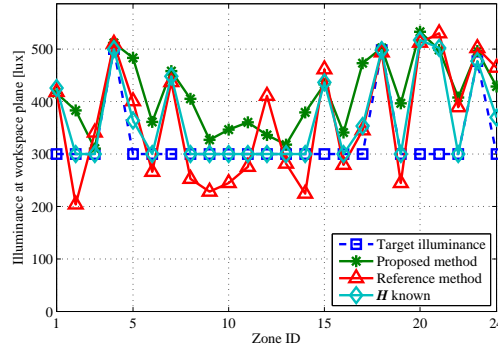


Figure 6.1: Achieved average illuminance levels at zones at the workspace plane for the proposed and reference method. Here, zones 4, 18 and 23 are occupied. For comparison, we show the target average illuminance levels at the zones and achieved average illuminance levels when the light sensors are located at the workspace plane (i.e. transfer matrix \mathbf{H} is known).

We simulate $K = 10^4$ instances of occupancy realizations for different occupancy level ($100\% \frac{\chi}{P}$, $\chi = 1, \dots, P$) without daylight. For each occupancy level, we distributed the occupants over all the zones randomly. In Fig. 6.1, we show the achieved average illuminance levels at the workspace plane for the reference method, proposed method and when light sensors are located at the workspace

plane for a single simulation instance where zones 4, 18 and 23 are occupied. We can see that the proposed method satisfies the illuminance constraints at the workspace while the reference method fails. In some zones (e.g. zone 2), the average illuminance levels for the reference method can be 100 lux below the target.

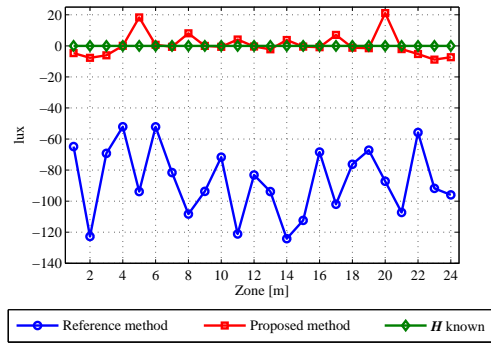


Figure 6.2: Difference between minimum achieved and target average illuminance, over all simulations and occupancy levels, at workspace in proposed and reference method (under no-daylight scenario). For comparison, we show the corresponding difference when the light sensors are located at the workspace plane (i.e. transfer matrix \mathbf{H} is known).

In Fig. 6.2, we plot the difference between the minimum (over all simulations and occupancy levels) achieved and target average illuminance level at zones at the workspace plane for the proposed method, i.e. for zone m , we plot

$$\min_{k,\chi} \left\{ w_m(\mathbf{d}^{*(k,\chi)}, 0) - W_m^{(k,\chi)} \right\}$$

where $\mathbf{d}^{*(k,\chi)}$ is the obtained dimming vector, and $w_m(\mathbf{d}^{*(k,\chi)}, 0)$ and $W_m^{(k,\chi)}$ are, respectively, the achieved and the target average illuminance level at zone m for simulation instance k with occupancy level $100\% \frac{\chi}{P}$. For comparison, we also plot the corresponding differences for the reference method and when the light sensors are located at the workspace plane. We can see that the minimum achieved illuminance of the proposed method is less than 10 lux below the target illuminance, whereas the reference method is as large as 120 lux below the target. The observed difference in achieved illuminance values in zones 1 – 3 and 22 – 24 for our method is because illuminance contributions from non-neighboring light sources was not accounted for.

CHAPTER 6. ROBUST CENTRALIZED LIGHTING CONTROL WITH LIGHT SENSOR MEASUREMENTS

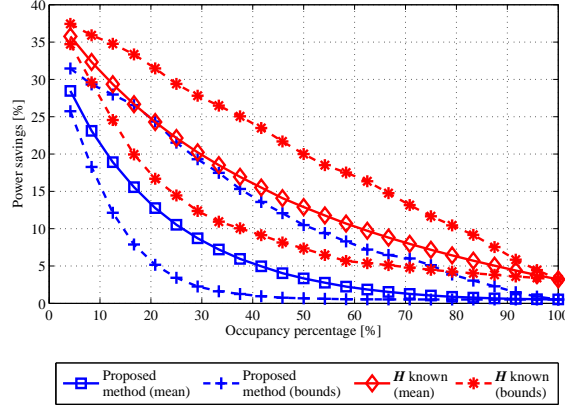


Figure 6.3: Power savings of proposed method with respect to a lighting system without adaptive control under no-daylight scenario. For comparison, we show the corresponding power savings when the light sensors are located at the workspace plane (i.e. transfer matrix \mathbf{H} is known).

In Fig. 6.3, for each simulated occupancy level of the proposed method, we plot the bounds, i.e.

$$\min_k \left\{ 100\% \frac{\mathbf{1}^T \mathbf{d}^{(no-control)} - \mathbf{1}^T \mathbf{d}^{*(k,\chi)}}{\mathbf{1}^T \mathbf{d}^{(no-control)}} \right\}, \text{ and}$$

$$\max_k \left\{ 100\% \frac{\mathbf{1}^T \mathbf{d}^{(no-control)} - \mathbf{1}^T \mathbf{d}^{*(k,\chi)}}{\mathbf{1}^T \mathbf{d}^{(no-control)}} \right\},$$

and mean, i.e.

$$\frac{100\%}{K} \sum_k \frac{\mathbf{1}^T \mathbf{d}^{(no-control)} - \mathbf{1}^T \mathbf{d}^{*(k,\chi)}}{\mathbf{1}^T \mathbf{d}^{(no-control)}},$$

of the power savings over all simulation instances. For comparison, we show also the corresponding power savings when the light sensors are located at the workspace plane. We can see that the proposed method achieves in average 10% less power savings than when the light sensors are located at the workspace plane. Above 25% occupancy level, the power savings can be as low as 0%. This is because, above 25% occupancy level, most of the zones are occupied or are in the neighborhood of an occupied zone and so in order to ensure sufficient illumination at the workspace the lighting system should be set close to dimming vector $\mathbf{d}^{(no-control)}$.

6.5.2 Daylight scenario

The daylight data was obtained from DIALux using clear sky settings for 11 November, 2011 in Amsterdam. The daylight distribution was simulated from 9:00 to 18:00 hours in 1 hour intervals. We simulated $K = 10^4$ instances of occupancy realizations with random number of occupants distributed randomly over all the zones for each hour.

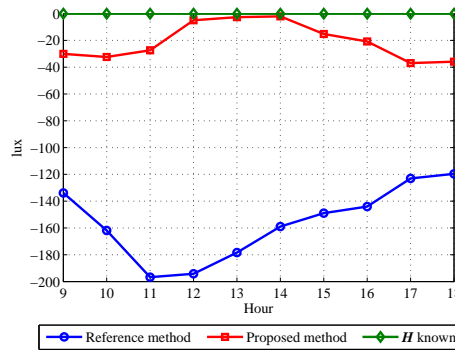


Figure 6.4: Difference between minimum achieved and target average illuminance at workspace in proposed and reference method (under daylight scenario). For comparison, we show the corresponding difference when the light sensors are located at the workspace plane (i.e. transfer matrix \mathbf{H} is known).

In Fig. 6.4, we plot the difference in achieved illuminance levels for each hour over all simulation instances, occupancy levels and zones, i.e. for the proposed method we plot

$$\min_{m,k,\chi} \left\{ w_m(\mathbf{d}^{*(k,\chi,h)}, u_m^{(k,\chi,h)}) - W_m^{(k,\chi,h)} \right\}$$

where $w_m(\mathbf{d}^{*(k,\chi,h)}, u_m^{(k,\chi,h)})$, $W_m^{(k,\chi,h)}$ and $u_m^{(k,\chi,h)}$ are, respectively, the achieved average illuminance, target average illuminance and daylight contribution at zone m in the workspace plane for simulation instance k , hour h and occupancy level $100\% \frac{\chi}{P}$. Here, $\mathbf{d}^{*(k,\chi,h)}$ is the dimming vector for simulation instance k , hour h and occupancy level $100\% \frac{\chi}{P}$. We can see that the minimum achieved illuminance of the proposed method is less than 40 lux below the target illuminance, whereas the reference method is as large as 200 lux below the target.

In Fig. 6.5, for each simulated hour of the proposed method, we plot the

CHAPTER 6. ROBUST CENTRALIZED LIGHTING CONTROL WITH LIGHT SENSOR MEASUREMENTS

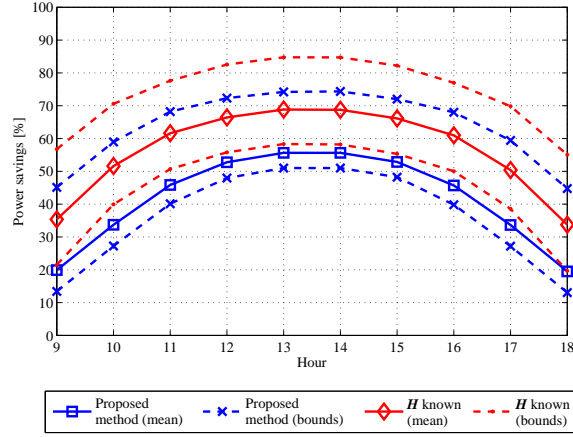


Figure 6.5: Power savings of proposed method with respect to a lighting system without adaptive control under different daylight scenarios. For comparison, we show the corresponding power savings when the light sensors are located at the workspace plane (i.e. transfer matrix \mathbf{H} is known).

bounds, i.e.

$$\min_{k,\chi} \left\{ 100\% \frac{\mathbf{1}^T \mathbf{d}^{(no-control)} - \mathbf{1}^T \mathbf{d}^{*(k,\chi,h)}}{\mathbf{1}^T \mathbf{d}^{(no-control)}} \right\} \text{ and}$$

$$\max_{k,\chi} \left\{ 100\% \frac{\mathbf{1}^T \mathbf{d}^{(no-control)} - \mathbf{1}^T \mathbf{d}^{*(k,\chi,h)}}{\mathbf{1}^T \mathbf{d}^{(no-control)}} \right\}$$

and mean, i.e.

$$\frac{100\%}{KP} \sum_{k,\chi} \frac{\mathbf{1}^T \mathbf{d}^{(no-control)} - \mathbf{1}^T \mathbf{d}^{*(k,\chi,h)}}{\mathbf{1}^T \mathbf{d}^{(no-control)}},$$

of the power savings over all simulation instances and occupancy levels. For comparison, we show also the corresponding power savings when the light sensors are located at the workspace plane. The proposed method achieves similar power savings as when the light sensors are located at the workspace plane (in average a difference of less than 10%), as seen in Fig. 6.5.

6.6 Conclusions

We presented a method for centralized lighting control by making use of calibration prior-information, such that the difference between target and achieved average illuminance at the workspace plane is bounded. The performance of the proposed algorithm was evaluated using simulations, under different daylight distributions. The achieved illuminance obtained under the proposed method was found to be close to the achieved illuminance when the light sensors are located at the workspace plane and substantially better than the reference method. Under different daylight conditions, power savings were obtained with limited difference between target and achieved average illuminance at the workspace plane.

Appendix

6.A Solution to linear programming problem (6.10)

Let us find an optimum solution to the linear programming problem [14, Chapter 4.3]

$$\max_{\mathbf{H}, t_m} t_m \text{ s.t.}$$

$$\begin{cases} \sum_{n \in \mathcal{N}_m} H_{m,n} d_n + t_m = W_m, & (6.31a) \\ \sum_{n \in \mathcal{N}_m} H_{m,n} d_n^* = W_m^*, & (6.31b) \\ \sum_{n \in \mathcal{N}_p} H_{p,n} d_n^* = W_p^*, p \neq m, & (6.31c) \\ H_{m,n} \leq \xi_{m,n} H_{m,m}, n \neq m \wedge n \in \mathcal{N}_m & (6.31d) \\ H_{p,n} \geq 0, \forall p, n \in \mathcal{N}_p. & (6.31e) \end{cases}$$

We obtain a solution to (6.31) by finding the minimum of the function [14, Chapter 5.5]

$$\begin{aligned} f(\{H_{p,n}\}, \{\lambda_p\}, \{\mu_p\}) &= \sum_{n \in \mathcal{N}_m} H_{m,n} d_n - W_m \\ &+ \sum_p \lambda_p \left(\sum_{n \in \mathcal{N}_p} H_{p,n} d_n^* - W_p^* \right) \\ &+ \sum_{\substack{n \neq m \\ \wedge n \in \mathcal{N}_m}} \mu_{m,n} (H_{m,n} - \xi_{m,n} H_{m,m}) \\ &- \sum_{p, n \in \mathcal{N}_p} \alpha_{p,n} \log H_{p,n} \end{aligned} \quad (6.32)$$

subject to (6.31a)-(6.31e) and

$$\begin{cases} \mu_{m,n} (H_{m,n} - \xi_{m,n} H_{m,m}) = 0, n \neq m \wedge n \in \mathcal{N}_m & (6.33a) \\ \mu_{m,n} \geq 0, n \neq m \wedge n \in \mathcal{N}_m. & (6.33b) \end{cases}$$

Here, the equality constraints in (6.31a)-(6.31c) and the inequality constraints in (6.31d) are included in (6.32) by using Lagrange multipliers $\{\lambda_p\}$ and $\{\mu_{m,n}\}$.

6.A. SOLUTION TO LINEAR PROGRAMMING PROBLEM (6.10)

The inequality constraints in (6.31e) are included in (6.32) by using logarithmic barrier functions [14, Chapter 11.2]. The values $\{\alpha_{p,n} \rightarrow 0^+\}$ are weighting factors of the logarithmic barrier functions.

The minimum of (6.32) satisfies the set of non-linear equations (partial derivatives of (6.32) with respect to variables $\{H_{p,n}\}$ are equal to zero)

$$\begin{cases} d_m + \lambda_m d_m^* - \sum_{\substack{n \neq m \\ \wedge n \in \mathcal{N}_m}} \mu_{m,n} \xi_{m,n} - \frac{\alpha_{m,m}}{H_{m,m}} = 0, & (6.34a) \\ d_n + \lambda_m d_n^* + \mu_{m,n} - \frac{\alpha_{m,n}}{H_{m,n}} = 0, n \neq m \wedge n \in \mathcal{N}_m & (6.34b) \\ \lambda_p d_n^* - \frac{\alpha_{p,n}}{H_{p,n}} = 0, p \neq m, n \in \mathcal{N}_p; & (6.34c) \end{cases}$$

and constraints (6.31a)-(6.31e), (6.33a) and (6.33b).

From (6.34a) and (6.34b), we obtain

$$\begin{cases} d_m = \frac{\alpha_{m,m}}{H_{m,m}} - \lambda_m d_m^* + \sum_{\substack{n \neq m \\ \wedge n \in \mathcal{N}_m}} \mu_{m,n} \xi_{m,n} & (6.35a) \\ d_n = \frac{\alpha_{m,n}}{H_{m,n}} - \lambda_m d_n^* - \mu_{m,n}, n \neq m \wedge n \in \mathcal{N}_m. & (6.35b) \end{cases}$$

Next, we replace (6.35a) and (6.35b) in (6.31a), obtaining

$$t_m - \lambda_m \sum_{n \in \mathcal{N}_m} H_{m,n} d_n^* + \sum_{n \in \mathcal{N}_m} \alpha_{m,n} + \sum_{\substack{n \neq m \\ \wedge n \in \mathcal{N}_m}} \mu_{m,n} (\xi_{m,n} H_{m,m} - H_{m,n}) = W_m$$

and by recalling (6.31c) and (6.33a), then

$$t_m - \lambda_m W_m^* + \sum_n \alpha_{m,n} = W_m$$

and thus

$$\lambda_m = \frac{t_m - W_m}{W_m^*} + \frac{\sum_{n \in \mathcal{N}_m} \alpha_{m,n}}{W_m^*}. \quad (6.36)$$

Further, replacing (6.36) in (6.34a) and (6.34b), we obtain

$$\begin{cases} d_m - C_m + \frac{t_m - W_m}{W_m^*} d_m^* - \sum_{\substack{q \neq m \\ \wedge q \in \mathcal{N}_m}} \mu_{m,q} \xi_{m,q} = 0, \\ d_n - C_n + \frac{t_m - W_m}{W_m^*} d_n^* + \mu_{m,n} = 0, n \neq m \wedge n \in \mathcal{N}_m \end{cases}$$

and thus

$$\begin{cases} t_m = W_m + \frac{W_m^*}{d_m^*} \left[C_m - d_m + \sum_{\substack{q \neq m \\ \wedge q \in \mathcal{N}_m}} \mu_{m,q} \xi_{m,q} \right], \\ t_m = W_m + \frac{W_m^*}{d_n^*} \left[C_n - d_n - \mu_{m,n} \right], n \neq m \wedge n \in \mathcal{N}_m, \end{cases} \quad (6.38)$$

where

$$C_n = \frac{\alpha_{m,n}}{H_{m,n}} - \frac{\sum_{q \in \mathcal{N}_m} \alpha_{m,q}}{W_m^*} d_n^*. \quad (6.39)$$

Note that when $\{\alpha_{m,q} \rightarrow 0^+\}$, then

$$\begin{cases} C_n = 0 & , \text{ if } H_{m,n} > 0, \\ C_n > 0 & , \text{ if } H_{m,n} \rightarrow 0^+. \end{cases} \quad (6.40)$$

Combining (6.31b), (6.31d), (6.31e) and (6.40) we have that the optimum solution must satisfy

$$\begin{cases} H_{m,m} > 0, \\ C_m = 0. \end{cases} \quad (6.41)$$

Finally, the optimum solution of (6.31) is the minimum value of t_m that satisfies the set of equations

$$\begin{cases} t_m = W_m - \frac{W_m^*}{d_m^*} \left[d_m - \sum_{\substack{q \neq m \\ \wedge q \in \mathcal{N}_m}} \mu_{m,q} \xi_{m,q} \right], \\ t_m \geq W_m - \frac{W_m^*}{d_n^*} \left[d_n + \mu_{m,n} \right], n \neq m \wedge n \in \mathcal{N}_m, \\ \mu_{m,n} \geq 0, n \neq m \wedge n \in \mathcal{N}_m. \end{cases}$$

Here, we use (6.33a), (6.33b), (6.38), (6.40) and (6.41).

6.B Solution to linear programming problem (6.6)

Let us find an optimum solution to the linear programming problem

$$\max_{\mathbf{H}, t_m} t_m \text{ s.t.}$$

6.B. SOLUTION TO LINEAR PROGRAMMING PROBLEM (6.6)

$$\left\{ \begin{array}{l} \sum_{n \in \mathcal{N}_m} H_{m,n} d_n + t_m = W_m, \\ \sum_{n \in \mathcal{N}_m} H_{m,n} d_n^* = W_m^*, \\ \sum_{n \in \mathcal{N}_p} H_{p,n} d_n^* = W_p^*, p \neq m, \\ H_{p,n} \geq 0, \forall p, n \in \mathcal{N}_p. \end{array} \right. \quad \begin{array}{l} (6.42a) \\ (6.42b) \\ (6.42c) \\ (6.42d) \end{array}$$

Using a similar procedure as in Appendix 6.A, we obtain a solution to (6.42) by finding the minimum of the function

$$\begin{aligned} \bar{f}(\{H_{p,n}\}, \{\lambda_p\}) &= \sum_{n \in \mathcal{N}_m} H_{m,n} d_n - W_m \\ &+ \sum_p \lambda_p \left(\sum_{n \in \mathcal{N}_m} H_{p,n} d_n^* - W_p^* \right) \\ &- \sum_{p,n \in \mathcal{N}_p} \alpha_{p,n} \log H_{p,n}. \end{aligned} \quad (6.43)$$

Note that function (6.43) is equal to (6.32) when $\{\mu_{m,n} = 0, \forall m, n \in \mathcal{N}_m\}$. Hence, the solution that minimizes (6.43) satisfies the set of equations

$$\left\{ \begin{array}{l} t_m = W_m + \frac{W_m^*}{d_m^*} [C_m - d_m], \\ t_m = W_m + \frac{W_m^*}{d_n^*} [C_n - d_n], \quad n \neq m \wedge n \in \mathcal{N}_m, \end{array} \right.$$

and (6.42b)-(6.42d), where the values $\{C_n\}$ are given by (6.39). Combining these equations, we can see that the solution that minimizes (6.43) has at least one value $\{H_{m,n}\}$ larger than zero (i.e. at least one value of $\{C_n\}$ is equal to zero). Then, the optimum solution to (6.42) is equal to

$$W_m - W_m^* \min_{n \in \mathcal{N}_m} \left\{ \frac{d_n}{d_n^*} \right\}.$$

REFERENCES

- [1] Energy Information Administration, “Commercial buildings energy consumption survey,” 2003.
- [2] B. Roisin, M. Bodart, A. Deneyer, and P. D. Herdt, “Lighting energy savings in offices using different control systems and their real consumption,” *Energy and Buildings*, vol. 40, no. 4, pp. 514 – 523, 2008.
- [3] S. Tanaka, M. Miki, A. Amamiya, and T. Hiroyasu, “An evolutionary optimization algorithm to provide individual illuminance in workplaces,” *IEEE International Conference on Systems, Man and Cybernetics*, pp. 941–947, 2009.
- [4] D. Caicedo and A. Pandharipande, “Distributed illumination control with local sensing and actuation in networked lighting systems,” *IEEE Sensors Journal*, pp. 1092–1104, March 2013.
- [5] J. A. Veitch, G. R. Newsham, P. R. Boyce, and C. C. Jones, “Lighting appraisal, well-being and performance in open-plan offices: A linked mechanisms approach,” *Lighting Research and Technology*, vol. 40, no. 2, pp. 133–151, 2008.
- [6] European Committee for Standardization, “EN 12464-1:2002. Light and lighting. Lighting of work places. Part 1: Indoor work places,” 2002.
- [7] A. Pandharipande and D. Caicedo, “Daylight integrated illumination control of LED systems based on enhanced presence sensing,” *Energy and Buildings*, vol. 43, pp. 944–950, April 2011.
- [8] D. Caicedo, A. Pandharipande, and G. Leus, “Occupancy based illumination control of LED lighting systems,” *Lighting Research and Technology*, vol. 43, no. 2, pp. 217–234, August 2011.
- [9] Y.-J. Wen and A. M. Agogino, “Personalized dynamic design of networked lighting for energy-efficiency in open-plan offices,” *Energy and Buildings*, vol. 43, no. 8, pp. 1919–1924, 2011.
- [10] M. Miki, A. Amamiya, and T. Hiroyasu, “Distributed optimal control of lighting based on stochastic hill climbing method with variable neighborhood,” *IEEE International Conference on Systems, Man and Cybernetics*, pp. 1676–1680, 2007.

REFERENCES

- [11] L.-W. Yeh, C.-Y. Lu, C.-W. Kou, Y.-C. Tseng, and C.-W. Yi, “Autonomous light control by wireless sensor and actuator networks,” *IEEE Sensors Journal*, pp. 1029–1041, June 2010.
- [12] Y.-W. Bai and Y.-T. Ku, “Automatic room light intensity detection and control using a microprocessor and light sensors,” *IEEE Transactions on Consumer Electronics*, vol. 54, no. 3, pp. 1173 – 1176, 2008.
- [13] <http://www.lighting.philips.com/pwc.li/main/products/controls/assets/lr11220ds.pdf>.
- [14] S. Boyd and L. Vandenberghe, *Convex Optimization*. Cambridge University Press, 2004.

CHAPTER 6. ROBUST CENTRALIZED LIGHTING CONTROL WITH
LIGHT SENSOR MEASUREMENTS

Distributed methods for light sensor calibration*

We consider a distributed lighting control system with multiple networked luminaires, each equipped with a light and presence sensor, and a local controller. Using local sensor inputs and information exchange with limited neighboring controllers, each local controller determines the optimum dimming level of its luminaire so that the lighting power consumption is minimized. This is done under net illumination constraints specified in terms of light sensor set-points. The underlying optimization problem requires knowledge of the contribution of a luminaire to the light sensor, termed illumination gain. The illumination gain is sensitive to reflectance changes, e.g. due to occupancy changes or object movements in the environment. We address the problem of illumination gain estimation and tracking in a lighting system with distributed asynchronous controllers. A Euclidean projection of the best linear unbiased estimator on the non-negative orthant is used as an initial illumination gain estimate and bounds on mean-squared error performance are obtained. A recursive calibration mechanism to track gain changes is proposed. Illumination performance improvements are shown by numerical results using photometric data.

*This chapter has been submitted as: D. Caicedo, A. Pandharipande and F. M. J. Willems. "Illumination gain estimation and tracking in a distributed lighting control system", *IEEE Multi-Conference on Systems and Control*, 2014

7.1 Introduction

Distributed lighting systems with networked, intelligent luminaires offer modularity and simplify commissioning [1–4]. An intelligent luminaire here refers to a light source with co-located light and presence sensors, a local controller and a communication module. The light and presence sensors respectively determine the illuminance value and occupancy state within the sensor field-of-view. Based on this sensor information and information exchange with neighboring controllers, a local controller determines the dimming level such that the total power consumption for lighting is minimized. The constraints on granular dimming, i.e. providing a higher average illuminance value in an occupied workspace and a lower value over unoccupied spaces by dimming individual luminaires, are specified in terms of set-points at the light sensors situated at the ceiling. The problem was solved using interior-point distributed optimization in [4]. Under different system settings, the lighting control problem has been treated in [5–8]. The underlying optimization problems in these works require knowledge of the illumination gains, i.e. the contributions of the luminaire light outputs to the light sensors. Further, the illumination gains may vary over time due to reflectance changes, e.g. user or object movements in the environment, resulting in a poorer illumination experience if not accounted for. If, for instance, the reflectance below a light sensor increases due to the introduction of a highly reflecting object, the resulting illumination over the zone would be lower than expected after lighting control since the light sensor set-point is at a lower value than required.

We address this problem by considering a method for estimating and tracking the illumination gains in a distributed lighting system of asynchronous luminaire controllers. In the proposed method, a difference of light sensor measurements is used to cancel out the daylight component and multiple such difference measurements are collected to ensure sufficient number of independent observations. An estimate for the illumination gains is obtained by projecting the best linear unbiased estimator on the non-negative orthant. We then obtain the minimum squared-error (MSE) bound for this estimator. The illumination gains are then tracked with new measurements as a recursive solution of a regularized weighted least-squares problem projected on the non-negative orthant. Photometric data from an open-plan office model is used to evaluate the performance gains obtained from the proposed method. In related work [9], the problem of designing dimming sequences with fixed length for estimating and tracking the illumination gains was considered.

The remainder of the paper is organized as follows. A description of the intelligent lighting system is provided in Section 7.2. The illumination gain estimation and tracking problem for illumination control is formulated in Section 7.3. In

Section 7.4, the proposed method for initial estimation of the illumination gains and tracking is presented. The proposed method is evaluated using photometric data from an open-plan office lighting system and results are presented in Section 7.5. Conclusions are presented in Section 7.6.

7.2 Lighting system description

We consider an indoor lighting system, with Fig. 7.1a depicting the lighting plan, with P luminaires located at the ceiling. Parallel to the ceiling is the workspace plane where the spatial illuminance distribution is of interest. The workspace plane is assumed to be divided into P logical zones, as shown in Fig. 7.1a. Denote $\mathbf{d}^{(k)} = [d_1^{(k)}, \dots, d_P^{(k)}]$ to be the dimming vector containing dimming levels, $d_p^{(k)}$ ($0 \leq d_p^{(k)} \leq 1$), of the p -th luminaire during the k -th control cycle. Each luminaire is embedded with a light sensor that has a limited field of view defined by its opening angle. A control cycle is the duration over which a controller samples its light sensor and changes the dimming level of the light source, if required, at the end of the cycle.

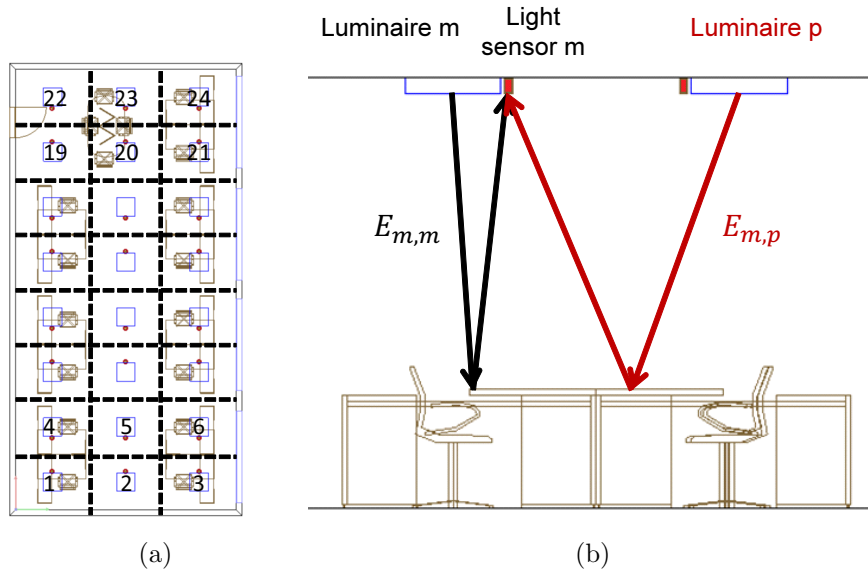


Figure 7.1: (a) Top view of office lighting plan showing zones and (b) illumination gains to light sensor m .

The measured illuminance at a light sensor at the ceiling is the net illuminance due to contributing luminaires and daylight reflected from objects (e.g. furniture)

CHAPTER 7. DISTRIBUTED METHODS FOR LIGHT SENSOR CALIBRATION

in the office (see Fig. 7.1b). Denote $E_{m,p}(d_p^{(k)})$ as the measured illuminance at the m -th light sensor and k -th control cycle when the p -th luminaire is at dimming level $d_p^{(k)}$, in the absence of daylight. We assume that the illuminance scales linearly with the dimming level [4], [8], $E_{m,p}(d_p^{(k)}) = d_p^{(k)} E_{m,p}(1)$. For notational convenience, we use $E_{m,p}$ instead of $E_{m,p}(1)$ hereafter to denote the illumination gain from luminaire p to sensor m .

The net illuminance at the m -th sensor at the ceiling, given that the lighting system is at dimming vector $\mathbf{d}^{(k)}$ and under daylight, can then be written as

$$i_m(\mathbf{d}^{(k)}, s_m^{(k)}) = \sum_{p=1}^P d_p^{(k)} E_{m,p} + s_m^{(k)}, \quad (7.1)$$

where $s_m^{(k)}$ is the illuminance due to daylight measured at the m -th sensor and k -th control cycle.

7.3 Problem setting

Let us consider a class of controllers that minimizes energy consumption such that a minimum illuminance level is achieved at the light sensors [4], i.e.

$$\begin{aligned} \mathbf{d}^* &= \arg \min_{\mathbf{d}} \sum_{p=1}^P d_p \\ \text{s.t. } &\begin{cases} \sum_{p \in \mathcal{N}_m} E_{m,p} d_p \geq L_m^{(k)} - s_m^{(k)}, & m = 1, \dots, P, \\ 0 \leq d_p \leq 1, & p = 1, \dots, P, \end{cases} \end{aligned} \quad (7.2)$$

where \mathbf{d}^* is the dimming level to be achieved in the following control cycle, $\mathcal{N}_m = \{1, \dots, m, \dots, N_m\}$ denotes indices of the neighbors of sensor m (including m),

$$L_m^{(k)} = \begin{cases} L_m^o, & \text{if the } m\text{-th zone is occupied at control cycle } k \\ L_m^u, & \text{otherwise,} \end{cases}$$

is the target illuminance level at the m -th light sensor. The target illuminance levels L_m^o and L_m^u , with $L_m^o > L_m^u$, are measured at the m -th light sensor when all the luminaires are at dimming level d^o and d^u , respectively, i.e. $L_m^o = d^o c_m$ and $L_m^u = d^u c_m$, where $c_m = \sum_{p \in \mathcal{N}_m} E_{m,p}$ is a calibration set-point for the m -th light sensor. Here, we assume that the major contributors to the illuminance at the m -th light sensor are those luminaires in its neighborhood

\mathcal{N}_m . This is a valid assumption because in a typical lighting system, the illuminance contribution of a luminaire to the net illuminance of a given light sensor decreases with the separation between the light sensor and the luminaire.

We can see that the problem in (7.2), requires that controller m has knowledge of the illuminance gains $\{E_{m,p}, p \in \mathcal{N}_m\}$. Our problem is to estimate and track these terms in a distributed way.

7.4 Proposed method

Let the difference in illuminance between two consecutive measurements from the m -th light sensor be given by

$$\begin{aligned}
\Delta i_m^{(k)} &= i_m(\mathbf{d}^{(k)}, s_m^{(k)}) - i_m(\mathbf{d}^{(k-1)}, s_m^{(k-1)}) \\
&= \sum_{p \in \mathcal{N}_m} E_{m,p} d_p^{(k)} + s_m^{(k)} + \bar{n}_m^{(k)} \\
&\quad - \sum_{p \in \mathcal{N}_m} E_{m,p} d_p^{(k-1)} - s_m^{(k-1)} - \bar{n}_m^{(k-1)} \\
&\approx \sum_{p \in \mathcal{N}_m} E_{m,p} \Delta d_p^{(k)} + \bar{n}_m^{(k)} - \bar{n}_m^{(k-1)}
\end{aligned} \tag{7.3}$$

where $\Delta d_p^{(k)} = d_p^{(k)} - d_p^{(k-1)}$ is the difference in dimming level between two consecutive cycles for the p -th luminaire and $\bar{n}_m^{(k)} = \sum_{p \notin \mathcal{N}_m} E_{m,p} d_p^{(k)} + n_m^{(k)}$ is the contribution from non-neighboring luminaires and the noise component at the m -th light sensor and k -th control cycle.

In this paper, we assume that

- [A1] the neighborhood of controller m , \mathcal{N}_m , includes all the other controllers within its communication range;
- [A2] daylight does not change between consecutive cycles, i.e. $s_m^{(k)} \approx s_m^{(k-1)}$; and
- [A3] the noise component $n_m^{(k)}$ follows a normal distribution with zero mean and variance σ_n^2 .

Assumption [A1] is reasonable because in general the communicating range of a wireless radio includes at least those luminaries with the largest illumination gain. Assumption [A2] holds because the elapsed time between consecutive cycles is small and daylight variations are typically slow. The last assumption is valid because the noise component is mainly due to electronic noise.

7.4.1 Initial calibration

During initial calibration, controller m collects $2K$ measurements represented by the following system of K equations

$$\Delta i_m^{(k)} \approx \sum_{p \in \mathcal{N}_m} E_{m,p} \Delta d_p^{(k)}, \quad k = 2, 4, \dots, 2K. \quad (7.4)$$

Let us rewrite (7.4) in matrix form,

$$\Delta \mathbf{D} \mathbf{x}_m = \Delta \mathbf{i}_m \quad (7.5)$$

where

$$\begin{aligned} \Delta \mathbf{i}_m &= \left[\Delta i_m^{(2)}, \quad \dots, \quad \Delta i_m^{(2K)} \right]^T, \\ \mathbf{x}_m &= \left[x_{m,1}, \quad \dots, \quad x_{m,N_m} \right]^T, \\ \Delta \mathbf{d}^{(k)} &= \left[\Delta d_1^{(k)}, \quad \dots, \quad \Delta d_{N_m}^{(k)} \right]^T, \\ \Delta \mathbf{D} &= \left[\Delta \mathbf{d}^{(2)}, \quad \dots, \quad \Delta \mathbf{d}^{(2K)} \right]^T \end{aligned}$$

and $E_{m,p} = x_{m,p}$.

Here, we are interested in estimating a non-negative vector $\mathbf{x}_m^{(0)}$ that reduces the MSE with respect to \mathbf{x}_m^* , the vector containing the actual contributions from neighboring luminaires to light sensor m , given that we have observed the measurements in (7.5). Note that the following relationships hold,

$$\mathbb{E}_{n,\{d_p\}} \left\{ \|\mathbf{x}_m^* - \mathbf{x}_m^{\text{opt}}\|^2 \right\} \leq \mathbb{E}_{n,\{d_p\}} \left\{ \|\mathbf{x}_m^* - \mathbf{x}_m^{(0)}\|^2 \right\} \quad (7.6)$$

and

$$\mathbb{E}_{n,\{d_p\}} \left\{ \|\mathbf{x}_m^* - \mathbf{x}_m^{(0)}\|^2 \right\} \leq \mathbb{E}_{n,\{d_p\}} \left\{ \|\mathbf{x}_m^* - \bar{\mathbf{x}}_m^{(0)}\|^2 \right\}, \quad (7.7)$$

where $\mathbf{x}_m^{\text{opt}}$ is an estimated non-negative vector with the minimum MSE,

$$\bar{\mathbf{x}}_m^{(0)} = (\Delta \mathbf{D}^T \Delta \mathbf{D})^{-1} \Delta \mathbf{D}^T \Delta \mathbf{i}_m \quad (7.8)$$

is a linear estimator given the measurements in (7.5), $\mathbf{x}_m^{(0)} = \text{Proj}\{\bar{\mathbf{x}}_m^{(0)}\}$ and $\text{Proj}\{\cdot\}$ is the Euclidean projection on the non-negative orthant. If there is no contribution from non-neighboring luminaires, $\{E_{m,p} = 0, p \notin \mathcal{N}_m\}$, then solution (7.8) is the best linear unbiased estimator given the measurements in (7.5). The inequality in (7.7) holds because every element in \mathbf{x}_m^* is non-negative, i.e.

the actual contributions from luminaires to light sensors are non-negative. We propose to use $\mathbf{x}_m^{(0)}$ as our solution with the corresponding calibration set-point, $c_m^{(0)} = \sum_p x_{m,p}^{(0)}$. The solution $\mathbf{x}_m^{(0)}$, as compared to $\mathbf{x}_m^{\text{opt}}$, allows further mathematical analysis and tractability in understanding the system performance better.

The associated MSE to solution $\mathbf{x}_m^{(0)}$ (considering only invertible matrices $\Delta \mathbf{D}^T \Delta \mathbf{D}$) is given by

$$\begin{aligned} \text{MSE}_m(K) &= \mathbb{E}_{n,\{d_p\}} \left\{ \left\| \mathbf{x}_m^* - \mathbf{x}_m^{(0)} \right\|^2 \right\} \\ &\leq \mathbb{E}_{n,\{d_p\}} \left\{ \left\| \mathbf{x}_m^* - \bar{\mathbf{x}}_m^{(0)} \right\|^2 \right\} \\ &= \mathbb{E}_{n,\{d_p\}} \left\{ \left\| (\Delta \mathbf{D}^T \Delta \mathbf{D})^{-1} \Delta \mathbf{D}^T \bar{\mathbf{n}} \right\|^2 \right\} \\ &= \text{tr} \left\{ \mathbb{E}_{n,\{d_p\}} \left\{ (\Delta \mathbf{D}^T \Delta \mathbf{D})^{-2} \Delta \mathbf{D}^T \bar{\mathbf{n}} \bar{\mathbf{n}}^T \Delta \mathbf{D} \right\} \right\}, \end{aligned}$$

where $\bar{\mathbf{n}} = [\bar{n}_m^{(2)} - \bar{n}_m^{(1)}, \dots, \bar{n}_m^{(2K)} - \bar{n}_m^{(2K-1)}]^T$ and $\text{tr}\{\}$ denotes the trace of a matrix. Here, we use (7.7), and properties $\|\mathbf{a}\|^2 = \text{tr}\{\mathbf{a}\mathbf{a}^T\}$ and $\text{tr}\{\mathbf{A}\mathbf{B}\mathbf{A}\} = \text{tr}\{\mathbf{A}^2\mathbf{B}\}$.

If we assume that all luminaires are synchronized, luminaire m changes its intensity with a fixed sequence of length $2K$, $[d_m^{(1)}, \dots, d_m^{(2K)}]$ where $\{d_{\min} \leq d_m^{(k)} \leq d_{\max}, \forall k\}$, and there is no contribution from non-neighboring luminaires, $\{E_{m,p} = 0, p \notin \mathcal{N}_m\}$, then the MSE reduces to

$$\begin{aligned} \text{MSE}_m(K) &\leq \text{tr} \left\{ (\Delta \mathbf{D}^T \Delta \mathbf{D})^{-2} \Delta \mathbf{D}^T \mathbb{E}_n \left\{ \mathbf{n}\mathbf{n}^T \right\} \Delta \mathbf{D} \right\}, \\ &= 2\sigma_n^2 \text{tr} \left\{ (\Delta \mathbf{D}^T \Delta \mathbf{D})^{-1} \right\}, \end{aligned} \quad (7.9)$$

where

$$\begin{aligned} \Delta \mathbf{D}^T \mathbb{E}_n \left\{ \mathbf{n}\mathbf{n}^T \right\} \Delta \mathbf{D} &= 2\sigma_n^2 \Delta \mathbf{D}^T \Delta \mathbf{D}, \\ \mathbb{E}_n \left\{ \mathbf{n}\mathbf{n}^T \right\} &= 2\sigma_n^2 \mathbf{I}, \\ \mathbf{n} &= \left[n_m^{(2)} - n_m^{(1)}, \dots, n_m^{(2K)} - n_m^{(2K-1)} \right]^T, \end{aligned}$$

and \mathbf{I} is the identity matrix of the right size.

Note that the expression in (7.9) is analogous to the MSE for the channel estimation problem in a MIMO system [10]. Here, the dimming sequences and constraints in dimming levels are analogous to the training sequences and power constraints in a MIMO system, respectively. Hence, optimal sequences that minimize (7.9), must maximize $\sigma_{\Delta d}^2$ such that $\Delta \mathbf{D}^T \Delta \mathbf{D} = K\sigma_{\Delta d}^2 \mathbf{I}$, $\sum_{k=1}^K (\Delta d_m^{(2k)})^2 = K\sigma_{\Delta d}^2$, $\forall m$ and $d_{\min} \leq d_m^{(k)} \leq d_{\max}, \forall k$.

CHAPTER 7. DISTRIBUTED METHODS FOR LIGHT SENSOR CALIBRATION

However, in the considered system: (i) the control of luminaires is not synchronous and (ii) there is contribution from non-neighboring luminaires. During initial calibration, we propose that the m -th luminaire at any given cycle k is either at intensity d_{\max} or d_{\min} with equal probability and independent of other luminaires. Therefore, $[\Delta d_i^{(2)}, \dots, \Delta d_i^{(2K)}]$ is a vector of K independent samples from the distribution of random variable Δd_i ,

$$\Delta d_i = \begin{cases} -(d_{\max} - d_{\min}) & , \text{ with probability } 0.25 \\ 0 & , \text{ with probability } 0.5 \\ d_{\max} - d_{\min} & , \text{ with probability } 0.25 \end{cases}$$

with properties

$$\begin{aligned} \mathbb{E}\{\Delta d_i\} &= 0, & \forall i, \\ \mathbb{E}\{(\Delta d_i)^2\} &= \sigma_{\Delta d}^2 = \frac{(d_{\max} - d_{\min})^2}{2}, & \forall i, \\ \mathbb{E}\{\Delta d_i \Delta d_j\} &= 0, & \forall i \neq j. \end{aligned}$$

Then, we have

$$\text{MSE}_m(K) \leq \text{tr} \left\{ \mathbb{E}_{\{d_p, p \in \mathcal{N}_m\}} \left\{ (\mathbf{\Delta D}^T \mathbf{\Delta D})^{-2} \mathbf{\Omega} \right\} \right\},$$

where

$$\begin{aligned} \mathbf{\Omega} &= \mathbf{\Delta D}^T \mathbb{E}_{n, \{d_p, p \notin \mathcal{N}_m\}} \left\{ \bar{\mathbf{n}} \bar{\mathbf{n}}^T \right\} \mathbf{\Delta D}, \\ &= \left(2\sigma_n^2 + \sigma_{\Delta d}^2 \sum_{p \notin \mathcal{N}_m} E_{m,p}^2 \right) (\mathbf{\Delta D}^T \mathbf{\Delta D}) \end{aligned}$$

and

$$\mathbb{E}_{n, \{d_p, p \notin \mathcal{N}_m\}} \left\{ \bar{\mathbf{n}} \bar{\mathbf{n}}^T \right\} = \left(2\sigma_n^2 + \sigma_{\Delta d}^2 \sum_{p \notin \mathcal{N}_m} E_{m,p}^2 \right) \mathbf{I}.$$

Note that

$$\frac{1}{K} [\mathbf{\Delta D}^T \mathbf{\Delta D}]_{i,j} = \frac{1}{K} \sum_{k \in \{2, \dots, 2K\}} \Delta d_i^{(k)} \Delta d_j^{(k)}$$

is the sample covariance between random variables Δd_i and Δd_j , where $[\mathbf{A}]_{i,j}$ is the (i, j) -th element of matrix \mathbf{A} . For large number of cycles, using the central limit theorem, we have that

$$\begin{aligned} \frac{1}{K} [\mathbf{\Delta D}^T \mathbf{\Delta D}]_{i,i} &\sim \mathcal{N} \left(\sigma_{\Delta d}^2, \frac{\sigma_{\Delta d}^4}{K^2} \right) \text{ and} \\ \frac{1}{K} [\mathbf{\Delta D}^T \mathbf{\Delta D}]_{i,j} &\sim \mathcal{N} \left(0, \frac{\sigma_{\Delta d}^4}{K^2} \right). \end{aligned}$$

Therefore, for large number of cycles we have

$$\Delta \mathbf{D}^T \Delta \mathbf{D} \approx K \sigma_{\Delta d}^2 \mathbf{I}.$$

and the MSE is upper bounded by

$$\text{MSE}_m(K) \leq \frac{N_m}{K} \left(\frac{2\sigma_n^2}{\sigma_{\Delta d}^2} + \sum_{p \notin \mathcal{N}_m} E_{m,p}^2 \right). \quad (7.10)$$

Note that (7.10) is valid for large number of cycles and when there is a unique solution to (7.8). A unique solution to (7.8) is obtained when we have sufficient number of independent measurements where gain values $\{E_{m,p}, p \in \mathcal{N}_m\}$ have not changed, i.e.

$$\text{Rank} \{\Delta \mathbf{D}\} = N_m \quad (7.11)$$

and the values $\{E_{m,p}, p \in \mathcal{N}_m\}$ are constant.

In Fig. 7.1, we plot the probability that condition (7.11) is not satisfied for different number of cycles, K , and $N_m = 9$. Additionally, we also plot the probability that condition (7.11) is not satisfied when $K = N_m$.

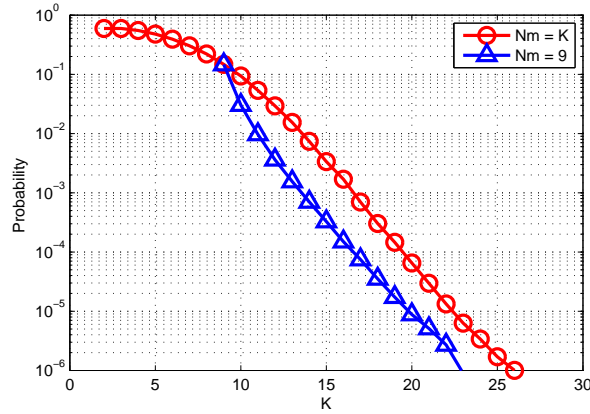


Figure 7.1: Probability that condition (7.11) is not satisfied for different number of measurements, $K \geq 2$, and $N_m = 9$, and also when $N_m = K$.

7.4.2 Calibration tracking

After the initial calibration, the system tracks the current value of gain terms $\{E_{m,n}\}$ and so the calibration set-point. We can see from (7.3) that a change in

CHAPTER 7. DISTRIBUTED METHODS FOR LIGHT SENSOR CALIBRATION

dimming levels is required to estimate the terms $\{E_{m,n}\}$, i.e. $\|\Delta \mathbf{d}^{(k)}\|^2 \geq \epsilon$ with $\epsilon > 0$.

Let $\mathcal{K}(k)$ be the list of indices at cycle k from measurements where a change of dimming level was observed,

$$\mathcal{K}(k) = \{\kappa : \|\Delta \mathbf{d}^{(\kappa)}\|^2 \geq \epsilon_d \text{ and } 2K < \kappa \leq k \text{ and } \kappa \text{ is even}\}.$$

Further, the indices in $\mathcal{K}(k)$ are sorted in ascending order, \mathcal{K}_q corresponds to the q -th entry in the list and Q is the total number of indices in $\mathcal{K}(k)$.

Note that the variations on illumination gains are mainly due to changes in the environment that cannot be accurately predicted or modelled in advance. Therefore, we propose a simple method for tracking the terms $\{E_{m,n}\}$. The estimated terms $\{E_{m,n}\}$ are updated with each additional measurement by

$$\mathbf{x}_m^{(Q)} = \text{Proj}\{\bar{\mathbf{x}}_m^{(Q)}\} \quad (7.12)$$

where

$$\begin{aligned} \bar{\mathbf{x}}_m^{(Q)} = \arg \min_{\mathbf{x}_m} & \left\{ (1-\gamma)\alpha^Q \|\Delta \mathbf{i}_m - \Delta \mathbf{D} \mathbf{x}_m\|^2 \right. \\ & + (1-\gamma) \|\widehat{\Delta \mathbf{i}}_m - \widehat{\Delta \mathbf{D}} \mathbf{x}_m\|^2 \\ & \left. + \gamma \|\mathbf{x}_m^{(Q-1)} - \mathbf{x}_m\|^2 \right\} \end{aligned} \quad (7.13)$$

is a regularized weighted least-square problem with solution given by [11]

$$\begin{aligned} \bar{\mathbf{x}}_m^{(Q)} &= \left((1-\gamma)(\alpha^Q \Delta \mathbf{D}^T \Delta \mathbf{D} + \widehat{\Delta \mathbf{D}}^T \widehat{\Delta \mathbf{D}}) + \gamma \mathbf{I} \right)^{-1} \\ &\times \left((1-\gamma)(\alpha^Q \Delta \mathbf{D}^T \Delta \mathbf{i}_m + \widehat{\Delta \mathbf{D}}^T \widehat{\Delta \mathbf{i}}_m) + \gamma \mathbf{x}_m^{(Q-1)} \right). \end{aligned} \quad (7.14)$$

The regularization term $\|\mathbf{x}_m^{(Q-1)} - \mathbf{x}_m\|^2$ in (7.13) ensures that the new solution vector is close to the previous vector $\mathbf{x}_m^{(Q-1)}$. Here,

$$\widehat{\Delta \mathbf{i}}_m = \begin{bmatrix} \alpha^{\frac{Q-1}{2}} \Delta i_m^{(\mathcal{K}_1)} \\ \vdots \\ \alpha^{\frac{Q-q}{2}} \Delta i_m^{(\mathcal{K}_q)} \\ \vdots \\ \Delta i_m^{(\mathcal{K}_Q)} \end{bmatrix} \quad \text{and} \quad \widehat{\Delta \mathbf{D}} = \begin{bmatrix} \alpha^{\frac{Q-1}{2}} (\Delta \mathbf{d}^{(\mathcal{K}_1)})^T \\ \vdots \\ \alpha^{\frac{Q-q}{2}} (\Delta \mathbf{d}^{(\mathcal{K}_q)})^T \\ \vdots \\ (\Delta \mathbf{d}^{(\mathcal{K}_Q)})^T \end{bmatrix}$$

are a weighted set of the last measurements. The parameters $0 \leq \gamma \leq 1$ and $0 \leq \alpha \leq 1$ determine the variation between consecutive solutions and the weight

of past measurements, respectively. Older measurements have a lower weight and so a lesser effect in the solution. The solution in (7.14) can be easily implemented in recursive form,

$$\begin{aligned}\bar{\mathbf{x}}_m^{(Q)} &= \left((1 - \gamma)\mathbf{A}^{(Q)} + \gamma\mathbf{I} \right)^{-1} \left((1 - \gamma)\mathbf{b}^{(Q)} + \gamma\bar{\mathbf{x}}_m^{(Q-1)} \right), \\ \mathbf{A}^{(Q)} &= \alpha\mathbf{A}^{(Q-1)} + \Delta\mathbf{d}^{(Q)}(\Delta\mathbf{d}^{(Q)})^T, \\ \mathbf{b}^{(Q)} &= \alpha\mathbf{b}^{(Q-1)} + \Delta\mathbf{d}^{(Q)}\Delta i_m^{(Q)},\end{aligned}$$

with

$$\mathbf{A}^{(0)} = \sum_{q=1}^K \Delta\mathbf{d}^{(q)}(\Delta\mathbf{d}^{(q)})^T \text{ and } \mathbf{b}^{(0)} = \sum_{q=1}^K \Delta\mathbf{d}^{(q)}\Delta i_m^{(q)}.$$

Finally, we update our calibration set-point as

$$c_m^{(Q)} = \sum_{p \in \mathcal{N}_m} x_{m,p}^{(Q)}, \quad Q > 0.$$

7.4.3 Re-calibration

The terms $\{E_{m,n}\}$ need to be re-computed when a major change in reflectance occurs. If the estimated error at light sensor m during cycle k given by

$$\alpha^Q \|\Delta\mathbf{i}_m - \Delta\mathbf{D}\mathbf{x}_m\|^2 + \|\widehat{\Delta\mathbf{i}_m} - \widehat{\Delta\mathbf{D}}\mathbf{x}_m\|^2,$$

is larger than $\epsilon_c > 0$, then we introduce a recalibration phase.

Here, luminaire m and its neighbors change their dimming level randomly around their current dimming level for around \bar{K} cycles, i.e. either $\{d_p^{(k)} - \delta d\}$ or $\{d_p^{(k)} + \delta d\}$ with equal probability.

7.5 Numerical results

We present results to evaluate the performance of the proposed method using photometric data from an office model with dimensions: 14.4 m (length) \times 7.4 m (width) \times 2.86 m (height), and $M = 24$ luminaires arranged in a grid of 3 by 8 as shown in Fig. 7.1a, with the workspace about 1.9 m from the ceiling. Light sensors co-located at the luminaires have a half-opening angle of 30 degrees. The luminaire indexing in Fig. 7.1a also corresponds to that of the controllers and zones. The office has windows on one side of the room for daylight.

We assume the neighborhood of the m -th luminaire to include the closest luminaires. In this case, the net illuminance due to non-neighboring luminaires

CHAPTER 7. DISTRIBUTED METHODS FOR LIGHT SENSOR CALIBRATION

is around 10% of the net illuminance from the entire lighting system. The target average illuminances at the workspace [12] when the m -th zone is occupied and unoccupied are $W_m^o = 500$ ($d^0 = 0.85$) and $W_m^u = 300$ ($d^u = 0.51$) lux, respectively.

We choose parameters $d_{\min} = 0$, $d_{\max} = 1$, $K = 30$, $\bar{K} = 10$, $\alpha = 0.98$, $\gamma = 0.3$, $\epsilon_c = 0.25$ and $\epsilon_d = 0.01$ for our simulation. During re-calibration, we choose $\gamma = 0.1$ and $\delta d = 0.05$. The controllers are asynchronous and the time between cycles is 0.75 seconds. The standard deviation of the noise, σ_n , is 10^{-3} times the initial set-point.

At the beginning of the simulation, there is a dark colored table between zones 20 and 23, and zone 20 is occupied. After 3 hours, a minor reflectance change is induced with objects like laptop and books placed on the table. At time instant 6 hours, the table with all objects is removed representing a large reflectance change. We assume that during the whole simulation, there is an occupant at zone 20.

For comparison, we first consider the system with only initial calibration. We can see in Figs. 7.1a and 7.1b that with initial calibration, the system achieves the target illuminance and calibration set-point respectively, over the first three hours of simulation time. Subsequently, the system cannot track the changes in the calibration set-point and thus cannot provide the required illumination.

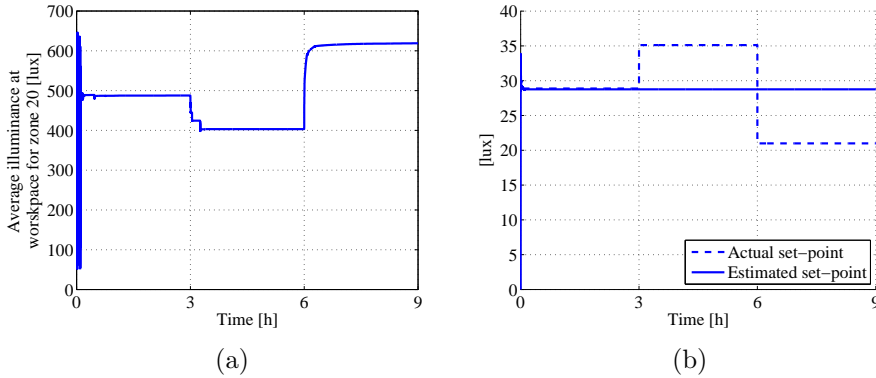


Figure 7.1: Simulation results of only initial calibration. We show (a) the average illumination at zone 20 and (b) the corresponding calibration set-point at controller 20.

Next, we simulate the system with initial calibration, calibration tracking and re-calibration. In Figs. 7.2a and 7.2b, we can see that the system provides the required illumination and tracks the changes in the calibration set-point.

Further, as seen in Fig. 7.3, the proposed method reduces the estimation error (defined as $\frac{\|\mathbf{x}_m^{(q)} - \mathbf{x}_m^*\|}{\|\mathbf{x}_m^*\|} \times 100\%$) for all controllers to less than 10%. At the time instant of reflectance change, the error shoots, but is reduced with calibration tracking and re-calibration.

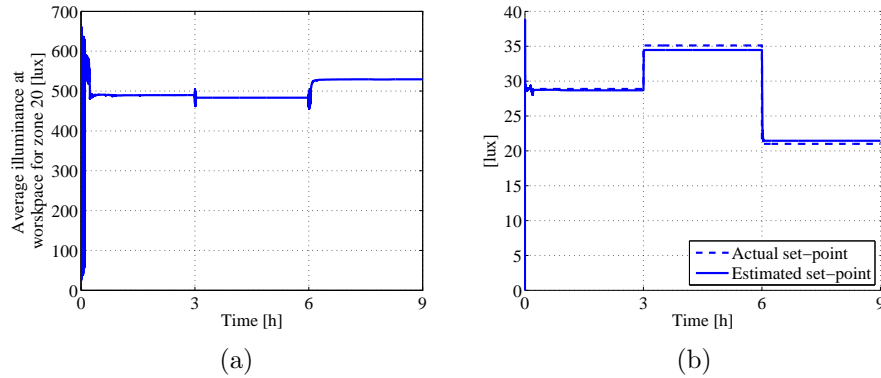


Figure 7.2: Simulation results of calibration tracking and re-calibration. We show (a) the average illumination at zone 20 and (b) the corresponding calibration set-point at controller 20.

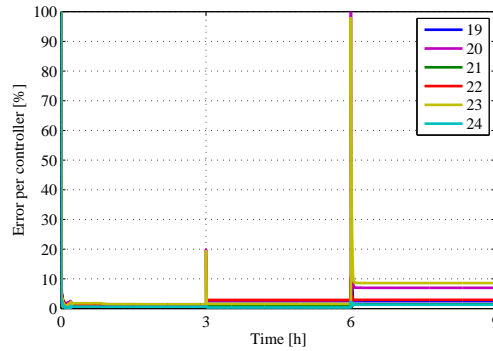


Figure 7.3: Estimation error for controllers 19 to 24, with calibration tracking and re-calibration.

7.6 Conclusions

We proposed a method for estimating and tracking the illumination gains in a distributed, asynchronous system of intelligent luminaires. From numerical

CHAPTER 7. DISTRIBUTED METHODS FOR LIGHT SENSOR CALIBRATION

results, we found that the estimation error in the illumination gains was less than 10% with calibration tracking and re-calibration, and the system was robust to minor and major reflectance changes and maintained the required illumination. We also noted the connection of a special case of the considered problem, when controllers are synchronous and the illumination gain from a non-neighboring luminaire to a light sensor is zero, to the MIMO channel estimation problem.

REFERENCES

- [1] S. Afshari, S. Mishra, A. Julius, F. Lizarralde, and J. T. Wen, “Modeling and feedback control of color-tunable LED lighting systems,” *American Control Conference*, pp. 3663–3668, 2012.
- [2] M. T. Koroglu and K. M. Passino, “Illumination balancing algorithm for smart lights,” *IEEE Transactions on Control Systems Technology*, vol. 2, pp. 557–567, March 2014.
- [3] A. E. Mady and G. Provan, “Co-design of wireless sensor-actuator networks for building controls,” *IEEE Conference on Decision and Control and European Control Conference*, pp. 5266–5273, 2011.
- [4] D. Caicedo and A. Pandharipande, “Distributed illumination control with local sensing and actuation in networked lighting systems,” *IEEE Sensors Journal*, pp. 1092–1104, March 2013.
- [5] L.-W. Yeh, C.-Y. Lu, C.-W. Kou, Y.-C. Tseng, and C.-W. Yi, “Autonomous light control by wireless sensor and actuator networks,” *IEEE Sensors Journal*, pp. 1029–1041, June 2010.
- [6] Y.-J. Wen and A. M. Agogino, “Personalized dynamic design of networked lighting for energy-efficiency in open-plan offices,” *Energy and Buildings*, vol. 43, no. 8, pp. 1919–1924, 2011.
- [7] M. Fischer, W. Kui, and P. Agathoklis, “Intelligent illumination model-based lighting control,” *International Conference on Distributed Computing Systems Workshops*, pp. 245 – 249, 2012.
- [8] A. Pandharipande and D. Caicedo, “Adaptive illumination rendering in LED lighting systems,” *IEEE Transactions on Systems, Man, and Cybernetics—Part A: Systems and Humans*, vol. 43, no. 5, pp. 1052 – 1062, May 2013.
- [9] D. Caicedo, A. Pandharipande, and F. M. J. Willems, “Light sensor calibration and dimming sequence design in distributed lighting control systems,” *IEEE International Conference on Networking, Sensing and Control*, 2014.
- [10] M. Biguesh and A. Gershman, “Training-based MIMO channel estimation: A study of estimator tradeoffs and optimal training signals,” *IEEE Transactions on Signal Processing*, pp. 884–893, March 2006.
- [11] S. Boyd and L. Vandenberghe, *Convex Optimization*. Cambridge University Press, 2004.

CHAPTER 7. DISTRIBUTED METHODS FOR LIGHT SENSOR
CALIBRATION

- [12] European Committee for Standardization, “EN 12464-1:2002. Light and lighting. Lighting of work places. Part 1: Indoor work places,” 2002.

Chapter 8

Conclusions and Further Research

8.1 Conclusions

Currently, artificial lighting accounts for a major fraction of energy consumption in office buildings and thus reducing the energy consumption due to artificial lighting has a beneficial effect on costs and on environmental impact. In this thesis, our main focus has been on the design of distributed smart lighting systems that minimize energy consumption while providing adequate illumination levels in offices. In distributed smart lighting systems, multiple occupancy sensors and light sensors, which are distributed across the office, provide detailed information about the occupancy state and daylight distribution in the office, respectively. This information is used by a central controller or a network of controllers in the system to adapt the artificial illumination. The development of lighting control algorithms that fully exploit this information is of vital importance for achieving minimum energy consumption in such systems.

In this thesis, in particular, we developed lighting control algorithms that reduce energy consumption by: (i) providing localized illumination (500 lux in occupied regions and 300 lux elsewhere) and (ii) reducing the artificial lighting in regions with sufficient daylight. In our simulations, distributed smart lighting systems that used these algorithms achieved power savings up to 40%, with respect to conventional lighting systems that do not adapt the illumination, in scenarios where daylight was not available (e.g. during night time). The largest power savings were achieved in the presence of daylight, up to 85% in clear sky conditions.

In general, adapting the artificial illumination to different illumination levels can only be performed over regions that are sufficiently far apart. We denote each such region as a control zone. In this thesis, we considered a different number of control zones depending on office sizes. In small-sized spaces, a single control zone was considered, while in medium-sized and large-sized spaces, multiple control zones were considered. The development of occupancy sensors that provide accurate and reliable occupancy information for each control zone is important for the proper functioning of distributed smart lighting systems that provide localized illumination.

In Chapter 2, we focused on the design of occupancy sensors that monitor several control zones in medium-sized spaces and provide reliable information about which monitored control zones are occupied, i.e. granular occupancy information. In large-sized spaces, we focused on the design of asynchronous and distributed systems of such occupancy sensors, known as granular occupancy sensors.

In Chapters 3 to 7, we focused on the development of lighting control algorithms for distributed smart lighting systems that maximize power savings,

with respect to conventional lighting systems that do not adapt the illumination, while providing adequate illumination levels. We developed such algorithms for different system architectures, depending on factors such as office sizes, communication capabilities between controllers and location of light sensors (see Chapter 1).

The main contributions of this thesis are:

- We developed and implemented a distributed system of ceiling-mounted ultrasonic array sensors that provide granular occupancy information (Chapter 2). The unique features of this system are:
 - Each ceiling-mounted ultrasonic array sensor is able to provide granular occupancy information using low complexity algorithms.
 - Our occupancy sensor has an improved reliability when compared to commercially available passive infrared (PIR) occupancy sensors.
 - In an asynchronous and distributed system of ultrasonic array sensors, each sensor is able to schedule its transmission such that no interference with neighboring sensors occurs, without the need of communication channels between the controllers.
- We developed lighting control algorithms for energy-efficient control of distributed smart lighting systems with light sensors located at the desk. The unique features of these algorithms are:
 - In systems with a central controller, our lighting control algorithm maximizes power savings, with respect to conventional lighting systems that do not adapt the illumination, while providing adequate illumination levels under the presence of daylight (Chapter 3).
 - In systems with a central controller or distributed networked controllers without constraints on the exchange of information between controllers, our lighting control algorithm achieves a balance between satisfying user illumination preferences and reducing energy consumption (Chapter 4).
- We developed distributed lighting control algorithms for energy-efficient control of distributed smart lighting systems with light sensors located at the ceiling, multiple controllers and communication limited to neighboring controllers. The unique features of these algorithms are:
 - In systems where accurate estimates of the illumination at the desks are obtained from the light sensors at the ceiling, our distributed lighting control algorithm achieves substantial power savings, with respect

to conventional lighting systems that do not adapt the illumination, while providing adequate illumination levels. The proposed algorithm achieves power savings similar to those of lighting control systems with a central controller (Chapters 5).

- In systems where coarse estimates of the illumination at the desks are obtained from the light sensors at the ceiling, our distributed lighting control algorithm compensates for these coarse estimates and achieves an adequate illumination at the desks while reducing power consumption. The proposed algorithm achieves a better illumination at the desks when compared with lighting systems that do not compensate for the coarse estimates of the illumination levels. (Chapters 6).

In the remainder of the section, we present a detailed description of the contributions and results from each chapter.

8.1.1 Granular occupancy sensing solutions

In Chapter 2, we focused on: (i) the design of reliable granular occupancy sensors and (ii) the design of asynchronous and distributed systems of such sensors without communication channels between controllers. For convenience we repeat the goals and then describe the key contributions of this chapter:

Subgoal 1: *To design a low complexity ceiling-mounted sensing solution for providing reliable granular occupancy information.*

Contributions:

In Chapter 2, we proposed a low complexity sensing solution that provides reliable granular occupancy information within the range of detection of a ceiling-mounted ultrasonic array sensor. The ultrasonic array sensor is operated in pulsed-mode configuration: a short-pulsed ultrasonic sinusoidal signal is transmitted and the echoes from the objects within detection range are received and processed. Echoes from the environment are filtered out by analyzing the differential signal between two consecutive pulses. Using the time-of-flight and angle of arrival of the strongest echoes in the differential signal, occupied control zones are determined. The zoning and detection performance of our algorithm is improved by tracking the occupant movements across control zones. In an experimental setup, our proposed algorithm achieved a more reliable detection of occupants when compared with commercially available PIR occupancy sensors. Several control zones were defined along the length of the room, where each control zone had a length of 0.5 meter. Our ultrasonic array sensor was able to provide granular occupancy information over these control zones with an accuracy of ± 1 zone.

Subgoal 2: *To enable the coexistence of multiple stand-alone ultrasonic occupancy sensors in an asynchronous distributed smart lighting system for large-sized spaces without communication channels between controllers.*

Contributions:

In Chapter 2, we also developed a time-multiplexing active transmission scheme for dealing with the coexistence problem in asynchronous distributed smart lighting systems for large-sized spaces without communication channels between controllers. Our method listens to the echoes from active transmission of neighboring ultrasonic array sensors. The deviation between the expected arrival time and the actual arrival time of these echoes is used to compensate for clock drifts and align the transmission slots. Furthermore, the absence of these echoes is used for determining free transmission slots and then for assigning them for transmission. The transmission of each ultrasonic sensor array has to be completed within the assigned transmission slot, so cross-interference between neighboring ultrasonic array sensors is avoided. We considered transmission slots of larger duration than required (around 5 ms longer) such that small drifts were tolerated without degrading the performance of each ultrasonic array sensor. In an experimental setup, the accuracy in the synchronization of transmission slots was found to be within range (less than 5 ms).

8.1.2 Lighting controls when light sensors are located at the workspace plane

The main objective of the lighting control algorithms in this thesis is to minimize energy consumption while providing adequate illumination. The most common criterion for assessing the quality of the illumination in offices is the average illuminance over a surface on the horizontal plane at the height of desk, i.e. the workspace plane. Illuminance is a measurement of the amount of light (due to daylight and artificial lighting) incident on a given surface. The controller adapts the artificial illumination at the workspace plane by controlling the light output of individual LED-based luminaires in the lighting system to a fraction of their nominal output. This procedure is known as dimming and the fraction to which the light output of LED-based luminaires is controlled is known as dimming level.

The illuminance levels are of interest at the workspace plane, in particular at the desks where the occupants perform their tasks. Therefore, in Chapters 3 and 4, we assumed that the illuminance levels were known at the workspace plane, e.g. by using wireless light sensor modules located at the desks. We summarize the goals and key contribution from these chapters:

Subgoal 3: *To design lighting control algorithms that minimize energy consumption while adapting to daylight, occupancy information and satisfying minimum illuminance requirements at the workspace plane.*

Contributions:

In Chapter 3, we developed an analytical framework that considers the effect of daylight distribution in the rendered illumination. Granular occupancy information was used to determine target illuminance levels at the workspace plane. We proposed a centralized lighting control algorithm that determines the most energy-efficient dimming vector for the lighting system such that the combination of artificial light and daylight was larger than the target illuminance level. The performance of our proposed algorithm was tested under different occupancy scenarios using simulations and compared to conventional lighting systems that do not adapt the illumination. Our algorithm achieves adequate illuminance distribution according to European norm EN12464-1 while maximizing the power savings with respect to conventional lighting systems that do not adapt the illumination. In our simulations, we achieved up to 70% in power savings depending on the occupancy scenario.

Subgoal 4: *To design lighting control algorithms that minimize energy consumption while taking into account user illumination preferences at the workspace plane.*

Contributions:

In Chapter 4, we extended the analytical framework developed in Chapter 3 to include user illumination preferences. We used a convex piecewise linear function for modeling user dissatisfaction with respect to different illuminance levels. In this chapter, we developed a lighting control algorithm that balances between the user dissatisfaction and energy consumption, under a localized illumination rendering strategy. Two implementations of the lighting control algorithm were considered and compared: (i) a centralized implementation and (ii) a distributed implementation without constraints in the communication requirements. The distributed implementation of the lighting control algorithm provided a maximum reduction of 45% in the required computational complexity per controller when compared with a central controller. The performance of the method was evaluated under different multiple-occupants scenarios using simulations.

8.1.3 Lighting controls when light sensors are located at the ceiling

The illuminance measurements from light sensors located at the desk are susceptible to movements of the occupant, e.g. the occupant could block the field-of-view of the light sensor. Therefore, in Chapters 5 and 6 we assumed that light sensors were located at the ceiling and not at the workspace plane. The illumination requirements are given at the workspace plane, therefore a mapping between the illuminance levels at the light sensors at the ceiling and the illuminance levels at the workspace plane is required. In practice, obtaining the mapping between the illuminance levels is a time-consuming procedure and thus a coarse mapping is usually performed. Different lighting control algorithms are proposed based on the available mapping: (i) a complete mapping (Chapter 5) or (ii) a coarse mapping (Chapter 6). We summarize the goals and key contribution from these chapters:

Subgoal 5: *To design distributed lighting control algorithms that minimize energy consumption while satisfying illumination constraints over the illuminance measurements from light sensors at the ceiling and with limited neighborhood communication requirements.*

Contributions:

The distributed lighting control algorithm proposed in Chapter 4 requires the exchange of control information between all controllers. In distributed smart lighting system for large-sized spaces, multiple controllers are commonly required and thus the communication requirements between controllers for the algorithm proposed in Chapter 4 would be extensive, limiting the practical use of the algorithm. Therefore, in Chapter 5, we developed a distributed lighting control algorithm that reduces power consumption while adapting to occupancy and daylight information with exchange of control information limited to neighboring controllers. Our proposed algorithm achieved a near-optimum solution to the power minimization problem (as formulated in Chapter 3) while limiting the exchange of control information to neighboring controllers. The performance of the method was evaluated using simulations and the power savings, with respect to conventional lighting systems that do not adapt the illumination, were shown to be comparable to the power savings achieved with a central controller. We achieved up to 80% in power savings under clear sky conditions.

Subgoal 6: *To design distributed lighting control algorithms that minimize energy consumption while ensuring a minimum level of illumination at the workspace plane under coarse mapping between the illuminance levels at the ceiling and workspace plane.*

Contributions:

In Chapter 5, we assumed that the illuminance levels at the workspace place were accurately inferred from the illuminance measurements of the light sensors at the ceiling, e.g. using an extensive mapping between illuminance levels at the workspace plane and illuminance levels at the light sensors at the ceiling. In Chapter 6, we relaxed this assumption by allowing coarse approximations of the illuminance measurements from the light sensors at the ceiling. In practice, a coarse mapping is obtained by measuring reference illuminance levels at the light sensors when the LED-based luminaires in the lighting system are at a known reference dimming vector. This procedure of mapping between the illuminance levels is known as calibration. Our solution uses prior information from the calibration phase, such as reference dimming vector and reference illuminance levels, to ensure that minimum illuminance levels are achieved at the workspace plane. The performance of our proposed method was evaluated using simulations for different daylight scenarios and occupants distributions. The achieved illuminance distribution at the workspace plane was found to be close to the desired illuminance level. Under clear sky daylight conditions, the power savings achieved by the proposed method, with respect to conventional lighting systems that do not adapt the illumination, were 10% lower than the power savings obtained with a central controller and light sensors located at the workspace (i.e. the method described in Chapter 3).

8.1.4 Calibration methods

The lighting control algorithms proposed in this thesis require knowledge of the contribution from LED-based luminaires to the illuminance level of neighboring light sensor, known as illumination gains. The illumination gains allow the controller to decide which LED-based luminaires could be dimmed while still satisfying the illuminance requirements at the light sensors. Methods for estimating the illumination gains are possible but are time-consuming, e.g. during night time, one luminaire at a time is turned on and the illuminance levels at the light sensors are then measured. Furthermore, the illumination gains depend on the environment, e.g. the reflectance of the furniture.

The focus of Chapter 7 was not directly related to reducing energy consumption in distributed smart lighting system but was centered on decreasing the

calibration efforts for these systems, in particular, the estimation and tracking of illumination gains.

First, we recall the subgoal and then list the key contributions from this chapter:

Subgoal 7: *To reduce the calibration efforts in asynchronous distributed smart lighting systems by developing automatic and distributed methods for computing the illumination gains.*

Contributions:

In Chapter 7, we developed an automatic method for estimating and tracking the illumination gains in asynchronous distributed smart lighting systems. We evaluated the performance of our method using simulations and found that our method achieved an error of less than 10% in the estimation of the illumination gains. The achieved accuracy in the estimation of illumination gains is good enough to ensure that the distributed smart lighting system could render the required illumination after changes in the environment. Furthermore, the proposed method was robust in adapting to minor and major reflectance changes by tracking the changes in the illumination gains.

8.2 Recommendations for future research

The scope of this thesis was limited to two important research topics for the proper functioning of distributed smart lighting systems: granular occupancy sensing and adaptive lighting control algorithms. The main focus on granular occupancy sensing was the development and implementation of algorithms for providing granular occupancy information using ultrasonic array sensors in medium-sizes and large-sized spaces. In the topic of lighting control algorithms for distributed smart lighting systems, the main focus was on developing lighting control algorithms that reduce energy consumption, with respect to conventional lighting systems that do not adapt the illumination, by adapting to occupancy information and available daylight.

We acknowledge that several challenges still remain for the successful deployment and adoption of smart lighting systems. In this section, we sketch several potential research topics and directions, which might help to close this gap.

8.2.1 Occupancy sensing

In Chapter 2, some of our design choices for granular occupancy sensing solutions based on ultrasonic array sensors were limited by the availability of commercial

components. In the future, we expect that new low-cost components will become available, enabling new research directions for occupancy sensing:

- Currently, the bulky size of commercially available ultrasonic transmitters limits the construction of a transmitter array. In the future, with advances in MEMS technology, we expect that MEMS-based ultrasonic transmitters become commercially available enabling the construction of an ultrasonic transmitter array. The existence of an ultrasonic transmitter array would enable the use of beamforming techniques for transmission. The combination of beamforming techniques at both the transmitter and receiver side would allow for the development of new occupancy detection algorithms and applications.
- Commercially available wide-beam ultrasonic transmitters have limited bandwidth. In the future, we expect that wide-beam ultrasonic transmitters with wide bandwidth will become available. A relevant research direction would be to develop distributed occupancy systems based on ultrasonic array sensors that exploit this wide bandwidth. For example, the wide bandwidth allows frequency multiplexing solutions to be considered for the coexistence problem.

8.2.2 Lighting controls

In Chapters 3 to 6, we developed an analytical framework for designing and evaluating lighting control algorithms in distributed smart lighting system with LED-based luminaires. The current framework uses illuminance level as the criterion for assessing the quality of the illumination and assumes a perfect communication channel between controllers (when a communication channel was required). Different research directions extending this analytical framework may include:

- We defined user dissatisfaction functions based on illuminance levels and modeled them as convex piecewise linear functions. In general, a user considers different factors while appraising the quality of lighting such as color, glare, contrast and so on. Note that a direct measurement of these factors is not always possible. Hence, modeling the effect of these factors in the user appraisal of lighting and including them in an analytical framework is a relevant research direction.
- The current framework for lighting control may be extended by considering practical constraints such as latency and errors in the communication channel. The study of distributed lighting control algorithms that are robust to different communication errors and failures is an interesting future step.

Summary

Distributed Smart Lighting Systems: Sensing and Control

The energy used by artificial lighting corresponds to a major part of the total energy consumed in office buildings. Energy consumption may be reduced by providing low illumination levels, but low illumination levels also reduce satisfaction of occupants in the office. Lighting control by adapting to daylight and occupancy levels is an effective way for providing the desired illumination while reducing energy consumption. Typically, light sensors are used to measure the illumination while occupancy sensors provide information about the presence of occupants.

Smart lighting systems have computing devices (controllers) that use available daylight and occupancy information to control the illumination and reduce energy consumption. Furthermore, distributed smart lighting systems, wherein the controllers and sensors are distributed across the space, have advantages of plug-and-play modularity and scalability that are desirable features. A key research theme in this thesis is *how to achieve maximum energy savings while providing the required illumination to the occupants using distributed smart lighting systems*.

Current occupancy sensors are based on detecting motion within their sensing region. Passive infrared-based occupancy sensors are widely used for providing information about the presence (or absence) of occupants in their sensing region, i.e. binary occupancy information. They are sensitive to major movements (e.g. walking) but cannot reliably detect minor movements (e.g. moving hands) of the occupant. In comparison, current ultrasonic-based occupancy sensors offer improved sensitivity over larger detection ranges as compared to passive infrared-based occupancy sensors at comparable costs. Occupancy sensors that provide accurate and reliable occupancy information are preferred in lighting systems.

However, both types of occupancy sensors cannot presently provide granular occupancy information, i.e. information about the location of the occupants within their sensing region. Granular occupancy information could conceivably be obtained by combining angular and distance information. The current minia-

SUMMARY

turization of technology has enabled the construction of arrays of ultrasonic elements and so the use of beam-forming techniques that could potentially provide angular information. Distance information can be obtained by using a pulsed waveform at the ultrasonic transmitter. In practical distributed smart lighting systems, occupancy sensors have additional constraints in cost and complexity. The first challenge in this thesis is *to develop low complexity algorithms for reliable granular occupancy information using an ultrasonic array sensor*.

In Chapter 2, we address the problem of how to process the raw data from a single ultrasonic array sensor to provide reliable granular occupancy information. An ultrasonic array sensor that transmits a probing pulse-sinusoid signal with a given pulse repetition interval is considered. Using differential processing on received echoes, further processing can be limited to time bins of possible occupancy. Time-of-flight and angular information is derived by processing the echoes at the receiver array based on which the occupants are localized. Furthermore, an algorithm for tracking the occupant movements is used to improve the reliability of the detection. The performance of the developed algorithms is evaluated on a prototype implementation.

In distributed smart lighting systems for large spaces such as open offices, several of these ultrasonic array sensors may be deployed to ensure detection coverage over the entire space. Due to low-cost constraints, such sensors typically have limited communication capabilities and clocks with low accuracy. For such a system to function properly, it is necessary to coordinate the active transmissions from the sensors properly. Under the constraints of the system, a time multiplex active transmission scheme is a preferred choice. Two challenges emerge in such a system. One is *how to allocate the transmission slots so that one transmission does not result in echoes over a transmission slot of another sensor within listening range*. The second is *to ensure that each sensor maintains its transmission slot, given that each sensor may exhibit clock drifts*. In Chapter 2, we also propose a solution to this coexistence problem, based on exploiting the cross-interference between sensors for identifying free transmission slots and clock drifts.

Current lighting control systems are conventionally designed to adapt to room-level occupancy and daylight availability within a pre-defined region, e.g. the lighting system in an office will be activated when occupancy is detected in any location within the office and only those luminaires close to the window will adapt to daylight levels. While this leads to low cost of system components, this lighting control approach has some disadvantages: (i) limited power savings and (ii) additional efforts for identifying those luminaires close to the windows. The identification of the luminaires close to the windows is part of a set of pro-

cedures required for the proper functioning of the lighting system, known as commissioning. In Chapters 3 to 7 of the thesis, we address the problem of *how to minimize the power consumption in a distributed smart lighting system with limited commissioning efforts while providing the required illumination levels*.

Granular occupancy information can be further used by the lighting control algorithm to provide localized illumination over the workspace plane, i.e. high illumination levels around the occupants (e.g. desk) and low illumination levels elsewhere. Low illumination levels are achieved by changing the light output of a luminaire to a fraction of its nominal value, hereafter referred to as dimming. In our first approach, the daylight and artificial light distribution at the workspace plane is assumed to be known, e.g. by using wireless light sensor modules at the desks. In Chapter 3, we investigate *how to determine the optimum dimming level of each luminaire so that the desired illumination levels at the workspace plane are achieved, when the daylight and artificial light distributions are known over the workspace plane*. Here, the illumination problem is formulated as a linear programming problem and solved using the Simplex Method.

The illumination problem is extended by considering user preferences. In general, different users may have different preferences and thus two major research challenges arise: (i) *how to balance between power savings and user satisfaction*, and (ii) *how to deal with conflicting user preferences*. The user preferences are modeled by piecewise linear functions and incorporated into the objective function of the constrained power minimization problem. The linearity of the problem is maintained and thus the Simplex Method can be used to obtain an optimum solution, as presented in Chapter 4.

In practice, light sensors are not located at the desks but rather at the ceiling where their view is not blocked by user movements. In Chapter 5, a networked distributed smart lighting system wherein luminaires have local sensing and limited communication capabilities within a neighborhood is considered. Here, we assume that the illuminance distribution at the workspace is accurately mapped to illuminance levels at the light sensors at the ceiling. The mapping of illuminance levels is known via a calibration that is part of the commissioning phase. Furthermore, we assume that each individual controller knows the illuminations gains from its neighboring luminaires, i.e. the illuminance contributions from neighboring luminaires to its own light sensor. The main challenge addressed in Chapter 5 is *how to find the dimming levels for distributed smart lighting systems with limited neighborhood communication capabilities so as to limit the energy consumption while satisfying minimum illumination constraints at light sensors at the ceiling*. Here, a near-optimum solution to the constrained power minimization problem is provided along with the corresponding bounds for opti-

mality.

In some scenarios, achieving the illumination constraints at the light sensors does not provide the desired illumination rendering at the workspace plane. This is because, in practice, only a coarse mapping between the illuminance levels at light sensors at the ceiling and workspace plane is available. Chapter 6 addresses the problem of *how to achieve a desired illumination at the workspace plane while maximizing power savings under limited knowledge of the mapping between illuminance levels at light sensors at the ceiling and workspace plane*. The proposed solution obtains a lower-bound in the illuminance distribution at the workspace plane when the lighting system is at a given dimming vector by using the information obtained during the calibration phase (i.e. reference dimming level and light sensor measurements). Power savings with respect to a lighting system that does not adapt the illumination are achieved such that the lower-bound in the illumination is close to the desired minimum illuminance level at the workspace plane.

In general, a dark-room calibration step is used to determine the individual illumination gains. The illumination gains are computed when the lighting system is set to known dimming vectors. This is a time-consuming procedure that is usually performed once, after the installation of the lighting system. However, the illumination gains may vary over time due to reflectance changes, e.g. user or object movements in the environment. In Chapter 7, the problem of *how to automatically estimate and track the individual illumination gains in an asynchronous distributed smart lighting system* is considered. The illumination gains are estimated and tracked by solving a system of linear equations. The system of linear equations is obtained by randomly blinking the luminaires in the lighting systems and measuring the corresponding illuminance levels at light sensors.

Finally, in Chapter 8, the main contributions and conclusions of this thesis are summarized, and future research challenges are identified.

Curriculum vitae

David Ricardo Caicedo Fernández was born in Guayaquil, Ecuador, on June 28, 1984. In 2006, he received an Engineering degree from the Faculty of Electrical and Computer Engineering, ESPOL, Guayaquil, Ecuador. In 2006, he did an internship in Nokia, Guayaquil, Ecuador. From 2007 to 2008, he was with Nokia Siemens Networks, Bogotá, Colombia, as a Radio Frequency Engineer.

From 2008 to 2010, he studied at Delft University of Technology, Delft, The Netherlands. He obtained the M.Sc. degree (cum laude) in electrical engineering, with specialization in the field of Telecommunications, from Delft University of Technology, Delft, The Netherlands, in June 2010. He spent one year at Philips Research, Eindhoven, The Netherlands, as part of his master program between 2009 and 2010.

In August 2010, he started working at Philips Research, Eindhoven, The Netherlands, while pursuing a Ph.D. degree with Eindhoven University of Technology, Eindhoven, The Netherlands.

His research interests are in the areas of sensor signal processing algorithms and applications, lighting control algorithms and applications, mobile wireless communications and wireless networking.

Curriculum vitae

Acknowledgement

Foremost, I would like to express my deepest appreciation to my daily supervisor at Philips Research and co-promotor, dr. Ashish Pandharipande, for all his support, guidance and encouragement throughout the past years. I owe him great gratitude, first, for offering me an internship at Philips Research during my master studies and later for recommending me for the van der Pol programme at Philips Research. I have learned a lot from his practical research style and from our daily discussions and interactions.

I would like to thank my promotor, prof. dr. ir. Jan Bergmans. Jan has been extremely patience and helpful with the coordination between Eindhoven University of Technology and Philips Research. His comments and suggestions during all the stages of my PhD work has greatly contributed to improved the quality of this disseration.

I am very thankful to dr. ir. Frans Willems. He has been my daily supervisor at Eindhoven University of Technology and co-promotor during this period. His challenging questions and critical comments during our weekly meetings have greatly improved the quality of my work. Our discussions has been an enriching experience for me.

Special thanks to prof. dr. U. Mitra, prof. dr. G. Q. Zhang, prof. dr. J. J. Lukkien and dr. S. Srinivasan for being part of the doctorate committee.

My sincere thanks also goes to dr. Martin Elixmann for his warm encouragement and support while working under his department group at Philips Research. During my time at Philips Research I have enjoyed working with numerous exceptional people. In particular, I would like to express my gratitude to some colleagues with whom I closely collaborated: Sriram Srinivasan, Hongming Yang, Sri Andari Husen, Oscar García-Morchon, Dee Denteneer and Eric Penning De Vries.

I want to thank Marc Aoun for his advices and help during the last stages of preparing my dissertation. I would like to thank Yvonne Lansink-Stroeve for her

Acknowledgement

help in dealing with many logistical issues. I have had a very nice time sharing offices and interesting discussions with Alessio Filippi, Esther van der Heide, Sandeep Kumar, Alexandre Sinitsyn and Ying Wang. Also, I have enjoyed our lively conversations with Oscar García-Morchon, Sandeep Kumar, Sye Loong Keoh, Ernest Ma, Henrik Ziegeldorf and Leandro Marín.

I thank Guido Vasquez, Steven Egbosimba and Liu Lei for their friendship and support during my time in The Netherlands. I would like to thank my friends in Ecuador for their long-lasting friendship.

I am very thankful to my aunt Narcisa and her family for receiving me and supporting me during all these years in The Netherlands.

Last but not least, a word of gratitude to my family in Ecuador. I would like to thank my parents, Martin and Amelia, and my brothers, Martin and Francisco, for their unconditional love and support. I thank my grandparents and relatives back home for their encouragement since my childhood.

Thank you all,

David Ricardo Caicedo Fernández
June 25, 2014